Metabolites from the Mangrove-derived Fungi: *Acremonium* sp. PSU-MA70 and *Pestalotiopsis* sp. PSU-MA92 and PSU-MA119

Aekkachai Rodglin

A Thesis Submitted in Partial Fulfillment of the Requirements
for the Degree of Master of Science in Organic Chemistry
Prince of Songkla University
2010

Thesis Title	Metabolites from the Mangrove-derived Fungi: *Acremonium* sp. PSU-MA70 and *Pestalotiopsis* sp. PSU-MA92 and PSU-MA119
Author	Mr. Aekkachai Rodglin
Major Program	Organic Chemistry

Major Advisor:

……..…

(Prof. Dr. Vatcharin Rukachaisirikul)

Co-advisor:

……..

(Dr. Yaowapa Sukpondma)

Examing Committee:

……...…….Chairperson

(Dr. Pattama Pittayakhajonwut)

……..……

(Prof. Dr. Vatcharin Rukachaisirikul)

……..……

(Dr. Yaowapa Sukpondma)

……..……

(Assoc. Prof. Dr. Chatchanok Karalai)

The Graduate School, Prince of Songkla University, has approved this thesis as partial fulfillment of the requirements for the Degree of Master of Science in Organic Chemistry

……

(Assoc. Prof. Dr. Krerkchai Thongnoo)

Dean of Graduate School

ชื่อวิทยานิพนธ์ เมทาบอไลต์จากเชื้อราพืชป่าชายเลน *Acremonium* sp. PSU-MA70 และ *Pestalotiopsis* sp. PSU-MA92 และ PSU-MA119

ผู้เขียน นายเอกชัย รอดกลิ่น

สาขาวิชา เคมีอินทรีย์

ปีการศึกษา 2552

บทคัดย่อ

งานวิจัยนี้ศึกษาองค์ประกอบทางเคมีของเชื้อราจากพืชป่าชายเลนจำนวน 3 ชนิด ได้แก่ *Acremonium* sp. PSU-MA70 และ *Pestalotiopsis* sp. PSU-MA92 และ PSU-MA119 โดยนำส่วนสกัดหยาบเอทิลอะซิเตทจากส่วนน้ำเลี้ยงเชื้อของเชื้อราดังกล่าวมาทำให้บริสุทธิ์ด้วยวิธีทางโครมาโทกราฟี สามารถแยกสารบริสุทธิ์ประเภทต่างๆ ได้ดังนี้

• สารใหม่จำนวน 10 สาร ได้แก่ อนุพันธ์ของ phthalide จำนวน 2 สาร (**AR11** และ **AR16**) อนุพันธ์ของ isochromanone จำนวน 3 สาร **(AR12**, **AR13** และ **AR17)** อนุพันธ์ของ isochromenone จำนวน 4 สาร **(AR14**, **AR18**, **AR19** และ **AR20)** และอนุพันธ์ของ lactone จำนวน 1 สาร **(AR15)** และสารที่มีการรายงานโครงสร้างแล้วจำนวน 10 สาร คือ อนุพันธ์ของ macrolide จำนวน 1 สาร (**AR1**) อนุพันธ์ของ cyclic depsipeptide จำนวน 2 สาร (**AR2** และ **AR3**) อนุพันธ์ของ sesquiterpene จำนวน 2 สาร (**AR4 และ AR7**) อนุพันธ์ของ hexanediol จำนวน 1 สาร (**AR5)** อนุพันธ์ของ pentanediol 1 สาร (**AR6)** อนุพันธ์ของ phthalide จำนวน 1 สาร (**AR8**) และอนุพันธ์ของ diketopiperazine จำนวน 2 สาร (**AR9** และ **AR10**) จากเชื้อรา *Acremonium* sp. PSU-MA70

• สารใหม่จำนวน 4 สาร คือ อนุพันธ์ของ α-pyrone จำนวน 4 สาร (**AR21**, **AR22**, **AR23** และ **AR24**) และสารที่มีการรายงานโครงสร้างแล้ว จำนวน 2 สาร คือ อนุพันธ์ของ phenol (**AR25)** และ อนุพันธ์ของ penicillide (**AR26**) จากเชื้อรา *Pestalotiopsis* sp. PSU-MA92

• สารใหม่จำนวน 2 สาร ได้แก่ อนุพันธ์ของ macrolide จำนวน 2 สาร (**AR27** และ **AR29**) และสารที่มีการรายงานโครงสร้างแล้วจำนวน 3 สาร คือ อนุพันธ์ของ macrolide จำนวน 1 สาร (**AR28**) และอนุพันธ์ของ phenol จำนวน 2 สาร (**AR30** และ **AR31**) จากเชื้อรา *Pestalotiopsis* sp. PSU-MA119 โดยสารประกอบ **AR27** แยกในรูปอนุพันธ์อะซิเทต

โครงสร้างสารทั้งหมดวิเคราะห์โดยใช้ข้อมูลทางสเปกโทรสโกปี โดยเฉพาะ 1D และ 2D NMR สเปกโทรสโกปี และเปรียบเทียบกับข้อมูลที่มีการรายงานไว้แล้ว สำหรับสเตอริโอเคมีของสาร **AR1** สามารถยืนยันได้ด้วยข้อมูล X-ray

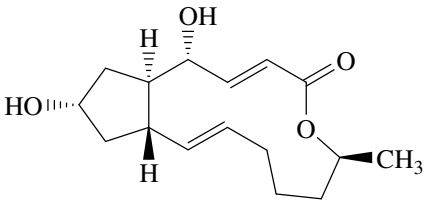

AR1

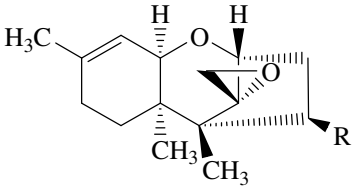

AR4 : R = $OCOCH\overset{Z}{=}CHCH_3$

AR7 : R = OH

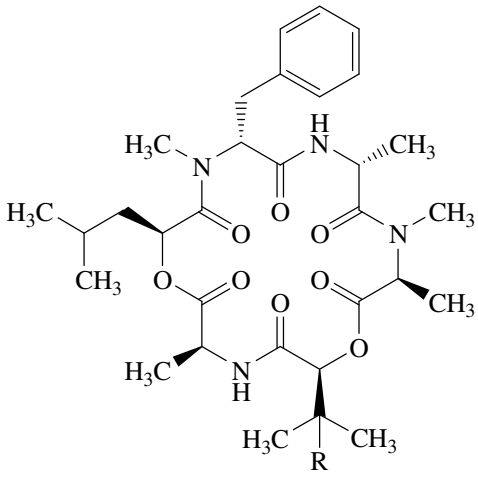

AR2 : R = OH

AR3 : R = H

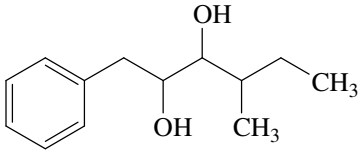

AR5

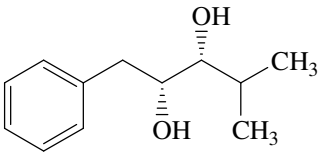

AR6

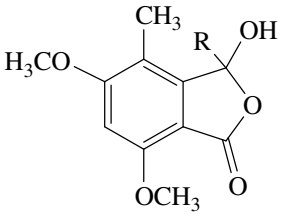

AR8 : R = CH_3

AR11 : R = CH_2OH

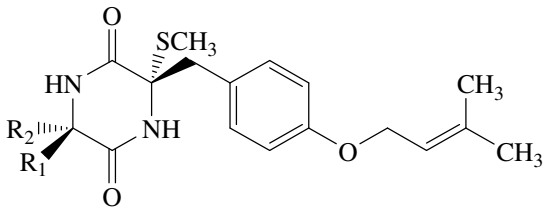

AR9 : R_1 = H, R_2 = SCH_3

AR10 : R_1 = SCH_3, R_2 = H

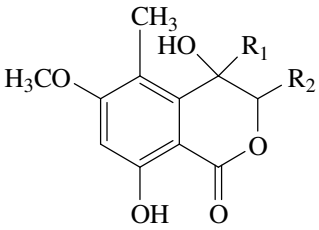

AR12 : $R_1 = COCH_3$, $R_2 = H$

AR13 : $R_1 = CH_2OH$, $R_2 = CH_3$

AR17 : $R_1 = CH(OH)CH_3$, $R_2 = H$

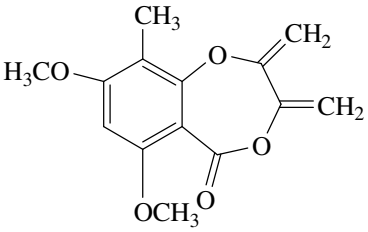

AR15

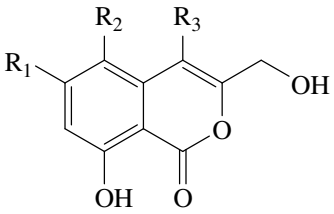

AR18 : $R_1 = OCH_3$, $R_2 = CH_3$, $R_3 = CH_2OH$

AR19 : $R_1 = OH$, $R_2 = H$, $R_3 = CH_3$

AR20 : $R_1 = OH$, $R_2 = CH_3$, $R_3 = CH_2OH$

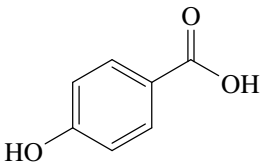

AR25

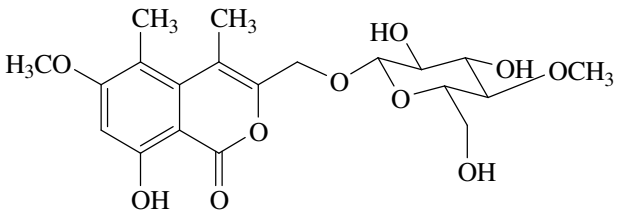

AR14

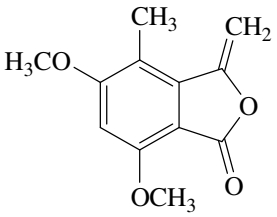

AR16

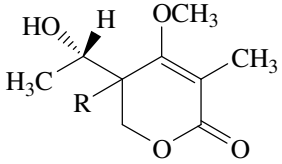

AR21 : R = α-H

AR22 : R = β-H

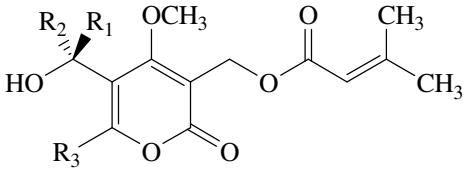

AR23 : $R_1 = R_3 = H$, $R_2 = OH$

AR24 : $R_1 = R_2 = H$, $R_3 = CH_3$

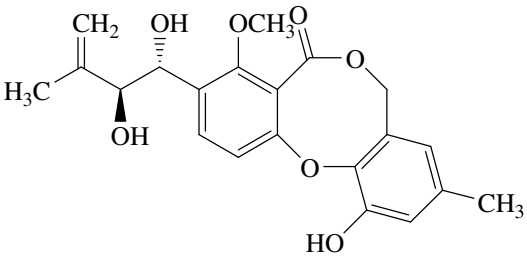

AR26

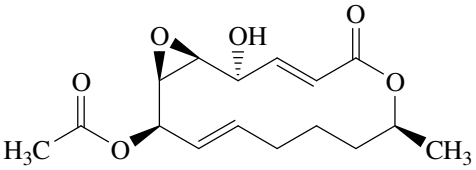

AR27

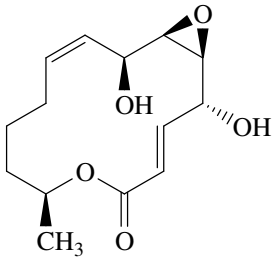

AR28

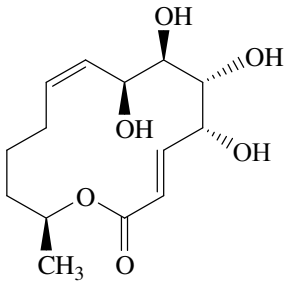

AR29

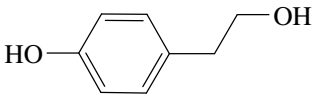

AR30

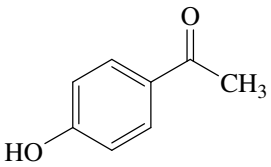

AR31

Thesis Title	Metabolites from the Mangrove-derived Fungi: *Acremonium* sp. PSU-MA70 and *Pestalotiopsis* sp. PSU-MA92 and PSU-MA119
Author	Mr. Aekkachai Rodglin
Major Program	Organic Chemistry
Academic Year	2009

ABSTRACT

This research investigated the ethyl acetate extracts from the culture broth of the mangrove-derived fungi; *Acremonium* sp. PSU-MA70 and *Pestalotiopsis* sp. PSU-MA92 and PSU-MA119. Each extract was purified by various chromatographic techniques. The investigation led to the isolation of various types of secondary metabolites as follows.

- Ten new compounds: two phthalide derivatives (**AR11** and **AR16**), three isochromanone derivatives **(AR12**, **AR13** and **AR17)**, four isochromenone derivatives **(AR14**, **AR18**, **AR19** and **AR20)** and one lactone derivative **(AR15)** together with ten known compounds: one macrolide (**AR1**), two cyclic depsipeptide derivatives (**AR2** and **AR3**), two sesquiterpene derivatives (**AR4** and **AR7**), one hexanediol derivative (**AR5)**, one pentanediol derivative **(AR6**), one phthalide derivative (**AR8**) and two diketopiperazine derivatives (**AR9** and **AR10**), from *Acremonium* sp. PSU-MA70.

- Four new α-pyrone derivatives (**AR21**, **AR22**, **AR23** and **AR24**) along with two known compounds: one phenol (**AR25)** and one penicillide derivative (**AR26**), from *Pestalotiopsis* sp. PSU-MA92.

- Two new macrolides (**AR27** and **AR29**) and three known compounds: one macrolide derivative (**AR28**) and two phenol derivatives (**AR30** and **AR31**), from *Pestalotiopsis* sp. PSU-MA119.

Their structures were elucidated by analysis of spectroscopic data, especially 1D and 2D NMR data, and comparison of the NMR data with those previously reported. The stereochemistry of **AR1**was confirmed by X-ray data.

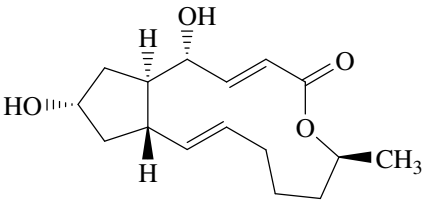

AR1

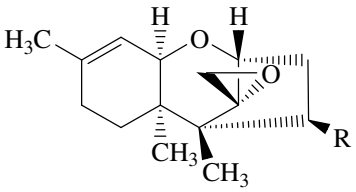

AR4 : R = $OCOCH\overset{Z}{=}CHCH_3$

AR7 : R = OH

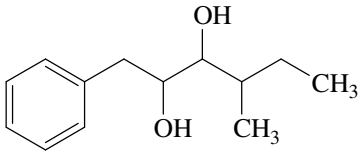

AR5

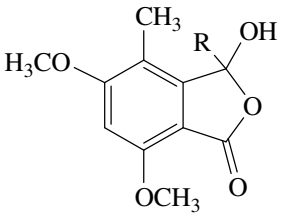

AR8 : R = CH_3

AR11 : R = CH_2OH

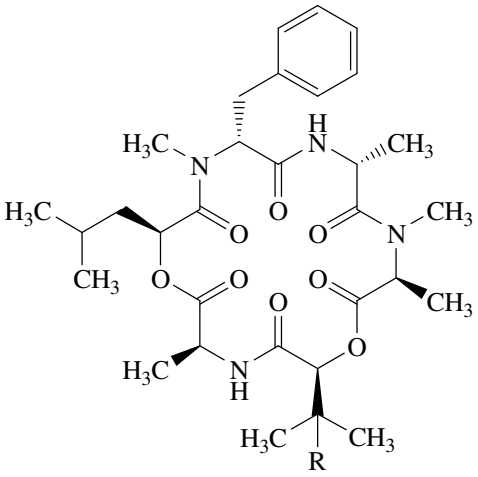

AR2 : R = OH

AR3 : R = H

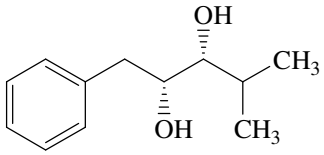

AR6

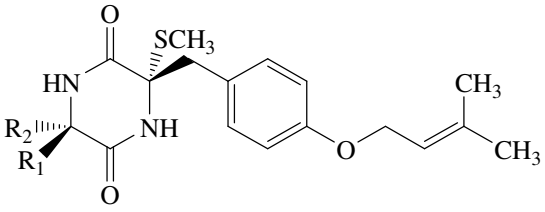

AR9 : R_1 = H, R_2 = SCH_3

AR10 : R_1 = SCH_3, R_2 = H

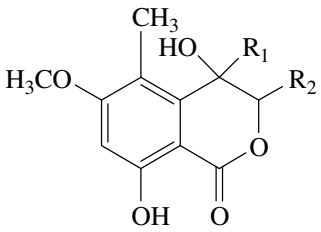

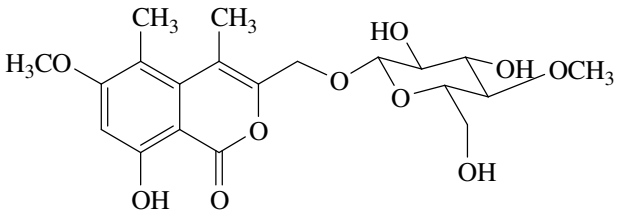

AR14

AR12 : $R_1 = COCH_3$, $R_2 = H$

AR13 : $R_1 = CH_2OH$, $R_2 = CH_3$

AR17 : $R_1 = CH(OH)CH_3$, $R_2 = H$

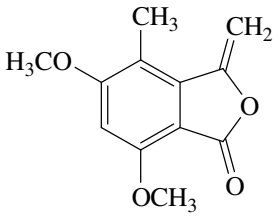

AR16

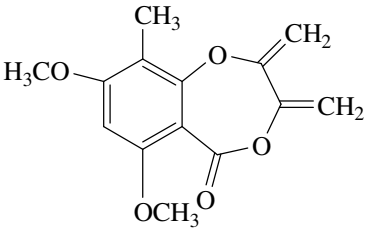

AR15

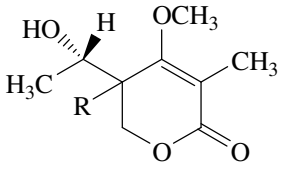

AR21 : R = α-H

AR22 : R = β-H

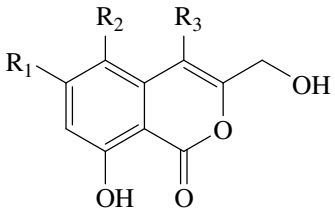

AR18 : $R_1 = OCH_3$, $R_2 = CH_3$, $R_3 = CH_2OH$

AR19 : $R_1 = OH$, $R_2 = H$, $R_3 = CH_3$

AR20 : $R_1 = OH$, $R_2 = CH_3$, $R_3 = CH_2OH$

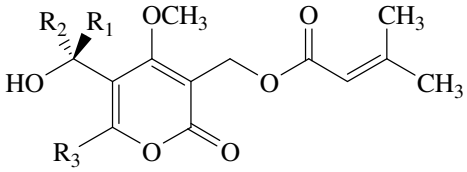

AR23 : $R_1 = R_3 = H$, $R_2 = OH$

AR24 : $R_1 = R_2 = H$, $R_3 = CH_3$

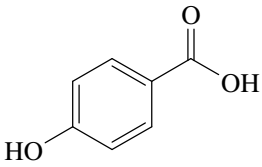

AR25

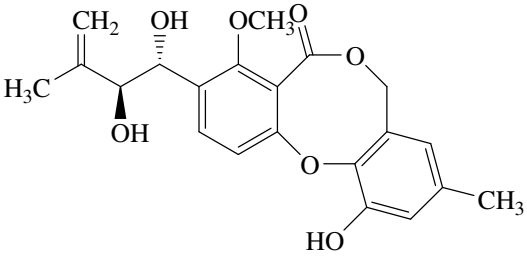

AR26

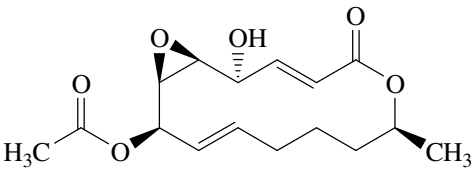

AR27

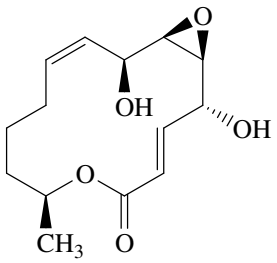

AR28

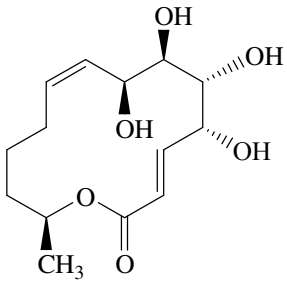

AR29

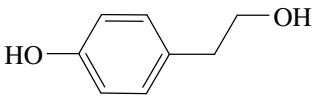

AR30

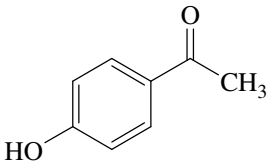

AR31

CONTENTS

CONTENTS (**Continued**)

CONTENTS (Continued)

LIST OF TABLES

LIST OF TABLES (Continued)

LIST OF TABLES (Continued)

LIST OF TABLES (Continued)

LIST OF TABLES (Continued)

LIST OF TABLES (Continued)

LIST OF TABLES (Continued)

LIST OF FIGURES

LIST OF FIGURES

LIST OF FIGURES (Continued)

LIST OF FIGURES (Continued)

PART I

METABOLITES FROM THE MANGROVE-DERIVED FUNGUS *ACREMONIUM* SP. PSU-MA70

CHAPTER 1.1

INTRODUCTION

1.1.1 Introduction

Fungi in the genus *Acremonium* producing various bioactive metabolites have drawn attention from many scientists to investigate their metabolites so far. Based on SciFinder Scholar Database, the secondary metabolites from the genus *Agremonium* with various biological activities since the year 2000 are summarized in **Table 1**. In this study, we conducted our research with the mangrove-derived fungus *Acremonium* sp. PSU-MA70. The crude ethyl acetate extract from its broth did not display antibacterial activity against *Staphylococcus aureus*, *Pseudomonas aeruginosa* and *Escherichia coli* at the concentration of 200 µg/mL. However, it showed antifungal activity against *Candida albicans* and *Cryptococcus neoformans* with the equal MIC value of 128 μg/mL and against *Microsporum gypseum* with the MIC value of 200 μg/mL.

This fungus was isolated from the twigs of *Rhizophora apiculata*, collected from Satun province, Thailand in the year 2007. It was deposited at the Department of Microbiology, Faculty of Science, Prince of Songkla University, as the fungus PSU-MA70.

Table 1 Compounds isolated from the *Acremonium* genus

Scientific name	Compound	Activity	Reference
A. crotocinige-num	6,8-Dimethoxy-4,5-dimeth-yl-3-methyleneisochroman-1-one, **1** 5,7-Dimethoxy-3,4-dimeth-yl-3-hydroxyisobenzofura-	-	Shim *et al*., 2008

Table 1 Continued

Scientific name	Compound	Activity	Reference
	none, **2**		
A. furcatum	(2*E*,4*E*)-2-Methylhexa-2,4-dienoic acid (2′*R*,3′*S*)-isoleucinol amide, **3** (2*E*,4*E*)-2-Methylhexa-2,4-dienoic acid (2′*S*,3′*S*)-isoleucinol amide, **4** (2*E*,4*E*)-2-Methylhexa-2,4-dienoic acid (2′*R*, 3′*S*)-isoleucinaldehyde, **5** (2*E*,4*E*)-2-Methylhexa-2,4-dienoic acid (2′*S*, 3′*S*)-isoleucinaldehyde, **6**	Antifungal	Gallardo *et al.*, 2006
Acremonium sp.	Acremonin A, **7** Acremonin A glugoside, **8** (3*R*,4*S*)-3,4-Dihydroxy-7-methyl-3,4-dihydro-1(2*H*)-naphthalenone, **9** (3*S*,4*S*)-3,4-Dihydroxy-7-methyl-3,4-dihydro-1(2*H*)-naphthalenone, **10** 2-(1-Methylethylidene)-pentanedioic acid, **11** Pentanedioic acid 2-(1-2-(1-Methylethylidene)-methylethylidene)-5-methyl ester, **12** Pentanedioic acid 2-(1-methylethylidene)-1-methyl	Antioxidant	Abdel-Lateff *et al.*, 2002

Table 1 Continued

Scientific name	Compound	Activity	Reference
	ester, **13** Pentanedioic acid 2-(1-methylethenyl)-5-methyl ester, **14** 2-(1-Hydroxy-1-methyl)-2,3-dihydrobenzofuran-5-ol, **15** 2,2-Dimethylchroman-3,6-diol, **16** 2-(2,3-Dihydroxy-3-methylbutyl)benzene-1,4-diol, **17**		
	Acremonisol A, **18**	-	Pontius *et al*., 2008
	Chlorocylindrocarpol, **19** Cylindrocarpol, **20** Acremofuranone A, **21** Acremofuranone B, **22** Dihydroxybergamotene, **23** Lignoren, **24** Ascofuranone, **25** Ascofuranol, **26** Ascochlorin, **27** Cylindrol B, **28** Ilicicolin C, **29** Ilicicolin F, **30** Deacetylchloronectrin, **31** LL-Z1272 ε, **32**	Anti-inflammatory	Zhang *et al*., 2009
	Awajanoran, **33**	Cytotoxic and	Jang *et al*.,

Table 1 Continued

Scientific name	Compound	Activity	Reference
		antimicrobial	2006
Acremonium sp. BCC 14080	3-Heptyl-5-hydroxyphenyl 2-(*β*-D-galactopyranosyl-oxy)-6-heptyl-4-hydroxy-benzoate, **34** 3-Heptyl-5-hydroxyphenyl 2-[(6-*O*-*β*-D-galactopyrano-syl-*β*-D-galactopyranosyl)-oxy]-6-heptyl-4-hydroxy-benzoate, **35** KS-501a, **36** 2-(3-Heptyl-5-hydroxyben-zyl)tetrahydro-6-(hydroxyl-methyl)-5-methoxy-2*H*-pyran-3,4-diol, **37**	Antiplasmo dial, cytotoxic and anti-HSV-1	Bunyapai-boonsri *et al*., 2008
Acremonium sp. BCC 31806	Acremoxanthone A, **38** Acremoxanthone B, **39** Acremonidin A, **40** Acremonidin C, **41**	Antibacterial, antifungal, antiplasmo dial, cytotoxic	Isaka *et al*., 2009
Acremonium sp. No. 27082	FR235222, **42**	Inhibitory lymphocyte proliferation, lymphokine production and activity of mammalian histone deacetylase (HDAC)	Mori *et al.*, 2003

Table 1 Continued

Scientific name	Compound	Activity	Reference
A. zeae	Curvularin, **43** Dihydroresorcylide, **44** (*R*)-7-Hydroxydihydro-resorcylide, **45** (*S*)-7-Hydroxydihydro-resorcylide, **46** Pyrrocidine A, **47** Pyrrocidine B, **48**	Antifungal	Poling *et al.*, 2008

Structures of the metabolites isolated from the *Acremonium* genus

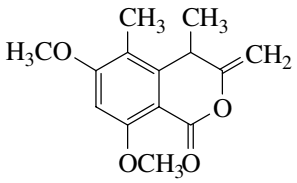

1 : 6,8-Dimethoxy-4,5-dimethyl-3-methyleneisochroman-1-one

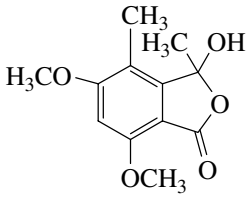

2 : 5,7-Dimethoxy-3,4-dimethyl-3-hydroxyisobenzofuran

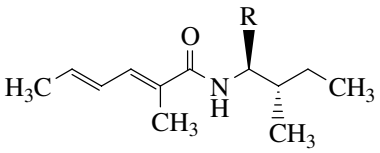

3 : R = CH_2OH
: (2*E*,4*E*)-2-Methylhexa-2,4-dienoic acid (2′*R*,3′*S*)-isoleucinol amide

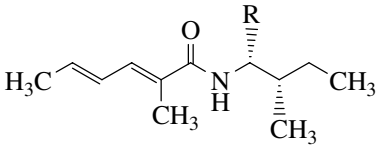

4 : R = CH_2OH
: (2*E*,4*E*)-2-Methylhexa-2,4-dienoic acid (2′*S*,3′*S*)-isoleucinol amide

5 : R = CHO
: (2*E*,4*E*)-2-Methylhexa-2,4-dienoic acid (2′*R*, 3′*S*)-isoleucinaldehyde

6 : R = CHO
: (2*E*,4*E*)-2-Methylhexa-2,4-dienoic acid (2′*S*, 3′*S*)-isoleucinaldehyde

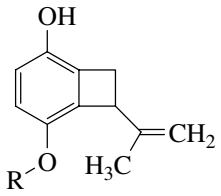

7 : R = H : Acremonin A

8 : R = 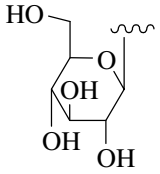

: Acremonin A glugoside

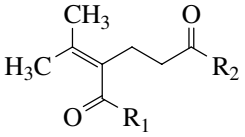

11 : R_1 = OH, R_2 = OH

: 2-(1-Methylethylidene)-pentanedioic acid

12 : R_1 = OH, R_2 = OCH_3

: Pentanedioic acid 2-(1-methylethylidene)-5-methyl ester

13 : R_1 = OCH_3, R_2 = OH

: Pentanedioic acid 2-(1-methylethylidene)-1-methyl ester

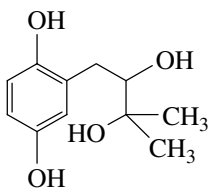

17 : 2-(2,3-Dihydroxy-3-methylbutyl)-benzene-1,4-diol

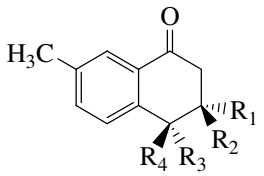

9 : R_1 = R_3 = H, R_2 = R_4 = OH

: (3*R*,4*S*)-3,4-Dihydroxy-7-methyl-3,4-dihydro-1(2*H*)-naphthalenone

10 : R_2 = R_3 = H, R_1 = R_4 = OH

: (3*S*,4*S*)-3,4-Dihydroxy-7-methyl-3,4-dihydro-1(2*H*)-naphthalenone

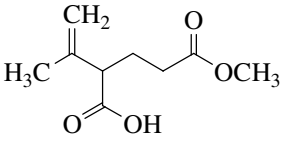

14 : Pentanedioic acid 2-(1-methylethenyl)-5-methyl ester

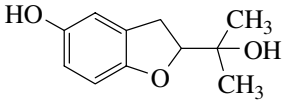

15 : 2-(1-Hydroxy-1-methyl)-2,3-dihydrobenzofuran-5-ol

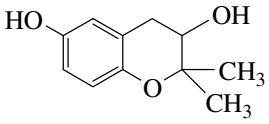

16 : 2,2-Dimethylchroman-3,6-diol

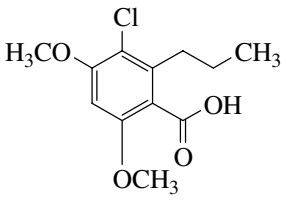

18 : Acremonisol A

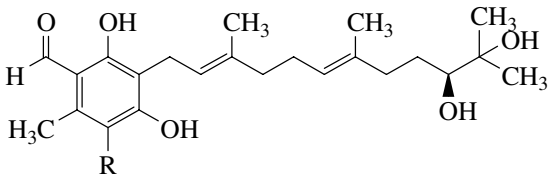

19 : R = Cl : Chlorocylindrocarpol

20 : R = H : Cylindrocarpol

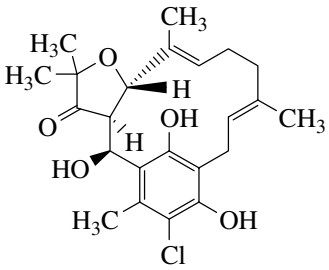

21 : Acremofuranone A

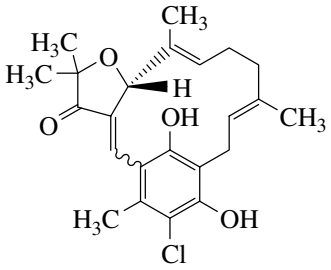

22 : Acremofuranone B

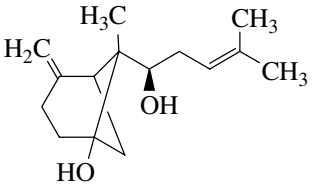

23 : Dihydroxybergamotene

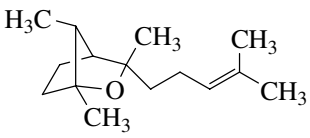

24 : Lignoren

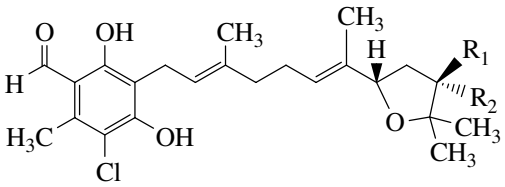

25 : $R_1 + R_2 = O$: Ascofuranone

26 : $R_1 = H$, $R_2 = OH$: Ascofuranol

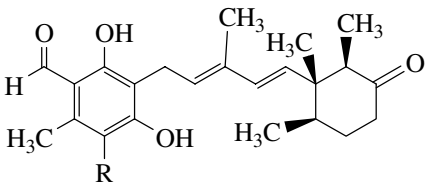

27 : R = Cl : Ascochlorin

28 : R = H : Cylindrol B

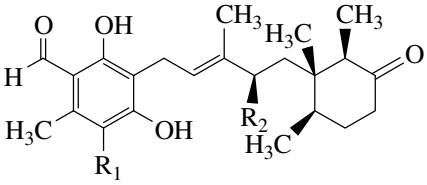

29 : $R_1 = Cl$, $R_2 = H$: Ilicicolin C

31 : $R_1 = Cl$, $R_2 = OH$

Deacetylchloronectrin

32 : $R_1 = H$, $R_2 = H$: LL-Z1272 ε

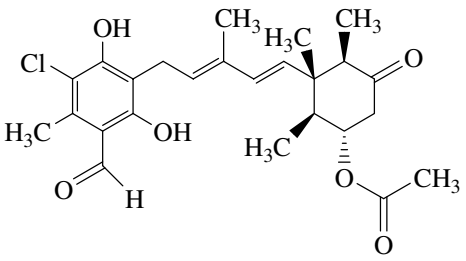

30 : Ilicicolin F

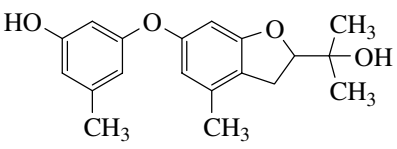

33 : Awajanoran

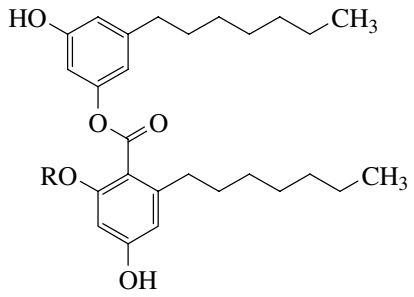

34 : R = 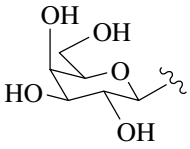

: 3-Heptyl-5-hydroxyphenyl 2-(*β*-D-galactopyranosyloxy)-6-heptyl-4-hydroxybenzoate

35 : R = 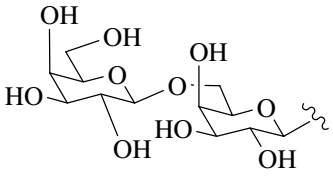

: 3-Heptyl-5-hydroxyphenyl 2-[(6-*O*-*β*-D-galactopyranosyl-*β*-D-galactopyranosyl)oxy]-6-heptyl-4-hydroxybenzoate

36 : R = H : KS-501a

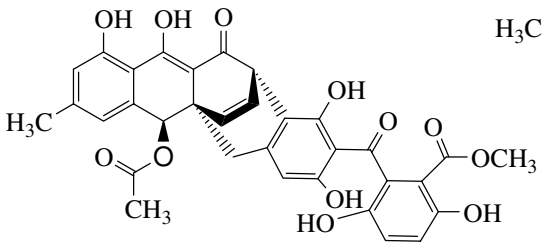

40 : Acremonidin A

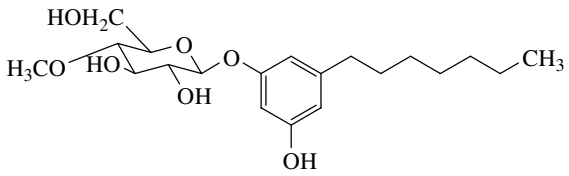

37 : 2-(3-Heptyl-5-hydroxybenzyl)-tetrahydro-6-(hydroxymethyl)-5-methoxy-2*H*-pyran-3,4-diol

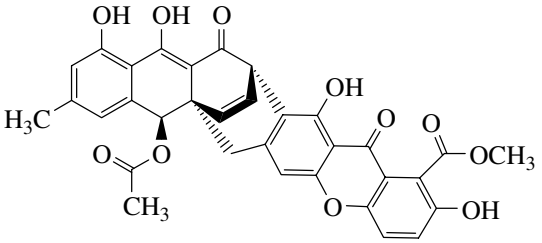

38 : Acremoxanthone A

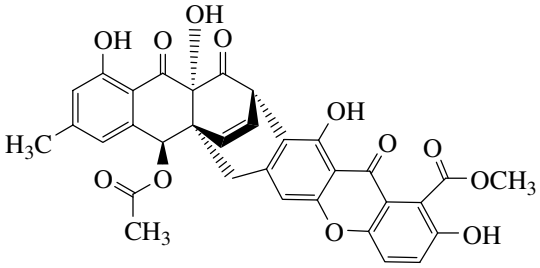

39 : Acremoxanthone B

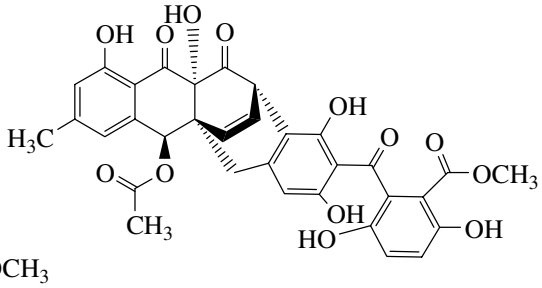

41 : Acremonidin C

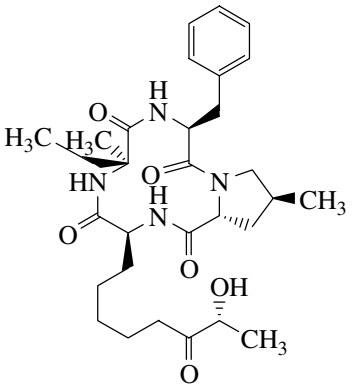

42 : FR235222

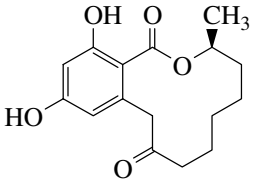

44 : Dihydroresorcylide

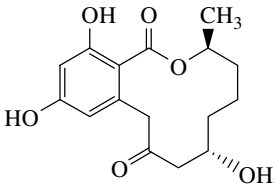

46 : *(S)*-7-Hydroxydihydro-resorcylide

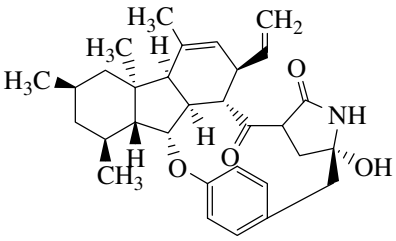

48 : Pyrrocidine B

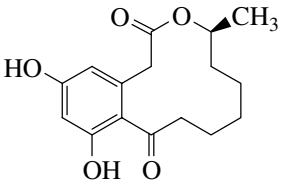

43 : Curvularin

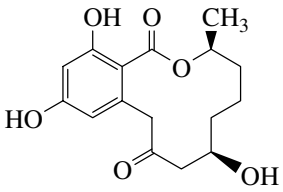

45 : (*R*)-7-Hydroxydihydroresorcylide

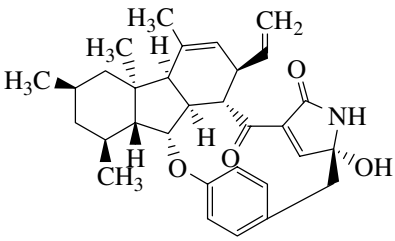

47 : Pyrrocidine A

1.1.2 The Objectives

1. To isolate the secondary metabolites from the mangrove-derived fungus *Pestalotiopsis* sp. PSU-MA92.
2. To elucidate the structures of the isolated compounds.

CHAPTER 1.2

EXPERIMENTAL

1.2.1 Instruments and chemicals

Infrared (IR) spectra were recorded using a Perkin-Elmer 783 FTS165 FT-IR spectrophotometer. Ultraviolet (UV) absorption spectra were measured on a SHIMADZU UV-160A and a SHIMADZU UV-1600 Series spectrophotometer. ^{1}H and ^{13}C NMR spectra were recorded on a 300 or a 500 MHz Bruker FTNMR Ultra Shield™ spectrometer using tetramethylsilane (TMS) as an internal standard. EIMS and HREIMS spectra were obtained on a MAT 95 XL Mass Spectrometer (Thermofinnigan). Optical rotation was measured in MeOH on a JASCO P-1020 polarimeter. Solvents for extraction and chromatography were distilled at their boiling point ranges prior to use except for analytical grade reagents. Thin-layer chromatography (TLC) and precoated TLC were performed on silica gel 60 GF_{254} (Merck). Column Chromatography (CC) was carried out on Sephadex LH-20, silica gel (Merck) type 60 (230-400 mesh ASTM) or type 100 (70-230 mesh ASTM), or reverse phase C_{18} silica gel.

1.2.2 Fermentation and extraction

The flask culture of the fungus PSU-MA70 (15 L) in potato dextrose broth was filtered to separate into the filtrate and wet mycelia. The filtrate was divided into 37 portions. Each portion was extracted twice with an equal amount of EtOAc (2 x 300 mL). The organic layer was dried over anhydrous Na_2SO_4 and evaporated *in vacuo* to obtain a dark brown gum (2.11 g).

1.2.3 Purification of the broth extract

The crude EtOAc extract was separated by dissolving with methanol to afford a methanol-soluble fraction (**70**) and a methanol-insoluble one (**70S**) as shown in **Table 2**.

Table 2 Fractions obtained from the crude EtOAc extract by dissolving with methanol

Fraction	Weight (g)	Physical appearance
70	1.2168	Brown gum
70S	0.8930	Colorless crystals

<u>Fraction 70S</u> (AR1) showed one UV-active spot on normal phase TLC using 5% methanol in dichloromethane as a mobile phase with the R_f value of 0.29.

m.p.	204-206 ^{0}C
$[\alpha]_D^{29}$	+90.4 (c = 0.2, MeOH)
UV λ_{max}(nm)(MeOH)(log ε)	208 (3.72)
FTIR(neat) : υ(cm^{-1})	3424 (O-H stretching), 1705 (C=O stretching)
^{1}H NMR(DMSO-d_6)(δ_{ppm}) : (300 MHz)	7.34 (*dd*, *J* = 15.6, 2.7 Hz, 1H), 5.71 (*dd, J* = 15.6, 1.8 Hz, 1H), 5.66 (*ddd*, *J* = 15.0, 10.2, 4.5 Hz, 1H), 5.20 (*dd*, *J* = 15.0, 9.6 Hz, 1H), 5.13 (*d*, *J* = 5.7 Hz, 1H), 4.70 (*sext*, *J* = 6.3 Hz, 1H), 4.51 (*d*, *J* = 3.9 Hz, 1H), 4.04 (*m*, 1H), 3.93 (*m*, 1H), 2.31 (*qn*, *J* = 8.1 Hz, 1H), 1.97 (*m*, 1H), 1.92 (*m*, 1H), 1.84 (*m*, 1H), 1.78 (*m*, 1H), 1.76 (*m*, 1H), 1.70 (*m*, 1H), 1.65 (*m*, 1H), 1.47 (*m*, 1H), 1.30 (*m*, 1H), 1.18 (*d*, *J* = 6.3 Hz, 3H), 0.74 (*m*, 1H)
^{13}C NMR(DMSO-d_6)(δ_{ppm}) : (75 MHz)	166.18, 154.83, 137.60, 129.71, 116.76, 74.83, 71.36, 71.00, 52.20, 43.82, 43.56,

	41.40, 33.91, 31.91, 26.91, 21.16
CH :	154.83, 137.60, 129.71, 116.76, 74.83, 71.36, 71.00, 52.20, 43.82
CH_2 :	43.56, 41.40, 33.91, 31.91, 26.91
CH_3 :	21.16

Fraction 70 was further separated by column chromatography over Sephadex LH-20. Elution was performed with 100% methanol. Fractions with the similar chromatogram were combined and evaporated to dryness under reduced pressure to afford seven fractions as shown in **Table 3**.

Table 3 Subfractions obtained from **Fraction 70** by column chromatography over Sephadex LH-20

Subfraction	Weight (mg)	Physical appearance
70A	111.5	Brown gum
70B	178.3	Brown gum
70C	794.7	Brown gum
70D	68.2	Brown gum
70E	48.7	Brown gum
70F	7.1	Brown gum
70G	8.3	Colorless crystals

Subfraction 70A did not show any UV-active spots on normal phase TLC using 3% methanol in dichloromethane but showed four spots after dipping the TLC plate in anisaldehyde reagent and subsequently heating with the R_f values of 0.13, 0.18, 0.53 and 0.58. It was further separated by column chromatography over silica gel. Elution was initially performed with 3% methanol in dichloromethane and gradually enriched with methanol until pure methanol. Fractions with the similar chromatogram were combined and evaporated to dryness under reduced pressure to afford four subfractions as shown in **Table 4**.

Table 4 Subfractions obtained from **subfraction 70A** by column chromatography over silica gel

Subfraction	Elution	Weight (mg)	Physical appearance
70A1	3% MeOH/CH_2Cl_2	30.8	Yellow solid
70A2	3% MeOH/CH_2Cl_2	25.8	Yellow gum
70A3	3-10% MeOH/CH_2Cl_2	4.9	Yellow gum
70A4	10% MeOH/CH_2Cl_2-100% MeOH	38.6	Yellow gum

Subfraction 70A1 showed three spots after dipping the TLC plate in anisaldehyde reagent and subsequently heating using 20% ethyl acetate in dichloromethane as a mobile phase (2 runs) with the R_f values of 0.25, 0.43 and 0.63. It was further separated by column chromatography over silica gel. Elution was initially performed with 40% ethyl acetate in dichloromethane and gradually enriched with ethyl acetate and then methanol until pure methanol. Fractions with the similar chromatogram were combined and evaporated to dryness under reduced pressure to afford five subfractions as shown in **Table 5**.

Table 5 Subfractions obtained from **subfraction 70A1** by column chromatography over silica gel

Subfraction	Elution	Weight (mg)	Physical appearance
70A11	20% EtOAc/CH_2Cl_2	3.5	Yellow gum
70A12	20% EtOAc/CH_2Cl_2	2.3	Yellow gum
70A13	20-50% EtOAc/CH_2Cl_2	5.0	Yellow gum
70A14	50-70% EtOAc/CH_2Cl_2	1.3	Yellow gum
70A15	100% EtOAc-100%MeOH	18.6	Yellow solid

Subfraction 70A11 showed two spots after dipping the TLC plate in anisaldehyde reagent and subsequently heating using 20% ethyl acetate in dichloromethane as a

mobile phase (2 runs) with the R_f values of 0.53 and 0.63. Its ^1H NMR spectrum indicated that the major compound was **AR5**. No further purification was carried out.

Subfraction 70A12 showed two spots after dipping the TLC plate in anisaldehyde reagent and subsequently heating using 20% ethyl acetate in dichloromethane as a mobile phase (2 runs) with the R_f values of 0.30 and 0.43. The ^1H NMR spectrum indicated the absence of olefinic and aromatic protons. Thus, it was not further investigated.

Subfraction 70A13 showed two spots after dipping the TLC plate in anisaldehyde reagent and subsequently heating using 20% ethyl acetate in dichloromethane as a mobile phase (2 runs) with the R_f values of 0.33 and 0.45. It was further separated by column chromatography over Sephadex LH-20. Elution was performed with 50% methanol in dichloromethane. Fractions with the similar chromatogram were combined and evaporated to dryness under reduced pressure to afford two subfractions as shown in **Table 6**.

Table 6 Subfractions obtained from **subfraction 70A13** by column chromatography over Sephadex LH-20

Subfraction	Weight (mg)	Physical appearance
70A131	2.0	Yellow gum
70A132	2.3	Colorless gum

Subfraction 70A131 showed three spots after dipping the TLC plate in anisaldehyde reagent and subsequently heating using 20% ethyl acetate in dichloromethane as a mobile phase (2 runs) with the R_f values of 0.28, 0.45 and 0.55. It was then purified by precoated TLC with 20% ethyl acetate in dichloromethane as a mobile phase to afford **AR3** as a white solid (1.2 mg). Its chromatogram showed one spot after dipping the TLC plate in anisaldehyde reagent and subsequently heating using 20% ethyl acetate in dichloromethane as a mobile phase (2 runs) with the R_f value of 0.44.

Subfraction 70A132 showed three spots after dipping the TLC plate in anisaldehyde reagent and subsequently heating using 20% ethyl acetate in dichloromethane as a mobile phase (2 runs) with the R_f values of 0.08, 0.20 and 0.30. The ^1H NMR spectrum displayed singnals in high field region. Thus, it was not investigated.

Subfraction 70A14 showed three spots after dipping the TLC plate in anisaldehyde reagent and subsequently heating using 20% ethyl acetate in dichloromethane as a mobile phase (2 runs) with the R_f values of 0.13, 0.20 and 0.30. Because of the minute quantity, it was not further investigated.

Subfraction 70A15 showed a long tail after dipping the TLC plate in anisaldehyde reagent and subsequently heating using 20% ethyl acetate in dichloromethane as a mobile phase (2 runs). It was further separated by column chromatography over Sephadex LH-20. Elution was performed with 50% methanol in dichloromethane. Fractions with the similar chromatogram were combined and evaporated to dryness under reduced pressure to afford two subfractions as shown in **Table 7**.

Table 7 Subfractions obtained from **subfraction 70A15** by column chromatography over Sephadex LH-20

Subfraction	Weight (mg)	Physical appearance
70A151	11.1	Yellow solid
70A152	7.4	Yellow gum

Subfraction 70A151 showed two spots after dipping the TLC plate in anisaldehyde reagent and subsequently heating using 2% methanol in dichloromethane as a mobile phase (2 runs) with the R_f values of 0.20 and 0.58. It was then purified by column chromatography over silica gel. Elution was initially performed with 2% methanol in dichloromethane and gradually enriched with methanol until pure methanol. Fractions with the similar chromatogram were combined and evaporated to dryness under reduced pressure to afford three subfractions as shown in **Table 8**.

Table 8 Subfractions obtained from **subfraction 70A151** by column chromatography over silica gel

Subfraction	Elution	Weight (mg)	Physical appearance
70A1511	2% MeOH/CH_2Cl_2	4.7	White solid
70A1512	2% MeOH/CH_2Cl_2	2.1	White solid
70A1513	3% MeOH/CH_2Cl_2-100% MeOH	2.8	Yellow gum

Subfraction 70A1511 (AR2) showed one spot after dipping the TLC plate in anisaldehyde reagent and subsequently heating using 2% methanol in dichloromethane as a mobile phase (2 runs) with the R_f value of 0.58.

m.p.	252-254 ^{0}C
$[\alpha]_D^{28}$	-40.2 (c = 0.8, $CHCl_3$)
UV λ_{max}(nm)(MeOH)(log ε)	203 (4.42)
FTIR(neat) : υ(cm^{-1})	3384 (O-H stretching), 3325 (N-H stretching), 1746 and 1640 (C=O stretching)
^{1}H NMR($CDCl_3$)(δ_{ppm})(300 MHz) :	8.22 (*d*, *J* = 8.7 Hz, 1H), 7.25 (*m*, 2H), 7.20 (*m*, 1H), 7.16 (*m*, 2H), 7.10 (*d*, *J* = 6.9 Hz, 1H), 5.76 (*dd*, *J* = 11.7, 5.1 Hz, 1H), 5.28 (*s*, 1H), 5.22 (*s*, 1H), 5.00 (*dd*, *J* = 8.7, 5.1 Hz, 1H), 4.96 (*m*, 1H), 4.86 (*qn*, *J* = 6.9 Hz, 1H), 3.70 (*q*, *J* = 6.9 Hz, 1H), 3.48 (*dd*, *J* = 15.3, 5.1 Hz, 1H), 3.20 (*s*, 3H), 2.92 (*s*, 3H), 2.91 (*dd*, *J* = 15.3, 11.7 Hz, 1H), 1.58 (*m*, 1H), 1.53 (*d*, *J* = 7.5 Hz, 3H), 1.52 (*d*, *J* = 6.9 Hz, 3H), 1.41 (*d*, *J* = 6.9 Hz, 3H), 1.25 (*s*, 3H), 1.17 (*s*, 3H), 1.12 (*m*, 1H), 0.97 (*ddd*, *J* = 14.1, 7.5, 5.1 Hz, 1H), 0.78 (*d*, *J* = 6.6 Hz, 3H), 0.72 (*d*, *J* = 6.6 Hz, 3H)
^{13}C NMR($CDCl_3$)(δ_{ppm})(75 MHz) :	172.60, 172.38, 171.39, 169.78, 168.95,

	168.50, 137.12, 128.63, 128.41, 126.60, 77.19, 71.77, 70.57, 60.53, 56.61, 47.10, 46.27, 38.83, 36.93, 33.18, 30.14, 26.75, 24.14, 23.85, 22.84, 22.24, 19.26, 18.10, 13.53
CH :	128.63, 128.41, 126.60, 77.19, 70.57, 60.53, 56.61, 47.10, 46.27, 23.85
CH_2 :	38.83, 33.18
CH_3 :	36.93, 30.14, 26.75, 24.14, 22.84, 22.24, 19.26, 18.10, 13.53

Subfraction 70A1512 showed three spots after dipping the TLC plate in anisaldehyde reagent and subsequently heating using 2% methanol in dichloromethane as a mobile phase (2 runs) with the R_f values of 0.30, 0.43 and 0.58. It contained **AR2** as a major component. No further purification was carried out.

Subfraction 70A1513 showed a long tail after dipping the TLC plate in anisaldehyde reagent and subsequently heating using 2% methanol in dichloromethane as a mobile phase (2 runs). The ^{1}H NMR spectrum indicated the absence of olefinic and aromatic protons. Thus, it was not further investigated.

Subfraction 70A152 showed a long tail after dipping the TLC plate in anisaldehyde reagent and subsequently heating using 20% ethyl acetate in dichloromethane as a mobile phase (3 runs). Because of the presence of broad signals in the ^{1}H NMR spectrum, it was not further investigated.

Subfraction 70A2 showed five spots after dipping the TLC plate in anisaldehyde reagent and subsequently heating using 95% ethyl acetate in petroleum ether as a mobile phase with the R_f values of 0.10, 0.30, 0.43, 0.63 and 0.70. It was further separated by flash column chromatography over silica gel. Elution was initially performed with 95% ethyl acetate in petroleum ether and gradually enriched with ethyl acetate and then methanol until pure methanol. Fractions with the similar

chromatogram were combined and evaporated to dryness under reduced pressure to afford four subfractions as shown in **Table 9**.

Table 9 Subfractions obtained from **subfraction 70A2** the by flash column chromatography over silica gel

Subfraction	Elution	Weight (mg)	Physical appearance
70A21	95% EtOAc/Petrol	2.2	Yellow gum
70A22	95% EtOAc/Petrol- 100% EtOAc	6.0	Yellow gum
70A23	100% EtOAc- 10% EtOAc/MeOH	5.5	Yellow gum
70A24	30% EtOAc/MeOH- 100% MeOH	11.9	Yellow gum

Subfraction 70A21 showed two spots after dipping the TLC plate in anisaldehyde reagent and subsequently heating using 95% ethyl acetate in petroleum ether as a mobile phase with the R_f values of 0.59 and 0.66. The ^{1}H NMR spectrum displayed singnals in the high field region. Thus, it was not investigated.

Subfraction 70A22 showed one UV-active spot on normal phase TLC using 95% ethyl acetate in petroleum ether as a mobile phase with the R_f value of 0.39. Its ^{1}H NMR spectrum indicated that the major compound was **AR1**. No further purification was carried out.

Subfraction 70A23 showed two spots after dipping the TLC plate in anisaldehyde reagent and subsequently heating using 95% ethyl acetate in petroleum ether as a mobile phase with the R_f values of 0.27 and 0.34. Because the ^{1}H NMR spectrum indicated the presence of many components, it was not further investigated.

Subfraction 70A24 showed a long tail after dipping the TLC plate in anisaldehyde reagent and subsequently heating using 95% ethyl acetate in petroleum ether as a

mobile phase. Because of the presence of broad signals in the ^{1}H NMR spectrum, it was not further investigated.

Subfraction 70A3 showed three spots after dipping the TLC plate in anisaldehyde reagent and subsequently heating using 5% methanol in dichloromethane as a mobile phase with the R_f values of 0.43, 0.50 and 0.65. Because the ^{1}H NMR spectrum indicated the presence of many components, it was not further investigated.

Subfraction 70A4 showed a long tail after dipping the TLC plate in anisaldehyde reagent and subsequently heating using 5% methanol in dichloromethane as a mobile phase. Because of the presence of broad signals in the ^{1}H NMR spectrum, it was not further investigated.

Subfraction 70B did not show any UV-active spots on normal phase TLC using 2% methanol in dichloromethane but showed four spots after dipping the TLC plate in anisaldehyde reagent and subsequently heating with the R_f values of 0.12, 0.32, 0.41 and 0.59. It was further separated by column chromatography over silica gel. Elution was initially performed with 2% methanol in dichloromethane and gradually enriched with methanol until pure methanol. Fractions with the similar chromatogram were combined and evaporated to dryness under reduced pressure to afford four subfractions as shown in **Table 10**.

Table 10 Subfractions obtained from **subfraction 70B** by column chromatography over silica gel

Subfraction	Elution	Weight (mg)	Physical appearance
70B1	2% MeOH/CH_2Cl_2	2.5	Yellow gum
70B2	2% MeOH/CH_2Cl_2	14.5	Yellow solid
70B3	3-10% MeOH/CH_2Cl_2	94.0	Yellow gum
70B4	30% MeOH/CH_2Cl_2-100% MeOH	55.8	Yellow gum

Subfraction 70B1 showed four spots after dipping the TLC plate in anisaldehyde reagent and subsequently heating using 2% methanol in dichloromethane as a mobile phase with the R_f values of 0.62, 0.69, 0.77 and 0.87. Because the ^1H NMR spectrum indicated the presence of many components, it was not further investigated.

Subfraction 70B2 showed a long tail after dipping the TLC plate in anisaldehyde reagent and subsequently heating using 2% methanol in dichloromethane as a mobile phase. It was further separated by column chromatography over Sephadex LH-20. Elution was performed with 50% methanol in dichloromethane. Fractions with the similar chromatogram were combined and evaporated to dryness under reduced pressure to afford three subfractions as shown in **Table 11**.

Table 11 Subfractions obtained from **subfraction 70B2** by column chromatography over Sephadex LH-20

Subfraction	Weight (mg)	Physical appearance
70B21	0.9	Yellow gum
70B22	8.5	White solid
70B23	4.7	Yellow solid

Subfraction 70B21 showed a long tail after dipping the TLC plate in anisaldehyde reagent and subsequently heating using 20% ethyl acetate in petroleum ether as a mobile phase. Because of the minute quantity, it was not further investigated.

Subfraction 70B22 (AR3) showed one spot after dipping the TLC plate in anisaldehyde reagent and subsequently heating using 20% ethyl acetate in dichloromethane as a mobile phase with the R_f value of 0.43.

m.p.	218-220 ^oC
$[\alpha]_D^{28}$	-16.7 (c = 0.9, $CHCl_3$)
UV λ_{max}(nm)(MeOH)(log ε)	203 (4.38)

FTIR(neat) : $\upsilon(cm^{-1})$	3345 (N-H stretching), 1744 and 1642 (C=O stretching)
^{1}H NMR($CDCl_3$)(δ_{ppm})(300 MHz) :	7.89 (*d*, *J* = 8.7 Hz, 1H), 7.22 (*m*, 2H), 7.18 (*m*, 1H), 7.16 (*m*, 2H), 7.13 (*d*, *J* = 6.9 Hz, 1H), 5.77 (*dd*, *J* = 11.4, 5.4 Hz, 1H), 5.23 (*d*, *J* = 2.4 Hz, 1H), 5.00 (*m*, 1H), 4.97 (*m*, 1H), 4.84 (*qn*, *J* = 6.9 Hz, 1H), 3.70 (*q*, *J* = 6.9 Hz, 1H), 3.47 (*dd*, *J* = 15.3, 5.4 Hz, 1H), 3.19 (*s*, 3H), 2.92 (*s*, 3H), 2.89 (*m*, 1H), 2.61 (*hept d*, *J* = 6.9, 2.4 Hz, 1H), 1.56 (*m*, 1H), 1.55 (*d*, *J* = 6.9 Hz, 3H), 1.51 (*d*, *J* = 7.2 Hz, 3H), 1.42 (*d*, *J* = 6.9 Hz, 3H), 1.17 (*hept*, *J* = 6.6 Hz, 1H), 0.98 (*m*, 1H), 0.93 (*d*, *J* = 6.9 Hz, 3H), 0.92 (*d*, *J* = 6.9 Hz, 3H), 0.78 (*d*, *J* = 6.6 Hz, 3H), 0.72 (*d*, *J* = 6.6 Hz, 3H)
^{13}C NMR($CDCl_3$)(δ_{ppm})(75 MHz) :	172.46, 172.95, 171.18, 169.68, 168.56, 168.52, 137.15, 128.64, 128.40, 126.58, 78.03, 70.34, 60.68, 56.53, 47.03, 46.34, 38.81, 36.87, 33.17, 30.12, 29.98, 23.84, 22.87, 22.20, 19.32, 19.19, 18.05, 15.84, 13.62
CH :	128.64, 128.40, 126.58, 78.03, 70.34, 60.68, 56.53, 47.03, 46.34, 29.98, 23.84
CH_2 :	38.81, 33.17
CH_3 :	36.87, 30.12, 22.87, 22.20, 19.32, 19.19, 18.05, 15.84, 13.62

Subfraction 70B23 showed three spots after dipping the TLC plate in anisaldehyde reagent and subsequently heating using 20% ethyl acetate in dichloromethane as a mobile phase with the R_f values of 0.40, 0.48 and 0.58. It contained **AR5** and **AR6** as major components. No further purification was carried out.

Subfraction 70B3 showed four spots after dipping the TLC plate in anisaldehyde reagent and subsequently heating using 50% acetone in petroleum ether as a mobile phase with the R_f values of 0.21, 0.40, 0.55 and 0.67. It was then purified by flash column chromatography over silica gel. Elution was initially performed with 50% acetone in petroleum ether and gradually enriched with acetone until pure acetone. Fractions with the similar chromatogram were combined and evaporated to dryness under reduced pressure to afford three subfractions as shown in **Table 12**.

Table 12 Subfractions obtained from **subfraction 70B3** by flash column chromatography over silica gel

Subfraction	Elution	Weight (mg)	Physical appearance
70B31	50% Acetone/Petrol	26.2	Yellow gum
70B32	50% Acetone/Petrol	23.9	Yellow gum
70B33	60% Acetone/Petrol-100% Acetone	36.2	Yellow gum

Subfraction 70B31 showed a long tail after dipping the TLC plate in anisaldehyde reagent and subsequently heating using 50% acetone in petroleum ether as a mobile phase. It was further separated by column chromatography over Sephadex LH-20. Elution was performed with 50% methanol in dichloromethane. Fractions with the similar chromatogram were combined and evaporated to dryness under reduced pressure to afford two subfractions as shown in **Table 13**.

Table 13 Subfractions obtained from **subfraction 70B31** by column chromatography over Sephadex LH-20

Subfraction	Weight (mg)	Physical appearance
70B311	13.2	Yellow gum
70B312	13.0	Yellow gum

Subfraction 70B311 showed two spots after dipping the TLC plate in anisaldehyde reagent and subsequently heating using 80% ethyl acetate in petroleum ether as a mobile phase (2 runs) with the R_f values of 0.50 and 0.55. Because of the presence of broad signals in the ^{1}H NMR spectrum, it was not further investigated.

Subfraction 70B312 showed two spots after dipping the TLC plate in anisaldehyde reagent and subsequently heating using 80% ethyl acetate in petroleum ether as a mobile phase (2 runs) with the R_f values of 0.38 and 0.50. It contained **AR1** as a major component. No further purification was carried out.

Subfraction 70B32 showed two spots after dipping the TLC plate in anisaldehyde reagent and subsequently heating using 50% acetone in petroleum ether as a mobile phase with the R_f values of 0.40 and 0.53. It contained **AR1** as a major component. No further purification was carried out.

Subfraction 70B33 showed a long tail after dipping the TLC plate in anisaldehyde reagent and subsequently heating using 50% acetone in petroleum ether as a mobile phase. Because of the presence of broad signals in the ^{1}H NMR spectrum, it was not further investigated.

Subfraction 70B4 showed a long tail after dipping the TLC plate in anisaldehyde reagent and subsequently heating using 2% methanol in dichloromethane as a mobile phase. Because of the presence of broad signals in the ^{1}H NMR spectrum, it was not further investigated.

Subfraction 70C showed six UV-active spots on normal phase TLC using 1% methanol in dichloromethane as a mobile phase with the R_f values of 0.12, 0.17, 0.24, 0.37, 0.56 and 0.85. It was further separated by column chromatography over silica gel. Elution was initially performed with 1% methanol in dichloromethane and gradually enriched with methanol until pure methanol. Fractions with the similar chromatogram were combined and evaporated to dryness under reduced pressure to afford seven subfractions as shown in **Table 14**.

Table 14 Subfractions obtained from **subfraction 70C** by column chromatography over silica gel

Subfraction	Elution	Weight (mg)	Physical appearance
70C1	1% MeOH/CH_2Cl_2	1.9	Yellow gum
70C2	1% MeOH/CH_2Cl_2	5.5	Yellow gum
70C3	1% MeOH/CH_2Cl_2	21.0	Yellow gum
70C4	1-2% MeOH/CH_2Cl_2	156.4	Yellow solid
70C5	2-3% MeOH/CH_2Cl_2	28.0	Brown gum
70C6	3-30% MeOH/CH_2Cl_2	258.6	Brown gum
70C7	30% MeOH/CH_2Cl_2-100% MeOH	294.7	Brown gum

Subfraction 70C1 showed three UV-active spots on normal phase TLC using 40% hexane in dichloromethane as a mobile phase (2 runs) with the R_f values of 0.30, 0.45 and 0.63. The ^1H NMR spectrum indicated the presence of many components. Because of the minute quantity, it was not further investigated.

Subfraction 70C2 showed three UV-active spots on normal phase TLC using 40% hexane in dichloromethane as a mobile phase (2 runs) with the R_f values of 0.30, 0.35 and 0.50. It contained **AR16** as a major component. No further purification was carried out.

Subfraction 70C3 showed five UV-active spots on normal phase TLC with a mixture of ethyl acetate, dichloromethane and petroleum ether in a ratio of 1:3:6 as a mobile phase with the R_f values of 0.20, 0.38, 0.50, 0.67 and 0.76. It was further separated by column chromatography over silica gel. Elution was performed with above mixture. Fractions with the similar chromatogram were combined and evaporated to dryness under reduced pressure to afford three subfractions as shown in **Table 15**.

Table 15 Subfractions obtained from **subfraction 70C3** by column chromatography over silica gel

Subfraction	Weight (mg)	Physical appearance
70C31	2.9	Yellow gum
70C32	13.2	Yellow gum
70C33	4.8	Yellow gum

Subfraction 70C31 showed a long tail under UV-S on normal phase TLC with a mixture of ethyl acetate, dichloromethane and petroleum ether in a ratio of 1:2:7 as a mobile phase (3 runs). Because the ^{1}H NMR spectrum indicated the presence of many components, it was not further investigated.

Subfraction 70C32 showed three UV-active spots on normal phase with a mixture of ethyl acetate, dichloromethane and petroleum ether in a ratio of 1:2:7 as a mobile phase (3 runs) with the R_f values of 0.33, 0.45 and 0.69. It was further separated by column chromatography over silica gel. Elution was performed with above mixture. Fractions with the similar chromatogram were combined and evaporated to dryness under reduced pressure to afford three subfractions as shown in **Table 16**.

Table 16 Subfractions obtained from **subfraction 70C32** by column chromatography over silica gel

Subfraction	Weight (mg)	Physical appearance
70C321	1.3	Yellow gum
70C322	4.0	Colorless gum
70C323	7.7	Yellow gum

Subfraction 70C321 showed a long tail under UV-S on normal phase TLC with a mixture of ethyl acetate, dichloromethane and petroleum ether in a ratio of 1:2:7 as a mobile phase. Because of the minute quantity, it was not further investigated.

Subfraction 70C322 (AR4) showed one UV-active spot on normal phase TLC with a mixture of ethyl acetate, dichloromethane and petroleum ether in a ratio of 1:2:7 as a mobile phase with the R_f value of 0.39.

$[\alpha]_D^{30}$	-12.8 (c = 1.4, $CHCl_3$)
UV λ_{max}(nm)(MeOH)(log ε)	212 (3.54)
FTIR(neat) : υ(cm^{-1})	1715 (C=O stretching)
^{1}H NMR($CDCl_3$)(δ_{ppm})(300 MHz) :	6.35 (*dq*, *J* = 9.9, 7.2 Hz, 1H), 5.83 (*dq*, *J* = 9.9, 1.8 Hz, 1H), 5.63 (*dd*, *J* = 7.8, 3.6 Hz, 1H), 5.42 (*dd*, *J* = 5.4, 1.2 Hz, 1H), 3.83 (*d*, *J* = 5.1 Hz, 1H), 3.63 (*d*, *J* = 5.4 Hz, 1H), 3.12 (*d*, *J* = 4.2 Hz, 1H), 2.83 (*d*, *J* = 4.2 Hz, 1H), 2.56 (*dd*, *J* = 15.6, 7.8 Hz, 1H), 2.16 (*dd*, *J* = 7.2, 1.8 Hz, 3H), 2.03 (*ddd*, *J* = 15.6, 5.1, 3.6 Hz, 1H), 2.02 (*m*, 1H), 1.99 (*m*, 1H), 1.92 (*m*, 1H), 1.72 (*s*, 3H), 1.42 (*m*, 1H), 0.96 (*s*, 3H), 0.73 (*s*, 3H)
^{13}C NMR($CDCl_3$)(δ_{ppm})(75 MHz) :	166.37, 145.46, 140.18, 120.70, 118.70, 79.21, 74.52, 70.58, 65.58, 49.03, 47.85, 40.47, 36.85, 28.03, 24.50, 23.23, 16.04, 15.44, 5.97
CH :	145.46, 120.70, 118.70, 79.21, 74.52, 70.58
CH_2 :	47.85, 36.85, 28.03, 24.50
CH_3 :	23.23, 16.04, 15.44, 5.97

Subfraction 70C323 showed two UV-active spots on normal phase TLC with a mixture of ethyl acetate, dichloromethane and petroleum ether in a ratio of 1:2:7 as a mobile phase with the R_f values of 0.34 and 0.39. It contained **AR4** as a major component. No further purification was carried out.

Subfraction 70C33 showed four UV-active spots on normal phase TLC with a mixture of ethyl acetate, dichloromethane and petroleum ether in a ratio of 1:2:7 as a mobile phase (3 runs) with the R_f values of 0.24, 0.33, 0.38 and 0.50. Because the ^1H NMR spectrum indicated the presence of many components, it was not further investigated.

Subfraction 70C4 showed a long tail under UV-S on normal phase TLC using 40% hexane in dichloromethane as a mobile phase (2 runs). It was further separated by column chromatography over Sephadex LH-20. Elution was performed with 50% methanol in dichloromethane. Fractions with the similar chromatogram were combined and evaporated to dryness under reduced pressure to afford four subfractions as shown in **Table 17**.

Table 17 Subfractions obtained from **subfraction 70C4** by column chromatography over Sephadex LH-20

Subfraction	Weight (mg)	Physical appearance
70C41	2.9	Yellow gum
70C42	90.4	Yellow gum
70C43	60.4	Yellow gum
70C44	2.3	Yellow gum

Subfraction 70C41 showed a long tail after dipping the TLC plate in anisaldehyde reagent and subsequently heating using 2% methanol in dichloromethane as a mobile phase. The ^1H NMR spectrum displayed singnals in the high field region. Thus, it was not investigated.

Subfraction 70C42 showed six UV-active spots on normal phase TLC with a mixture of ethyl acetate, dichloromethane and petroleum ether in a ratio of 2:3:5 as a mobile phase with the R_f values of 0.10, 0.22, 0.34, 0.51, 0.63 and 0.71. It was further separated by column chromatography over silica gel. Elution was performed with above mixture. Fractions with the similar chromatogram were combined and

evaporated to dryness under reduced pressure to afford five subfractions as shown in **Table 18**.

Table 18 Subfractions obtained from **subfraction 70C42** by column chromatography over silica gel

Subfraction	Weight (mg)	Physical appearance
70C421	4.9	Yellow gum
70C422	37.7	Yellow solid
70C423	10.0	Yellow gum
70C424	30.9	Yellow solid
70C425	6.8	Yellow gum

Subfraction 70C421 showed two UV-active spots on normal phase TLC with a mixture of ethyl acetate, dichloromethane and petroleum ether in a ratio of 2:3:5 as a mobile phase with the R_f values of 0.76 and 0.85. It contained **AR4** as a major component. No further purification was carried out.

Subfraction 70C422 showed three UV-active spots on normal phase TLC using 20% ethyl acetate in petroleum ether as a mobile phase (2 runs) with the R_f values of 0.23, 0.43 and 0.58. It was further separated by column chromatography over silica gel. Elution was initially performed with 20% ethyl acetate in petroleum ether and gradually enriched with ethyl acetate and then methanol until pure methanol. Fractions with the similar chromatogram were combined and evaporated to dryness under reduced pressure to afford three subfractions as shown in **Table 19**.

Table 19 Subfractions obtained from **subfraction 70C422** by column chromatography over silica gel

Subfraction	Elution	Weight (mg)	Physical appearance
70C4221	20% EtOAc/Petrol	17.0	White solid
70C4222	40-60% EtOAc/Petrol	10.6	White solid

Table 19 Continued

Subfraction	Elution	Weight (mg)	Physical appearance
70C4223	60% EtOAc/Petrol-100%MeOH	8.3	Yellow gum

Subfraction 70C4221 (AR5) showed one UV-active spot on normal phase TLC using 20% ethyl acetate in petroleum ether as a mobile phase (2 runs) with the R_f value of 0.56.

m.p.	90-92 ^{0}C
$[\alpha]_D^{22}$	+12.5 (c = 1.4, $CHCl_3$)
UV λ_{max}(nm)(MeOH)(log ε)	209 (3.52), 261 (2.11)
FTIR(neat) : υ(cm^{-1})	3296 (O-H stretching)
^{1}H NMR($CDCl_3$)(δ_{ppm})(300 MHz) :	7.33 (*d*, *J* = 6.6 Hz, 2H), 7.26 (*d*, *J* = 6.6 Hz, 2H), 7.23 (*t*, *J* = 6.6 Hz, 1H), 3.91 (*dd*, *J* = 8.1, 2.0 Hz, 1H), 3.52 (*dd*, *J* = 8.1, 2.0 Hz, 1H), 2.91 (*dd*, *J* = 13.8, 2.4 Hz, 1H), 2.70 (*dd*, *J* = 13.8, 8.1 Hz, 1H), 2.26 (*brs*, 1H), 2.23 (*brs*, 1H), 1.90 (*m*, 1H), 1.62 (*m*, 1H), 1.24 (*m*, 1H), 0.97 (*d*, *J* = 6.9 Hz, 3H), 0.95 (*d*, *J* = 7.2 Hz, 3H)
^{13}C NMR($CDCl_3$)(δ_{ppm})(75 MHz) :	138.59, 129.46, 128.75, 126.60, 77.74, 73.11, 36.51, 36.24, 24.94, 14.80, 10.84
CH :	129.46, 128.75, 126.60, 73.11, 77.74, 36.24
CH_2 :	36.51, 24.94
CH_3 :	14.80, 10.84

Subfraction 70C4222 showed two UV-active spots on normal phase TLC using 20% ethyl acetate in petroleum ether as a mobile phase (2 runs) with the R_f values of 0.48.

and 0.56. It contained **AR6** as a major component. No further purification was carried out.

Subfraction 70C4223 showed six UV-active spots on normal phase TLC using 20% ethyl acetate in petroleum ether as a mobile phase (2 runs) with the R_f values of 0.10, 0.22, 0.29, 0.39, 0.41 and 0.48. Because the ^{1}H NMR spectrum indicated the presence of many components, it was not further investigated.

Subfraction 70C423 contained many spots on TLC without major components. No further separation was conducted.

Subfraction 70C424 showed two UV-active spots on normal phase TLC with a mixture of ethyl acetate, dichloromethane and petroleum ether in a ratio of 2:3:5 as a mobile phase with the R_f values of 0.24 and 0.34. It contained **AR7** and **AR9** as major components. No further purification was carried out.

Subfraction 70C425 showed a long tail under UV-S on normal phase TLC with a mixture of ethyl acetate, dichloromethane and petroleum ether in a ratio of 2:3:5 as a mobile phase. Because the ^{1}H NMR spectrum indicated the presence of many components, it was not further investigated.

Subfraction 70C43 showed five UV-active spots on normal phase TLC using 20% acetone in hexane as a mobile phase with the R_f values of 0.10, 0.28, 0.38, 0.48 and 0.58. It was further separated by column chromatography over silica gel. Elution was performed with 20% acetone in hexane and gradually enriched with acetone until pure acetone. Fractions with the similar chromatogram were combined and evaporated to dryness under reduced pressure to afford four subfractions as shown in **Table 20**.

Table 20 Subfractions obtained from **subfraction 70C43** by column chromatography over silica gel

Subfraction	Elution	Weight (mg)	Physical appearance
70C431	20% Acetone/Hexane	3.5	White solid
70C432	20% Acetone/Hexane	39.7	White solid
70C433	20% Acetone/Hexane	10.6	White solid
70C434	20% Acetone/Hexane-100% Acetone	6.3	Yellow gum

Subfraction 70C431 showed one UV-active spot on normal phase TLC using 20% acetone in hexane as a mobile phase with the R_f value of 0.59. The ^{1}H NMR spectrum indicated that it was **AR5**.

Subfraction 70C432 showed two UV-active spots on normal phase TLC using 2% acetone in dichloromethane as a mobile phase with the R_f values of 0.53 and 0.63. It was further separated by column chromatography over silica gel. Elution was performed with 2% acetone in dichloromethane and gradually enriched with acetone until pure acetone. Fractions with the similar chromatogram were combined and evaporated to dryness under reduced pressure to afford four subfractions as shown in **Table 21**.

Table 21 Subfractions obtained from **subfraction 70C432** by column chromatography over silica gel

Subfraction	Elution	Weight (mg)	Physical appearance
70C4321	2% Acetone/CH_2Cl_2	10.3	White solid
70C4322	2-10% Acetone/CH_2Cl_2	27.1	White solid
70C4323	30-70% Acetone/CH_2Cl_2	3.9	White solid
70C4324	70% Acetone/CH_2Cl_2 - 100% Acetone	3.9	Yellow gum

Subfraction 70C4321 showed one UV-active spot on normal phase TLC using 2% acetone in dichloromethane as a mobile phase with the R_f value of 0.35. The ^1H NMR spectrum indicated that it was **AR5**.

Subfraction 70C4322 showed two UV-active spots on normal phase TLC using 2% acetone in dichloromethane as a mobile phase with the R_f values of 0.35 and 0.45. It was further separated by column chromatography over silica gel. Elution was performed with 2% acetone in dichloromethane and gradually enriched with acetone until pure acetone. Fractions with the similar chromatogram were combined and evaporated to dryness under reduced pressure to afford three subfractions as shown in **Table 22**.

Table 22 Subfractions obtained from **subfraction 70C4322** by column chromatography over silica gel

Subfraction	Elution	Weight (mg)	Physical appearance
70C43221	2% Acetone/CH_2Cl_2	8.3	White solid
70C43222	2-10% Acetone/CH_2Cl_2	16.5	White solid
70C43223	70% Acetone/CH_2Cl_2 - 100% Acetone	1.4	White solid

Subfraction 70C43221 showed one UV-active spot on normal phase TLC using 2% acetone in dichloromethane as a mobile phase with the R_f value of 0.35. The ^1H NMR spectrum indicated that it was **AR5**.

Subfraction 70C43222 showed two UV-active spots on normal phase TLC using 2% acetone in dichloromethane as a mobile phase with the R_f values of 0.30 and 0.35. The ^1H NMR spectrum indicated that it was **AR5** and **AR6**. No further separation was conducted.

Subfraction 70C43223 showed one UV-active spot on normal phase TLC using 2% acetone in dichloromethane as a mobile phase with the R_f value of 0.30. The ^1H NMR spectrum indicated that it was **AR6**.

Subfraction 70C4323 showed two UV-active spots on normal phase TLC using 2% acetone in dichloromethane as a mobile phase with the R_f values of 0.35 and 0.30. It was then purified by precoated TLC with 2% acetone in dichloromethane as a mobile phase (5 runs) to afford **AR6** as a white solid (2.5 mg). Its chromatogram showed one UV-active spot on normal phase TLC using 2% acetone in dichloromethane as a mobile phase with the R_f value of 0.30.

m.p.	87-89 ^{0}C
$[\alpha]_D^{22}$	+16.0 (c = 1.4, $CHCl_3$)
UV λ_{max}(nm)(MeOH)(log ε)	205 (3.54)
FTIR(neat) : υ(cm^{-1})	3283 (O-H stretching)
^1H NMR($CDCl_3$)(δ_{ppm})(300 MHz) :	7.34 (*t*, *J* = 6.3 Hz, 2H), 7.26 (*d*, *J* = 6.3 Hz, 2H), 7.24 (*t*, *J* = 6.3 Hz, 1H), 3.89 (*ddd*, *J* = 10.2, 4.5, 3.0 Hz, 1H), 3.42 (*dd*, *J* = 7.2, 4.5 Hz, 1H), 2.96 (*dd*, *J* = 13.8, 3.0 Hz, 1H), 2.71 (*dd*, *J* = 13.8, 10.2 Hz, 1H), 2.10 (*brs*, 1H), 2.09 (*brs*, 1H), 1.89 (*sext*, *J* = 7.2 Hz, 1H), 1.05 (*d*, *J* = 7.2 Hz, 3H), 0.98 (*d*, *J* = 7.2 Hz, 3H)
^{13}C NMR($CDCl_3$)(δ_{ppm})(75 MHz) :	138.48, 129.44, 128.74, 126.61, 79.05, 73.16, 37.20, 29.70, 18.98, 18.31
CH :	129.44, 128.74, 126.61, 79.05, 73.16, 29.70
CH_2 :	37.20
CH_3 :	18.98, 18.31

Subfraction 70C4324 showed two UV-active spots on normal phase TLC using 2% acetone in dichloromethane as a mobile phase with the R_f values of 0.18 and 0.26.

Its ^{1}H NMR spectrum indicated the presence of many components. Thus, it was not further investigated.

Subfraction 70C433 showed three UV-active spots on normal phase TLC using 20% acetone in hexane as a mobile phase with the R_f values of 0.28, 0.50 and 0.59. The ^{1}H NMR spectrum indicated that it was **AR5** and **AR6**. No further separation was conducted.

Subfraction 70C434 showed four UV-active spots on normal phase TLC using 20% acetone in hexane as a mobile phase with the R_f values of 0.10, 0.18, 0.26 and 0.38. Its ^{1}H NMR spectrum indicated the presence of many components. Thus, it was not further investigated.

Subfraction 70C44 showed three UV-active spots on normal phase TLC using 2% methanol in dichloromethane as a mobile phase with the R_f values of 0.19, 0.50 and 0.57. Because of the low quantity, it was not further investigated.

Subfraction 70C5 showed four UV-active spots on normal phase TLC using 10% ethyl acetate in dichloromethane as a mobile phase (2 runs) with the R_f values of 0.26, 0.38, 0.48 and 0.60. It was further separated by column chromatography over silica gel. Elution was performed with 10% ethyl acetate in dichloromethane and gradually enriched with ethyl acetate and then methanol until pure methanol. Fractions with the similar chromatogram were combined and evaporated to dryness under reduced pressure to afford three subfractions as shown in **Table 23**.

Table 23 Subfractions obtained from **subfraction 70C5** by column chromatography over silica gel

Subfraction	Elution	Weight (mg)	Physical appearance
70C51	10% EtOAc/CH_2Cl_2	4.6	Yellow gum
70C52	10-30% EtOAc/CH_2Cl_2	15.1	Yellow gum

Table 23 Continued

Subfraction	Elution	Weight (mg)	Physical appearance
70C53	30% EtOAc/CH_2Cl_2 - 100% MoOH	8.1	Yellow gum

Subfraction 70C51 showed five UV-active spots on normal phase TLC using 15% ethyl acetate in petroleum ether as a mobile phase (2 runs) with the R_f values of 0.24, 0.41, 0.46, 0.54 and 0.80. Its ^1H NMR spectrum indicated the presence of many components. Thus, it was not further investigated.

Subfraction 70C52 showed five UV-active spots on normal phase TLC using 30% ethyl acetate in petroleum ether as a mobile phase (5 runs) with the R_f values of 0.18, 0.33, 0.40, 0.55 and 0.58. It was further separated by column chromatography over silica gel. Elution was initially performed with 30% ethyl acetate in petroleum ether and gradually enriched with ethyl acetate and then methanol until pure methanol. Fractions with the similar chromatogram were combined and evaporated to dryness under reduced pressure to afford three subfractions as shown in **Table 24**.

Table 24 Subfractions obtained from **subfraction 70C52** by column chromatography over silica gel

Subfraction	Elution	Weight (mg)	Physical appearance
70C521	30% EtOAc/Petrol	4.0	Yellow gum
70C522	30% EtOAc/Petrol	6.1	Colorless gum
70C523	30% EtOAc/Petrol-100%MeOH	5.0	Yellow gum

Subfraction 70C521 showed four UV-active spots on normal phase TLC using 30% ethyl acetate in petroleum ether as a mobile phase (5 runs) with the R_f values of 0.54, 0.63, 0.71 and 0.76. It contained **AR7** as a major component. No further purification was carried out.

Subfraction 70C522 (AR7) showed one UV-active spot on normal phase TLC using 30% ethyl acetate in petroleum ether as a mobile phase (5 runs) with the R_f value of 0.54.

$[\alpha]_D^{25}$	-31.4 (c = 1.1, $CHCl_3$)
UV λ_{max}(nm)(MeOH)(log ε)	224 (3.06)
FTIR(neat) : υ(cm^{-1})	3448 (O-H stretching)
^{1}H NMR($CDCl_3$)(δ_{ppm})(300 MHz) :	5.38 (*brd*, *J* = 5.4 Hz, 1H), 4.33 (*brs*, 1H), 3.82 (*d*, *J* = 5.4 Hz, 1H), 3.50 (*d*, *J* = 5.4 Hz, 1H), 3.10 (*d*, *J* = 3.9 Hz, 1H), 2.81 (*d*, *J* = 3.9 Hz, 1H), 2.61 (*dd*, *J* = 15.6, 7.5 Hz, 1H), 2.00 (*m*, 1H), 1.97 (*m*, 1H), 1.93 (*m*, 1H), 1.88 (*m*, 1H), 1.70 (*s*, 3H), 1.44 (*m*, 1H), 0.85 (*s*, 3H), 0.80 (*s*, 3H)
^{13}C NMR($CDCl_3$)(δ_{ppm})(75 MHz) :	140.14, 118.71, 78.72, 74.05, 70.26, 65.73, 49.12, 47.56, 40.15, 39.78, 27.99, 24.41, 23.22, 15.80, 6.20
CH :	118.71, 78.72, 74.05, 70.26
CH_2 :	47.56, 40.15, 27.99, 24.41
CH_3 :	23.22, 15.80, 6.20

Subfraction 70C523 showed four UV-active spots on normal phase TLC using 30% ethyl acetate in petroleum ether as a mobile phase (5 runs) with the R_f values of 0.14, 0.20, 0.32 and 0.39. Its ^{1}H NMR spectrum indicated the presence of many components. Thus, it was not further investigated.

Subfraction 70C53 contained many spots on TLC without major components. No further separation was conducted.

Subfraction 70C6 showed six UV-active spots on normal phase TLC using 40% acetone in hexane as a mobile phase (2 runs) with the R_f values of 0.18, 0.28, 0.33,

0.40, 0.50 and 0.63. It was further separated by column chromatography over silica gel. Elution was performed with 40% acetone in hexane and gradually enriched with acetone until pure acetone. Fractions with the similar chromatogram were combined and evaporated to dryness under reduced pressure to afford four subfractions as shown in **Table 25**.

Table 25 Subfractions obtained from **subfraction 70C6** by column chromatography over silica gel

Subfraction	Elution	Weight (mg)	Physical appearance
70C61	40% Acetone/Hexane	18.2	Yellow gum
70C62	40-50% Acetone/Hexane	115.0	Yellow gum
70C63	50-60% Acetone/Hexane	41.9	Yellow gum
70C64	70% Acetone/Hexane-100% Acetone	82.8	Brown gum

Subfraction 70C61 showed three UV-active spots on normal phase TLC using 40% acetone in hexane as a mobile phase with the R_f values of 0.43, 0.48 and 0.65. Because of the presence of broad signals in the ^1H NMR spectrum, it was not further investigated.

Subfraction 70C62 showed three UV-active spots on reverse phase TLC using 60% methanol in water as a mobile phase with the R_f values of 0.33, 0.48 and 0.70. It was further separated by column chromatography over reverse phase silica gel. Elution was initially performed with 60% methanol in water, followed by reducing the polarity with methanol until pure methanol. Fractions with the similar chromatogram were combined and evaporated to dryness under reduced pressure to afford seven subfractions as shown in **Table 26**.

Table 26 Subfractions obtained from **subfraction 70C62** by column chromatography over reverse phase silica gel

Subfraction	Elution	Weight (mg)	Physical appearance
70C621	60% MeOH/H_2O	13.9	Yellow gum
70C622	60% MeOH/H_2O	7.6	Yellow gum
70C623	60% MeOH/H_2O	8.2	Yellow gum
70C624	60% MeOH/H_2O	43.5	Yellow solid
70C625	60% MeOH/H_2O	7.4	Yellow gum
70C626	60-80% MeOH/H_2O	24.5	Yellow solid
70C627	80% MeOH/H_2O-100% MeOH	9.6	Yellow gum

Subfraction 70C621 showed three UV-active spots on normal phase TLC using 40% ethyl acetate in petroleum ether as a mobile phase (5 runs) with the R_f values of 0.23, 0.38 and 0.68. It contained **AR30** as a major component. No further purification was carried out.

Subfraction 70C622 showed four UV-active spots on normal phase TLC using 40% ethyl acetate in petroleum ether as a mobile phase (5 runs) with the R_f values of 0.20, 0.37, 0.49 and 0.63. It was then purified by precoated TLC with 40% ethyl acetate in petroleum ether as a mobile phase (5 runs) to afford **AR8** as a white solid (3.1 mg). Its chromatogram showed one UV-active spot on normal phase TLC using 40% ethyl acetate in petroleum ether as a mobile phase (5 runs) with the R_f value of 0.48.

m.p.	151-153 ^{0}C
$[\alpha]_D^{25}$	-21.5 (c = 1.0, $CHCl_3$)
UV λ_{max}(nm)(MeOH)(log ε)	214 (3.57), 221 (3.59), 259 (3.32), 301 (3.13)
FTIR(neat) : υ(cm^{-1})	3352 (O-H stretching), 1738 (C=O stretching)
^{1}H NMR($CDCl_3$)(δ_{ppm})(300 MHz) :	6.38 (*s*, 1H), 3.92 (*s*, 3H), 3.90 (*s*, 3H), 2.18

	(*s*, 3H), 1.79 (*s*, 3H), 1.60 (*brs*, 1H)
^{13}C NMR($CDCl_3$)(δ_{ppm})(75 MHz) :	166.01, 164.84, 157.79, 150.14, 113.90, 105.37, 95.61, 56.18, 56.09, 25.50, 10.04
CH :	95.61
CH_3 :	56.18, 56.09, 25.50, 10.04

Subfraction 70C623 showed four UV-active spots on normal phase TLC using 40% ethyl acetate in petroleum ether as a mobile phase (5 runs) with the R_f values of 0.23, 0.43, 0.53 and 0.60. Because of the presence of broad signals in the ^{1}H NMR spectrum, it was not further investigated.

Subfraction 70C624 showed four UV-active spots on normal phase TLC using 50% ethyl acetate in petroleum ether as a mobile phase (3 runs) with the R_f values of 0.32, 0.49, 0.56 and 0.68. It was further separated by column chromatography over silica gel. Elution was initially performed with 50% ethyl acetate in petroleum ether and gradually enriched with ethyl acetate and then methanol until pure methanol. Fractions with the similar chromatogram were combined and evaporated to dryness under reduced pressure to afford two subfractions as shown in **Table 27**.

Table 27 Subfractions obtained from **subfraction 70C624** by column chromatography over silica gel

Subfraction	Elution	Weight (mg)	Physical appearance
70C6241	50-70% EtOAc/Petrol	5.8	Yellow gum
70C6242	70% EtOAc/Petrol-100%MeOH	37.2	White solid

Subfraction 70C6241 showed four UV-active spots on normal phase TLC using 50% ethyl acetate in petroleum ether as a mobile phase (3 runs) with the R_f values of 0.34, 0.56, 0.66 and 0.76. Its ^{1}H NMR spectrum indicated the presence of many components. Thus, it was not further investigated.

Subfraction 70C6242 showed a long tail under UV-S on normal phase TLC using 50% ethyl acetate in petroleum ether as a mobile phase (3 runs). Its ^{1}H NMR spectrum indicated that the major compound was **AR1**. No further purification was carried out.

Subfraction 70C625 showed two UV-active spots on normal phase TLC using 40% ethyl acetate in petroleum ether as a mobile phase (5 runs) with the R_f values of 0.40 and 0.90. It contained **AR1** as a major component. No further purification was carried out.

Subfraction 70C626 showed five UV-active spots on normal phase TLC using 3% methanol in dichloromethane as a mobile phase with the R_f values of 0.17, 0.27, 0.34, 0.41 and 0.54. It was further separated by column chromatography over silica gel. Elution was initially performed with 3% methanol in dichloromethane and gradually enriched with methanol until pure methanol. Fractions with the similar chromatogram were combined and evaporated to dryness under reduced pressure to afford two subfractions as shown in **Table 28**.

Table 28 Subfractions obtained from **subfraction 70C626** by column chromatography over silica gel

Subfraction	Elution	Weight (mg)	Physical appearance
70C6261	3% MeOH/CH_2Cl_2	14.1	Yellow solid
70C6262	3% MeOH/CH_2Cl_2-100% MeOH	10.2	Yellow gum

Subfraction 70C6261 showed three UV-active spots on normal phase TLC using 2% methanol in dichloromethane as a mobile phase with the R_f values of 0.29, 0.39 and 0.59. It was further separated by column chromatography over silica gel. Elution was initially performed with 2% methanol in dichloromethane and gradually enriched with methanol until pure methanol. Fractions with the similar chromatogram were combined and evaporated to dryness under reduced pressure to afford four subfractions as shown in **Table 29**.

Table 29 Subfractions obtained from **subfraction 70C6261** by column chromatography over silica gel

Subfraction	Elution	Weight (mg)	Physical appearance
70C62611	2% MeOH/CH_2Cl_2	1.6	White solid
70C62612	2% MeOH/CH_2Cl_2	1.5	White solid
70C62613	2-3% MeOH/CH_2Cl_2	3.7	White solid
70C62614	10% MeOH/CH_2Cl_2-100% MeOH	5.8	Yellow solid

Subfraction 70C62611 showed two UV-active spots on normal phase TLC using 2% methanol in dichloromethane as a mobile phase with the R_f values of 0.41 and 0.52. It contained **AR9** as a major component. Thus, it was not further investigated.

Subfraction 70C62612 (AR9) showed one UV-active spot on normal phase TLC using 2% methanol in dichloromethane as a mobile phase with the R_f value of 0.51.

m.p.	199-201 ^{0}C
$[\alpha]_D^{25}$	-67.8 (c = 0.1, MeOH)
UV λ_{max}(nm)(MeOH)(log ε)	203 (3.48), 226 (3.10), 277 (2.36)
FTIR(neat) : υ(cm^{-1})	3176, 3059 (N-H stretching), 1674 (C=O stretching)
^{1}H NMR($CDCl_3$)(δ_{ppm})(300 MHz) :	7.14 (*d*, *J* = 8.7 Hz, 2H), 6.85 (*d*, *J* = 8.7 Hz, 2H), 6.02 (*brs*, 1H), 5.94 (*brs*, 1H), 5.47 (*tm*, *J* = 6.9 Hz, 1H), 4.48 (*d*, *J* = 6.9 Hz, 2H), 4.23 (*d*, *J* = 2.1 Hz, 1H), 3.45 (*d*, *J* = 13.8 Hz, 1H), 2.95 (*d*, *J* = 13.8 Hz, 1H), 2.27 (*s*, 3H), 2.22 (*s*, 3H), 1.80 (*s*, 3H), 1.74 (*s*, 3H)
^{13}C NMR($CDCl_3$)(δ_{ppm})(75 MHz) :	165.71, 164.83, 158.75, 138.40, 131.84, 124.77, 119.47, 114.98, 67.78, 64.83, 58.40,

	44.83, 25.83, 18.23, 13.94, 13.74
CH :	131.84, 119.47, 114.98, 58.40
CH_2 :	64.83, 44.83
CH_3 :	25.83, 18.23, 13.94, 13.74

Subfraction 70C62613 (AR10) showed one UV-active spot on normal phase TLC using 2% methanol in dichloromethane as a mobile phase with the R_f value of 0.37.

m.p.	208-210 ^{0}C
$[\alpha]_D^{25}$	-22.2 (c = 0.1, MeOH)
UV λ_{max}(nm)(MeOH)(log ε)	202 (3.51), 228 (2.97), 277 (2.36)
FTIR(neat) : υ(cm^{-1})	3176, 3059 (N-H stretching), 1670 (C=O stretching)
^{1}H NMR($CDCl_3$)(δ_{ppm})(500 MHz) :	7.10 (*d*, *J* = 8.5 Hz, 2H), 6.78 (*d*, *J* = 8.5 Hz, 2H), 6.05 (*brs*, 1H), 5.97 (*brs*, 1H), 5.39 (*tm*, *J* = 7.0 Hz, 1H), 4.90 (*d*, *J* = 1.5 Hz, 1H), 4.41 (*d*, *J* = 6.5 Hz, 2H), 3.50 (*d*, *J* = 14.0 Hz, 1H), 2.95 (*d*, *J* = 14.0 Hz, 1H), 2.16 (*s*, 3H), 1.72 (*s*, 3H), 1.67 (*s*, 3H), 1.64 (*s*, 3H)
^{13}C NMR($CDCl_3$)(δ_{ppm})(125 MHz) :	165.34, 164.47, 158.77, 138.25, 132.05, 125.08, 119.58, 115.00, 67.75, 64.86, 58.47, 43.03, 25.76, 18.17, 13.28, 11.34
CH :	132.05, 119.58, 115.00, 58.47
CH_2 :	64.86, 43.03
CH_3 :	25.76, 18.17, 13.28, 11.34

Subfraction 70C62614 showed a long tail under UV-S on normal phase TLC using 2% methanol in dichloromethane as a mobile phase. The ^{1}H NMR spectrum indicated the absence of olefinic and aromatic protons. Thus, it was not further investigated.

Subfraction 70C6262 showed four UV-active spots on normal phase TLC using 3% methanol in dichloromethane as a mobile phase with the R_f values of 0.28, 0.35, 0.43 and 0.50. Because of the presence of broad signals in the ^{1}H NMR spectrum, it was not further investigated.

Subfraction 70C627 showed a long tail after dipping the TLC plate in anisaldehyde reagent and subsequently heating using 40% ethyl acetate in petroleum ether as a mobile phase (5 runs). Because of the presence of broad signals in the ^{1}H NMR spectrum, it was not further investigated.

Subfraction 70C63 showed three UV-active spots on normal phase TLC using 40% acetone in hexane as a mobile phase (3 runs) with the R_f values of 0.38, 0.45 and 0.55. Its ^{1}H NMR spectrum indicated that the major compound was **AR1**. No further purification was carried out.

Subfraction 70C64 showed a long tail under UV-S on normal phase TLC using 40% acetone in hexane as a mobile phase (3 runs). Because of the presence of broad signals in the ^{1}H NMR spectrum, it was not further investigated.

Subfraction 70C7 showed a long tail under UV-S on normal phase TLC using 3% methanol in dichloromethane as a mobile phase (3 runs). Because of the presence of broad signals in the ^{1}H NMR spectrum, it was not further investigated.

Subfraction 70D showed four UV-active spots on reverse phase TLC using 50% methanol in water as a mobile phase with the R_f values of 0.05, 0.14, 0.29 and 0.51. It was further separated by column chromatography over reverse phase silica gel. Elution was initially performed with 50% methanol in water, followed by reducing the polarity with methanol until pure methanol. Fractions with the similar chromatogram were combined and evaporated to dryness under reduced pressure to afford six subfractions as shown in **Table 30**.

Table 30 Subfractions obtained from **subfraction 70D** by column chromatography over reverse phase silica gel

Subfraction	Elution	Weight (mg)	Physical appearance
70D1	50% MeOH/H_2O	9.9	Brown gum
70D2	50% MeOH/H_2O	17.2	Brown gum
70D3	50-60% MeOH/H_2O	15.3	Brown gum
70D4	60-70% MeOH/H_2O	13.4	Brown solid
70D5	70-80% MeOH/H_2O	9.0	Brown solid
70D6	80% MeOH/H_2O-100% MeOH	3.2	Brown gum

Subfraction 70D1 showed two UV-active spots on normal phase TLC using 40% ethyl acetate in dichloromethane as a mobile phase (3 runs) with the R_f values of 0.30 and 0.55. It was then purified by precoated TLC with 40% ethyl acetate in dichloromethane as a mobile phase (5 runs) to afford two bands.

Band 1 (70D11) was a colorless gum (3.8 mg). Its chromatogram showed one UV-active spot on normal phase TLC using 40% ethyl acetate in petroleum ether as a mobile phase with the R_f value of 0.48. The ^{1}H NMR spectrum indicated that it was **AR30**.

Band 2 (70D12) was a white solid (1.3 mg). Its chromatogram showed one UV-active spot on normal phase TLC using 40% ethyl acetate in petroleum ether as a mobile phase with the R_f value of 0.18. The ^{1}H NMR spectrum indicated that it was **AR11**.

Subfraction 70D2 showed three UV-active spots on normal phase TLC using 2% methanol in dichloromethane as a mobile phase (4 runs) with the R_f values of 0.14, 0.26 and 0.43. It was further separated by column chromatography over silica gel. Elution was initially performed with 2% methanol in dichloromethane and gradually enriched with methanol until pure methanol. Fractions with the similar chromatogram were combined and evaporated to dryness under reduced pressure to afford five subfractions as shown in **Table 31**.

Table 31 Subfractions obtained from **subfraction 70D2** by column chromatography over silica gel

Subfraction	Elution	Weight (mg)	Physical appearance
70D21	2% MeOH/CH_2Cl_2	1.3	Yellow gum
70D22	2% MeOH/CH_2Cl_2	7.1	Yellow gum
70D23	2-3% MeOH/CH_2Cl_2	1.0	Yellow gum
70D24	3-5% MeOH/CH_2Cl_2	2.1	White solid
70D25	10% MeOH/CH_2Cl_2-100% MeOH	5.6	Yellow gum

Subfraction 70D21 showed two UV-active spots on normal phase TLC using 4% methanol in dichloromethane as a mobile phase (2 runs) with the R_f values of 0.44 and 0.51. Because of the minute quantity, it was not further investigated.

Subfraction 70D22 showed two UV-active spots on normal phase TLC using 4% methanol in dichloromethane as a mobile phase (2 runs) with the R_f values of 0.32 and 0.37. Its ^{1}H NMR spectrum indicated that the major compound was **AR30**. No further purification was carried out.

Subfraction 70D23 showed three UV-active spots on normal phase TLC using 4% methanol in dichloromethane as a mobile phase (2 runs) with the R_f values of 0.24, 0.29 and 0.37. Because of the minute quantity, it was not further investigated.

Subfraction 70D24 (AR11) showed one UV-active spot on normal phase TLC using 4% methanol in dichloromethane as a mobile phase (2 runs) with the R_f value of 0.24.

m.p.	120-122 ^{0}C
$[\alpha]_D^{25}$	-10.1 (c = 1.0, $CHCl_3$)
UV λ_{max}(nm)(MeOH)(log ε)	204 (3.56), 224 (3.40), 261 (3.03), 300 (2.81)
FTIR(neat) : υ(cm^{-1})	3362 (O-H stretching), 1738 (C=O stretching)

^{1}H NMR($CDCl_3$)(δ_{ppm})(500 MHz) :	6.40 (*s*, 1H). 3.97 (*d*, *J* = 11.5 Hz, 1H), 3.92 (*s*, 3H), 3.86 (*s*, 3H), 3.78 (*d*, *J* = 11.5 Hz, 1H), 2.15 (*s*, 3H)
^{13}C NMR($CDCl_3$)(δ_{ppm})(125 MHz) :	166.20, 164.99, 158.11, 145.97, 114.91, 106.80, 104.12, 96.06, 66.42, 56.20, 56.15, 10.25
CH :	96.06
CH_2 :	66.42
CH_3 :	56.20, 56.15, 10.25
EIMS *m/z* (% relative intensity) :	254 (2), 227 (10), 143 (20), 87 (73), 74 (100)

Subfraction 70D25 showed four UV-active spots on normal phase TLC using 4% methanol in dichloromethane as a mobile phase (2 runs) with the R_f values of 0.05, 0.10, 0.24 and 0.44. Its ^{1}H NMR spectrum indicated the presence of many components. Thus, it was not further investigated.

Subfraction 70D3 showed five UV-active spots on normal phase TLC using 1% methanol in dichloromethane as a mobile phase with the R_f values of 0.10, 0.15, 0.21, 0.28 and 0.67. It was further separated by column chromatography over silica gel. Elution was initially performed with 1% methanol in dichloromethane and gradually enriched with methanol until pure methanol. Fractions with the similar chromatogram were combined and evaporated to dryness under reduced pressure to afford five subfractions as shown in **Table 32**.

Table 32 Subfractions obtained from **subfraction 70D3** by column chromatography over silica gel

Subfraction	Elution	Weight (mg)	Physical appearance
70D31	1% MeOH/CH_2Cl_2	3.9	Yellow gum
70D32	1% MeOH/CH_2Cl_2	2.0	Yellow gum

Table 32 Continued

Subfraction	Elution	Weight (mg)	Physical appearance
70D33	2-5% MeOH/CH_2Cl_2	3.0	Yellow gum
70D34	5-10% MeOH/CH_2Cl_2	4.3	Yellow gum
70D35	30% MeOH/CH_2Cl_2-100% MeOH	3.4	Yellow gum

Subfraction 70D31 showed three UV-active spots on normal phase TLC using 1% methanol in dichloromethane as a mobile phase with the R_f values of 0.31, 0.52 and 0.69. It was then purified by precoated TLC with 1% methanol in dichloromethane as a mobile phase (2 runs) to afford **AR12** as a pale yellow gum (2.2 mg). Its chromatogram showed one UV-active spot on normal phase TLC using 1% methanol in dichloromethane as a mobile phase (2 runs) with the R_f value of 0.69.

$[\alpha]_D^{25}$	-67.8 (c = 1.0, $CHCl_3$)
UV λ_{max}(nm)(MeOH)(log ε)	217 (3.84), 268 (3.45), 315 (3.26)
FTIR(neat) : υ(cm^{-1})	3432 (O-H stretching), 1716 and 1673 (C=O stretching)
^{1}H NMR($CDCl_3$)(δ_{ppm})(500 MHz) :	11.59 (*s*, 1H), 6.52 (*s*, 1H), 4.50 (*s*, 1H), 4.39 (*d*, *J* = 12.0 Hz, 1H), 4.19 (*d*, *J* = 12.0 Hz, 1H), 3.87 (*s*, 3H), 2.26 (*s*, 3H), 1.96 (*s*, 3H)
^{13}C NMR($CDCl_3$)(δ_{ppm})(125 MHz) :	206.39, 169.36, 165.31, 164.40, 136.89, 118.30, 100.20, 99.86, 76.06, 71.44, 56.03, 25.39, 11.35
CH :	99.86
CH_2 :	71.44
CH_3 :	56.03, 25.39, 11.35
EIMS *m/z* (% relative intensity) :	266 (22), 223 (81), 206 (32), 195 (100), 165 (20), 150 (19)

Subfraction 70D32 showed three UV-active spots on normal phase TLC using 1% methanol in dichloromethane as a mobile phase with the R_f values of 0.10, 0.26 and 0.31. It was then purified by precoated TLC with 1% methanol in dichloromethane as a mobile phase (4 runs) to afford two bands.

Band 1 (AR13) was a pale yellow gum (0.6 mg). Its chromatogram showed one UV-active spot on normal phase TLC using 1% methanol in dichloromethane as a mobile phase (2 runs) with the R_f value of 0.23.

$[\alpha]_D^{29}$	-24.8 (c = 0.04, $CHCl_3$)
UV λ_{max}(nm)(MeOH)(log ε)	203 (3.84), 217 (3.81), 268 (3.39), 312 (3.18)
FTIR(neat) : $\upsilon(cm^{-1})$	3394 (O-H stretching), 1652 (C=O stretching)
^{1}H NMR($CDCl_3$)(δ_{ppm})(500 MHz) :	11.52 (*s*, 1H), 6.39 (*s*, 1H), 4.44 (*q*, *J* = 6.5 Hz, 1H), 4.02 (*d*, *J* = 11.0 Hz, 1H), 3.79 (*s*, 3H), 3.72 (*d*, *J* = 11.0 Hz, 1H), 2.97 (*s*, 1H), 2.27 (*s*, 3H), 1.51 (*d*, *J* = 6.5 Hz, 3H)
^{13}C NMR($CDCl_3$)(δ_{ppm})(125 MHz) :	169.89, 165.18, 163.35, 141.02, 117.30, 100.30, 98.97, 79.48, 73.42, 62.57, 55.93, 14.68, 12.22
CH :	98.97, 79.48
CH_2 :	62.57
CH_3 :	55.93, 14.68, 12.22
EIMS *m/z* (% relative intensity) :	268 (43), 237 (100), 209 (73), 191 (44)

Band 2 (70D322) was a white solid (0.6 mg). Its chromatogram showed one UV-active spot on normal phase TLC using 1% methanol in dichloromethane as a mobile phase (2 runs) with the R_f value of 0.13. The ^{1}H NMR spectrum indicated that it was **AR8**.

Subfraction 70D33 showed four UV-active spots on normal phase TLC using 3% methanol in dichloromethane as a mobile phase with the R_f values of 0.10, 0.15, 0.34 and 0.54. Its ^{1}H NMR spectrum indicated the presence of many components. Thus, it was not further investigated.

Subfraction 70D34 showed three UV-active spots on normal phase TLC using 60% ethyl acetate in dichloromethane as a mobile phase (5 runs) with the R_f values of 0.28, 0.33 and 0.38. It was then purified by precoated TLC with 60% ethyl acetate in dichloromethane as a mobile phase (7 runs) to afford **AR14** as a white solid (2.0 mg). Its chromatogram showed one UV-active spot on normal phase TLC using 60% ethyl acetate in dichloromethane as a mobile phase (5 runs) with the R_f value of 0.28.

m.p.	180-182 ^{0}C
$[\alpha]_D^{26}$	-46.0 (c = 0.05, MeOH)
UV λ_{max}(nm)(MeOH)(log ε)	202 (3.86), 249 (3.75), 305 (2.33), 335 (2.85)
FTIR(neat) : υ(cm^{-1})	3370 (O-H stretching), 1654 (C=O stretching)
^{1}H NMR($CDCl_3$)(δ_{ppm})(500 MHz) :	11.85 (*s*, 1H), 6.58 (*s*, 1H), 4.68 (*d*, *J* = 12.5 Hz, 1H), 4.62 (*d*, *J* = 12.5 Hz, 1H), 4.43 (*d*, *J* = 8.0 Hz, 1H), 3.92 (*m*, 1H), 3.92 (*s*, 3H), 3.76 (*brd*, *J* = 12.0 Hz, 1H), 3.66 (*t*, *J* = 9.0 Hz, 1H), 3.60 (*s*, 3H), 3.41 (*dd*, *J* = 9.0, 8.0 Hz, 1H), 3.36 (*ddd*, *J* = 9.0, 4.5, 3.0 Hz, 1H), 3.24 (*t*, *J* = 9.0 Hz, 1H), 2.38 (*s*, 3H), 2.41 (*s*, 3H)
^{13}C NMR($CDCl_3$)(δ_{ppm})(125 MHz) :	167.00, 147.00, 165.50, 162.93, 137.50, 115.30, 114.50, 102.11, 100.50, 98.81, 79.06, 76.41, 75.70, 73.96, 66.49, 62.03, 60.70, 56.03, 17.18, 13.69
CH :	102.11, 98.81, 79.06, 76.41, 75.70, 73.96
CH_2 :	66.49, 62.03

CH_3 :	60.70, 56.03, 17.18, 13.69
EIMS *m/z* (% relative intensity) :	426 (13), 250 (25), 234 (100), 205 (29)

Subfraction 70D35 showed two UV-active spots on normal phase TLC using 5% methanol in dichloromethane (2 runs) as a mobile phase with the R_f values of 0.21 and 0.64. Because of the presence of broad signals in the ^{1}H NMR spectrum, it was not further investigated.

Subfraction 70D4 showed three UV-active spots on normal phase TLC using 20% ethyl acetate in dichloromethane as a mobile phase (2 runs) with the R_f values of 0.08, 0.38 and 0.68. It was then purified by precoated TLC with 20% ethyl acetate in dichloromethane as a mobile phase (4 runs) to afford three bands.

Band 1 (70D41) was a white solid (1.3 mg). Its chromatogram showed one UV-active spot on normal phase TLC using 20% ethyl acetate in dichloromethane as a mobile phase (2 runs) with the R_f value of 0.63. The ^{1}H NMR spectrum indicated that it was **AR9**.

Band 2 (70D42) was a white solid (2.0 mg). Its chromatogram showed one UV-active spot on normal phase TLC using 20% ethyl acetate in dichloromethane as a mobile phase (2 runs) with the R_f value of 0.30. The ^{1}H NMR spectrum indicated that it was **AR10**.

Band 3 (70D43) was a colorless crystals (5.6 mg). Its chromatogram showed one UV-active spot on normal phase TLC using 30% ethyl acetate in dichloromethane as a mobile phase (5 runs) with the R_f value of 0.25. The ^{1}H NMR spectrum indicated that it was **AR1**.

Subfraction 70D5 showed two UV-active spots on normal phase TLC using 2% methanol in dichloromethane as a mobile phase with the R_f values of 0.64 and 0.74. It was then purified by precoated TLC with 10% ethyl acetate in petroleum ether as a mobile phase (7 runs) to afford two bands.

Band 1 (AR15) was a white solid (3.1 mg). Its chromatogram showed one UV-active spot on normal phase TLC using 20% ethyl acetate in petroleum ether as a mobile phase (3 runs) with the R_f value of 0.41.

m.p.	184-186 ^{0}C
UV λ_{max}(nm)(MeOH)(log ε)	212 (3.67), 254 (3.08), 296 (2.93)
FTIR(neat) : υ(cm^{-1})	1745 (C=O stretching)
^{1}H NMR($CDCl_3$)(δ_{ppm})(300 MHz) :	6.31 (*s*, 1H), 5.16 (*d*, *J* = 1.8 Hz, 1H), 5.11 (*d*, *J* = 1.8 Hz, 1H), 4.95 (*d*, *J* = 1.5 Hz, 1H), 4.86 (*d*, *J* = 1.5 Hz, 1H), 3.89 (*s*, 3H), 3.88 (*s*, 3H), 2.10 (*s*, 3H)
^{13}C NMR($CDCl_3$)(δ_{ppm})(75 MHz) :	162.35, 162.27, 158.88, 156.16, 153.33, 148.90, 114.24, 106.63, 105.00, 97.30, 92.48, 56.44, 55.79, 7.85
CH :	92.48
CH_2 :	106.63, 97.30
CH_3 :	56.44, 55.79, 7.85
EIMS *m/z* (% relative intensity) :	262 (36), 218 (34), 192 (100), 163 (24), 134 (54)

<u>Band 2</u> (AR16) was a white solid (2.7 mg). Its chromatogram showed one UV-active spot on normal phase TLC using 20% ethyl acetate in petroleum ether as a mobile phase (3 runs) with the R_f value of 0.27.

m.p.	167-169 ^{0}C
UV λ_{max}(nm)(MeOH)(log ε)	202 (3.55), 240 (3.63), 278 (3.06), 331 (2.93)
FTIR(neat) : υ(cm^{-1})	1774 (C=O stretching)
^{1}H NMR($CDCl_3$)(δ_{ppm})(300 MHz) :	5.30 (*d*, *J* = 2.7 Hz, 1H), 5.19 (*d*, *J* = 2.7 Hz, 1H), 4.01 (*s*, 3H), 3.96 (*s*, 3H), 2.30 (*s*, 3H)
^{13}C NMR($CDCl_3$)(δ_{ppm})(75 MHz) :	164.28, 157.80, 152.36, 139.11, 114.13, 105.50, 96.00, 95.23, 56.35, 56.13, 10.95
CH_2 :	95.23
CH_3 :	56.35, 56.13, 10.95

EIMS *m/z* (% relative intensity) : 220 (100), 191 (56), 162 (26), 149 (45)

Subfraction 70D6 showed a long tail under UV-S on normal phase TLC using 2% methanol in dichloromethane as a mobile phase. The ^{1}H NMR spectrum indicated the absence of olefinic and aromatic protons. Thus, it was not further investigated.

Subfraction 70E showed six UV-active spots on normal phase TLC using 1% methanol in dichloromethane as a mobile phase with the R_f values of 0.09, 0.20, 0.39, 0.59, 0.66 and 0.86. It was further separated by column chromatography over silica gel. Elution was initially performed with 1% methanol in dichloromethane and gradually enriched with methanol until pure methanol. Fractions with the similar chromatogram were combined and evaporated to dryness under reduced pressure to afford six subfractions as shown in **Table 33**.

Table 33 Subfractions obtained from **subfraction 70E** by column chromatography over silica gel

Subfraction	Elution	Weight (mg)	Physical appearance
70E1	1% MeOH/CH_2Cl_2	1.0	Yellow gum
70E2	1% MeOH/CH_2Cl_2	5.7	Brown gum
70E3	1-2% MeOH/CH_2Cl_2	5.9	Brown gum
70E4	2-3% MeOH/CH_2Cl_2	8.0	Yellow gum
70E5	3-5% MeOH/CH_2Cl_2	9.7	Yellow gum
70E6	10% MeOH/CH_2Cl_2-100% MeOH	18.1	Brown gum

Subfraction 70E1 showed two UV-active spots on normal phase TLC using 1% methanol in dichloromethane as a mobile phase with the R_f values of 0.70 and 0.80. Because of the minute quantity, it was not further investigated.

Subfraction 70E2 showed four UV-active spots on normal phase TLC using 10% ethyl actate in petroleum ether as a mobile phase (3 runs) with the R_f values of 0.12, 0.22, 0.32 and 0.49. It was then purified by precoated TLC with 10% ethyl acetate in petroleum ether as a mobile phase (7 runs) to afford two bands.

Band 1 (70E21) was a pale yellow gum (2.2 mg). Its chromatogram showed one UV-active spot on normal phase TLC using 10% ethyl acetate in petroleum ether as a mobile phase (3 runs) with the R_f value of 0.54. The ^{1}H NMR spectrum indicated that it was **AR12**.

Band 2 (70E22) was a pale yellow gum (1.0 mg). Its chromatogram showed one UV-active spot on normal phase TLC using 10% ethyl acetate in petroleum ether as a mobile phase (3 runs) with the R_f value of 0.20. The ^{1}H NMR spectrum indicated that it was **AR17**.

Subfraction 70E3 showed five UV-active spots on normal phase TLC using 1% methanol in dichloromethane as a mobile phase with the R_f values of 0.25, 0.30, 0.34, 0.55 and 0.59. Its ^{1}H NMR spectrum indicated the presence of many components. Thus, it was not further investigated.

Subfraction 70E4 showed four UV-active spots on normal phase TLC using 30% ethyl actate in petroleum ether as a mobile phase (3 runs) with the R_f values of 0.07, 0.24, 0.50 and 0.62. It was then purified by precoated TLC with 30% ethyl acetate in petroleum ether as a mobile phase (5 runs) to afford two bands.

Band 1 (70E41) was a yellow solid (1.8 mg). Its chromatogram showed one UV-active spot on normal phase TLC using 30% ethyl acetate in petroleum ether as a mobile phase (3 runs) with the R_f value of 0.61. Its ^{1}H NMR spectrum indicated the presence of many components. Thus, it was not further investigated.

Band 2 (70E42) was a yellow gum (2.9 mg). Its chromatogram showed two UV-active spots on normal phase TLC using 10% ethyl acetate in dichloromethane as a mobile phase (2 runs) with the R_f values of 0.32 and 0.49. It was then purified by precoated TLC with 10% ethyl acetate in dichloromethane as a mobile phase (5 runs) to afford two bands.

Band 1 (70E421) was a colorless gum (0.7 mg). Its chromatogram showed one UV-active spot on normal phase TLC using 10% ethyl acetate in dichloromethane as a mobile phase (2 runs) with the R_f value of 0.41. The ^{1}H NMR spectrum indicated that it was **AR13**.

Band 2 (AR17) was a pale yellow gum (0.7 mg). Its chromatogram showed one UV-active spot on normal phase TLC using 10% ethyl acetate in dichloromethane as a mobile phase (2 runs) with the R_f value of 0.27.

$[\alpha]_D^{25}$	-33.2 (c = 1.0, $CHCl_3$)
UV λ_{max}(nm)(MeOH)(log ε)	204 (3.91), 217 (3.77), 230 (3.47), 270 (3.35), 314 (3.14)
FTIR(neat) : υ(cm^{-1})	3370 (O-H stretching), 1654 (C=O stretching)
^{1}H NMR($CDCl_3$)(δ_{ppm})(500 MHz) :	11.64 (*s*, 1H), 6.46 (*s*, 1H), 4.46 (*d*, *J* = 10.5 Hz, 1H), 4.17 (*q*, *J* = 6.5 Hz, 1H), 4.14 (*d*, *J* = 10.5 Hz, 1H), 3.88 (*s*, 3H), 2.75 (*s*, 1H), 2.42 (*s*, 3H), 1.20 (*d*, *J* = 6.5 Hz, 3H)
^{13}C NMR($CDCl_3$)(δ_{ppm})(125 MHz) :	169.90, 165.14, 138.97, 117.87, 99.61, 98.67, 74.32, 70.36, 69.04, 55.85, 17.36, 12.33
CH :	98.67, 69.04
CH_2 :	70.36
CH_3 :	55.85, 17.36, 12.33
EIMS *m/z* (% relative intensity) :	268 (32), 224 (70), 206 (100), 195 (54), 178 (48)

Subfraction 70E5 showed three UV-active spots on normal phase TLC using 30% ethyl actate in petroleum ether as a mobile phase (3 runs) with the R_f values of 0.21, 0.36 and 0.55. It was then purified by precoated TLC with 30% ethyl acetate in petroleum ether as a mobile phase (5 runs) to afford three bands.

Band 1 (70E51) was a yellow solid (1.2 mg). Its chromatogram showed one UV-active spot on normal phase TLC using 30% ethyl acetate in

petroleum ether as a mobile phase (3 runs) with the R_f value of 0.54. Its ^{1}H NMR spectrum indicated the presence of many components. Thus, it was not further investigated.

Band 2 (70E52) was a colorless gum (2.7 mg). Its chromatogram showed one UV-active spot on normal phase TLC using 30% ethyl acetate in petroleum ether as a mobile phase (3 runs) with the R_f value of 0.39. The ^{1}H NMR spectrum indicated that it was **AR30**.

Band 3 (AR18) was a pale yellow gum (1.6 mg). Its chromatogram showed one UV-active spot on normal phase TLC using 30% ethyl acetate in petroleum ether as a mobile phase (3 runs) with the R_f value of 0.17.

UV λ_{max}(nm)(MeOH)(log ε)	202 (3.80), 249 (3.84), 333 (2.73)
FTIR(neat) : υ(cm^{-1})	3352 (O-H stretching), 1666 (C=O stretching)
^{1}H NMR(Acetone-d_6)(δ_{ppm}) : (500 MHz)	11.93 (*s*, 1H), 6.67 (*s*, 1H), 4.76 (*d*, *J* = 4.5 Hz, 2H), 4.60 (*d*, *J* = 5.5 Hz, 2H), 4.94 (*m*, 1H), 4.49 (*m*, 1H), 3.98 (*s*, 3H), 2.56 (*s*, 3H)
^{13}C NMR(Acetone-d_6)(δ_{ppm}) : (125 MHz)	167.32, 166.67, 163.92, 156.80, 137.69, 116.76, 114.79, 101.22, 99.12, 60.34, 57.60, 56.74, 12.09
CH :	99.12
CH_2 :	60.34, 57.60
CH_3 :	56.74, 12.09
EIMS *m/z* (% relative intensity) :	266 (49), 248 (35), 219 (41), 207 (95), 189 (100), 165 (55)

Subfraction 70E6 showed a long tail under UV-S on normal phase TLC using 1% methanol in dichloromethane as a mobile phase. The ^{1}H NMR spectrum indicated the absence of olefinic and aromatic protons. Thus, it was not further investigated.

Subfraction 70F showed three UV-active spots on normal phase TLC using 2% methanol in dichloromethane as a mobile phase with the R_f values of 0.12, 0.32 and

0.44. It was then purified by precoated TLC with 2% methanol in dichloromethane as a mobile phase (8 runs) to afford three bands.

Band 1 (**70F1**) was a pale yellow gum (2.1 mg). Its chromatogram showed one UV-active spot on normal phase TLC using 2% methanol in dichloromethane as a mobile phase (5 runs) with the R_f value of 0.40. The ^{1}H NMR spectrum indicated that it was **AR18**.

Band 2 (**AR19**) was a pale yellow gum (0.8 mg). Its chromatogram showed one UV-active spot on normal phase TLC using 2% methanol in dichloromethane as a mobile phase (5 runs) with the R_f value of 0.31.

UV λ_{max}(nm)(MeOH)(log ε)	201 (3.84), 219 (3.41), 246 (3.72), 328 (2.25)
FTIR(neat) : υ(cm^{-1})	3356 (O-H stretching), 1674 (C=O stretching)
^{1}H NMR(Acetone-d_6)(δ_{ppm}) : (500 MHz)	11.49 (*s*, 1H), 6.56 (*d*, *J* = 2.0 Hz, 1H), 6.46 (*d*, *J* = 2.0 Hz, 1H), 4.65 (*m*, 1H), 4.51 (*d*, *J* = 5.5 Hz, 2H), 2.19 (*s*, 3H)
^{13}C NMR(Acetone-d_6)(δ_{ppm}) : (125 MHz)	167.00, 166.63, 165.00, 153.01, 142.00, 111.80, 102.71, 102.23, 100.50, 59.64, 11.95
CH :	102.71, 102.23
CH_2 :	59.64
CH_3 :	11.95
EIMS *m/z* (% relative intensity) :	222 (100), 193 (78), 163 (68), 135 (46)

Band 3 (**AR20**) was a pale yellow gum (0.8 mg). Its chromatogram showed one UV-active spot on normal phase TLC using 2% methanol in dichloromethane as a mobile phase (5 runs) with the R_f value of 0.12.

UV λ_{max}(nm)(MeOH)(log ε)	200 (3.86), 247 (3.47)
FTIR(neat) : υ(cm^{-1})	3369 (O-H stretching), 1666 (C=O stretching)
^{1}H NMR(Acetone-d_6)(δ_{ppm}) :	11.84 (*s*, 1H), 6.58 (*s*, 1H), 4.84 (*m*, 1H),

(500 MHz)	4.78 (*d*, *J* = 4.5 Hz, 2H), 4.61 (*d*, *J* = 5.5 Hz, 2H), 4.38 (*m*, 1H), 2.58 (*s*, 3H)
^{13}C NMR(Acetone-d_6)(δ_{ppm}) : (125 MHz)	167.00, 165.40, 163.50, 156.80, 138.80, 117.00, 113.90, 102.63, 101.00, 60.39, 57.55, 12.06
CH :	102.63
CH_2 :	60.39, 57.55
CH_3 :	12.06
EIMS *m/z* (% relative intensity) :	252 (75), 234 (50), 205 (47), 193 (100), 175 (98), 149 (33)

Subfraction 70G showed a long tail under UV-S on normal phase TLC using 1% methanol in dichloromethane as a mobile phase. Its ^{1}H NMR spectrum indicated that the major compound was **AR1**. No further purification was carried out.

CHAPTER 1.3

RESULTS AND DISCUSSION

Ten new compounds **(AR11-20)** along with ten known compounds **(AR1-10)** were isolated from the broth extract.

1.3.1 Compound AR1

Compound **AR1** with the melting point 204-206 ^{0}C was obtained as colorless crystals. The UV spectrum displayed an absorption band at 208 nm, indicating the presence of an α,β-unsaturated ester chromophore. The IR spectrum exhibited absorption bands at 3424 cm^{-1} for a hydroxy group, and 1705 cm^{-1} for a conjugated ester carbonyl group. Comparision of its ^{1}H (**Figure 1**) and ^{13}C NMR (**Figure 2**) data (**Table 34**), TLC chromatogram and optical rotation, $[\alpha]_D^{29}$ +90.4 (c = 0.2, MeOH), with the previously reported data of (+)-brefeldin A, $[\alpha]_D^{29}$ +89.0 (c = 0.2, MeOH), indicated that compound **AR1** was (+)-brefeldin A which was isolated from broth extract of *Penicillium* sp. PSU-F44 (Trisuwan *et al*., 2009). The structure was confirmed by X-ray data (**Figure 3**).

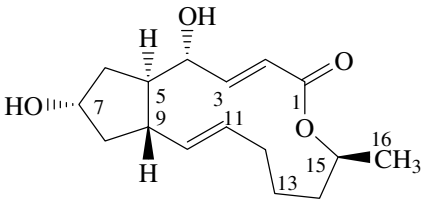

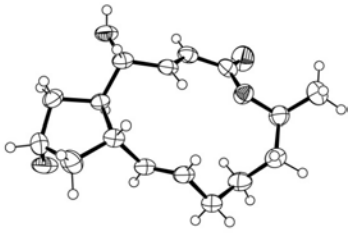

Table 34 The ^{1}H and ^{13}C NMR data of compound **AR1** and (+)-brefeldin A in DMSO-d_6

Position	**AR1**		**(+)-Brefeldin A**	
	δ_H (*mult.*, J_{Hz})	δ_C (C-type)	δ_H (*mult.*, J_{Hz})	δ_C (C-type)
1	-	166.18 (C=O)	-	166.19 (C=O)
2	5.71 (*dd*, 15.6, 1.8)	116.76 (CH)	5.70 (*dd*, 15.3, 1.8)	116.71 (CH)
3	7.34 (*dd*, 15.6, 2.7)	154.83 (CH)	7.34 (*dd*, 15.3, 2.7)	154.87 (CH)
4	3.93 (*m*)	74.83 (CH)	3.92 (*m*)	74.80 (CH)
4-OH	5.13 (*d*, 5.7)	-	5.16 (*d*, 5.7)	-
5	1.70 (*m*)	52.20 (CH)	1.70 (*m*)	52.17 (CH)
6	a: 1.84 (*m*) b: 1.65 (*m*)	41.40 (CH_2)	a: 1.84 (*m*) b: 1.65 (*m*)	41.35 (CH_2)
7	4.04 (*m*)	71.00 (CH)	4.03 (*m*)	71.01 (CH)
7-OH	4.51 (*d*, 3.9)	-	4.55 (*d*, 3.6)	
8	a: 1.97 (*m*) b: 1.30 (*m*)	43.56 (CH_2)	a: 1.97 (*m*) b: 1.30 (*m*)	43.49 (CH_2)
9	2.31 (*qn*, 8.1)	43.82 (CH)	2.31 (*qn*, 8.4)	43.78 (CH)
10	5.20 (*dd*, 15.0, 9.6)	137.60 (CH)	5.19 (*dd*, 15.3, 9.6)	137.58 (CH)
11	5.66 (*ddd*, 15.0, 10.2, 4.5)	129.71 (CH)	5.66 (*ddd*, 15.3, 10.2, 4.5)	129.71 (CH)
12	a: 1.92 (*m*) b: 1.76 (*m*)	31.91 (CH_2)	a: 1.92 (*m*) b: 1.76 (*m*)	31.92 (CH_2)
13	a: 1.78 (*m*) b: 0.74 (*m*)	26.91 (CH_2)	a: 1.78 (*m*) b: 0.74 (*m*)	26.94 (CH_2)
14	a: 1.70 (*m*) b: 1.47 (m)	33.91 (CH_2)	a: 1.70 (*m*) b: 1.45 (m)	33.85 (CH_2)
15	4.70 (*sext*, 6.3)	71.36 (CH)	4.70 (*sext*, 6.3)	71.39 (CH)

Table 34 Continued

Position	AR1		(+)-Brefeldin A	
	δ_H (*mult.*, J_{Hz})	δ_C (C-type)	δ_H (*mult.*, J_{Hz})	δ_C (C-type)
16	1.18 (*d*, 6.3)	21.16 (CH_3)	1.18 (*d*, 6.3)	21.17 (CH_3)

Trisuwan *et al*., 2009.

1.3.2 Compound AR2

Compound **AR2** with the melting point 252-254 ^{0}C was obtained as a white solid. It showed an UV absorption band at 203 nm. The IR spectrum exhibited absorption bands at 3384, 3325, 1746 and 1640 cm^{-1} for hydroxyl, amino, ester carbonyl and amide carbonyl groups, respectively. The ^{1}H NMR spectrum (**Figure 4**) (**Table 35**) contained signals for one 2-oxy-4-methylpentanoyl unit [δ_H 5.00 (*dd*, *J* = 8.7, 5.1 Hz, 1H), 1.58 (*m*, 1H)/0.97 (*ddd*, *J* = 14.1, 7.5, 5.1 Hz, 1H), 1.12 (*m*, 1H), 0.78 (*d*, *J* = 6.6 Hz, 3H) and 0.72 (*d*, *J* = 6.6 Hz, 3H)], two 2-aminopropenonyl units [δ_H 8.22 (*d*, *J* = 8.7 Hz, 1H), 4.96 (*m*, 1H) and 1.53 (*d*, *J* = 7.5 Hz, 3H); 7.10 (*d*, *J* = 6.9 Hz, 1H), 4.86 (*qn*, *J* = 6.9 Hz, 1H), and 1.41 (*d*, *J* = 6.9 Hz, 3H)], one 3-hydroxy-2-oxy-3-methylbutanoyl unit [δ_H 5.28 (*s*, 1H), 5.22 (*s*, 1H), 1.17 (*s*, 3H) and 1.25 (*s*, 3H)], one 2-(methylamino)propanoyl unit [δ_H 3.70 (*q*, *J* = 6.9 Hz, 1H), 3.20 (*s*, 3H) and 1.52 (*d*, *J* = 6.9 Hz, 3H)] and one 2-(methylamino)-3-phenylpropanoyl unit [δ_H 7.25 (*m*, 2H), 7.20 (*m*, 1H), 7.16 (*m*, 2H), 5.76 (*dd*, *J* = 11.7, 5.1 Hz, 1H), 3.48 (*dd*, *J* = 15.3, 5.1 Hz, 1H)/2.91 (*dd*, *J* = 15.3, 11.7 Hz, 1H) and 2.92 (*s*, 3H)]. The ^{13}C NMR spectrum (**Figure 5**) (**Table 35**) displayed two ester carbonyl carbons (δ_C 172.60 and 168.95), four amide carbonyl carbons (δ_C 172.38, 171.39, 169.78 and 168.50), two quaternary carbons (δ_C 137.12 and 71.77), ten resonances for twelve methine carbons (δ_C 128.63, 128.41, 126.60, 77.19, 70.57, 60.53, 56.61, 47.10, 46.27 and 23.85), two methylene carbons (δ_C 38.83 and 33.18) and nine methyl carbons (δ_C 36.93, 30.14, 26.75, 24.14, 22.84, 22.24, 19.26, 18.10 and 13.53). The methine proton (H-4, δ_H 1.12) exhibited ^{1}H-^{1}H COSY cross peaks with H_3-5 (δ_H 0.78), H_3-6 (δ_H 0.72) and H_{ab}-3 (δ_H 1.58 and 0.97) (**Table 36**) which were further coupled with H-2 (δ_H 5.00). H-2

gave the HMBC correlation with C-1 (δ_C 172.38) (**Table 36**), constructing the 2-oxy-4-methylpentanoyl unit (1). The methine proton (H-9, δ_H 4.96) displayed ^{1}H-^{1}H COSY cross peaks with H_3-10 (δ_H 1.53) and 11-NH (δ_H 8.22). H-9 gave the HMBC correlation with C-8 (δ_C 172.60), establishing the 2-aminopropenoyl unit (2). The methine proton (H-13, δ_H 5.22) showed the HMBC correlations with C-12 (δ_C 169.78), C-14 (δ_C 71.77), C-15 (δ_C 26.75), and C-16 (δ_C 24.14) and 14-OH (δ_H 5.28) displayed the HMBC correlations with C-14, C-15 and C-16, constructing the 3-hydroxy-2-oxy-3-methylbutanoyl unit (3). The methine proton (H-19, δ_H 3.70) exhibited ^{1}H-^{1}H COSY cross peaks with H_3-20 (δ_H 1.52). H-19 gave the HMBC correlations with C-18 (δ_C 168.95) and C-22 (δ_C 36.93), establishing the 2-(methylamino)propanoyl unit (4). The methine proton (H-24, δ_H 4.86) displayed ^{1}H-^{1}H COSY cross peaks with H_3-25 (δ_H 1.41) and 26-NH (δ_H 7.10). H-24 gave the HMBC correlation with C-23 (δ_C 171.39), constructing the 2-aminopropenoyl unit (5). An aromatic proton (H-33, δ_H 7.20) displayed ^{1}H-^{1}H COSY cross peaks with H-31 and H-31′ (δ_H 7.16) and H-32 and H-32′ (δ_H 7.25), indicating the presence of a monosubstituted benzene. The methine proton (H-28, δ_H 5.76) showed ^{1}H-^{1}H COSY cross peaks with H_{ab}-29 (δ_H 3.48 and 2.91). H_{ab}-29 gave the HMBC correlations with C-30 (δ_C 137.12), C-31 and C-31′ (δ_C 128.63). The methyl protons (H_3-35, δ_H 2.92) showed the HMBC correlation with C-28 (δ_C 56.61) as well as H-28 displayed the HMBC correlation with C-27 (δ_C 168.50), constructing the 2-(methylamino)-3-phenylpropanoyl unit (6).

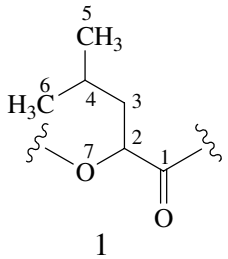

1

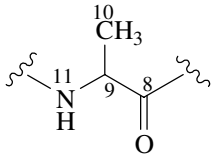

2

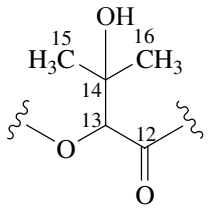

3

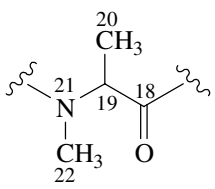

4

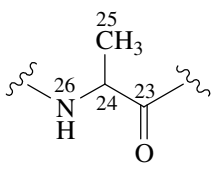

5

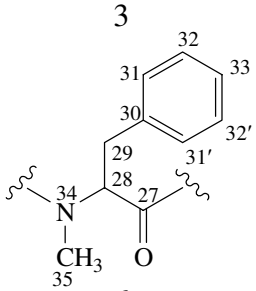

6

The subunits 1-6 were sequentially connected on the basis of the ^{3}J HMBC correlation of H-2/C-8, H-9/C-12, H-13/C-18, H-19/C-23, H-24/C-27 and H-28/C-1. Consequently, compound **AR2** was identified as guangomide A (Amagata *et al*., 2006). The observed optical rotation of compound **AR2**, $[\alpha]_D^{28}$ -40.2 (c = 0.8, $CHCl_3$), was similar to that of guangomide A, $[\alpha]_D^{28}$ -44.6 (c = 0.8, $CHCl_3$), indicating that all chiral carbons of compound **AR2** possessed the same absolute configuration as those of guangomide A.

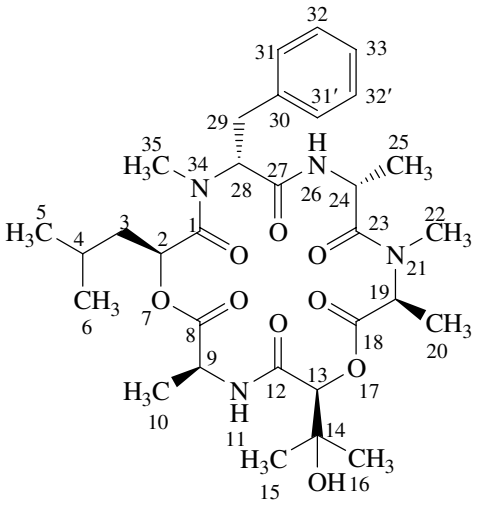

Table 35 The ^{1}H and ^{13}C NMR data of compound **AR2** and guangomide A in $CDCl_3$

Position	**AR2**		**Guangomide A**	
	δ_H (*mult.*, J_{Hz})	δ_C (C-type)	δ_H (*mult.*, J_{Hz})	δ_C (C-type)
1	-	172.38 (C=O)	-	172.4 (C=O)
2	5.00 (*dd*, 8.7, 5.1)	70.57 (CH)	5.00 (*dd*, 8.7, 6.2)	70.5 (CH)
3	a: 1.58 (*m*)	38.83 (CH_2)	1.55 (*ddd*, 14.2, 8.7, 6.7)	38.8 (CH_2)
	b: 0.97 (*ddd*, 14.1, 7.5, 5.1)		0.98 (*ddd*, 14.2, 6.2, 5.3)	
4	1.12 (*m*)	23.85 (CH)	1.15 (*m*)	23.8 (CH)
5	0.78 (*d*, 6.6)	22.84 (CH_3)	0.78 (*d*, 6.6)	22.8 (CH_3)
6	0.72 (*d*, 6.6)	22.24 (CH_3)	0.72 (*d*, 6.6)	22.3 (CH_3)
8	-	172.60 (C=O)	-	172.6 (C=O)

Table 35 Continued

Position	AR2		Guangomide A	
	δ_H (*mult.*, J_{Hz})	δ_C (C-type)	δ_H (*mult.*, J_{Hz})	δ_C (C-type)
9	4.96 (*m*)	47.10 (CH)	4.97 (*dq*, 8.7, 7.1)	47.1 (CH)
10	1.53 (*d*, 7.5)	19.26 (CH_3)	1.53 (*d*, 7.1)	19.3 (CH_3)
11-NH	8.22 (*d*, 8.7)	-	8.22 (*d*, 8.7)	-
12	-	169.78 (C=O)	-	169.8 (C=O)
13	5.22 (*s*)	77.19 (CH)	5.22 (*s*)	76.5 (CH)
14	-	71.77 (C)	-	71.8 (C)
14-OH	5.28 (*s*)	-	5.27 (*brs*)	-
15	1.17 (*s*)	26.75 (CH_3)	1.17 (*s*)	26.7 (CH_3)
16	1.25 (*s*)	24.14 (CH_3)	1.26 (*s*)	24.1 (CH_3)
18	-	168.95 (C=O)	-	169.0 (C=O)
19	3.70 (*q*, 6.9)	60.53 (CH)	3.69 (*q*, 6.8)	60.5 (CH)
20	1.52 (*d*, 6.9)	13.53 (CH_3)	1.52 (*d*, 6.8)	13.5 (CH_3)
22	3.20 (*s*)	36.93 (CH_3)	3.20 (*s*)	36.9 (CH_3)
23	-	171.39 (C=O)	-	171.3 (C=O)
24	4.86 (*qn*, 6.9)	46.27 (CH)	4.85 (*qn*, 7.1)	46.2 (CH)
25	1.41 (*d*, 6.9)	18.10 (CH_3)	1.41 (*d*, 6.8)	18.1 (CH_3)
26-NH	7.10 (*d*, 6.9)	-	7.09 (*d*, 7.3)	-
27	-	168.50 (C=O)	-	168.5 (C=O)
28	5.76 (*dd*, 11.7, 5.1)	56.61 (CH)	5.76 (*dd*, 11.9, 5.3)	56.6 (CH)
29	a: 3.48 (*dd*, 15.3, 5.1) b: 2.91 (*dd*, 15.3, 11.7)	33.18 (CH_2)	3.49 (*dd*, 15.3, 5.3) 2.92 (*dd*, 15.3, 11.8)	33.2 (CH_2)
30	-	137.12 (C)	-	137.1 (C)
31, 31′	7.16 (*m*)	128.63 (CH)	7.16 (*m*)	128.6 (CH)
32, 32′	7.25 (*m*)	128.41 (CH)	7.24 (*m*)	128.4 (CH)
33	7.20 (*m*)	126.60 (CH)	7.19 (*m*)	126.6 (CH)

Table 35 Continued

Position	**AR2**		**Guangomide A**	
	δ_H (*mult.*, J_{Hz})	δ_C (C-type)	δ_H (*mult.*, J_{Hz})	δ_C (C-type)
35	2.92 (*s*)	30.14 (CH_3)	2.92 (*s*)	30.2 (CH_3)

Amagata *et al*., 2006.

Table 36 The HMBC and COSY data of compound **AR2** in $CDCl_3$

Proton	HMBC	COSY
H-2	C-1, C-3, C-4, C-8	H_{ab}-3
H_a-3	C-2, C-4, C-6	H-2, H_b-3, H-4
H_b-3	C-2, C-4, C-6	H-2, H_a-3, H-4
H-4	C-3, C-6	H_{ab}-3, H_3-5, H_3-6
H_3-5	C-3, C-4, C-6	H-4
H_3-6	C-3, C-4, C-5	H-4
H-9	C-8, C-10, C-12	H_3-10, 11-NH
H_3-10	C-8, C-9	H-9
11-NH	C-12	H-9
H-13	C-12, C-14, C-15, C-16, C-18	-
14-OH	C-13, C-14, C-15, C-16	-
H_3-15	C-13, C-14, C-16	-
H_3-16	C-13, C-14, C-15	-
H-19	C-18, C-20, C-22, C-23	H_3-20
H_3-20	C-18, C-19	H-19
H_3-22	C-19, C-23	-
H-24	C-23, C-25, C-27	H_3-25, 26-NH
H_3-25	C-23, C-24	H-24
26-NH	C-23, C-27	H-24
H-28	C-1, C-27, C-29, C-30	H_{ab}-29

Table 36 Continued

Proton	HMBC	COSY
H_a-29	C-27, C-28, C-30, C-31, C-31′	H-28, H_b-29
H_b-29	C-27, C-28, C-30, C-31, C-31′	H-28, H_a-29
H-31, H-31′	C-29, C-33	H-32, H-32′, H-33
H-32, H-32′	C-30, C-33	H-31, H-31′, H-33
H-33	C-31, C-31′	H-31, H-31′, H-32, H-32′
H_3-35	C-1, C-28	-

1.3.3 Compound AR3

Compound **AR3** with the melting point 218-220 ^{0}C was obtained as a white solid and exhibited an UV absorption band similar to that of compound **AR2**. The IR spectrum exhibited absorption bands at 3345, 1744 and 1642 cm^{-1} for amino, ester carbonyl and amide carbonyl groups, respectively. The ^{1}H NMR data (**Figure 6**) (**Table 37**) were almost identical to those of compound **AR2** except that a signal of the hydroxyl group (14-OH, δ_H 5.28) was replaced by a signal for a methine proton (H-14, δ_H 2.61, *hept d*, J = 6.9, 2.4 Hz). All substitutents were located at the same position as those in compound **AR2** according to the HMBC correlations shown in **Table 38**. Therefore, compound **AR3** was identified as guangomide B (Amagata *et al*., 2006). The observed optical rotation of compound **AR3**, $[\alpha]_D^{28}$ -16.7 (c = 0.9, $CHCl_3$), was almost identical to that of guangomide B, $[\alpha]_D^{28}$ -18.1 (c = 0.9, $CHCl_3$), indicating that all chiral carbons of compound **AR3** possessed the same absolute configuration as those of guangomide B.

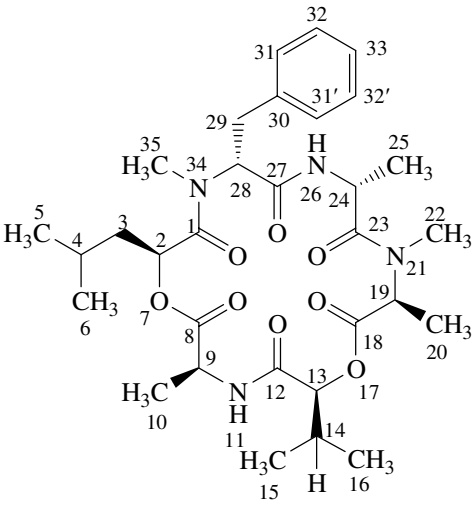

Table 37 The ^{1}H and ^{13}C NMR data of compound **AR3** and guangomide B in $CDCl_3$

Position	**AR3**		**Guangomide B**	
	δ_H (*mult.*, J_{Hz})	δ_C (C-type)	δ_H (*mult.*, J_{Hz})	δ_C (C-type)
1	-	172.46 (C=O)	-	172.4 (C=O)
2	5.00 (*m*)	70.34 (CH)	5.00 (*dd*, 8.9, 6.4)	70.3 (CH)
3	a: 1.56 (*m*)	38.81 (CH_2)	1.54 (*m*)	38.8 (CH_2)
	b: 0.98 (*m*)		0.96 (*ddd*, 14.2, 6.4, 5.3)	
4	1.17 (*hept*, 6.6)	23.84 (CH)	1.19 (*hept*, 6.7)	23.8 (CH)
5	0.78 (*d*, 6.6)	22.87 (CH_3)	0.78 (*d*, 6.6)	22.9 (CH_3)
6	0.72 (*d*, 6.6)	22.20 (CH_3)	0.72 (*d*, 6.6)	22.2 (CH_3)
8	-	172.95 (C=O)	-	172.9 (C=O)
9	4.97 (*m*)	47.03 (CH)	4.98 (*dq*, 8.9, 7.4)	47.0 (CH)
10	1.51 (*d*, 7.2)	19.32 (CH_3)	1.52 (*d*, 7.4)	19.3 (CH_3)
11-NH	7.89 (*d*, 8.7)	-	7.89 (*d*, 8.7)	-
12	-	168.52 (C=O)	-	168.5 (C=O)
13	5.23 (*d*, 2.4)	78.03 (CH)	5.23 (*d*, 2.5)	78.0 (CH)
14	2.61 (*hept d*, 6.9, 2.4)	29.98 (CH)	2.61 (*hept d*, 6.7, 2.5)	30.0 (CH)
15	0.93 (*d*, 6.9)	19.19 (CH_3)	0.93 (*d*, 6.7)	19.2 (CH_3)

Table 37 Continued

Position	AR3		Guangomide B	
	δ_H (*mult.*, J_{Hz})	δ_C (C-type)	δ_H (*mult.*, J_{Hz})	δ_C (C-type)
16	0.92 (*d*, 6.9)	15.84 (CH_3)	0.92 (*d*, 6.7)	15.8 (CH_3)
18	-	169.68 (C=O)	-	169.7 (C=O)
19	3.70 (*q*, 6.9)	60.68 (CH)	3.69 (*q*, 6.8)	60.7 (CH)
20	1.55 (*d*, 6.9)	13.62 (CH_3)	1.54 (*d*, 6.9)	13.6 (CH_3)
22	3.19 (*s*)	36.87 (CH_3)	3.19 (*s*)	36.9 (CH_3)
23	-	171.18 (C=O)	-	171.1 (C=O)
24	4.84 (*qn*, 6.9)	46.34 (CH)	4.84 (*qn*, 7.1)	46.3 (CH)
25	1.42 (*d*, 6.9)	18.05 (CH_3)	1.42 (*d*, 6.7)	18.1 (CH_3)
26-NH	7.13 (*d*, 6.9)	-	7.12 (*d*, 7.4)	-
27	-	168.56 (C=O)	-	168.5 (C=O)
28	5.77 (*dd*, 11.4, 5.4)	56.53 (CH)	5.76 (*dd*, 11.8, 5.3)	56.5 (CH)
29	a: 3.47 (*dd*, 15.3, 5.4) b: 2.89 (*m*)	33.17 (CH_2)	3.47 (*dd*, 15.1, 5.3) 2.92 (*dd*, 15.1, 11.8)	33.2 (CH_2)
30	-	137.15 (C)	-	137.1 (C)
31, 31′	7.16 (*m*)	128.64 (CH)	7.16 (*m*)	128.6 (CH)
32, 32′	7.22 (*m*)	128.40 (CH)	7.24 (*m*)	128.4 (CH)
33	7.18 (*m*)	126.58 (CH)	7.19 (*m*)	126.6 (CH)
35	2.92 (*s*)	30.12 (CH_3)	2.92 (*s*)	30.1 (CH_3)

Amagata *et al*., 2006.

Table 38 The HMBC and COSY data of compound **AR3** in $CDCl_3$

Proton	HMBC	COSY
H-2	C-1, C-3, C-4, C-8	H_{ab}-3
H_a-3	C-1, C-2, C-6	H-2, H_b-3, H-4

Table 38 Continued

Proton	HMBC	COSY
H_b-3	C-1, C-2, C-6	H-2, H_a-3, H-4
H-4	C-2, C-3, C-5, C-6	H_{ab}-3, H_3-5, H_3-6
H_3-5	C-3, C-4, C-6	H-4
H_3-6	C-3, C-4, C-5	H-4
H-9	C-8, C-10, C-12	H_3-10, 11-NH
H_3-10	C-8, C-9	H-9
11-NH	C-12	H-9
H-13	C-12, C-14, C-15, C-16, C-18	H-14
H-14	C-15, C-16	H-13, H_3-15, H_3-16
H_3-15	C-13, C-14, C-16	H-14
H_3-16	C-13, C-14, C-15	H-14
H-19	C-18, C-20, C-23	H_3-20
H_3-20	C-18, C-19	H-19
H_3-22	C-19, C-23	-
H-24	C-23, C-25, C-27	H_3-25, 26-NH
H_3-25	C-23, C-24	H-24
26-NH	C-23, C-27	H-24
H-28	C-1, C-27, C-29, C-30	H_{ab}-29
H_a-29	C-27, C-28, C-30, C-31, C-31′	H-28, H_b-29
H_b-29	C-27, C-28, C-30, C-31, C-31′	H-28, H_a-29
H-31, H-31′	C-29, C-33	H-32, H-32′, H-33
H-32, H-32′	C-30, C-33	H-31, H-31′, H-33
H-33	C-31, C-31′	H-31, H-31′, H-32, H-32′
H_3-35	C-1, C-28	-

1.3.4 Compound AR4

Compound **AR4** was obtained as a colorless gum. It showed an UV absorption band at 212 nm. A carbonyl absorption band was found at 1715 cm^{-1} in the IR spectrum. The ^{1}H NMR spectrum (**Figure 8**) (**Table 39**) contained signals for two *cis*-olefinic protons of an α,β-unsaturated carbonyl compound [δ_H 6.35 (*dq*, *J* = 9.9, 7.2 Hz, 1H) and 5.83 (*dq*, *J* = 9.9, 1.8 Hz, 1H)], three oxymethine protons [δ_H 5.63 (*dd*, *J* = 7.8, 3.6 Hz, 1H), 3.83 (*d*, *J* = 5.1 Hz, 1H) and 3.63 (*d*, *J* = 5.4 Hz, 1H)], one olefinic proton of a trisubstituted double bond (δ_H 5.42, *dd*, *J* = 5.4, 1.2 Hz, 1H), one set of nonequivalent epoxymethylene protons [δ_H 3.12 (*d*, *J* = 4.2 Hz, 1H) and 2.83 (*d*, *J* = 4.2 Hz, 1H)], three sets of nonequivalent methylene protons [δ_H 2.56 (*dd*, *J* = 15.6, 7.8 Hz, 1H)/2.03 (*ddd*, *J* = 15.6, 5.1, 3.6 Hz, 1H), 2.02 (*m*, 1H)/1.99 (*m*, 1H) and 1.92 (*m*, 1H)/1.42 (*m*, 1H)] and four methyl groups [δ_H 2.16 (*dd*, *J* = 7.2, 1.8 Hz, 3H), 1.72 (*s*, 3H), 0.96 (*s*, 3H) and 0.73 (*s*, 3H)]. The ^{13}C NMR spectrum (**Figure 9**) (**Table 39**) displayed one typical carbonyl carbon of an α,β-unsaturated ester (δ_C 166.37), four quaternary carbons (δ_C 140.18, 65.58, 49.03 and 40.47), six methine carbons (δ_C 145.46, 120.70, 118.70, 79.21, 74.52 and 70.58), four methylene carbons (δ_C 47.85, 36.85, 28.03 and 24.50) and four methyl carbons (δ_C 23.23, 16.04, 15.44 and 5.97). The nonequivalent epoxymethylene protons at δ_H 3.12 and 2.83 were assigned as H_{ab}-13. They showed the HMBC correlations with C-2 (δ_C 79.21), C-5 (δ_C 49.03) and C-12 (δ_C 65.58) (**Table 40**). H_{ab}-3 (δ_H 2.56 and 2.03) gave the ^{1}H-^{1}H COSY cross peaks with H-2 (δ_H 3.83) and H-4 (δ_H 5.63) (**Table 40**) and also exhibited the same HMBC correlations as H_{ab}-13. The methyl protons (H_3-14, δ_H 0.73) displayed the HMBC correlations with C-4 (δ_C 74.52), C-5 and C-12. These results together with ^{13}C chemical shifts of C-4, C-12 and C-13 (δ_C 47.85) established a cyclopentane with a spiro epoxide, a methyl and an alkoxyl units at C-12, C-5 and C-4, respectively. The *cis*-olefinic proton (H-3′, δ_H 6.35) showed ^{1}H-^{1}H COSY cross peaks with H-2′ (δ_H 5.83) and H_3-4′ (δ_H 2.16). Moreover, H-3′ gave the HMBC correlations with C-1′ (δ_C 166.37) and C-4′ (δ_C 15.44). Thus, a 1-butenoyl unit was established. It was then attached to C-4 of the cyclopentane ring on the basis of the HMBC correlation from H-4 to C-1′ to establish substructure 1.

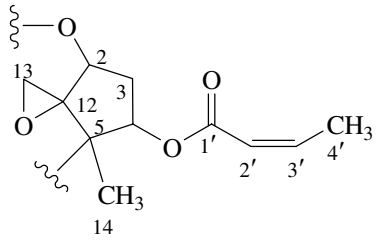

Substructure 1

The olefinic proton (H-10, δ_H 5.42) exhibited ^{1}H-^{1}H COSY cross peaks with H_{ab}-8 (δ_H 2.02 and 1.99) and H-11 (δ_H 3.63). H_{ab}-8 were further coupled with H_{ab}-7 (δ_H 1.92 and 1.42). The methyl protons (H_3-15, δ_H 0.96) showed the HMBC correlations with C-6 (δ_C 40.47), C-7 (δ_C 24.50) and C-11 (δ_C 70.58) while the methyl protons (H_3-16, δ_H 1.72) displayed the HMBC cross peaks with C-8 (δ_C 28.03), C-9 (δ_C 140.18) and C-10 (δ_C 118.70). Accordingly, substructure unit 2 was formed.

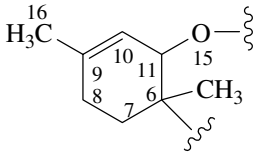

Substructure 2

The oxymethine proton (H-2) and the methyl protons (H_3-14) exhibited the ^3J HMBC correlations with C-11 and C-6, respectively. Thus, substructure 1 was fused with substructure 2 by forming an ether linkage between C-2 and C-11 and a C-C bond between C-5 and C-6 to construct a tetracyclic skeleton. Irradiation of H_{ab}-13 in the NOEDIFF experiment (**Table 40**) enhanced signal intensity of H-2, while irradiation of H_3-14 affected signal intensity of H_b-13. These results indicated that they had *cis*-relationship. Moreover, irradiation of H_3-15 enhanced signal intensity of H-4 and H-11, indicating that H-4, H-11 and H_3-15 were *cis* but *trans* to H-2, H_{ab}-13 and H_3-14. Therefore, compound **AR4** was identified as 8-deoxytrichothecin (Chinworrungsee *et al.*, 2008). The observed optical rotation of compound **AR4**, $[\alpha]_D^{30}$ -12.8 (c = 1.4, $CHCl_3$), was similar to that of 8-deoxytrichothecin, $[\alpha]_D^{30}$ -9.1 (c = 1.4, $CHCl_3$), indicating that all chiral carbons of compound **AR4** possessed the same absolute configuration as those of 8-deoxytrichothecin.

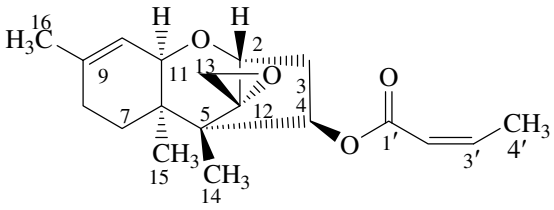

Table 39 The ^{1}H and ^{13}C NMR data of compound **AR4** and 8-deoxytrichothecin in $CDCl_3$

Position	**AR4**		**8-Deoxytrichothecin**	
	δ_H (*mult.*, J_{Hz})	δ_C (C-type)	δ_H (*mult.*, J_{Hz})	δ_C (C-type)
2	3.83 (*d*, 5.1)	79.21 (CH)	3.84 (*d*, 5.2)	79.2 (CH)
3	a: 2.56 (*dd*, 15.6, 7.8) b: 2.03 (*ddd*, 15.6, 5.1, 3.6)	36.85 (CH_2)	2.57 (*dd*, 15.4, 7.8) 1.90-2.07 (*m*)	36.8 (CH_2)
4	5.63 (*dd*, 7.8, 3.6)	74.52 (CH)	5.64 (*dd*, 7.8, 3.6)	74.5 (CH)
5	-	49.03 (C)	-	49.0 (C)
6	-	40.47 (C)	-	40.5 (C)
7	a: 1.92 (*m*) b: 1.42 (*m*)	24.50 (CH_2)	1.90-2.07 (*m*) 1.43 (*m*)	24.5 (CH_2)
8	a: 2.02 (*m*) b: 1.99 (*m*)	28.03 (CH_2)	1.90-2.07 (*m*) 1.90-2.07 (*m*)	28.0 (CH_2)
9	-	140.18 (C)	-	140.2 (C)
10	5.42 (*dd*, 5.4, 1.2)	118.70 (CH)	5.42 (*dd*, 5.4, 1.3)	118.7 (CH)
11	3.63 (*d*, 5.4)	70.58 (CH)	3.64 (*d*, 5.4)	70.6 (CH)
12	-	65.58 (C)	-	65.6 (C)
13	a: 3.12 (*d,* 4.2) b: 2.83 (*d*, 4.2)	47.85 (CH_2)	3.13 (*d,* 4.1) 2.84 (*d,* 4.1)	47.9 (CH_2)
14	0.73 (*s*)	5.97 (CH_3)	0.73 (*s*)	6.0 (CH_3)
15	0.96 (*s*)	16.04 (CH_3)	0.97 (*s*)	16.0 (CH_3)
16	1.72 (*s*)	23.23 (CH_3)	1.72 (*s*)	23.3 (CH_3)
1′	-	166.37 (C=O)	-	166.4 (C=O)

Table 39 Continued

Position	AR4		8-Deoxytrichothecin	
	δ_H (*mult.*, J_{Hz})	δ_C (C-type)	δ_H (*mult.*, J_{Hz})	δ_C (C-type)
2′	5.83 (*dq*, 9.9, 1.8)	120.70 (CH)	5.84 (*dq*, 11.5, 1.8)	120.7 (CH)
3′	6.35 (*dq*, 9.9, 7.2)	145.46 (CH)	6.36 (*dq*, 11.5, 7.3)	145.5 (CH)
4′	2.16 (*dd*, 7.2, 1.8)	15.44 (CH_3)	2.17 (*dd*, 7.3, 1.8)	15.5 (CH_3)

Chinworrungsee *et al*., 2008.

Table 40 The HMBC, COSY and NOE data of compound **AR4** in $CDCl_3$

Proton	HMBC	COSY	NOE
H-2	C-4, C-5, C-11, C-12	H_{ab}-3	H_b-3, H_a-13
H_a-3	C-2, C-5, C-12	H-2, H_b-3, H-4	*
H_b-3	C-2, C-5, C-12	H-2, H_a-3, H-4	*
H-4	C-1′, C-2, C-5, C-6, C-12	H_{ab}-3	H_a-3, H-11, H_3-14, H_3-15
H_a-7	C-6, C-9	H_b-7, H_{ab}-8	*
H_b-7	C-6, C-9	H_a-7, H_{ab}-8	*
H_a-8	-	H_b-8, H_{ab}-7, H_3-16	*
H_b-8	-	H_a-8, H_{ab}-7, H_3-16	*
H-10	C-6, C-8, C-16	H_{ab}-8, H-11, H_3-16	H-11, H_3-16
H-11	C-7, C-9, C-10	H-10	H_b-3, H-4, H-10, H_3-15
H_a-13	C-2, C-5, C-12	H_b-13	H-2, H_b-13
H_b-13	C-2, C-5, C-12	H_a-13	H-2, H_a-13
H_3-14	C-4, C-5, C-6, C-12	-	H_b-13
H_3-15	C-5, C-6, C-7, C-11	-	H-4, H-7, H-11
H_3-16	C-8, C-9, C-10	-	*
H-2′	C-1′, C-4′	H-3′, H_3-4′	*

Table 40 Continued

Proton	HMBC	COSY	NOE
H-3′	C-1′, C-4′	H-2′, H_3-4′	*
H_3-4′	C-2′, C-4′	H-2′, H-3′	*

* not determined

1.3.5 Compound AR7

Compound **AR7** was obtained as a colorless gum. It exhibited an UV absorption band at 224 nm. A hydroxyl absorption band was found at 3448 cm^{-1} in the IR spectrum. The ^1H NMR data (**Figure 10**) (**Table 41**) were almost identical to those of compound **AR4** except for the appearance of an oxymethine proton, H-4, at higher field and the absence of signals for the α,β-unsaturated ester moiety. All substitutents were located at the same position as those in **AR4** according to the HMBC correlations and NOEDIFF data (**Table 42**). Thus, compound **AR7** was identified as trichodermol (Ayer *et al*., 1993). The observed optical rotation of compound **AR7**, $[\alpha]_D^{25}$ -31.4 (c = 1.1, $CHCl_3$), was almost identical to that of trichodermol, $[\alpha]_D^{25}$ -33.0 (c = 1.1, $CHCl_3$), indicating that all chiral carbons of compound **AR7** possessed the same absolute configuration as those of trichodermol.

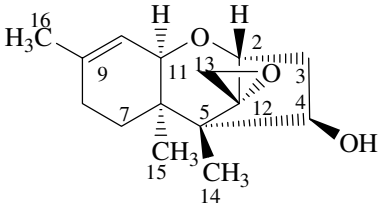

Table 41 The ^1H and ^{13}C NMR data of compound **AR7** and the ^1H NMR data of trichodermol in $CDCl_3$

Position	**AR7**		**Trichodermol**
	δ_H (*mult., J_{Hz}*)	δ_C (C-type)	δ_H (*mult., J_{Hz}*)
2	3.82 (*d*, 5.4)	78.72 (CH)	3.82 (*d*, 5.4)
3	a: 2.61 (*dd*, 15.6, 7.5)	40.15 (CH_2)	2.60 (*dd*, 15.6, 7.4)

Table 41 Continued

Position	**AR7**		**Trichodermol**
	δ_H (*mult.*, J_{Hz})	δ_C (C-type)	δ_H (*mult.*, J_{Hz})
	b: 1.88 (*m*)		1.90-2.00 (*m*)
4	4.33 (*brs*)	74.05 (CH)	4.33 (*td*, 8.6, 2.9)
5	-	49.12 (C)	-
6	-	39.78 (C)	-
7	a: 1.93 (*m*)	24.41 (CH_2)	1.90-2.00 (*m*)
	b: 1.44 (*m*)		1.44 (*m*)
8	a: 2.00 (*m*)	27.99 (CH_2)	1.90-2.00 (*m*)
	b: 1.97 (*m*)		1.90-2.00(*m*)
9	-	140.14 (C)	-
10	5.38 (*brd*, 5.4)	118.71 (CH)	5.39 (*brd*, 5.6)
11	3.50 (*d*, 5.4)	70.26 (CH)	3.51 (*brd*, 5.6)
12	-	65.73 (C)	-
13	a: 3.10 (*d,* 3.9)	47.56 (CH_2)	3.10 (*d,* 3.9)
	b: 2.81 (*d*, 3.9)		2.81 (*d,* 4.0)
14	0.80 (*s*)	6.20 (CH_3)	0.80 (*s*)
15	0.85 (*s*)	15.80 (CH_3)	0.85 (*s*)
16	1.70 (*s*)	23.22 (CH_3)	1.71 (*brs*)

Ayer *et al*., 1993.

Table 42 The HMBC, COSY and NOE data of compound **AR7** in $CDCl_3$

Proton	HMBC	COSY	NOE
H-2	C-3, C-4, C-11, C-12, C-13	H_{ab}-3	H_{ab}-3, H_a-13
H_a-3	C-2, C-4, C-5, C-11, C-12, C-13	H-2, H_b-3, H-4	H-2, H_b-3, H-4
H_b-3	C-2, C-4, C-5, C-12	H-2, H_a-3, H-4	H-2, H_b-3
H-4	-	H_{ab}-3	H_a-3, H-11, H_3-15

Table 42 Continued

Proton	HMBC	COSY	NOE
H_a-7	C-6, C-8, C-9, C-11, C-15	H_b-7, H_{ab}-8	*
H_b-7	C-6, C-8, C-9, C-11, C-15	H_a-7, H_{ab}-8	*
H_a-8	C-7, C-10	H_b-8, H_{ab}-7, H_3-16	*
H_b-8	C-7, C-10	H_a-8, H_{ab}-7, H_3-16	*
H-10	C-6, C-8, C-16	H_{ab}-8, H-11, H_3-16	H-11, H_3-16
H-11	C-7, C-9, C-10, C-15	H-10	H_a-3, H-4, H-10, H_3-15
H_a-13	C-2, C-5, C-12	H_b-13	H-2, H_b-13
H_b-13	C-2, C-5, C-12	H_a-13	H_a-13, H_3-14
H_3-14	C-4, C-5, C-6, C-12	-	H_b-13
H_3-15	C-5, C-6, C-7, C-11	-	H-4, H-11
H_3-16	C-8, C-9, C-10	-	H_{ab}-8, H-10

* not determined

1.3.6 Compound AR5

Compound **AR5** with the melting point 90-92 ^{0}C was obtained as a white solid. The UV spectrum displayed absorption bands at 209 and 261 nm, indicating the presence of a benzene chromophore. The IR spectrum exhibited an absorption band at 3296 cm^{-1} for a hydroxyl group. The ^{1}H NMR spectrum (**Figure 12**) (**Table 43**) contained signals for one monosubstituted benzene [δ_H 7.33 (*d*, *J* = 6.6 Hz, 2H), 7.26 (*d*, *J* = 6.6 Hz, 2H) and 7.23, *t*, *J* = 6.6 Hz, 1H)] and one 2,3-dihydroxy-4-methylhexyl moiety [δ_H 3.91 (*dd*, *J* = 8.1, 2.0 Hz, 1H), 3.52 (*dd*, *J* = 8.1, 2.0 Hz, 1H), 2.91 (*dd*, *J* = 13.8, 2.4 Hz, 1H), 2.70 (*dd*, *J* = 13.8, 8.1 Hz, 1H), 2.26 (*brs*, 1H), 2.23 (*brs*, 1H), 1.90 (*m*, 1H), 1.62 (*m*, 1H), 1.24 (*m*, 1H), 0.97 (*d*, *J* = 6.9 Hz, 3H) and 0.95 (*d*, *J* = 7.2 Hz, 3H)]. The ^{13}C NMR spectrum (**Figure 13**) (**Table 43**) contained one quaternary carbon (δ_C 138.59), six resonances for eight methine carbons (δ_C 129.46 (x2), 128.75 (x2), 126.60, 77.74, 73.11 and 36.24), two methylene carbons (δ_C 36.51 and 24.94) and two methyl carbons (δ_C 14.80 and 10.84). The aromatic protons

resonating at δ_H 7.33, 7.26 and 7.23 were assigned as H-2, H-2′, H-3, H-3′ and H-4, based on their multiplicity and the HMBC correlations. The 2,3-dihydroxy-4-methylhexyl unit was established based on the following ^1H-^1H COSY correlations (**Table 43**): H-6 (δ_H 3.91)/H_{ab}-5 (δ_H 2.91 and 2.70) and H-7 (δ_H 3.52) and H-8 (δ_H 1.62)/H-7 and H_{ab}-9 (δ_H 1.90 and 1.24) and H_3-11 (δ_H 0.97) and H_3-10 (δ_H 0.95)/H_{ab}-9. The chemical shifts of C-6 (δ_C 73.11) and C-7 (δ_C 77.74) revealed the presence of hydroxyl groups at C-6 and C-7. The 2,3-dihydroxy-4-methylhexyl unit was attached at C-1 (δ_C 138.59) of the aromatic ring because H_{ab}-5 showed the HMBC correlations with C-1, C-2 (δ_C 128.75), and C-2′ (δ_C 128.75). Consequently, compound **AR5** was identified as 4-methyl-1-phenyl-2,3-hexanediol (Kashiyama *et al*., 2009).

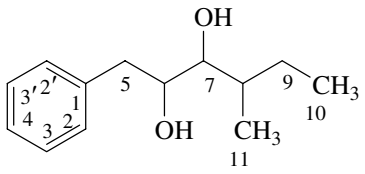

Table 43 The NMR data of compound **AR5** in $CDCl_3$

Position	δ_H (*mult*., J_{Hz})	δ_C (C-Type)	HMBC	COSY
1	-	138.59 (C)	-	-
2, 2′	7.33 (*t,* 6.6)	128.75 (CH)	C-1, C-3, C-3′, C-4, C-5	H-3,H-3′
3, 3′	7.26 (*d,* 6.6)	129.46 (CH)	C-1, C-2, C-2′, C-4	H-2, H-2′, H-4
4	7.23 (*t,* 6.6)	126.60 (CH)	C-2, C-2′, C-3, C-3′	H-3,H-3′
5	a : 2.91 (*dd,* 13.8, 2.4)	36.51 (CH_2)	C-1, C-2, C-2′, C-6, C-7	H_a-5, H-6
	b : 2.70 (*dd,* 13.8, 8.1)	-	C-1, C-2, C-2′, C-6, C-7	H_b-5, H-6
6	3.91 (*dd,* 8.1, 2.0)	73.11 (CH)	C-1	H_{ab}-5, 6-OH, H-7
6-OH	2.26 (*brs*)	-	C-5	H-6

Table 43 Continued

Position	δ_H (*mult.*, J_{Hz})	δ_C (C-Type)	HMBC	COSY
7	3.52 (*dd,* 8.1, 2.0)	77.74 (CH)	C-5, C-6, C-9	H-6, 7-OH, H-8
7-OH	2.23 (*brs*)	-	C-11	H-7
8	1.62 (*m)*	36.24 (CH)	C-6, C-7, C-10, C-11	H-7, H_{ab}-9, H_3-11
9	a : 1.90 (*m*)	24.94 (CH_2)	C-7, C-8, C-10, C-11	H-8, H_b-9, H_3-10
	b : 1.24 (*m*)	-	C-7, C-8, C-10, C-11	H-8, H_a-9, H_3-10
10	0.95 (*d,* 7.2)	10.84 (CH_3)	C-8, C-9	H_{ab}-9
11	0.97 (*d,* 6.9)	14.80 (CH_3)	C-7, C-8, C-9	H-8

1.3.7 Compound AR6

Compound **AR6** with the melting point 87-89 ^{0}C was obtained as a white solid and exhibited UV and IR absorption bands similar to those of compound **AR5**. The ^{1}H NMR data (**Figure 14**) (**Table 44**) were almost identical to those of compound **AR5** except for the replacement of the 2,3-dihydroxy-4-methylhexyl group in compound **AR5** with a 2,3-dihydroxy-4-methylpentyl unit. The presence of this side chain was confirmed by ^{1}H-^{1}H COSY and the HMBC correlations shown in **Table 44**. Therefore, compound **AR6** was identified as 4-methyl-1-phenyl-2,3-pentanediol (Jiao *et al*., 2009). The observed optical rotation of compound **AR6**, $[\alpha]_D^{22}$ +16.0 (c = 1.4, $CHCl_3$), was almost identical to that of (2*R*,3*R*)-4-methyl-1-phenyl-2,3-pentanediol, $[\alpha]_D^{22}$ +15.5 (c = 1.4, $CHCl_3$) (Jiao *et al*., 2009), indicating that they possessed the same absolute configuration at all chiral carbons.

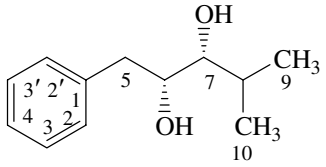

Table 44 The NMR data of compound **AR6** in $CDCl_3$

Position	δ_H (*mult*., J_{Hz})	δ_C (C-Type)	HMBC	COSY
1	-	138.48 (C)	-	-
2, 2′	7.34 (*t,* 6.3)	128.74 (CH)	C-4, C-5	H-3, H-3′
3, 3′	7.26 (*d,* 6.3)	129.44 (CH)	C-1, C-4	H-2, H-2′, H-4
4	7.24 (*t,* 6.3)	126.61 (CH)	C-2, C-2′	H-3, H-3′
5	a : 2.96 (*dd,* 13.8, 3.0)	37.20 (CH_2)	C-1, C-2, C-2′, C-6, C-7	H_b-5, H-6
	b : 2.71 (*dd,* 13.8, 10.2)	-	C-1, C-2, C-2′, C-6, C-7	H_a-5, H-6
6	3.89 (*ddd,* 10.2, 4.5, 3.0)	73.16 (CH)	-	H_{ab}-5, 6-OH, H-7
6-OH	2.10 (*brs*)	-	-	-
7	3.42 (*dd,* 7.2, 4.5)	79.05 (CH)	C-5, C-6, C-9, C-10	H-6, 7-OH, H-8
7-OH	2.09 (*brs*)	-	-	-
8	1.89 (*sext,* 7.2)	29.70 (CH)	C-7, C-9, C-10	H-7, H_3-9, H_3-10
9	0.98 (*d,* 7.2)	18.98 (CH_3)	C-7, C-8, C-10	H-8
10	1.05 (*d,* 7.2)	18.31 (CH_3)	C-7, C-8, C-9	H-8

1.3.8 Compound AR8

Compound **AR8** with the melting point 151-153 ^{0}C was obtained as a white solid. The UV spectrum displayed absorption bands at 214, 221, 259 and 301 nm, indicating the presence of a conjugated benzene chromophore. The IR spectrum exhibited absorption bands at 3352 and 1738 cm^{-1} for hydroxyl and carbonyl groups, respectively. The ^{1}H NMR data (**Figure 16**) (**Table 45**) contained signals for one aromatic proton (δ_H 6.38, *s*, 1H), two methoxyl groups [δ_H 3.92 (*s*, 3H) and 3.90 (*s*,

3H)], two methyl groups [δ_H 2.18 (*s*, 3H) and 1.79 (*s*, 3H)] and one hydroxyl group (δ_H 1.60, *s*, 1H). The ^{13}C NMR spectrum (**Figure 17**) (**Table 45**) contained one carbonyl carbon (δ_C 166.01), five resonances for six quaternary carbons (δ_C 164.84, 157.79, 150.14, 113.90 and 105.37), one methine carbon (δ_C 95.61), two methoxy carbons (δ_C 56.18 and 56.09) and one methyl group (δ_C 10.04). The aromatic proton at δ_H 6.38 was assigned as H-6 and displayed the ^2J HMBC correlations with C-5 (δ_C 164.84) and C-7 (δ_C 157.79). The methoxyl groups at δ_H 3.90 (H_3-10) and 3.92 (H_3-11) were attached at C-5 and C-7, respectively, on the basis of the HMBC correlations of H_3-10/C-5 and H_3-11/C-7. The methyl protons at δ_H 2.18 (H_3-9) showed the HMBC correlations with C-3a (δ_C 150.14), C-4 (δ_C 113.90) and C-5, indicating that it was connected to C-4. The methyl protons at δ_H 1.79 (H_3-8) and the hydroxyl group (3-OH, δ_H 1.60) were attached at the same carbon, C-3 (δ_C 105.37) due to the HMBC correlations of H_3-8/C-3 and C-3a as well as the carbon chemical shift of C-3. These also linked C-3 with C-3a. The HMBC correlation of H-6 with the ester carbonyl carbon (δ_C 166.01, C-1) as well as the UV data attached the ester carbonyl moiety at C-7a. The chemical shift of C-3 established a lactone moiety. The ^1H and ^{13}C NMR spectra of compound **AR8** were almost identical to those of 5,7-dimethoxy-3,4-dimethyl-3-hydroxyphthalide (Shim *et al*., 2008). Therefore, **AR8** was identified as 5,7-dimethoxy-3,4-dimethyl-3-hydroxyphthalide.

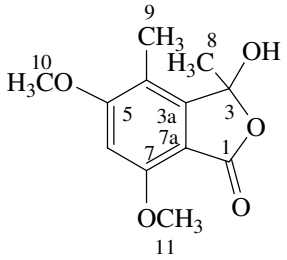

Table 45 The ^{1}H and ^{13}C NMR data of compound **AR8** and 5,7-dimethoxy-3,4-dimethyl-3-hydroxyphthalide in $CDCl_3$

Position	**AR8**		**5,7-Dimethoxy-3,4-dimethyl-3-hydroxyphthalide**	
	δ_H (*mult.*, J_{Hz})	δ_C (C-type)	δ_H (*mult.*, J_{Hz})	δ_C (C-Type)
1	-	166.01 (C=O)	-	165.5 (C=O)
3	-	105.37 (C)	-	104.5 (C)
3-OH	1.60 (*brs*)	-	-	-
3a	-	150.14 (C)	-	150.4 (C)
4	-	113.90 (C)	-	114.1 (C)
5	-	164.84 (C)	-	166.4 (C)
6	6.38 (*s*)	95.61 (CH)	6.38 (*s*)	95.8 (CH)
7	-	157.79 (C)	-	160.0 (C)
7a	-	105.37 (C)	-	105.6 (C)
8	1.79 (*s*)	25.50 (CH_3)	1.82 (*s*)	25.7 (CH_3)
9	2.18 (*s*)	10.04 (CH_3)	2.21 (*s*)	10.3 (CH_3)
10	3.90 (*s*)	56.18 (CH_3)	3.90 (*s*)	56.3 (CH_3)
11	3.92 (*s*)	56.09 (CH_3)	3.92 (*s*)	56.4 (CH_3)

Shim *et al*., 2008.

Table 46 The HMBC data of compound **AR8** in $CDCl_3$

Proton	HMBC
3-OH	-
H-6	C-1, C-4, C-5, C-7, C-7a
H_3-8	C-3, C-3a
H_3-9	C-3a, C-4, C-5, C-6
H_3-10	C-5
H_3-11	C-6

1.3.9 Compound AR11

Compound **AR11** with the molecular formula $C_{12}H_{14}O_6$ by EIMS [*m/z* 222 $(M\text{-}MeOH)^+$] (**Figure 20**) and the melting point 120-122 ^{0}C was obtained as a white solid and exhibited UV and IR absorption bands similar to those of compound **AR8**. The ^{1}H NMR data (**Figure 18**) (**Table 47**) were almost identical to those of compound **AR8** except for replacement of the methyl signal (H_3-8, δ_H 1.79) in compound **AR8** with the hydroxymethyl signals (H_{ab}-8, δ_H 3.97 and 3.78) in compound **AR11**. All substitutents were located at the same position as those in compound **AR8** according to the HMBC correlations. Consequently, compound **AR11** was identified as a new phthalide derivative.

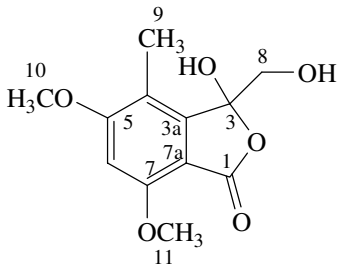

Table 47 The NMR data of compound **AR11** in $CDCl_3$

Position	δ_H (*mult.*, J_{Hz})	δ_C (C-Type)	HMBC
1	-	166.20 (C=O)	-
3	-	104.12 (C)	-
3a	-	145.97 (C)	-
4	-	114.91 (C)	-
5	-	164.99 (C)	-
6	6.40 (*s*)	96.06 (CH)	C-4, C-5, C-7, C-7a
7	-	158.11 (C)	-
7a	-	106.80 (C)	-
8	a : 3.97 (*d*, 11.5)	66.42 (CH_2)	C-3, C-3a
	b : 3.78 (*d*, 11.5)		C-3, C-3a
9	2.15 (*s*)	10.25 (CH_3)	C-1, C-3a, C-4, C-5
10	3.86 (*s*)	56.15 (CH_3)	C-5

Table 47 Continued

Position	δ_H (*mult*., J_{Hz})	δ_C (C-Type)	HMBC
11	3.92 (*s*)	56.20 (CH_3)	C-7

1.3.10 Compound AR15

Compound **AR15** with the molecular formula $C_{14}H_{14}O_5$ by EIMS (**Figure 23**) and the melting point 184-186 ^{0}C was obtained as a white solid. The UV spectrum displayed absorption bands at 212, 254, and 296 nm, indicating the presence of a benzoyl chromophore. The IR spectrum exhibited an absorption band at 1745 cm^{-1} for an ester carbonyl group. The ^{1}H NMR and HMBC data (**Figure 21**) (**Table 48**) indicated that it possessed a pentasubstituted benzene, similar to that of Compound **AR8**. The chemical shift of C-6 (δ_C 153.33) in compound **AR15** attached an alkoxyl substituent at this carbon, instead of the alkyl group as found in compound **AR8**. Two sets of terminal olefinic protons [δ_H 5.16 (*d*, *J* = 1.8 Hz, 1H)/5.11 (*d*, *J* = 1.8 Hz, 1H) and 4.95 (*d*, *J* = 1.5 Hz, 1H)/4.86 (*d*, *J* = 1.5 Hz, 1H)] were observed. The ^{13}C NMR spectrum (**Figure 22**) (**Table 48**) contained one carbonyl carbon (δ_C 162.35), seven quaternary carbons (δ_C 162.27, 158.88, 156.16, 153.33, 148.90, 114.24 and 105.00), one methine carbon (δ_C 92.48), two terminal olefinic carbons (δ_C 106.63 and 97.30), two methoxy carbons (δ_C 56.44 and 55.79) and one methyl carbon (δ_C 7.85). All the nonequivalent gem-olefinic protons [H_{ab}-12 (δ_H 5.16 and 5.11) and H_{ab}-13 (δ_H 4.95 and 4.86)] exhibited the same HMBC correlations with C-3 (δ_C 156.16) and C-4 (δ_C 148.90) (**Table 49**). These results along with signal enhancement of H_a-13 and H_a-12 upon irradiation of H_b-13 in the NOEDIFF experiment (**Table 49**) constructed a 1,3-butadienyl unit with alkoxyl groups at C-3 and C-4. According to the chemical shift of C-6 (δ_C 153.33) as well as the HMBC correlation of H_{ab}-12/C-1 (δ_C 162.35), this unit was linked to C-6 and C-1 through an ether and an ester linkage, respectively. Thus, compound **AR15** was identified as a new lactone derivative.

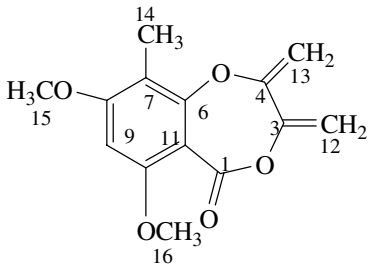

Table 48 The ^{1}H and ^{13}C NMR data of compound **AR15** in $CDCl_3$

Position	δ_H (*mult*., J_{Hz})	δ_C (C-Type)
1	-	162.35 (C=O)
3	-	156.16 (C)
4	-	148.90 (C)
6	-	153.33 (C)
7	-	114.24 (C)
8	-	162.27 (C)
9	6.31 (*s*)	92.48 (CH)
10	-	158.88 (C)
11	-	105.00 (C)
12	a : 5.16 (*d*, 1.8)	106.63 (CH_2)
	b : 5.11 (*d*, 1.8)	
13	a : 4.95 (*d*, 1.5)	97.30 (CH_2)
	b : 4.86 (*d*, 1.5)	
14	2.10 (*s*)	7.85 (CH_3)
15	3.88 (*s*)	55.79 (CH_3)
16	3.89 (*s*)	56.44 (CH_3)

Table 49 The HMBC, COSY and NOE data of compound **AR15** in $CDCl_3$

Proton	HMBC	COSY	NOE
H-9	C-1, C-7, C-8, C-10, C-11	-	H_3-15, H_3-16
H_a-12	C-1, C-3, C-4	H_b-12	H_b-12
H_b-12	C-1, C-3, C-4	H_a-12	H_a-12
H_a-13	C-3, C-4	H_b-13	H_b-13, H_3-14

Table 49 Continued

Proton	HMBC	COSY	NOE
H_b-13	C-3, C-4	H_a-13	H_a-12, H_a-13
H_3-14	C-6, C-7, C-8	-	H_a-13, H_3-15
H_3-15	C-8	-	H-9, H_3-14
H_3-16	C-10	-	H-9

1.3.11 Compound AR16

Compound **AR16** with the molecular formula $C_{12}H_{12}O_4$ by EIMS (**Figure 26**) and the melting point 167-169 ^{0}C was obtained as a white solid. The UV spectrum displayed absorption bands at 202, 240, 278 and 331 nm, indicating the presence of a benzoyl chromophore. The IR spectrum exhibited an absorption band at 1774 cm^{-1} for an ester carbonyl group. The ^{1}H NMR data (**Figure 24**) (**Table 50**) were almost identical to those of compound **AR8** except that signals for the methyl (H_3-8, δ_H 1.79) and hydroxyl (3-OH, δ_H 1.60) groups in **AR8** were replaced by signals of gem-olefinic protons (H_{ab}-10, δ_H 5.30 and 5.19). These gem-olefinic protons were assigned as H_{ab}-10 on the basis of their HMBC correlations with C-3 (δ_C 152.36) and C-4 (δ_C 139.11). Signal enhancement of H_b-10 (δ_H 5.19) after irradiation of H_3-11 (δ_H 2.30) in the NOEDIFF experiment supported the assigned location of H_{ab}-10. Therefore, compound **AR16** was identified as a dehydrated product of **AR8**, a new derivative of phthalide.

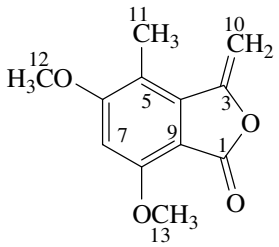

Table 50 The ^{1}H and ^{13}C NMR data of compound **AR16** in $CDCl_3$

Position	δ_H (*mult*., J_{Hz})	δ_C (C-Type)
1	-	157.80 (C=O)
3	-	152.36 (C)
4	-	139.11 (C)
5	-	114.13 (C)
6	-	164.28 (C)
7	-	96.00 (C)
8	-	157.80 (C)
9	-	105.50 (C)
10	a : 5.30 (*d*, 2.7)	95.23 (CH_2)
	b : 5.19 (*d*, 2.7)	
11	2.30 (*s*)	10.95 (CH_3)
12	3.96 (*s*)	56.35 (CH_3)
13	4.01 (*s*)	56.13 (CH_3)

Table 51 The HMBC, COSY and NOE data of compound **AR16** in $CDCl_3$

Proton	HMBC	COSY	NOE
H-7	C-1, C-5, C-6, C-9	-	H_3-12, H_3-13
H_a-10	C-3, C-4	H_b-10	H_b-10
H_b-10	C-3, C-4	H_a-10	H_a-10, H_3-11
H_3-11	C-4, C-5, C-6	-	H_b-10
H_3-12	C-6, C-7	-	H-7
H_3-13	C-1, C-7, C-8	-	H-7

1.3.12 Compound AR9

Compound **AR9** with the melting point 199-201 ^{0}C was obtained as a white solid. The UV spectrum displayed absorption bands at 203, 226 and 277 nm, indicating the presence of a benzene chromophore. The IR spectrum exhibited absorption bands at 3176 and 3059 cm^{-1} for amino groups, and 1674 cm^{-1} for an

amide carbonyl group. Comparision of its ^{1}H (**Figure 27**) and ^{13}C NMR (**Figure 28**) data (**Table 52**) and optical rotation, $[\alpha]_D^{25}$ -67.8 (c = 0.1, MeOH), with the previously reported data of Sch 54794 which was isolated from the broth extract of *Tolypocladium* sp., $[\alpha]_D^{25}$ -70.0 (c = 0.1, DMSO) (Chu *et al*., 1993), indicated that compound **AR9** was Sch 54794.

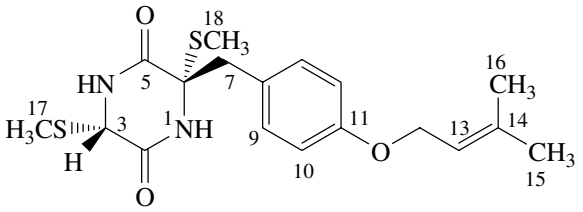

Table 52 The ^{1}H and ^{13}C NMR data of compound **AR9** and Sch 54794 in $CDCl_3$

Position	**AR9**		**Sch 54794**	
	δ_H (*mult., J_{Hz}*)	δ_C (C-type)	δ_H (*mult., J_{Hz}*)	δ_C (C-type)
1-NH	5.94 (*brs*)	-	-	-
2	-	164.83 (C=O)	-	165.5 (C=O)
3	4.23 (*d*, 2.1)	58.40 (CH)	4.25 (*s*)	58.1 (CH)
4-NH	6.02 (*brs*)	-	-	-
5	-	165.71 (C=O)	-	166.0 (C=O)
6	-	67.78 (C)	-	67.6 (C)
7	a: 3.45 (*d*, 13.8)	44.83 (CH_2)	3.49 (*d*, 13.7)	44.3 (CH_2)
	b: 2.95 (*d*, 13.8)		2.97 (*d*, 13.7)	
8	-	124.77 (C)	-	125.2 (C)
9, 9′	7.14 (*d*, 8.7)	131.84 (CH)	7.16 (*d*, 8.6)	131.7 (CH)
10, 10′	6.85 (*d*, 8.7)	114.98 (CH)	6.86 (*d*, 8.6)	114.7 (CH)
11	-	158.75 (C)	-	158.4 (C)
12	4.48 (*d*, 6.9)	64.83 (CH_2)	4.50 (*d*, 6.8)	64.7 (CH_2)
13	5.47 (*tm*, 6.9)	119.47 (CH)	5.49 (*t*, 6.8)	119.3 (CH)
14	-	138.40 (C)	-	138.3 (C)
15	1.74 (*s*)	25.83 (CH_3)	1.76 (*s*)	25.6 (CH_3)
16	1.80 (*s*)	18.23 (CH_3)	1.82 (*s*)	18.0 (CH_3)
17	2.22 (*s*)	13.94 (CH_3)	2.24 (*s*)	13.9 (CH_3)

Table 52 Continued

Position	**AR9**		**Sch 54794**	
	δ_H (*mult., J_{Hz}*)	δ_C (C-type)	δ_H (*mult., J_{Hz}*)	δ_C (C-type)
18	2.27 (*s*)	13.74 (CH_3)	2.30 (*s*)	13.5 (CH_3)

Chu *et al*., 1993.

1.3.13 Compound AR10

Compound **AR10** with the melting point 208-210 ^{0}C was obtained as a white solid and exhibited UV and IR absorption bands similar to those of compound **AR9**. The ^{1}H NMR data (**Figure 29**) (**Table 53**) were almost identical to those of compound **AR9** except for the appearance of a singlet signal for H_3-17 (δ_H 1.64) (**Table 53**) at much higher field. Comparision of its ^{13}C NMR data (**Figure 30**) (**Table 53**) and optical rotation, $[\alpha]_D^{25}$ -22.2 (c = 0.1, MeOH), with the previously reported data of Sch 54796 which was isolated from the broth extract of *Tolypocladium* sp., $[\alpha]_D^{25}$ -25.0 (c = 0.1, DMSO) (Chu *et al*., 1993), indicated that **AR10** was Sch 54796.

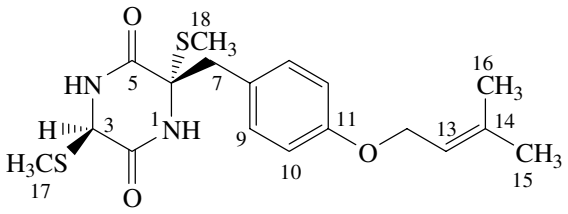

Table 53 The ^{1}H and ^{13}C NMR data of compound **AR10** and Sch 54796 in $CDCl_3$

Position	**AR10**		**Sch 54796**	
	δ_H (*mult., J_{Hz}*)	δ_C (C-type)	δ_H (*mult., J_{Hz}*)	δ_C (C-type)
1-H	5.97 (*brs*)	-	-	-
2	-	164.47 (C=O)	-	165.6 (C=O)
3	4.90 (*d*, 1.5)	58.47 (CH)	4.93 (*s*)	57.8 (CH)
4-H	6.05 (*brs*)	-	-	-
5	-	165.34 (C=O)	-	165.9 (C=O)
6	-	67.75 (C)	-	68.1 (C)

Table 53 Continued

Position	AR10		Sch 54796	
	δ_H (*mult.*, J_{Hz})	δ_C (C-type)	δ_H (*mult.*, J_{Hz})	δ_C (C-type)
7	a: 3.50 (*d*, 14.0)	43.03 (CH_2)	3.60 (*d*, 13.7)	42.3 (CH_2)
	b: 2.95 (*d*, 14.0)		2.95 (*d*, 13.7)	
8	-	125.08 (C)	-	126.1 (C)
9, 9′	7.10 (*d*, 8.5)	132.05 (CH)	7.19 (*d*, 8.7)	132.0 (CH)
10, 10′	6.78 (*d*, 8.5)	115.00 (CH)	6.83 (*d*, 8.7)	114.6 (CH)
11	-	158.77 (C)	-	158.5 (C)
12	4.41 (*d*, 6.5)	64.86 (CH_2)	4.47 (*d*, 6.7)	64.5 (CH_2)
13	5.39 (*tm*, 7.0)	119.58 (CH)	5.46 (*t*, 6.7)	119.4 (CH)
14	-	138.25 (C)	-	138.3 (C)
15	1.72 (*s*)	25.76 (CH_3)	1.74 (*s*)	25.1 (CH_3)
16	1.67 (*s*)	18.17 (CH_3)	1.79 (*s*)	17.5 (CH_3)
17	1.64 (*s*)	11.34 (CH_3)	1.48 (*s*)	9.8 (CH_3)
18	2.16 (*s*)	13.28 (CH_3)	2.22 (*s*)	12.2 (CH_3)

Chu *et al*., 1993.

1.3.14 Compound AR12

Compound **AR12** with the molecular formula $C_{13}H_{14}O_6$ by EIMS (**Figure 33**) was obtained as a pale yellow gum. The UV spectrum displayed absorption bands at 217, 268 and 315 nm, indicating the presence of a benzene chromophore. The IR spectrum exhibited absorption bands at 3432, 1716 and 1673 cm^{-1} for hydroxyl, ketone carbonyl and ester carbonyl groups, respectively. The ^1H NMR spectrum (**Figure 31**) (**Table 54**) contained signals for one chelated hydroxy proton (δ_H 11.59, *s*, 1H), one hydroxy proton (δ_H 4.50, *s*, 1H), one aromatic proton (δ_H 6.52, *s*, 1H), one set of nonequivalent oxymethylene protons ([δ_H 4.39 (*d*, J = 12.0 Hz, 1H) and 4.19 (*d*, J = 12.0 Hz, 1H)], one methoxyl group (δ_H 3.87, *s*, 3H) and two methyl groups [δ_H 2.26 (*s*, 3H) and 1.96 (*s*, 3H)]. The ^{13}C NMR spectrum (**Figure 32**) (**Table 54**) contained one ketone carbonyl carbon (δ_C 206.39), one ester carbonyl

carbon (169.36), six quaternary carbons (δ_C 165.31, 164.40, 136.89, 118.30, 100.20 and 76.06), one methine carbon (δ_C 99.86), one oxymethylene carbon (δ_C 71.44), one methoxy carbon (δ_C 56.03) and two methyl carbons (δ_C 25.39 and 11.35). The chelated hydroxy proton (δ_H 11.59) was placed at C-9, a *peri* position to the ester carbonyl carbon (δ_C 169.36), and showed the HMBC correlations with C-8 (δ_C 99.86), C-9 (δ_C 164.40) and C-10 (δ_C 100.20). The aromatic proton at δ_H 6.52 was assigned as H-8 according to its HMQC with C-8. Irradiation of H_3-14 (δ_H 3.87) in the NOEDIFF experiment (**Table 54**) affected signal intensity of H-8 and H_3-13 (δ_H 1.96). These results together with the HMBC correlation of H_3-14/C-7 (δ_C 165.31) and that of H_3-13/C-6 (δ_C 118.30) attached the methoxyl and the methyl groups at C-7 and C-6, respectively. The nonequivalent oxymethylene protons (H_{ab}-3, δ_H 4.39 and 4.19) exhibited the HMBC correlations with C-4 (δ_C 76.06), C-5 (δ_C 136.89) and C-11 (δ_C 206.39) while the methyl protons (H_3-12, δ_H 2.26) exhibited the HMBC correlations with C-4 and C-11. These data together with the HMBC correlation of H_{ab}-3 with C-1 established an isochromanone derivative with a hydroxyl group and an acetyl moiety at C-4. Irradiation of H_3-12 in the NOEDIFF experiment enhanced signal intensity of H_3-13, supporting above assignment. Thus, **AR12** was assigned as a new isochromanone derivative.

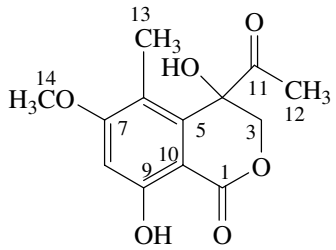

Table 54 The NMR data of compound **AR12** in $CDCl_3$

Position	δ_H (*mult.*, J_{Hz})	δ_C (C-Type)	HMBC	NOE
1	-	169.36 (C=O)	-	*
3	a : 4.39 (*d*, 12.0)	71.44 (CH_2)	C-1, C-4, C-5, C-11	*
	b : 4.19 (*d*, 12.0)		C-1, C-4, C-5, C-11	*
4	-	76.06 (C)	-	*

Table 54 Continued

Position	δ_H (*mult*., J_{Hz})	δ_C (C-Type)	HMBC	NOE
4-OH	4.50 (*s*)	-	C-3, C-4, C-5	*
5	-	136.89 (C)	-	*
6	-	118.30 (C)	-	*
7	-	165.31 (C)	-	*
8	6.52 (*s*)	99.86 (CH)	C-1, C-6, C-7, C-9, C-10	*
9	-	164.40 (C)	-	*
9-OH	11.59 (*s*)	-	C-8, C-9, C-10	*
10	-	100.20 (C)	-	*
11	-	206.39 (C=O)	-	*
12	2.26 (*s*)	25.39 (CH_3)	C-1, C-4	H_b-3, H_3-13
13	1.96 (*s*)	11.35 (CH_3)	C-5, C-6, C-7	H_3-12, H_3-14
14	3.87 (*s*)	56.03 (CH_3)	C-7, C-8	H-8, H_3-13

* not determined

1.3.15 Compound AR13

Compound **AR13** with the molecular formula $C_{13}H_{16}O_6$ by EIMS (**Figure 36**) was obtained as a pale yellow gum. The UV spectrum displayed absorption bands at 203, 217, 268, and 312 nm. The IR spectrum exhibited absorption bands at 3394 and 1652 cm^{-1} for hydroxyl and ester carbonyl groups, respectively. The ^1H NMR data (**Figure 34**) (**Table 55**) were almost identical to those of compound **AR12** except for the replacement of signals for nonequivalent oxymethylene protons (H_{ab}-3, δ_H 4.39 and 4.19) and the acetyl group (H_3-12, δ_H 2.26) in compound **AR12** with those for a 1-substituted oxyethyl group (H_3-11, δ_H 1.51, *d*, *J* = 6.5 Hz and H-3, δ_H 4.44, *q*, *J* = 6.5 Hz) and nonequivalent hydroxymethyl group (H_{ab}-12, δ_H 4.02 and 3.72), respectively. The location of the 1-substituted oxyethyl group and the hydroxymethyl unit was confirmed by HMBC correlations of H_{ab}-12/C-3 (δ_C 79.48), C-4 (δ_C 73.42) and C-5 (δ_C 141.02) and those of H_3-11 with C-3 and C-4

(**Table 55**). Irradiation of H_{ab}-12 affected signal intensity of H_3-11 in the NOEDIFF experiment (**Table 55**), indicating that H_{ab}-12 and H_3-11 were *cis*. Therefore, compound **AR13** was identified as a new isochromanone derivative.

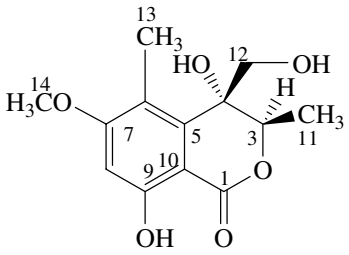

Table 55 The NMR data of compound **AR13** in $CDCl_3$

Position	δ_H (*mult.*, J_{Hz})	δ_C (C-Type)	HMBC	NOE
1	-	169.89 (C=O)	-	*
3	4.44 (*q*, 6.5)	79.48 (CH)	C-4, C-5, C-11, C-12	H_3-11
4	-	73.42 (C)	-	*
4-OH	2.97 (*s*)	-	C-4, C-5, C-12	*
5	-	141.02 (C)	-	*
6	-	117.30 (C)	-	*
7	-	165.18 (C)	-	*
8	6.39 (*s*)	98.97 (CH)	C-1, C-6, C-7, C-9, C-10	*
9	-	163.35 (C)	-	*
9-OH	11.52 (*s*)	-	C-8, C-9, C-10	*
10	-	100.30 (C)	-	*
11	1.51 (*d*, 6.5)	14.68 (CH_3)	C-3, C-4	H-3, H_{ab}-12
12	a : 4.02 (*d*, 11.0)	62.57 (CH_2)	C-3, C-4, C-5	H_b-12, H_3-11
	b : 3.72 (*d*, 11.0)		C-3, C-4, C-5	H_a-12, H_3-13
13	2.27 (*s*)	12.22 (CH_3)	C-5, C-6, C-7	H_b-12, H_3-14

Table 55 Continued

Position	δ_H (*mult*., J_{Hz})	δ_C (C-Type)	HMBC	NOE
14	3.79 (*s*)	55.93 (CH_3)	C-7	H-8, H_3-13

* not determined

1.3.16 Compound AR17

Compound **AR17** with the molecular formula $C_{13}H_{16}O_6$ by EIMS (**Figure 39**) was obtained as a pale yellow gum. The UV spectrum displayed absorption bands at 204, 217, 230, 270 and 314 nm. The IR spectrum exhibited absorption bands at 3370 and 1654 cm^{-1} for hydroxyl and ester carbonyl groups, respectively. The ^{1}H NMR data (**Figure 37**) (**Table 56**) were almost identical to those of compound **AR12** except for signal replacement of the acetyl group (H_3-12, δ_H 2.26) with a 1-hydroxyethyl unit [H-11 (δ_H 4.17, *q*, *J* = 6.5 Hz) and H_3-12 (δ_H 1.20, *d*, *J* = 6.5 Hz)]. The ^3J HMBC correlations of H-11 with C-3 (δ_C 70.36) and C-5 (δ_C 138.97) (**Table 56**) confirmed the assigned position for the 1-hydroxyethyl group. Irradiation of H_3-12 enhanced signal intensity of H_3-13 (δ_H 2.42) in the NOEDIFF experiment (**Table 56**), supporting above assignment. Consequently, compound **AR17** was identified as a new isochromanone derivative.

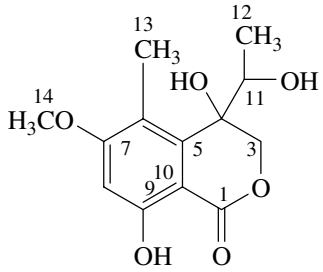

Table 56 The NMR data of compound **AR17** in $CDCl_3$

Position	δ_H (*mult*., J_{Hz})	δ_C (C-Type)	HMBC	NOE
1	-	169.90 (C=O)	-	*
3	a : 4.46 (*d*, 10.5)	70.36 (CH_2)	C-1, C-4, C-5, C-11	H_b-3, H-11
	b : 4.14 (*d*, 10.5)		C-1, C-4, C-5, C-11	*

Table 56 Continued

Position	δ_H (*mult*., J_{Hz})	δ_C (C-Type)	HMBC	NOE
4	-	74.32 (C)	-	*
4-OH	2.75 (*s*)	-	C-4, C-5, C-11	*
5	-	138.97 (C)	-	*
6	-	117.87 (C)	-	*
7	-	165.14 (C)	-	*
8	6.46 (*s*)	98.67 (CH)	C-1, C-6, C-7, C-9, C-10	*
9-OH	11.64 (*s*)	-	C-8, C-9, C-10	*
10	-	99.61 (C)	-	*
11	4.17 (*q*, 6.5)	69.04 (CH)	C-3, C-5, C-12	*
12	1.20 (*d*, 6.5)	17.36 (CH_3)	C-4, C-11	H-11, H_3-13
13	2.42 (*s*)	12.33 (CH_3)	C-5, C-6, C-7	H_3-12
14	3.88 (*s*)	55.85 (CH_3)	C-7	*

* not determined

1.3.17 Compound AR18

Compound **AR18** with the molecular formula $C_{13}H_{14}O_6$ by EIMS (**Figure 42**) was obtained as a pale yellow gum. The UV spectrum displayed absorption bands at 202, 249 and 333 nm, indicating the presence of a benzene chromophore. The IR spectrum exhibited absorption bands at 3352 and 1666 cm^{-1} for hydroxyl and ester carbonyl groups, respectively. The ^1H (**Figure 40)** and ^{13}C (**Figure 41)** NMR data (**Table 57**) indicated that compound **AR18** possessed a pentasubstituted benzene, identical to that of **AR12**, **AR13**, and **AR17**. In addition the ^1H NMR spectrum consisted of signals for two hydroxyl groups [δ_H 4.94 (*m*, 1H) and 4.49 (*m*, 1H)] and two sets of hydroxymethyl protons [δ_H 4.76 (*d*, J = 4.5 Hz, 2H) and 4.49 (*m*, 1H); 4.60 (*d*, J = 5.5 Hz, 2H) and 4.94 (*m*, 1H)]. The ^{13}C NMR spectrum (**Figure 41**) (**Table 57**) contained, apart from the ^{13}C signals of the pentasubstituted benzoyl moiety, two quarternary sp^2 carbons (δ_C 156.80 and 116.76) and two oxymethylene carbons (δ_C 60.34 and 57.60). The hydroxymethyl protons (H_2-11, δ_H

4.60) exhibited the HMBC correlations with C-3 (δ_C 156.80), C-4 (δ_C 116.76) and C-12 (δ_C 57.60) while the other hydroxymethyl protons (H_2-12, δ_H 4.76) displayed the same correlation with C-3, C-4 and C-5 (δ_C 137.69) (**Table 58**). These data established an isochromenone unit having two hydroxymethyl groups at C-3 and C-4. Signal enhancement of H_3-13 (δ_H 2.56) and H_2-11 upon irradiation of H_2-12 in the NOEDIFF experiment (**Table 58**) confirmed this assignment. Therefore, **AR18** was assigned as a new isochromenone derivative.

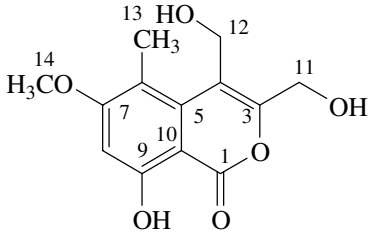

Table 57 The ^{1}H and ^{13}C NMR data of compound **AR18** in Acetone-d_6

Position	δ_H (*mult.*, J_{Hz})	δ_C (C-Type)
1	-	167.32 (C=O)
3	-	156.80 (C)
4	-	116.76 (C)
5	-	137.69 (C)
6	-	114.79 (C)
7	-	166.67 (C)
8	6.67 (*s*)	99.12 (CH)
9	-	163.92 (C)
9-OH	11.93 (*s*)	-
10	-	101.22 (C)
11	4.60 (*d*, 5.5)	60.34 (CH_2)
11-OH	4.94 (*m*)	-
12	4.76 (*d*, 4.5)	57.60 (CH_2)
12-OH	4.49 (*m*)	-
13	2.56 (*s*)	12.09 (CH_3)

Table 57 Continued

Position	δ_H (*mult*., J_{Hz})	δ_C (C-Type)
14	3.98 (*s*)	56.74 (CH_3)

Table 58 The HMBC, COSY and NOE data of compound **AR18** in Acetone-d_6

Proton	HMBC	COSY	NOE
H-8	C-6, C-7, C-9, C-10	-	*
9-OH	C-7, C-8, C-9, C-10	-	*
H_2-11	C-3, C-4, C-12	11-OH	H_2-12
11-OH	C-11	H_2-11	*
H_2-12	C-3, C-4, C-5	12-OH	H_2-11, H_3-13
12-OH	C-4, C-12	H_2-12	*
H_3-13	C-5, C-6, C-7	-	H_2-12
H_3-14	C-7	-	H-8

* not determined

1.3.18 Compound AR14

Compound **AR14** with the molecular formula $C_{20}H_{26}O_{10}$ by EIMS (**Figure 45**) and the melting point 180-182 ^{0}C was obtained as a white solid. The UV spectrum displayed absorption bands at 202, 249, 305 and 335 nm. The IR spectrum exhibited absorption bands similar to those of **AR18**. The ^{1}H NMR data (**Figure 43**) (**Table 59**) were almost identical to those of compound **AR18** except for the presence of typical signals for *β*-glucopyranose unit [δ_H 4.43 (*d*, *J* = 8.0 Hz, 1H), 3.92 (*m*, 1H)/3.76 (*brd*, *J* = 12.0 Hz, 1H), 3.66 (*t*, *J* = 9.0 Hz, 1H), 3.41 (*dd*, *J* = 9.0, 8.0 Hz, 1H), 3.36 (*ddd*, *J* = 9.0, 4.5, 3.0 Hz, 1H) and 3.24 (*t*, *J* = 9.0 Hz, 1H)] (Bunyapaiboonsri *et al*., 2008) and signal replacement for one of the hydroxymethyl group with a methyl group (δ_H 2.41, *s*, 3H). The methyl group was located at C-4 (δ_C 115.30) on the basis of their HMBC correlations with C-3 (δ_C 147.00), C-4 and C-5 (δ_C 137.50) (**Table 60**). The anomeric proton, H-1′ (δ_H 4.43), displayed the ^3J HMBC correlation with C-11 (δ_C 66.49), thus connecting the glucose unit at C-11. In

addition, the ^{1}H NMR spectrum displayed an addition signal of a methoxyl group (δ_H 3.60, *s*, 3H). These methoxy protons established the ^{3}J HMBC correlation with C-4′ (δ_C 79.06), thus linking the methoxyl group at C-4′. Consequently, compound **AR14** was identified as a new isochromenone glucoside.

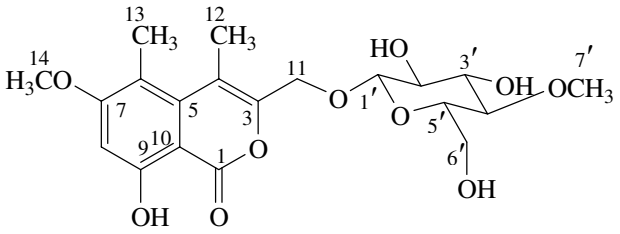

Table 59 The ^{1}H and ^{13}C NMR data of compound **AR14** in $CDCl_3$

Position	δ_H (*mult*., J_{Hz})	δ_C (C-Type)
1	-	167.00 (C=O)
3	-	147.00 (C)
4	-	115.30 (C)
5	-	137.50 (C)
6	-	114.50 (C)
7	-	165.50 (C)
8	6.58 (*s*)	98.81 (CH)
9	-	162.93 (C)
9-OH	11.85 (*s*)	-
10	-	100.50 (C)
11	a : 4.68 (*d*, 12.5)	66.49 (CH_2)
	b : 4.62 (*d*, 12.5)	
12	2.41 (*s*)	17.18 (CH_3)
13	2.38 (*s*)	13.69 (CH_3)
14	3.92 (*s*)	56.03 (CH_3)
1′	4.43 (*d*, 8.0)	102.11 (CH)
2′	3.41 (*dd*, 9.0, 8.0)	73.96 (CH)
3′	3.66 (*t*, 9.0)	76.41 (CH)
4′	3.24 (*t*, 9.0)	79.06 (CH)
5′	3.36 (*ddd*, 9.0, 4.5, 3.0)	75.70 (CH)

Table 59 Continued

Position	δ_H (*mult*., J_{Hz})	δ_C (C-Type)
6′	a : 3.92 (*m)*	62.03 (CH_2)
	b : 3.76 (*brd*, 12.0)	
7′	3.60 (*s*)	60.70 (CH_3)

Table 60 The HMBC, COSY and NOE data of compound **AR14** in $CDCl_3$

Proton	HMBC	COSY	NOE
H-8	C-6, C-7, C-9, C-10	-	*
9-OH	C-8, C-9, C-10	-	*
H_a-11	C-3, C-4, C-1′	H_b-11	*
H_b-11	C-3, C-4, C-1′	H_a-11	*
H_3-12	C-3, C-4, C-5	-	*
H_3-13	C-5, C-6, C-7	-	*
H_3-14	C-7	-	H-8
H-1′	C-11	H-2′	H-3′, H-5′, H_{ab}-11
H-2′	C-1′, C-3′	H-1′, H-3′	*
H-3′	C-2′, C-4′	H-2′, H-4′	*
H-4′	C-3′, C-5′, C-7′	H-3′, H-5′	H_3-7′
H-5′	C-4′	H-4′, H_{ab}-6′	*
H_a-6′	-	H-5′, H_b-6′	*
H_b-6′	-	H-5′, H_a-6′	*
H_3-7′	C-4′	-	H-4′, H_a-6′

* not determined

1.3.19 Compound AR20

Compound **AR20** with the molecular formula $C_{12}H_{12}O_6$ by EIMS (**Figure 48**) was obtained as a pale yellow gum. The UV spectrum displayed absorption bands at 200 and 247 nm. The IR spectrum exhibited absorption bands similar to those of compound **AR18**. The ^{1}H NMR data (**Figure 46**) (**Table 61**) were

almost identical to those of compound **AR18** except for the disappearance of the methoxy signal in compound **AR20**. The chemical shift of C-7 (δ_C 165.40) established a hydroxyl substituent at this carbon. All substitutents were located at the same position as those in compound **AR18** according to the HMBC correlations and NOEDIFF data (**Table 61**). Thus, compound **AR20** was identified as a demethylated **AR18**, a new isochromenone derivative.

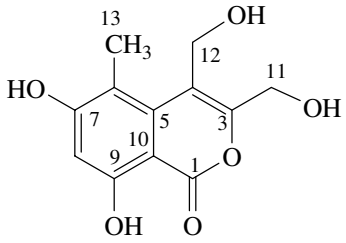

Table 61 The NMR data of compound **AR20** in Acetone-d_6

Position	δ_H (*mult*., J_{Hz})	δ_C (C-Type)	HMBC	NOE
1	-	167.00 (C=O)	-	*
3	-	156.80 (C)	-	*
4	-	117.00 (C)	-	*
5	-	138.80 (C)	-	*
6	-	113.90 (C)	-	*
7	-	165.40 (C)	-	*
8	6.58 (*s*)	102.63 (CH)	C-6, C-7, C-9, C-10	*
9	-	163.50 (C)	-	*
9-OH	11.84 (*s*)	-	C-8, C-9, C-10	*
10	-	101.00 (C)	-	*
11	4.61 (*d*, 5.5)	60.39 (CH_2)	C-3, C-4	H_2-12
11-OH	4.84 (*m*)	-	-	*
12	4.78 (*d*, 4.5)	57.55 (CH_2)	C-3, C-4, C-5	H_2-11, H_3-13
12-OH	4.38 (*m*)	-	-	*
13	2.58 (*s*)	12.06 (CH_3)	C-5, C-6, C-7	H_2-12

* not determined

1.3.20 Compound AR19

Compound **AR19** with the molecular formula $C_{11}H_{10}O_5$ by EIMS (**Figure 51**) was obtained as a pale yellow gum. The UV spectrum displayed absorption bands at 201, 219, 246, and 328 nm. The IR spectrum exhibited absorption bands similar to those of compound **AR20**. The ^{1}H NMR data (**Figure 49**) (**Table 62**) were almost identical to those of compound **AR20** except for signal replacement of one hydroxymethyl group in compound **AR20** with a methyl group (δ_H 2.19) in compound **AR19**. The ^3J HMBC correlations of the methyl protons with C-3 (δ_C 153.01) and C-5 (δ_C 142.00) (**Table 62**) indicated the attachment of the methyl group at C-4 (δ_C 111.80). Signal enhancement of H-6 (δ_H 6.56) and H_2-11 (δ_H 4.51) in the NOEDIFF experiment upon irradiation of H_3-12 (**Table 62**) supported the assigned location of the methyl group. Accordingly, compound **AR19** was identified as a new isochromenone derivative.

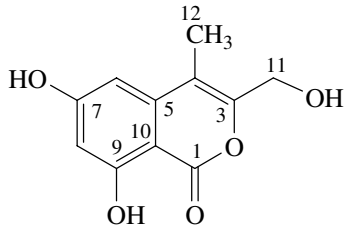

Table 62 The ^{1}H and ^{13}C NMR data of compound **AR19** in Acetone-d_6

Position	δ_H (*mult.*, J_{Hz})	δ_C (C-Type)
1	-	167.00 (C=O)
3	-	153.01 (C)
4	-	111.80 (C)
5	-	142.00 (C)
6	6.56 (*d*, 2.0)	102.23 (CH)
7	-	166.63 (C)
8	6.46 (*d*, 2.0)	102.71 (CH)
9	-	165.00 (C)
9-OH	11.49 (*s*)	-

Table 62 Continued

Position	δ_H (*mult*., J_{Hz})	δ_C (C-Type)
10	-	100.50 (C)
11	4.51 (*d*, 5.5)	59.64 (CH_2)
11-OH	4.65 (*m*)	-
12	2.19 (*s*)	11.95 (CH_3)

Table 63 The HMBC, COSY and NOE data of compound **AR19** in Acetone-d_6

Proton	HMBC	COSY	NOE
H-6	C-1, C-4, C-8, C-10	H-8	H_3-12
H-8	C-6, C-7, C-9, C-10	H-6	*
9-OH	C-8, C-9, C-10	-	*
H_2-11	C-3, C-4	11-OH	H_3-12
11-OH	C-11	H_2-11	*
H_3-12	C-3, C-4, C-5	-	H-6, H_2-11

* not determined

PART II

METABOLITES FROM THE MANGROVE-DERIVED FUNGUS *PESTALOTIOPSIS* SP. PSU-MA92

CHAPTER 2.1

INTRODUCTION

2.1.1 Introduction

In the literatures, the research on metabolites from fungi in the genus *Pestalotiopsis* has displayed that these fungi produce many types of secondary metabolites. Some of them showed interesting biological activities such as antifungal jesterone (Li *et al*., 2001), antibacterial 6-hydroxypunctaporonin A (Deyrup *et al*., 2006), and anti-HIV-1 pestalazine A (Ding *et al*., 2008). Based on SciFinder Scholar Database, secondary metabolites isolated from the genus *Pestalotiopsis* since the year 2000 are summarized in **Table 64** The ethyl acetate extract from the broth of *Pestalotiopsis* sp. PSU-MA92 exhibited no antibacterial activity against *S. aureus*, *P. aeruginosa* and *E. coli* at the concentration of 200 µg/mL. However, it showed antioxidant activity in $DPPH^{\bullet}$ assay with the IC_{50} value of 2.97 mg/mL.

Pestalotiopsis sp. PSU-MA92 was isolated from the twigs of *R. apiculata*, collected from Trang province, Thailand in the year 2006. It was deposited at the Department of Microbiology, Faculty of Science, Prince of Songkla University.

Table 64 Compounds isolated from the *Pestalotiopsis* genus

Scientific name	Compound	Activity	Reference
P. adusta	Pestalachloride A, **49** Pestalachloride B, **50** Pestalachloride C, **51**	Antifungal	Li *et al.*, 2008
P. disseminata	6-Hydroxypunctaporonin A, **52** 6-Hydroxypunctaporonin B, **53** 6-Hydroxypunctaporonin E, **54**	Antibacterial	Deyrup *et al*., 2006

Table 64 Continued

Scientific name	Compound	Activity	Reference
P. fici	Pestaloficiol A, **55** Pestaloficiol B, **56** Pestaloficiol C, **57** Pestaloficiol D, **58** Pestaloficiol E, **59**	Anti-HIV-1	Liu *et al*., 2008
	Pestalofone A, **60** Pestalofone B, **61** Pestalofone C, **62** Pestalofone D, **63** Pestalofone E, **64** Isosulochrin, **65** Isosulochrin dehydrate, **66** *iso*-A82775C, **67**	Anti-HIV-1 and antifungal	Liu *et al*., 2009
	Chloropestolide A, **68** Chloropupukeananin, **69**	Anti-HIV-1 and anticancer	Liu *et al*., 2009
	Pestaloficiol F, **70** Pestaloficiol G, **71** Pestaloficiol H, **72** Pestaloficiol I, **73** Pestaloficiol J, **74** Pestaloficiol K, **75** Pestaloficiol L, **76**	Anti-HIV-1 and cytotoxic	Liu *et al*., 2009
P. foedan	Pestafolide A, **77** Pestaphthalide A, **78** Pestaphthalide B, **79**	Antifungal	Ding *et al*., 2008
P. jesteri	Jesterone, **80** Hydroxyjesterone, **81**	Antimycotic	Li *et al*., 2001

Table 64 Continued

Scientific name	Compound	Activity	Reference
P. microspora	Pestacin, **82**	Antifungal and antioxidant	Harper *et al*., 2003
	Isopestacin, **83**	Antifungal and antioxidant	Strobel *et al*., 2002
P. photiniae	Photinide A, **84** Photinide B, **85** Photinide C, **86** Photinide D, **87** Photinide E, **88** Photinide F, **89**	Cytotoxic	Ding *et al*., 2009
Pestalotiopsis sp.	Ambuic acid, **90** (2*E*)-4-[(1*R*,5*R*,6*R*)-4-[(acetyloxy)methyl]-3-(1*E*)-1-hepten-1-yl-5-hydroxy-2-oxo-7-oxabicyclo[4.1.0]hept-3-en-1-yl]-2-methyl-2-butenoic acid, **91** (2*E*)-4-[(1*R*,5*R*,6*R*)-5-hydroxy-4-(hydroxymethyl)-2-oxo-3-[(1*E*)-5-oxo-1-hepten-1-yl]-7-oxabicyclo[4.1.0]hept-3-en-1-yl]-2-methyl-2-butenoic acid, **92** (2*E*)-4-[(1*R*,5*R*,6*R*)-3-heptyl-5-hydroxy-4-(hydroxymethyl)-2-oxo-7-oxabicyclo[4.1.0]-hept-3-en-1-yl]-2-methyl-2-	Antibacterial	Ding *et al*., 2009

Table 64 Continued

Scientific name	Compound	Activity	Reference
	butenoic acid, **93** (2*E*)-4-[(1*R*,5*R*,6*R*)-3-(1*E*,3*E*)-1,3-heptadien-1-yl-5-hydroxy-4-(hydroxymethyl)-2-oxo-7-oxabicyclo[4.1.0]hept-3-en-1-yl]-2-methyl-2-butenoic acid, **94** (2*E*)-4-[(6a*R*,7a*R*,7b*R*)-5-(1*E*)-1-hepten-1-yl-4,6,7a,7b-tetrahydro-2,2-dimethyl-6-oxo-6a*H*-oxireno[h]-1,3-benzodioxin-6a-yl]-2-methyl-2-butenoic acid, **95** (2*E*)-4-[(1*R*,2*S*)-3-(1*E*)-1-hepten-1-yl-1,2-dihydroxy-4-(hydroxymethyl)-5-oxo-3-cyclohexen-1-yl]-2-methyl-2-butenoic acid, **96** (2*E*,2'*E*)-4,4'-[(1a*R*,5*R*,5a*S*,-6*R*,7a*S*,8a*S*,9*S*,10*R*,10a*S*,11a*S*,-13*S*)-1a,2,5a,6,7,8a,9,10-octahydro-9-hydroxy-2,7,11-trioxo-5,13-dipentyl-10,6-(epoxymethano)bisoxireno-[4,5]benzo[1,2-d:1',2'-g][2]-benzopyran-7a,11a(5*H*,11*H*)-diyl]bis[2-methyl-2-butenoic acid, **97**		

Table 64 Continued

Scientific name	Compound	Activity	Reference
	Pestalodiopsolide A, **98** Taedolidol, **99** 6-Epitaedolidol, **100**	-	Magnani, *et al*., 2003
	Pestalotiopsone A, **101** Pestalotiopsone B, **102** Pestalotiopsone C, **103** Pestalotiopsone D, **104** Pestalotiopsone E, **105** Pestalotiopsone F, **106** 7-Hydroxy-2-(2-hydroxypropyl)-5-methylchromone, **107**	Cytotoxic	Xu *et al*., 2009
	Cytosporone C, **108** Cytosporone J, **109** Cytosporone K, **110** Cytosporone L, **111** Cytosporone M, **112** Cytosporone N, **113** Dothiorelone B, **114** Pestalasin A, **115** Pestalasin B, **116** Pestalasin C, **117** Pestalasin D, **118** Pestalasin E, **119** 3-Hydroxymethyl-6,8-dimethoxycoumarin, **120** Pestalotiopsiod A, **121**	Cytotoxic	Xu *et al*., 2009

Table 64 Continued

Scientific name	Compound	Activity	Reference
P. theae	Pestalazine A, **122** Pestalazine B, **123** Pestalamide A, **124** Pestalamide B, **125** Asperazine, **126** Pestalamide C, **127** Aspernigrin A, **128** Carbonarone A, **129**	Antifungal and anti-HIV-1	Ding *et al*., 2008
	Pestalotheol A, **130** Pestalotheol B, **131** Pestalotheol C, **132** Pestalotheol D, **133**	Anti-HIV-1	Li *et al*., 2008
	Chloroisosulochrin, **134** Chloroisosulochrin dehydrate, **135** Pestheic acid, **136**	Plant growth reculators	Shimada, *et al*., 2001

Structures of the metabolites isolated from the *Pestalotiopsis* genus

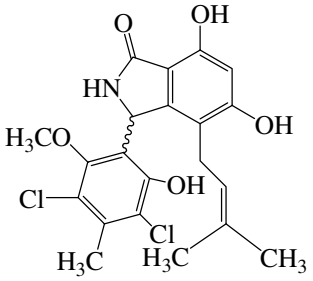

49 : Pestalachloride A

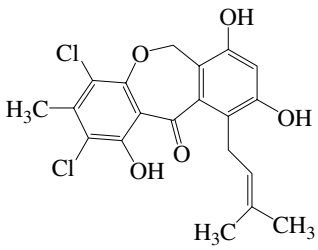

50 : Pestalachloride B

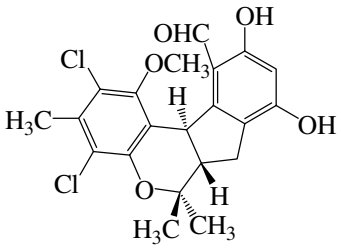

51 : Pestalachloride C

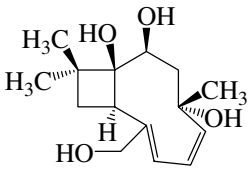

53 : 6-Hydroxypunctaporonin B

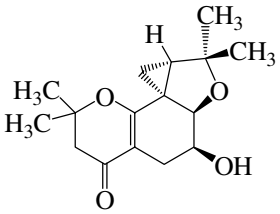

55 : Pestaloficiol A

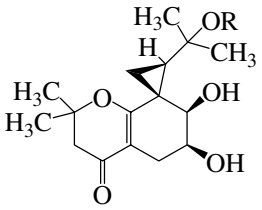

58 : R = H : Pestaloficiol D

59 : R = CH_3 : Pestaloficiol E

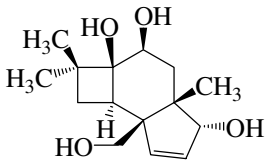

52 : 6-Hydroxypunctaporonin A

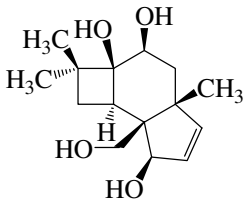

54 : 6-Hydroxypunctaporonin E

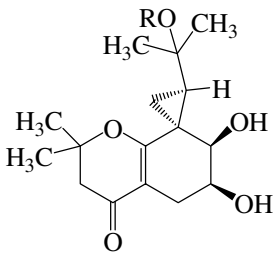

56 : R = H : Pestaloficiol B

57 : R = CH_3 : Pestaloficiol C

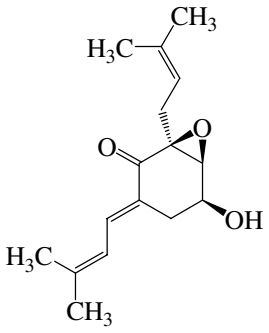

60 : Pestalofone A

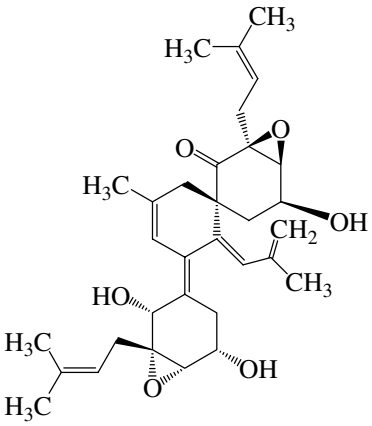

61 : Pestalofone B

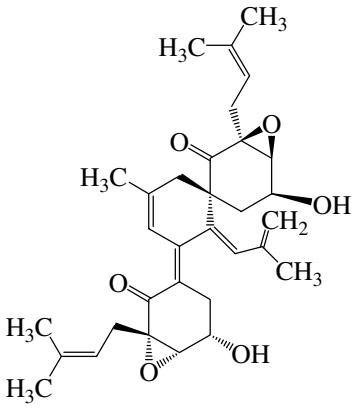

62 : Pestalofone C

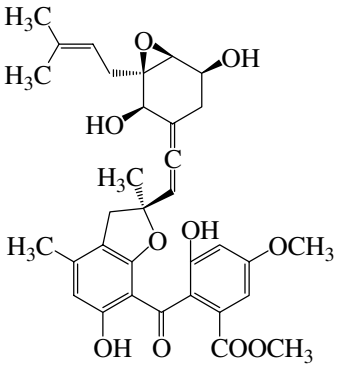

63 : Pestalofone D

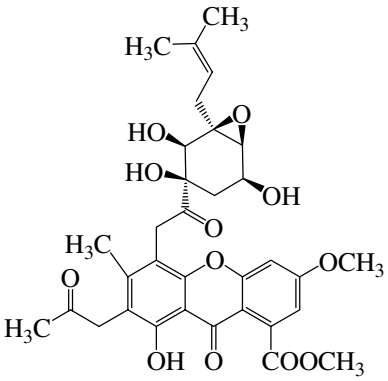

64 : Pestalofone E

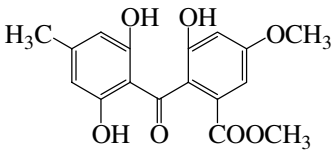

65 : Isosulochrin

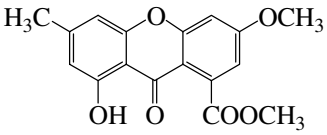

66 : Isosulochrin dehydrate

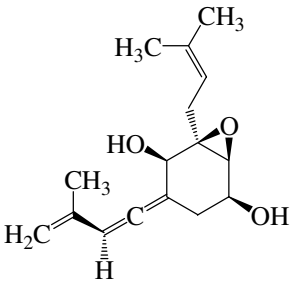

67 : *iso*-A82775C

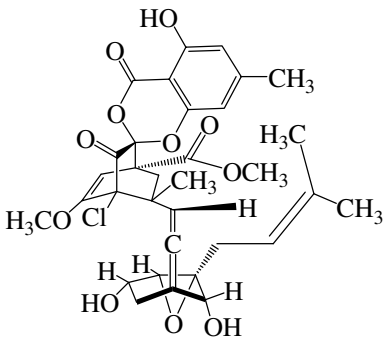

68 : Chloropestolide A

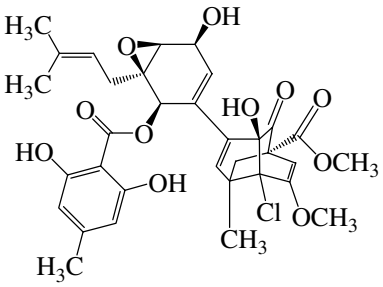

69 : Chloropupukeananin

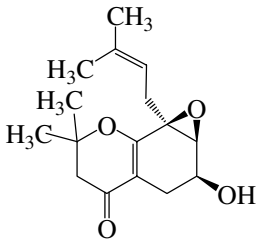

70 : Pestaloficiol F

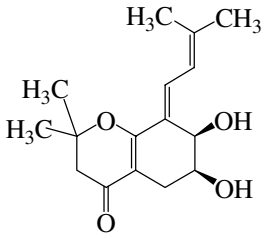

71 : Pestaloficiol G

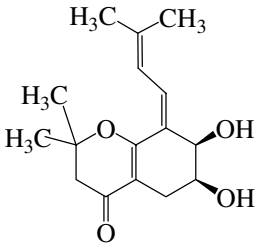

72 : Pestaloficiol H

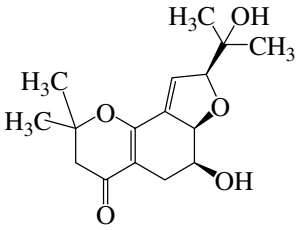

73 : Pestaloficiol I

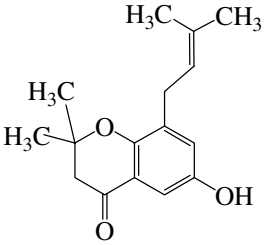

74 : Pestaloficiol J

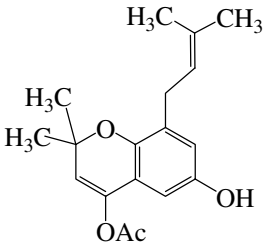

75 : Pestaloficiol K

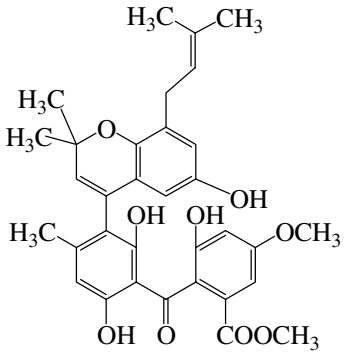

76 : Pestaloficiol L

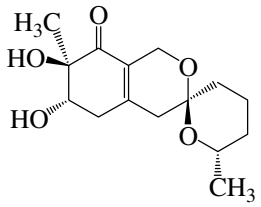

77 : Pestafolide A

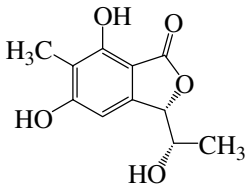

78 : Pestaphthalide A

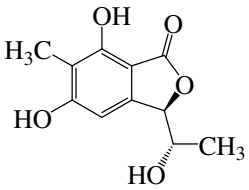

79 : Pestaphthalide B

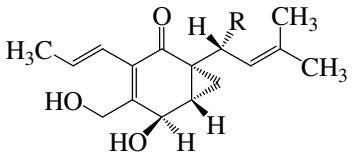

80 : R = H : Jesterone

81 : R = OH : Hydroxyjesterone

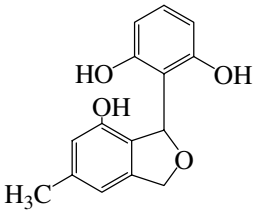

82 : Pestacin

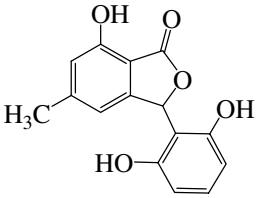

83 : Isopestacin

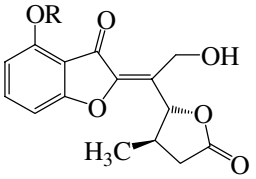

84 : R = CH_3 : Photinide A

86 : R = H : Photinide C

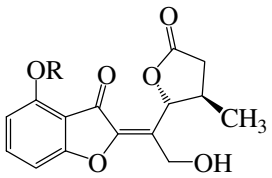

85 : R = CH_3 : Photinide B

87 : R = H : Photinide D

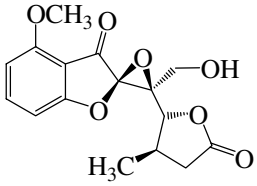

88 : Photinide E

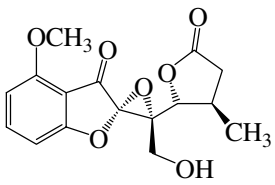

89 : Photinide F

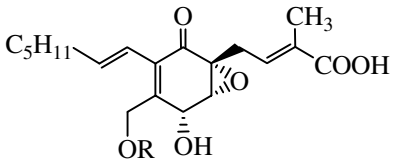

90 : R = H : Ambuic acid

91 : R = Ac : (2*E*)-4-[(1*R*,5*R*,6*R*)-4-[(acetyloxy)methyl]-3-(1*E*)-1-hepten-1-yl-5-hydroxy-2-oxo7-oxabicyclo[4.1.0]hept-3-en-1-yl]-2-methyl-2-butenoic acid

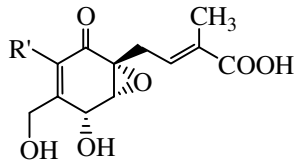

92 : R′ = 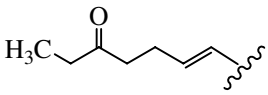

: (2*E*)-4-[(1*R*,5*R*,6*R*)-5-hydroxy-4-(hydroxymethyl)-2-oxo-3-[(1*E*)-5-oxo-1-hepten-1-yl]-7-oxabicyclo-[4.1.0]hept-3-en-1-yl]-2-methyl-2-butenoic acid

93 : R′ = 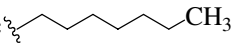

: (2*E*)-4-[(1*R*,5*R*,6*R*)-3-heptyl-5-hydroxy-4-(hydroxymethyl)-2-oxo-7-oxabicyclo[4.1.0]hept-3-en-1-yl]-2-methyl-2-butenoic acid

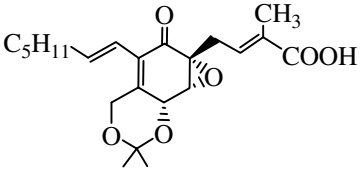

95 : (2*E*)-4-[(6a*R*,7a*R*,7b*R*)-5-(1*E*)-1-hepten-1-yl-4,6,7a,7b-tetrahydro-2,2-dimethyl-6-oxo-6a*H*-oxireno[h]-1,3-benzodioxin-6a-yl]-2-methyl-2-butenoic acid

94 : R′ = 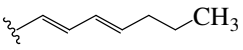

: (2*E*)-4-[(1*R*,5*R*,6*R*)-3-(1*E*,3*E*)-1,3-heptadien-1-yl-5-hydroxy-4-(hydroxymethyl)-2-oxo-7-oxabicyclo[4.1.0]hept-3-en-1-yl]-2-methyl-2-butenoic acid

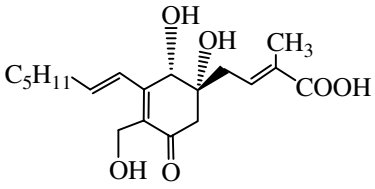

96 : (2*E*)-4-[(1*R*,2*S*)-3-(1*E*)-1-hepten-1-yl-1,2-dihydroxy-4-(hydroxymethyl)-5-oxo-3-cyclohexen-1-yl]-2-methyl-2-butenoic acid

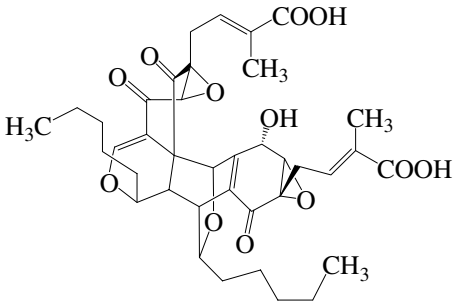

97 : (2*E*,2'*E*)-4,4'-[(1a*R*,5*R*,5a*S*,6*R*,7a*S*,8a*S*,9*S*,-10*R*,10a*S*,11a*S*,13*S*)-1a,2,5a,6,7,8a,9,10-octahydro-9-hydroxy-2,7,11-trioxo-5,13-dipentyl-10,6-(epoxymethano)bisoxireno-[4,5]benzo[1,2-d:1',2'-g][2]benzopyran-7a,11a(5*H*,11*H*)-diyl]bis[2-methyl-2-butenoic acid

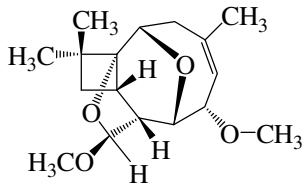

98 : Pestalodiopsolide A

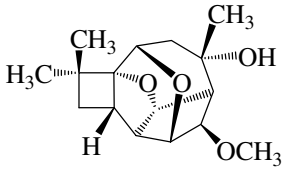

99 : Taedolidol

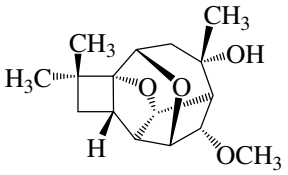

100 : 6-Epitaedolidol

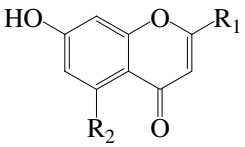

	R_1	R_2
101 :	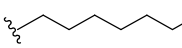	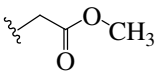
	: Pestalotiopsone A	
102 :	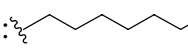	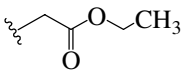
	: Pestalotiopsone B	
103 :	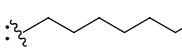	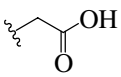
	: Pestalotiopsone C	
104 :	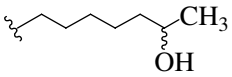	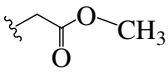
	: Pestalotiopsone D	

	R_1	R_2
105 :	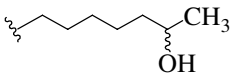	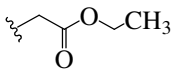
	: Pestalotiopsone E	
106 :	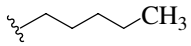	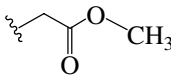
	: Pestalotiopsone F	
107 :	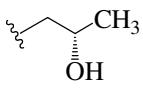	CH_3

: 7-Hydroxy-2-(2-hydroxypropyl)-5-methylchromone

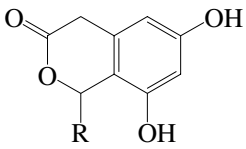

108 : R = 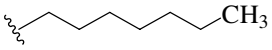

: Cytosporone C

109 : R = 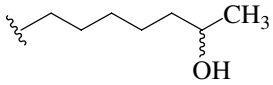

: Cytosporone J

110 : R = 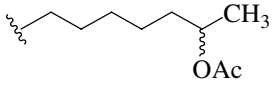

: Cytosporone K

111 : R = 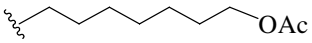

: Cytosporone L

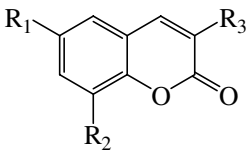

	R_1	R_2	R_3
115 :	OCH_3	OCH_3	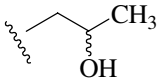
116 :	OCH_3	OCH_3	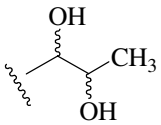
117 :	OCH_3	OCH_3	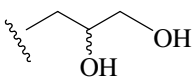
118 :	OCH_3	OH	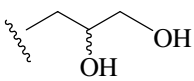

: Pestalasin A

: Pestalasin B

: Pestalasin C

: Pestalasin D

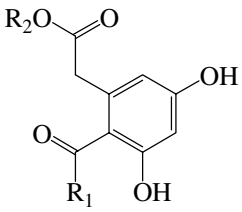

	R_1	R_2
112 :	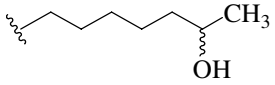	CH_3
113 :	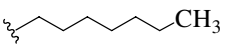	CH_3

: Cytosporone M

: Cytosporone N

	R_1	R_2
114 :	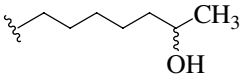	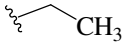

: Dothiorelone B

	R_1	R_2	R_3
119 :	OH	OCH_3	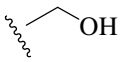
120 :	OCH_3	OCH_3	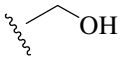

: Pestalasin E

: 3-Hydroxymethyl-6,8-dimethoxycoumarin

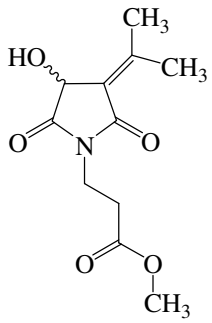

121 : Pestalotiopsiod A

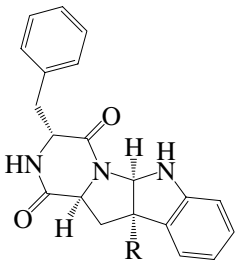

122 : R =

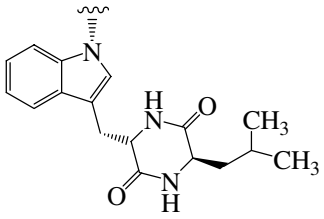

: Pestalazine A

123 : R =

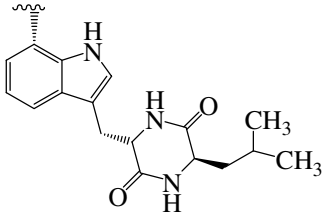

: Pestalazine B

126 : R =

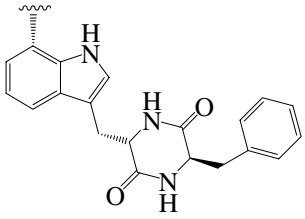

: Asperazine

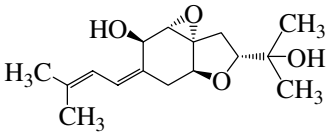

132 : Pestalotheol C

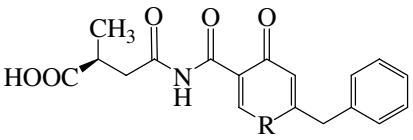

124 : R = O : Pestalamide A

125 : R = NH : Pestalamide B

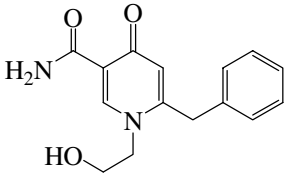

127 : Pestalamide C

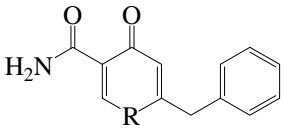

128 : R = NH : Aspernigrin A

129 : R = O : Carbonarone A

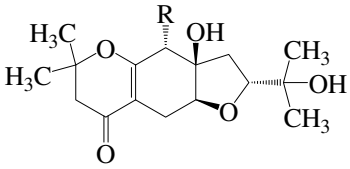

130 : R = OH : Pestalotheol A

131 : R = H : Pestalotheol B

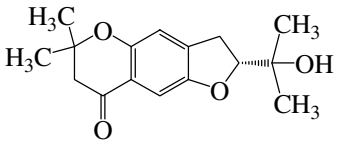

133 : Pestalotheol D

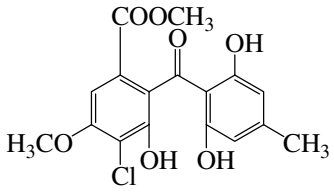

134 : Chloroisosulochrin

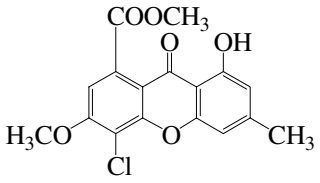

135 : Chloroisosulochrin dehydrate

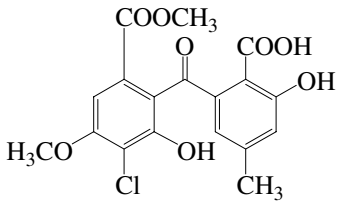

136 : Pestheic acid

2.1.2 The Objectives

1. To isolate the secondary metabolites from the mangrove-derived fungus *Pestalotiopsis* sp. PSU-MA92.
2. To elucidate the structures of the isolated compounds.

CHAPTER 2.2

EXPERIMENTAL

2.2.1 Fermentation and extraction

The flask culture of the fungus PSU-MA92 (15 L) in potato dextrose broth was filtered to separate into the filtrate and wet mycelia. The filtrate was divided into 37 portions. Each portion was extracted twice with an equal amount of EtOAc (2 x 300 mL). The organic layer was dried over anhydrous Na_2SO_4 and evaporated in *vacuo* to obtain a dark brown gum (340 mg). The crude extract was subjected to chromatographic purification.

2.2.2 Purification of the broth extract

The crude EtOAc extract was separated by column chromatography over Sephadex LH-20. Elution was performed with 100% methanol. Fractions with similar chromatogram were combined and evaporated to dryness under reduced pressure to afford four fractions, as shown in **Table 65**.

Table 65 Fractions obtained from the crude EtOAc extract by column chromatography over Sephadex LH-20

Fraction	Weight (mg)	Physical appearance
92A	36.4	Brown gum
92B	87.9	Brown gum
92C	68.1	Brown gum
92D	86.4	Brown gum

Fraction 92A did not show any UV-active spots on normal phase TLC using 2% methanol in dichloromethane as a mobile phase. The ^{1}H NMR spectrum displayed signals in high field region. Thus, it was not investigated.

Fraction 92B showed two UV-active spots on reverse phase TLC using 50% methanol in water as a mobile phase with the R_f values of 0.25 and 0.53. It was further separated by column chromatography over reverse phase silica gel. Elution was performed initially with 50% methanol in water, followed by pure methanol. Fractions with similar chromatogram were combined and evaporated to dryness under reduced pressure to afford five subfractions, as shown in **Table 66**.

Table 66 Subfractions obtained from **fraction 92B** by column chromatography over reverse phase silica gel

Subfraction	Elution	Weight (mg)	Physical appearance
92B1	50% MeOH/H_2O	24.6	Yellow gum
92B2	50% MeOH/ H_2O	13.9	Yellow gum
92B3	50% MeOH/ H_2O	4.1	Yellow gum
92B4	50% MeOH/ H_2O	19.2	Yellow gum
92B5	50% MeOH/ H_2O -100% MeOH	25.3	Brown gum

Subfraction 92B1 showed one UV-active spot on reverse phase TLC using 50% methanol in water as a mobile phase with the R_f value of 0.71. Its ^{1}H NMR spectrum displayed sugar signals. Thus, it was not investigated.

Subfraction 92B3 showed three UV-active spots on reverse phase TLC using 50% methanol in water as a mobile phase with the R_f values of 0.29, 0.43 and 0.55. It was further separated by column chromatography over silica gel. Elution was performed initially with 2% methanol in dichloromethane, followed by increasing the polarity with methanol and finally with pure methanol. Fractions with similar

chromatogram were combined and evaporated to dryness under reduced pressure to afford seven subfractions, as shown in **Table 67**.

Table 67 Subfractions obtained from **subfraction 92B2** by column chromatography over silica gel

Subfraction	Elution	Weight (mg)	Physical appearance
92B21	2% MeOH/CH_2Cl_2	3.0	Yellow gum
92B22	2% MeOH/CH_2Cl_2	4.2	Yellow gum
92B23	2% MeOH/CH_2Cl_2	0.4	Yellow gum
92B24	2% MeOH/CH_2Cl_2	1.4	Yellow gum
92B25	2% MeOH/CH_2Cl_2	2.0	Yellow gum
92B26	2-5% MeOH/CH_2Cl_2	0.2	Yellow gum
92B27	100% MeOH	2.7	Yellow gum

Subraction 92B21 showed three UV-active spots on normal phase TLC using 20% ethyl acetate in petroleum ether as a mobile phase (5 runs) with the R_f values of 0.73, 0.85 and 0.93. Because of the low quantity, it was not further investigated.

Subfraction 92B22 showed two UV-active spots on normal phase TLC using 20% ethyl acetate in petroleum ether as a mobile phase (5 runs) with the R_f values of 0.61, and 0.71. It was then purified by precoated TLC with 10% ethyl acetate in chloroform as a mobile phase (10 runs) to afford two bands.

Band 1 (AR21) was a colorless gum (1.6 mg). Its chromatogram showed one UV-active spot on normal phase TLC using 10% ethyl acetate in chloroform as a mobile phase (10 runs) with the R_f value of 0.60.

$[\alpha]_D^{25}$	+38.2 (c = 1.0, $CHCl_3$)
UV λ_{max}(nm)(MeOH)(log ε)	207 (3.03), 254 (3.45)
FTIR(neat) : υ(cm^{-1})	3407 (O-H stretching), 1679 (C=O stretching)
^{1}H NMR($CDCl_3$)(δ_{ppm})(300 MHz) :	4.40 (*dd, J* = 12.0, 1.5, Hz, 1H), 4.28 (*dd, J* = 12.0, 3.6, Hz, 1H), 4.16 (*qn*, *J* = 6.9 Hz,

	1H), 3.88 (*s*, 3H), 2.69 (*dd*, *J* = 6.9, 3.6, Hz, 1H), 1.83 (*s*, 3H), 1.36 (*d*, *J* = 6.9 Hz, 3H)
^{13}C NMR($CDCl_3$)(δ_{ppm})(125 MHz) :	167.64, 166.87, 105.24, 67.81, 65.29, 56.52, 40.92, 20.97, 9.28
CH :	67.81, 40.92
CH_2 :	65.29
CH_3 :	56.52, 20.97, 9.28
EIMS *m/z* (% relative intensity) :	186 (7), 142 (100), 124 (24), 109 (19), 97 (10)

Band 2 (AR22) was a colorless gum (1.4 mg). Its chromatogram showed one UV-active spot on normal phase TLC using 10% ethyl acetate in chloroform as a mobile phase (10 runs) with the R_f value of 0.53.

$[\alpha]_D^{25}$	-29.3 (c = 1.0, $CHCl_3$)
UV λ_{max}(nm)(MeOH)(log ε)	207 (3.18), 250 (3.51)
FTIR(neat) : υ(cm^{-1})	3405 (O-H stretching), 1679 (C=O stretching)
^{1}H NMR($CDCl_3$)(δ_{ppm})(300 MHz) :	4.58 (*d, J* = 11.7, Hz, 1H), 4.24 (*dd, J* = 11.7, 3.6, Hz, 1H), 4.05 (*m*, 1H), 3.83 (*s*, 3H), 2.62 (*brs*, 1H), 1.93 (*brs*, 1H), 1.84 (*s*, 3H), 1.32 (*d*, *J* = 6.6, Hz, 3H)
^{13}C NMR($CDCl_3$)(δ_{ppm})(125 MHz) :	167.73, 165.83, 107.39, 67.12, 65.49, 57.05, 40.90, 21.35, 9.54
CH :	67.12, 40.90
CH_2 :	65.49
CH_3 :	57.05, 21.35, 9.54
EIMS *m/z* (% relative intensity) :	186 (5), 142 (100), 124 (25), 109 (21), 97 (15)

Subfraction 92B23 showed one UV-active spot on normal phase TLC using 20% ethyl acetate in petroleum ether as a mobile phase (5 runs) with the R_f value of 0.59. Its ^{1}H NMR spectrum displayed many signals. Thus, it was not further investigated.

Subfraction 92B24 showed two UV-active spots on normal phase TLC using 20% ethyl acetate in petroleum ether as a mobile phase (5 runs) with the R_f values of 0.05 and 0.10. Because of the minute quantity and the presence of proton signals in high field region, it was not further investigated.

Subfraction 92B25 showed one UV-active spot on normal phase TLC using 20% ethyl acetate in petroleum ether as a mobile phase (5 runs) with the R_f value of 0.41. Because of the minute quantity and the presence of signals in high field region, it was not further investigated.

Subfraction 92B26 showed one UV-active spot on normal phase TLC using 20% ethyl acetate in petroleum ether as a mobile phase (5 runs) with the R_f value of 0.32. Because of the minute quantity, it was not further investigated.

Subfraction 92B27 showed two UV-active spots on normal phase TLC using 20% ethyl acetate in petroleum ether as a mobile phase (5 runs) with the R_f values of 0.17 and 0.29. Because of the low quantity and the presence of broad signals in the ^{1}H NMR spectrum, it was not further investigated.

Subfraction 92B3 showed two UV-active spots on reverse phase TLC using 50% methanol in water as a mobile phase with the R_f values of 0.24 and 0.29. It contained **AR24** as a major component. No further purification was carried out.

Subfraction 92B4 showed three UV-active spots on normal phase TLC using 40% ethyl acetate in petroleum ether as a mobile phase (5 runs) with the R_f values of 0.34, 0.59, and 0.76. It was further separated by column chromatography over silica gel. Elution was performed initially with 30% ethyl acetate in petroleum ether, followed by increasing the polarity with ethyl acetate and then methanol and finally with pure

methanol. Fractions with similar chromatogram were combined and evaporated to dryness under reduced pressure to afford nine subfractions, as shown in **Table 68**.

Table 68 Subfractions obtained from **subfraction 92B4** by column chromatography over silica gel

Subfraction	Elution	Weight (mg)	Physical appearance
92B41	30-40% EtOAc/Petrol	1.3	Yellow gum
92B42	40-50% EtOAc/Petrol	0.6	Yellow gum
92B43	50% EtOAc/Petrol	0.6	Yellow gum
92B44	50-60% EtOAc/Petrol	1.4	Yellow gum
92B45	60-70% EtOAc/Petrol	0.5	Yellow gum
92B46	70-80% EtOAc/Petrol	2.1	Colorless gum
92B47	80-90% EtOAc/Petrol	0.5	Yellow gum
92B48	90% EtOAc/Petrol-100% EtOAc	11.7	Colorless gum
92B49	100% EtOAc-100% MeOH	0.5	Yellow gum

Subfraction 92B41 did not show any UV-active spots on normal phase TLC using 1% methanol in dichloromethane but showed two spots after dipping the TLC plate in anisaldehyde reagent and subsequently heating the plate with the R_f values of 0.24 and 0.56. Because of the minute quantity, it was not further investigated

Subfraction 92B42 showed one UV-active spot on normal phase TLC using 40% ethyl acetate in petroleum ether as a mobile phase (5 runs) with the R_f value of 0.79. Because of the minute quantity and the absence of olefinic and aromatic protons in the ^{1}H NMR spectrum, it was not further investigated.

Subfraction 92B43 did not show any UV-active spots on normal phase TLC using 40% ethyl acetate in petroleum ether as a mobile phase (5 runs). Because of the minute quantity, it was not further investigated.

Subfraction 92B44 showed one UV-active spot on normal phase TLC using 40% ethyl acetate in petroleum ether as a mobile phase (5 runs) with the R_f value of 0.67. Unfortunately, it was decomposed.

Subfraction 92B45 did not show any UV-active spots on normal phase TLC using 40% ethyl acetate in petroleum ether as a mobile phase (5 runs). Because of the minute quantity, it was not further investigated.

Subfraction 92B46 (AR23) showed one UV-active spot on normal phase TLC using 40% ethyl acetate in petroleum ether as a mobile phase (5 runs) with the R_f value of 0.50.

$[\alpha]_D^{25}$	-44.07 (c = 0.33, MeOH)
UV λ_{max}(nm)(MeOH)(log ε)	210 (3.96), 287 (3.40)
FTIR(neat) : υ(cm^{-1})	3410 (O-H stretching), 1722, 1711 (C=O stretching)
^{1}H NMR(Acetone-d_6)(δ_{ppm}) : (300 MHz)	7.64 (*d*, *J* = 0.9 Hz, 1H), 5.69 (*hept*, *J* = 1.2 Hz, 1H), 5.05 (*s*, 2H), 4.81 (*m*, 1H), 4.42 (*d*, *J* = 4.5 Hz, 1H), 4.15 (*s*, 3H), 2.16 (*d*, *J* = 1.2 Hz, 3H), 1.90 (*d*, *J* = 1.2 Hz, 3H), 1.40 (*d*, *J* = 6.3 Hz, 3H)
^{13}C NMR(Acetone-d_6)(δ_{ppm}) : (75 MHz)	169.23, 165.62, 163.95, 157.13, 148.63, 122.42, 115.32, 106.14, 62.30, 61.67, 56.22, 26.29, 23.24, 19.23
CH :	148.63, 115.32, 62.30
CH_2 :	56.22
CH_3 :	61.67, 26.29, 23.24, 19.23
EIMS *m/z* (% relative intensity) :	282 (1), 199 (100), 183 (28), 153 (9), 139 (10), 83 (54)

Subfraction 92B47 did not show any UV-active spots on normal phase TLC using 40% ethyl acetate in petroleum ether as a mobile phase (5 runs) but showed one spot, after dipping the TLC plate in anisaldehyde reagent and subsequently heating the plate, with the R_f value of 0.36. Because of the minute quantity, it was not further investigated.

Subfraction 92B48 (AR24) showed one UV-active spot on normal phase TLC using 40% ethyl acetate in petroleum ether as a mobile phase (5 runs) with the R_f value of 0.33.

UV λ_{max}(nm)(MeOH)(log ε)	212 (3.54), 273 (3.79)
FTIR(neat) : υ(cm^{-1})	3414 (O-H stretching), 1720, 1712 (C=O stretching)
^{1}H NMR($CDCl_3$)(δ_{ppm})(300 MHz) :	5.68 (*s*, 1H), 5.07 (*s*, 2H), 4.46 (*s*, 2H), 4.09 (*s*, 3H), 2.35 (*s*, 3H), 2.17 (*s*, 3H), 1.88 (*s*, 3H)
^{13}C NMR($CDCl_3$)(δ_{ppm})(75 MHz) :	170.52, 166.31, 164.37, 161.86, 157.74, 148.63, 115.50, 113.07, 104.99, 62.41, 56.26, 56.03, 27.41, 20.29, 17.37
CH :	115.50
CH_2 :	56.26, 56.03
CH_3 :	62.41, 27.41, 20.29, 17.37
EIMS *m/z* (% relative intensity) :	282 (1), 199 (100), 183 (13), 153 (9), 139 (5), 123 (14), 83 (58)

Subfraction 92B49 displayed a long tail under UV-S on normal phase TLC using 40% ethyl acetate in petroleum ether as a mobile phase (5 runs). Because of the minute quantity, it was not further investigated.

Subfraction 92B5 displayed a long tail under UV-S on reverse phase TLC using 50% methanol in water as a mobile phase. Because the ^{1}H NMR spectrum showed broad signals, it was not further investigated.

Fraction 92C showed three UV-active spots on reverse phase TLC using 50% methanol in water as a mobile phase with the R_f values of 0.43, 0.64 and 0.77. It was further separated by column chromatography over reverse phase silica gel. Elution was performed initially with 50% methanol in water, followed by reducing the polarity with methanol and finally with pure methanol. Fractions with similar chromatogram were combined and evaporated to dryness under reduced pressure to afford four subfractions, as shown in **Table 69**.

Table 69 Subfractions obtained from **fraction 92C** by column chromatography over reverse phase silica gel

Subfraction	Elution	Weight (mg)	Physical appearance
92C1	50% MeOH/ H_2O	42.4	Brown gum
92C2	50% MeOH/ H_2O	9.2	Brown gum
92C3	50-60% MeOH/ H_2O	4.9	Brown gum
92C4	100% MeOH	12.0	Brown gum

Subfraction 92C1 showed three UV-active spots on reverse phase TLC using 50% methanol in water as a mobile phase with the R_f values of 0.38, 0.55 and 0.72. It was further separated by column chromatography over reverse phase silica gel. Elution was performed initially with 50% methanol in water, followed by reducing the polarity with methanol and finally with pure methanol. Fractions with similar chromatogram were combined and evaporated to dryness under reduced pressure to afford six subfractions, as shown in **Table 70**.

Table 70 Subfractions obtained from **subfraction 92C1** by column chromatography over reverse phase silica gel

Subfraction	Elution	Weight (mg)	Physical appearance
92C11	50% MeOH/ H_2O	22.3	Brown gum
92C12	50% MeOH/ H_2O	9.3	Brown gum
92C13	50% MeOH/ H_2O	3.5	Brown gum
92C14	50% MeOH/ H_2O	1.7	Brown gum
92C15	50% MeOH/ H_2O	1.5	Brown gum
92C16	50% MeOH/ H_2O -100% MeOH	4.3	Brown gum

Subfraction 92C11 showed two UV-active spots on normal phase TLC using 10% methanol in dichloromethane as a mobile phase with the R_f values of 0.07 and 0.22. The ^1H NMR spectrum displayed sugar signals. Thus, it was not investigated.

Subfraction 92C12 showed four UV-active spots on normal phase TLC using 10% methanol in dichloromethane as a mobile phase with the R_f values of 0.15, 0.29, 0.41 and 0.49. It was further separated by column chromatography over Sephadex LH-20. Elution was performed with 50% methanol in dichloromethane. Fractions with similar chromatogram were combined and evaporated to dryness under reduced pressure to afford four subfractions, as shown in **Table 71**.

Table 71 Subfractions obtained from **subfraction 92C12** by column chromatography over Sephadex LH-20

Subfraction	Weight (mg)	Physical appearance
92C121	1.0	Brown gum
92C122	4.1	Brown gum
92C123	1.1	Brown gum
92C124	3.5	Brown gum

Subfraction 92C121 showed two UV-active spots on normal phase TLC using 3% methanol in dichloromethane as a mobile phase (3 runs) with the R_f values of 0.20 and 0.28. Because of the minute quantity, it was not further investigated.

Subfraction 92C122 showed three UV-active spots on normal phase TLC using 3% methanol in dichloromethane as a mobile phase (3 runs) with the R_f values of 0.13, 0.23 and 0.33. Because of the low quantity, it was not further investigated.

Subfraction 92C123 showed two UV-active spots on normal phase TLC using 3% methanol in dichloromethane as a mobile phase (3 runs) with the R_f values of 0.13 and 0.33. Because of the minute quantity, it was not further investigated.

Subfraction 92C124 showed two UV-active spots on normal phase TLC using 3% methanol in dichloromethane as a mobile phase (3 runs) with the R_f values of 0.13 and 0.23. Because of the low quantity, it was not further investigated.

Subfraction 92C13 showed three UV-active spots on normal phase TLC using 10% methanol in dichloromethane as a mobile phase with the R_f values of 0.46, 0.56 and 0.71. Because of the low quantity, it was not further investigated.

Subfraction 92C14 showed two UV-active spots on normal phase TLC using 10% methanol in dichloromethane as a mobile phase with the R_f values of 0.44 and 0.56. Because of the minute quantity, it was not further investigated.

Subfraction 92C15 showed one UV-active spot on normal phase TLC using 10% methanol in dichloromethane as a mobile phase with the R_f value of 0.54. Because of the minute quantity, it was not further investigated.

Subfraction 92C16 did not show any UV-active spots on normal phase TLC using 10% methanol in dichloromethane as a mobile phase. Because of the low quantity and the presence of proton signals in high field region, it was not further investigated.

Subfraction 92C2 showed six UV-active spots on normal phase TLC using 2% methanol in dichloromethane (2 runs) as a mobile phase with the R_f values of 0.15, 0.22, 0.34, 0.41, 0.51 and 0.78. It was further separated by column chromatography over Sephadex LH-20. Elution was performed with 50% methanol in dichloromethane. Fractions with similar chromatogram were combined and evaporated to dryness under reduced pressure to afford five subfractions, as shown in **Table 72**.

Table 72 Subfractions obtained from **subfraction 92C2** by column chromatography over Sephadex LH-20

Subfraction	Elution	Weight (mg)	Physical appearance
92C21	50% MeOH/CH_2Cl_2	1.3	Colorless gum
92C22	50% MeOH/CH_2Cl_2	1.7	Brown gum
92C23	50% MeOH/CH_2Cl_2	4.1	Brown gum
92C24	50% MeOH/CH_2Cl_2	1.0	Brown gum
92C25	50% MeOH/CH_2Cl_2	1.1	Brown gum

Subfraction 92C21 (AR25) showed one UV-active spot on normal phase TLC using 2% methanol in dichloromethane as a mobile phase (3 runs) with the R_f value of 0.08.

UV λ_{max}(nm)(MeOH)(log ε)	253 (3.18), 273 (2.98)
FTIR(neat) : υ(cm^{-1})	3373 (O-H stretching), 1650 (C=O stretching)
^{1}H NMR(Acetone-d_6)(δ_{ppm}) : (300 MHz)	7.93 (*d*, *J* = 8.7 Hz, 2H), 6.93 (*d*, *J* = 8.7 Hz, 2H)
^{13}C NMR(Acetone-d_6)(δ_{ppm}) : (75 MHz)	166.87, 161.75, 131.84, 121.73, 115.09
CH :	131.84, 115.09

Subfraction 92C22 showed one UV-active spot on normal phase TLC using 2% methanol in dichloromethane as a mobile phase (3 runs) with the R_f value of 0.58. It contained **AR24** as a major component. No further purification was carried out.

Subfraction 92C23 showed one UV-active spot on normal phase TLC using 2% methanol in dichloromethane as a mobile phase (3 runs) with the R_f value of 0.30. It was then purified by precoated TLC with 3% methanol in dichloromethane as a mobile phase (6 runs) to afford **AR26** as a brown gum (2.3 mg). Its chromatogram showed one UV-active spot on normal phase TLC using 3% methanol in dichloromethane as a mobile phase with the R_f value of 0.24.

$[\alpha]_D^{25}$	+25.6 (c = 0.17, $CHCl_3$)
UV λ_{max}(nm)(MeOH)(log ε)	206 (3.91), 246 (3.30), 273 (2.88)
FTIR(neat) : υ(cm^{-1})	3395 (O-H stretching), 1734 (C=O stretching)
^{1}H NMR($CDCl_3$)(δ_{ppm})(500 MHz) :	7.60 (*d*, *J* = 8.5 Hz, 1H), 6.84 (*d*, *J* = 8.5 Hz, 1H), 6.79 (*brs*, 1H), 6.32 (*brs*, 1H), 5.02 (*d*, *J* = 6.5 Hz, 1H), 4.98 (*brs*, 2H), 4.87 (*brs*, 1H), 4.83 (*brs*, 1H), 4.27 (*d*, *J* = 6.5 Hz, 1H), 3.93 (*s*, 3H), 2.18 (*s*, 3H), 1.67 (*s*, 3H)
^{13}C NMR($CDCl_3$)(δ_{ppm})(125 MHz) :	167.40, 155.55, 152.04, 147.27, 144.31, 141.50, 135.11, 132.36, 132.17, 125.79, 120.94, 119.50, 117.50, 117.42, 114.30, 78.61, 69.21, 68.85, 62.87, 20.83, 18.44
CH :	132.17, 120.94, 117.50, 117.42, 78.61, 69.21
CH_2 :	114.30, 68.85
CH_3 :	62.87, 20.83, 18.44

Subfraction 92C24 showed two UV-active spots on normal phase TLC using 2% methanol in dichloromethane as a mobile phase (3 runs) with the R_f values of 0.13 and 0.30. Because of the minute quantity, it was not investigated.

Subfraction 92C25 did not show any UV-active spots on normal phase TLC using 2% methanol in dichloromethane as a mobile phase (3 runs). Because of the minute quantity, it was not further investigated.

Subfraction 92C3 showed one UV-active spot on normal phase TLC using 2% methanol in dichloromethane as a mobile phase (2 runs) with the R_f value of 0.54. Its ^{1}H NMR spectrum indicated the presence of many components. Thus, it was not further investigated.

Subfraction 92C4 showed a long tail under UV-S on normal phase TLC using 2% methanol in dichloromethane as a mobile phase (2 runs). Because of the absence of olefinic and aromatic protons in the ^{1}H NMR spectrum, it was not further investigated.

Fraction 92D showed three UV-active spots on normal phase TLC using 2% methanol in dichloromethane (2 runs) as a mobile phase with the R_f values of 0.05, 0.12 and 0.21. It was further separated by column chromatography over Sephadex LH-20. Elution was performed with 50% methanol in dichloromethane. Fractions with similar chromatogram were combined and evaporated to dryness under reduced pressure to afford three subfractions, as shown in **Table 73**.

Table 73 Subfractions obtained from **fraction 92D** by column chromatography over Sephadex LH-20

Subfraction	Elution	Weight (mg)	Physical appearance
92D1	50% MeOH/CH_2Cl_2	6.0	Brown gum
92D2	50% MeOH/CH_2Cl_2	9.9	Brown gum
92D3	50% MeOH/CH_2Cl_2	70.5	Brown gum

Subfraction 92D1 showed four UV-active spots on normal phase TLC using 2% methanol in dichloromethane as a mobile phase with the R_f values of 0.24, 0.37, 0.44 and 0.93. Because of the low quantity, it was not further investigated.

Subfraction 92D2 showed three UV-active spots on normal phase TLC using 2% methanol in dichloromethane as a mobile phase with the R_f values of 0.15, 0.24 and 0.32. Because the ^1H NMR spectrum indicated the presence of many compounds, it was not further investigated.

Subfraction 92D3 did not show any UV-active spots on normal phase TLC using 2% methanol in dichloromethane as a mobile phase and displayed a long tail under UV-S on reverse phase TLC using 70% methanol in water as a mobile phase. The ^1H NMR spectrum exhibited the broad signals. Therefore, no further purification was performed.

CHAPTER 2.3

RESULTS AND DISCUSSION

Four new compounds **(AR21-24)** and two known compounds **(AR25-26)** were isolated from the broth extract.

2.3.1 Compound AR21

Compound **AR21** with the molecular formula $C_9H_{14}O_4$ by EIMS (**Figure 54**) was obtained as a colorless gum. It exhibited UV absorption bands at 207 and 254 nm while hydroxyl and carbonyl absorption bands were found at 3407 and 1679 cm^{-1}, respectively, in the IR spectrum. The ^1H NMR spectrum (**Figure 52**) (**Table 74**) contained signals for one set of nonequivalent oxymethylene protons [δ_H 4.40 (*dd, J* = 12.0, 1.5, Hz, 1H)/4.28 (*dd, J* = 12.0 and 3.6, Hz, 1H)], one oxymethine proton (δ_H 4.16, *qn*, *J* = 6.9 Hz, 1H), one methoxyl group (δ_H 3.88, *s*, 3H), one methine proton (δ_H 2.69, *dd*, *J* = 6.9 and 3.6, Hz, 1H) and two methyl groups [δ_H 1.83 (*s*, 3H) and 1.36 (*d*, *J* = 6.9 Hz, 3H)]. The ^{13}C NMR spectrum (**Figure 53**) (**Table 74**) displayed one typical carbonyl carbon of an α,β-unsaturated ester moiety (δ_C 167.64), two quaternary carbons (δ_C 166.87 and 105.24), one oxymethine carbon (δ_C 67.81), one oxymethylene carbon (δ_C 65.29), one methoxy carbon (δ_C 56.52), one methine carbon (δ_C 40.92), and two methyl carbons (δ_C 20.97 and 9.28). The methyl protons at δ_H 1.83 (H_3-7) gave the ^3J HMBC correlations (**Table 75**) with C-2 (δ_C 167.64) and C-4 (δ_C 166.87) while the methoxy protons at δ_H 3.88 (H_3-8) showed the ^3J HMBC correlation with C-4. These data indicated the attachment of the methyl and methoxyl groups at C-3 (δ_C 105.24) and C-4, respectively. The following ^1H-^1H COSY correlations (**Table 75**): H-5 (δ_H 2.69)/H_{ab}-6 (δ_H 4.40 and 4.28) and H-9 (δ_H 4.16) and H_3-10 (δ_H 1.36)/H-9, as well as the HMBC correlations of H-5/C-4 and H_{ab}-6/C-2, constructed a 5,6-dihydropyrone having a 1-hydroxyethyl unit at C-5 (δ_C 40.92). Signal enhancement of H_{ab}-6, H_3-8 and H_3-10 upon irradiation of H-5 in the

NOEDIFF experiment confirmed the assigned location of the 1-hydroxyethyl group. Futhermore, these results suggested that H-5 and H-9 were located at opposite direction. As compounds **AR21** and **AR23** were co-metabolites, we proposed that C-9 in compound **AR21** would have *S*-configuration. Consequently, C-5 was assigned to possess *S*-configuration. Therefore, **AR21** was identified as a new α-pyrone derivative.

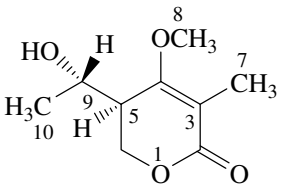

Table 74 The ^{1}H and ^{13}C NMR data of compound **AR21** in $CDCl_3$

Position	δ_H (*mult.*, J_{Hz})	δ_C (C-Type)
2	-	167.64 (C=O)
3	-	105.24 (C)
4	-	166.87 (C)
5	2.69 (*dd*, 6.9, 3.6)	40.92 (CH)
6	a: 4.40 (*dd,* 12.0, 1.5)	65.29 (CH_2)
	b: 4.28 (*dd,* 12.0, 3.6)	
7	1.83 (*s*)	9.28 (CH_3)
8	3.88 (*s*)	56.52 (CH_3)
9	4.16 (*qn,* 6.9)	67.81 (CH)
10	1.36 (*d*, 6.9)	20.97 (CH_3)

Table 75 The HMBC, COSY and NOE data of compound **AR21** in $CDCl_3$

Proton	HMBC	COSY	NOE
H-5	C-4, C-9	H_{ab}-6, H-9	H_{ab}-6, H_3-8, H_3-10
H_a-6	C-2, C-4, C-5, C-9	H-5, H_b-6	*
H_b-6	C-2, C-4, C-5, C-9	H-5, H_a-6	*
H_3-7	C-2, C-3, C-4	-	*

Table 75 Continued

Proton	HMBC	COSY	NOE
H_3-8	C-4	-	H-5
H-9	C-6	H-5, H_3-10	H_3-10
H_3-10	C-5, C-9	H-9	*

* not determined

2.3.2 Compound AR22

Compound **AR22** was obtained as a colorless gum and possessed the same molecular formula as **AR21** from EIMS (**Figure 57**). It exhibited UV and IR absorption bands similar to those of **AR21**. The ^{1}H and ^{13}C NMR spectra (**Figure 55** and **56**) (**Table 76**) were also similar to those of compound **AR21**. In addition, all substitutents were attached at the same position as those in **AR21** according to the HMBC correlations. In contrast, irradiation of H-9 in the NOEDIFF experiment did enhance signal intensity of H-5 and vice versa, suggesting their close proximity. Thus, compound **AR22** was a diastereomer of compound **AR21** with the *R*-configuration at C-5. Therefore, **AR22** was identified as a new α-pyrone derivative.

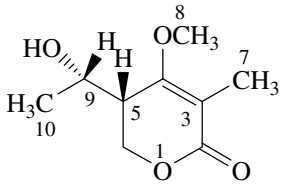

Table 76 The ^{1}H and ^{13}C NMR data of compound **AR22** in $CDCl_3$

Position	δ_H (*mult.*, J_{Hz})	δ_C (C-Type)
2	-	167.73 (C=O)
3	-	107.39 (C)
4	-	165.83 (C)
5	2.62 (*brs*)	40.90 (CH)
6	a: 4.58 (*d,* 11.7)	65.49 (CH_2)

Table 76 Continued

Position	δ_H (*mult*., J_{Hz})	δ_C (C-Type)
	b: 4.24 (*dd,* 11.7, 3.6)	
7	1.84 (*s*)	9.54 (CH_3)
8	3.83 (*s*)	57.05 (CH_3)
9	4.05 (*m*)	67.12 (CH)
9-OH	1.93 (*brs*)	-
10	1.32 (*d*, 6.6)	21.35 (CH_3)

Table 77 The HMBC, COSY and NOE data of compound **AR22** in $CDCl_3$

Proton	HMBC	COSY	NOE
H-5	-	H_{ab}-6	H_{ab}-6, H_3-8, H-9
H_a-6	C-2, C-4, C-9	H_b-6, H-5	*
H_b-6	C-2, C-4, C-9	H_a-6, H-5	*
H_3-7	C-2, C-3, C-4	-	H_3-8
H_3-8	C-4	-	H-5, H_3-7, H_3-10
H-9	-	H_3-10	H-5, H_3-10
H_3-10	C-5, C-9	H-9	*

* not determined

2.3.3 Compound AR23

Compound **AR23** with the molecular formula $C_{14}H_{18}O_6$ by EIMS (**Figure 60**) was obtained as a colorless gum. It exhibited UV absorption bands at 210 and 287 nm. A hydroxyl absorption band was found at 3410 cm^{-1} while carbonyl ones were found at 1722 and 1711 cm^{-1} in the IR spectrum. The ^1H NMR and ^1H-^1H COSY spectra (**Figure 58**) (**Table 78**) contained signals for two olefinic protons [δ_H 7.64 (*d*, J = 0.9 Hz, 1H) and 5.69 (*hept*, J = 1.2 Hz, 1H)], one set of oxymethylene protons (δ_H 5.05, *s*, 2H), a 1-hydroxyethyl group [δ_H 4.81 (*m*, 1H), 4.42 (*d*, J = 4.5 Hz, 1H) and 1.40 (*d*, J = 6.3 Hz, 3H)], one methoxyl group (δ_H 4.15, *s*, 3H) and two methyl

groups [δ_H 2.16 (*d*, *J* = 1.2 Hz, 3H) and 1.90 (*d*, *J* = 1.2 Hz, 3H)]. The ^{13}C NMR spectrum (**Figure 59**) (**Table 78**) displayed one typical carbonyl carbon of a α-pyrone unit (δ_C 163.95), one ester carbonyl carbon (δ_C 165.62), four quaternary carbons (δ_C 169.23, 157.13, 122.42 and 106.14), three methine carbons (δ_C 148.63, 115.32 and 62.30), one oxymethylene carbon (δ_C 56.22), one methoxy carbon (δ_C 61.67) and three methyl carbons (δ_C 26.29, 23.24 and 19.23). One of the olefinic protons at δ_H 7.64 was assigned as H-6 of the α-pyrone unit on the basis of its HMBC correlation (**Table 79**) with C-2 (δ_C 163.95). The 1-hydroxyethyl unit was attached at C-5 of the α-pyrone moiety because H-6 displayed the ^3J HMBC correlation with C-15 (δ_C 62.30). This assignment was confirmed by a ^1H-^1H COSY correlation of H-6 and H-15. In addition, both H-6 and the methoxy protons at δ_H 4.15 (H_3-14) showed the ^3J HMBC correlation with C-4 (δ_C 169.23), indicating that the methoxyl group was attached at C-4. The oxymethylene protons (H_2-7, δ_H 5.05) displayed the HMBC correlations (**Table 79**) with C-3 (δ_C 106.14) and C-4, indicating its location at C-3. The remaining olefinic proton (δ_H 5.69, H-10) exhibited ^1H-^1H COSY cross peaks with H_3-12 (δ_H 1.90) and H_3-13 (δ_H 2.16). Furthermore, H-10 displayed the ^3J HMBC correlations with C-12 (δ_C 26.29) and C-13 (δ_C 19.23). These data indicated the presence of a 2-methyl-1-propenyl unit. The HMBC correlations of H_3-12, H_3-13 and H_2-7 with the ester carbonyl carbon (C-9, δ_C 165.62) connected the methylene substituent of the α-pyrone moiety and the 2-methyl-1-propenyl unit through an ester linkage. Signal enhancement of H-15 and H-7 upon irradiation of H_3-14 in the NOEDIFF experiment confirmed the assigned location of all substituents on the α-pyrone unit. Since it was obtained in minute quantity, no attempts were made to identify the absolute configuration at C-15. However, the observed optical rotation of **AR23**, $[\alpha]_D^{25}$ -44.07 (c = 0.33, MeOH), was almost identical to that of taiwapyrone, $[\alpha]_D^{22}$ -48.50 (c = 0.33, MeOH), We proposed that a chiral carbon of **AR23** would possess *S* configuration, the same as that of taiwapyrone (Camarda *et al*., 1976). Therefore, **AR23** was identified as a new α-pyrone derivative.

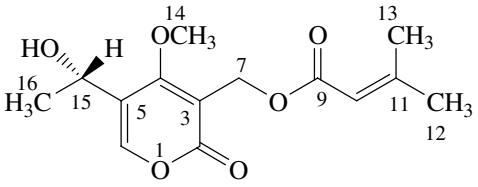

AR23

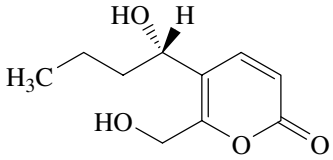

Taiwapyrone

Table 78 The ^{1}H and ^{13}C NMR data of compound **AR23** in Acetone-d_6

Position	δ_H (*mult*., J_{Hz})	δ_C (C-Type)
2	-	163.95 (C=O)
3	-	106.14 (C)
4	-	169.23 (C)
5	-	122.42 (C)
6	7.64 (*d,* 0.9)	148.63 (CH)
7	5.05 (*s*)	56.22 (CH_2)
9	-	165.62 (C=O)
10	5.69 (*hept,* 1.2)	115.32 (CH)
11	-	157.13 (C)
12	1.90 (*d*, 1.2)	26.29 (CH_3)
13	2.16 (*d*, 1.2)	19.23 (CH_3)
14	4.15 (*s*)	61.67 (CH_3)
15	4.81 (*m*)	62.30 (CH)
15-OH	4.42 (*d*, 4.5)	-
16	1.40 (*d*, 6.3)	23.24 (CH_3)

Table 79 The HMBC, COSY and NOE data of compound **AR23** in Acetone-d_6

Proton	HMBC	COSY	NOE
H-6	C-2, C-4, C-5, C-15	H-15	H-15, H_3-16
H_2-7	C-2, C-3, C-4, C-9	-	H_3-14
H-10	C-11, C-12, C-13	H_3-12, H_3-13	*
H_3-12	C-9, C-10, C-11, C-13	H-10	*
H_3-13	C-9, C-10, C-11, C-12	H-10	*

Table 79 Continued

Proton	HMBC	COSY	NOE
H_3-14	C-4	-	H_2-7, H-15
H-15	C-16	H-6, 15-OH, H_3-16	H-6, H_3-14, 15-OH, H_3-16
15-OH	-	H-15	*
H_3-16	C-5, C-15	H-15	H_3-14, H-15

* not determined

2.3.4 Compound AR24

Compound **AR24** was obtained as a colorless gum and possessed the same molecular formula as **AR23** from EIMS (**Figure 63**). It also exhibited UV and IR absorption bands similar to those of **AR23**. The ^{1}H and ^{13}C NMR data (**Figure 61** and **62**) (**Table 80**) were almost identical to those of compound **AR23** except for the replacement of signals for the 1-hydroxyethyl unit and the α-pyrone proton (H-6) in compound **AR23** with those of one hydroxymethyl unit (δ_H 4.46, *s*, 2H) and one methyl group (δ_H 2.35, *s*, 3H), respectively. The HMBC correlations of H_3-16 (δ_H 2.35) to C-5 (δ_C 113.07) and C-6 (δ_C 161.86) indicated that the methyl group was attached at C-6 of the α-pyrone unit. Irradiation of the above methyl protons enhanced signal intensity of H_2-15 (δ_H 4.46), thus indicating that the 1-hydroxymethyl unit was attached at C-5. The remaining substitutents were located at the same position as those in **AR23** according to the HMBC correlations and NOEDIFF data. Therefore, **AR24** was identified as a new α-pyrone derivative.

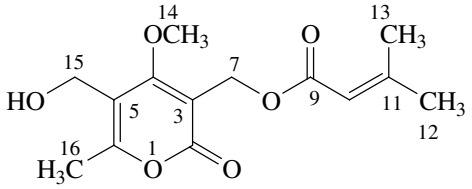

Table 80 The ^{1}H and ^{13}C NMR data of compound **AR24** in $CDCl_3$

Position	δ_H (*mult*., J_{Hz})	δ_C (C-Type)
2	-	164.37 (C=O)
3	-	104.99 (C)
4	-	170.52 (C)
5	-	113.07 (C)
6	-	161.86 (C)
7	5.07 (*s*)	56.26 (CH_2)
9	-	166.31 (C=O)
10	5.68 (*s*)	115.50 (CH)
11	-	157.74 (C)
12	1.88 (*s*)	27.41 (CH_3)
13	2.17 (*s*)	20.29 (CH_3)
14	4.09 (*s*)	62.41 (CH_3)
15	4.46 (*s*)	56.03 (CH_2)
16	2.35 (*s*)	17.37 (CH_3)

Table 81 The HMBC, COSY and NOE data of compound **AR24** in $CDCl_3$

Proton	HMBC	COSY	NOE
H_2-7	C-2, C-3, C-4, C-9	-	H_3-14
H-10	-	H_3-12, H_3-13	H_3-12
H_3-12	C-10, C-11, C-13	-	H-10, H_3-13
H_3-13	C-9, C-10, C-11, C-12	H_3-12	H_3-12
H_3-14	C-2	-	H_2-7, H_2-15
H_2-15	C-4, C-5, C-6	-	H_3-14, H_3-16
H_3-16	C-4, C-5, C-6	-	H_2-15

2.3.5 Compound AR25

Compound **AR25** was obtained as a colorless gum. The UV spectrum showed absorption bands at λ_{max} 253 and 273 nm, indicating the presence of a benzene chromophore. The IR spectrum exhibited absorption bands at 3372 and 1650 cm^{-1} for hydroxyl and carbonyl groups, respectively. The ^{1}H NMR spectrum displayed characteristic signals of a 1,4-disubstituted benzene [δ_H 7.93 (*d*, *J* = 8.7 Hz, 2H) and 6.93 (*d*, *J* = 8.7 Hz, 2H)]. The presence of a carbonyl carbon at δ_C 166.9 in the ^{13}C NMR spectrum related to the IR data. Comparison of its ^{1}H and ^{13}C NMR data with those of 4-hydroxybenzoic acid indicated that compound **AR25** was 4-hydroxybenzoic acid which was isolated from the rice hulls of *Oryza sativa* (Cho *et al*., 1998).

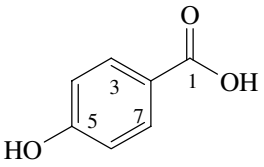

Table 82 The ^{1}H and ^{13}C NMR data of compound **AR25** in Acetone-d_6 and 4-hydroxybenzoic acid in DMSO-d_6

Position	AR25		4-Hydroxybenzoic acid	
	δ_H (*mult.*, J_{Hz})	δ_C (C-type)	δ_H (*mult.*, J_{Hz})	δ_C (C-type)
1	-	166.87 (C=O)	-	169.4 (C=O)
2	-	121.73 (C)	-	127.5 (C)
3, 7	7.93 (*d*, 8.7)	131.84 (CH)	7.73 (*d*, 8.0)	131.1 (CH)
4, 6	6.93 (*d*, 8.7)	115.09 (CH)	6.71 (*d*, 8.6)	114.4 (CH)
5	-	161.75 (C)	-	159.9 (C)

Cho *et al*., 1998.

2.3.6 Compound AR26

Compound **AR26** was obtained as a brown gum. It showed UV absorption bands at 206, 246 and 273 nm. A hydroxyl absorption band was found at 3395 cm^{-1} while a carbonyl one was observed at 1734 cm^{-1} in the IR spectrum. The ^{1}H NMR spectrum (**Figure 66**) (**Table 83**) contained signals for two-*ortho*-coupled aromatic protons [δ_H 7.60 (*d*, *J* = 8.5 Hz, 1H) and 6.84 (*d*, *J* = 8.5 Hz, 1H)], two *meta*-coupled ones [δ_H 6.79 (*brs*, 1H) and 6.32 (*brs*, 1H)], one set of oxymethylene protons (δ_H 4.98, *brs*, 2H), one set of nonequivalent gem-olefinic protons [δ_H 4.87 (*brs*, 1H) and 4.83 (*brs*, 1H)], two coupled oxymethine protons [δ_H 5.02 (*d*, *J* = 6.5 Hz, 1H) and 4.27 (*d*, *J* = 6.5 Hz, 1H)], one methoxyl group (δ_H 3.93, *s*, 3H) and two methyl groups [δ_H 2.18 (*s*, 3H) and 1.67 (*s*, 3H)]. The ^{13}C NMR spectrum (**Figure 67**) (**Table 83**) displayed one typical carbonyl carbon of a lactone ring (δ_C 167.40), nine quaternary carbons (δ_C 155.55, 152.04, 147.27, 144.31, 141.50, 135.11, 132.36, 125.79 and 119.50), six methine carbons (δ_C 132.17, 120.94, 117.50, 117.42, 78.61 and 69.21), two methylene carbons (δ_C 114.30 and 68.85), one methoxy carbon (δ_C 62.87) and two methyl carbons (δ_C 20.83 and 18.44). The *ortho*-coupled aromatic protons at δ_H 6.84 and 7.60 were assigned as H-1 and H-2, respectively. The ester carbonyl functionality was connected to C-4a (δ_C 119.50) on the basis of the HMBC correlation of H-1/C-5 and the ^{1}H chemical shift of H-2. A 1,2-dihydroxy-3-methyl-3-butenyl unit was established based on the following ^{1}H-^{1}H COSY correlations (**Table 84**): H-1′ (δ_H 5.02)/H-2′ (δ_H 4.27) and H_{ab}-4′ (δ_H 4.87 and 4.83)/H_3-5′ (δ_H 1.67) as well as the HMBC correlations of H-2′ to C-3′ (δ_C 144.31) and C-4' (δ_C 114.30) and those of H_{ab}-4′ to C-2′ (δ_C 78.16) and C-5′ (δ_C 18.44). This substituent was attached at C-3 of the aromatic ring because H-1′ displayed the ^{3}J HMBC correlations with C-2 (δ_C 132.17) and C-4 (δ_C 155.55). H_3-13 (δ_H 3.93) showed the ^{3}J HMBC correlation with C-4, indicating its attachment at C-4. This assignment was confirmed by signal enhancement of H-1′ upon irradiation of H_3-13. According to the HMBC correlation of H-1 to C-5 (δ_C 167.40) and the chemical shift of C-12a (δ_C 152.04), substructure 1 was established.

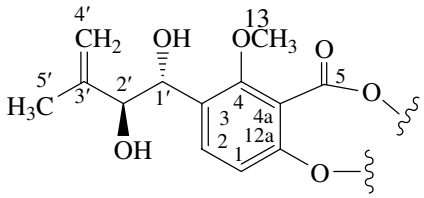

Substructure 1

The *meta*-coupled aromatic protons at δ_H 6.32 and 6.79 were assigned as H-8 and H-10, respectively. In the NOEDIFF experiment, irradiation of H-8 enhanced signals intensity of H_2-7 (δ_H 4.98) and H_3-14 (δ_H 2.18), indicating that the oxymethylene and methyl groups were connected to C-7a (δ_C 125.79) and C-9 (δ_C 135.11), respectively. The ^3J HMBC correlations of H_3-14 with C-8 (δ_C 120.94) and C-10 (δ_C 117.50) confirm this assignment. A hydroxyl group was attached at C-11 (δ_C 147.27) according to its chemical shift. Thus, substructure 2 was proposed.

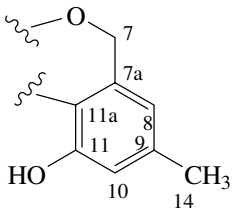

Substructure 2

Substructure 1 was connected with substructure 2 by forming an ester bond between C-5 and C-7 and an ether linkage between C-11a and C-12a to afford an octacyclic lactone ring on the basis of the ^{1}H chemical shift of H_2-7. The observed optical rotation of compound **AR26**, $[\alpha]_D^{25}$ +25.6 (c = 0.17, $CHCl_3$), was almost identical to that of 2′-hydroxy-3′,4′-didehydropenicillide, $[\alpha]_D^{25}$ +29.1 (c = 0.17, $CHCl_3$), indicating that all chiral carbons of compound **AR26** possessed the same configuration as those of 2′-hydroxy-3′,4′-didehydropenicillide (Kawamura *et al.*, 2000).

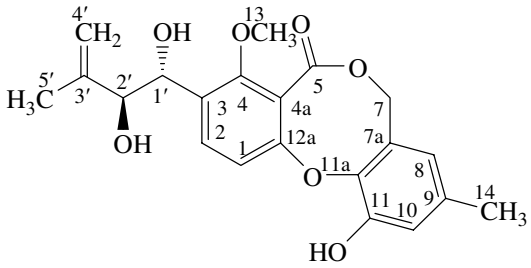

Table 83 The ^{1}H and ^{13}C NMR data of compound **AR26** and 2′-hydroxy-3′,4′-didehydropenicillide in $CDCl_3$

Position	**AR26**		**2′-Hydroxy-3′,4′-didehydropenicillide**	
	δ_H (*mult.*, J_{Hz})	δ_C (C-type)	δ_H (*mult.*, J_{Hz})	δ_C (C-type)
1	6.84 (*d*, 8.5)	117.42 (CH)	6.99 (*d*, 8.8)	118.8 (CH)
2	7.60 (*d*, 8.5)	132.17 (CH)	7.72 (*d*, 8.8)	133.9 (CH)
3	-	132.36 (C)	-	135.2 (C)
4	-	155.55 (C)	-	156.8 (C)
4a	-	119.50 (C)	-	120.9 (C)
5	-	167.40 (C=O)	-	169.9 (C=O)
7	4.98 (*brs*)	68.85 (CH_2)	a: 5.13 (*brd*, 14.6)	70.3 (CH_2)
			b: 5.05 (*brd*, 14.6)	
7a	-	125.79 (C)	-	128.2 (C)
8	6.32 (*brs*)	120.94 (CH)	6.40 (*d*, 2.0)	121.1 (CH)
9	-	135.11 (C)	-	135.9 (C)
10	6.79 (*brs*)	117.50 (CH)	6.77 (*d*, 2.0)	119.2 (CH)
11	-	147.27 (C)	-	149.7 (C)
11a	-	141.50 (C)	-	143.3 (C)
12a	-	152.04 (C)	-	153.4 (C)
13	3.93 (*s*)	62.87 (CH_3)	3.93 (*s*)	63.4 (CH_3)
14	2.18 (*s*)	20.83 (CH_3)	2.20 (*s*)	20.8 (CH_3)
1′	5.02 (*d*, 6.5)	69.21 (CH)	5.04 (*d*, 7.3)	69.2 (CH)
2′	4.27 (*d*, 6.5)	78.61 (CH)	4.24 (*d*, 7.3)	79.5 (CH)
3′	-	144.31 (C)	-	146.5 (C)

Table 83 Continued

Position	**AR26**		**2′-Hydroxy-3′,4′-didehydropenicillide**	
	δ_H (*mult., J_{Hz}*)	δ_C (C-type)	δ_H (*mult., J_{Hz}*)	δ_C (C-type)
4′	a: 4.87 (*brs*) b: 4.83 (*brs*)	114.30 (CH_2)	4.86 (*brs*)	114.1 (CH_2)
5′	1.67 (*s*)	18.44 (CH_3)	1.80 (*s*)	18.4 (CH_3)

Kawamura *et al*., 2000.

Table 84 The HMBC, COSY and NOE data of compound **AR26** in $CDCl_3$

Proton	HMBC	COSY	NOE
H-1	C-2, C-4a, C-5, C-12a	H-2	*
H-2	C-1́, C-4, C-12a	H-1	H-1
H_2-7	-	-	*
H-8	C-7, C-10, C-11a, C-14	-	H_2-7, H_3-14
H-10	C-8, C-9, C-11, C-11a, C-14	-	*
H_3-13	C-4	-	H-1′
H_3-14	C-8, C-9, C-10	-	H-8, H-10
H-1′	C-2, C-2′, C-3′, C-4	H-2′	*
H-2′	C-1′, C-3′, C-4′, C-5′	H-1′	H-1′, H_b-4′
H_a-4′	C-2′, C-5′	H_b-4′, H_3-5′	*
H_b-4′	C-2′, C-5′	H_a-4′, H_3-5′	*
H-5′	C-2′, C-3′, C-4′	-	H-1′, H_b-4′

* not determined

PART III

METABOLITES FROM THE MANGROVE-DERIVED FUNGUS *PESTALOTIOPSIS* SP. PSU-MA119

CHAPTER 3.1

INTRODUCTION

3.1.1 Introduction

Metabolites of the genus *Pestalotiopsis* are summarized in the **Table 64**. The mangrove-derived fungus *Pestalotiopsis* sp. PSU-MA119 was isolated from the twigs of *R. mucronata*, collected from Satun province, Thailand in the year 2007. It was deposited at the Department of Microbiology, Faculty of Science, Prince of Songkla University. The ethyl acetate extract from the broth of *Pestalotiopsis* sp. PSU-MA119 displayed no antibacterial activity against *S. aureus*, *P. aeruginosa* and *E. coli* at the concentration of 200 µg/mL. However, it showed antioxidant activity in $DPPH^{\bullet}$ assay with the IC_{50} value of 2.21 mg/mL.

3.1.2 The Objectives

1. To isolate the secondary metabolites from the mangrove-derived fungus *Pestalotiopsis* sp. PSU-MA119.
2. To elucidate the structures of the isolated compounds.

CHAPTER 3.2

EXPERIMENTAL

3.2.1 Fermentation and extraction

The flask culture of the fungus PSU-MA119 (15 L) in potato dextrose broth was filtered to separate into the filtrate and wet mycelia. The filtrate was divided into 37 portions. Each portion was extracted twice with an equal amount of EtOAc (2 x 300 mL). The organic layer was dried over anhydrous Na_2SO_4 and evaporated in *vacuo* to obtain a dark brown gum (976 mg). The extract was subjected to chromatographic fractionation.

3.2.2 Purification of the broth extract

The crude EtOAc extract was separated by column chromatography over Sephadex LH-20. Elution was performed with 100% methanol. Fractions with the similar chromatogram were combined and evaporated to dryness under reduced pressure to afford five fractions as shown in **Table 85**.

Table 85 Fractions obtained from the crude EtOAc extract by column chromatography over Sephadex LH-20

Fraction	Weight (mg)	Physical appearance
ZA	52.4	Brown gum
ZB	96.4	Brown gum
ZC	501.2	Brown gum
ZD	101.2	Brown gum
ZE	217.8	Brown gum

Fraction ZA did not show UV-active spots on normal phase TLC using 3% methanol in dichloromethane as a mobile phase. The ^{1}H NMR spectrum indicated the absence of olefinic and aromatic protons. Thus, it was not further investigated.

Fraction ZB displayed a long tail under UV-S on normal phase TLC using 3% methanol in dichloromethane as a mobile phase. The ^{1}H NMR spectrum indicated the absence of olefinic and aromatic protons. Therefore, it was not further investigated.

Fraction ZC showed four UV-active spots on reverse phase TLC using 50% methanol in water as a mobile phase with the R_f values of 0.27, 0.36, 0.42 and 0.80. It was further separated by column chromatography over reverse phase silica gel. Elution was initially performed with 50% methanol in water, followed by reducing the polarity with methanol until pure methanol. Fractions with the similar chromatogram were combined and evaporated to dryness under reduced pressure to afford nine subfractions as shown in **Table 86**.

Table 86 Subfractions obtained from **fraction ZC** by column chromatography over reverse phase silica gel

Subfraction	Elution	Weight (mg)	Physical appearance
ZC1	50% MeOH/H_2O	101.3	Brown gum
ZC2	50% MeOH/H_2O	131.3	Brown gum
ZC3	50% MeOH/H_2O	57.5	Brown gum
ZC4	50% MeOH/H_2O	36.3	Brown gum
ZC5	50% MeOH/H_2O	6.6	Brown gum
ZC6	50% MeOH/H_2O	15.6	Brown gum
ZC7	50-60% MeOH/H_2O	6.3	Brown gum
ZC8	60-70% MeOH/H_2O	5.5	Brown gum
ZC9	70% MeOH/H_2O-100% MeOH	127.5	Brown gum

Subfraction ZC1 displayed a long tail under UV-S on normal phase TLC using 3% methanol in dichloromethane. The ^{1}H NMR spectrum indicated the presence of sugar signals. Thus, it was not investigated.

Subfraction ZC2 displayed a long tail under UV-S on normal phase TLC using 3% methanol in dichloromethane. It was further separated by column chromatography over Sephadex LH-20. Elution was performed with 50% methanol in dichloromethane. Fractions with the similar chromatogram were combined and evaporated to dryness under reduced pressure to afford four subfractions as shown in **Table 87**.

Table 87 Subfractions obtained from **subfraction ZC2** by column chromatography over Sephadex LH-20

Subfraction	Weight (mg)	Physical appearance
ZC21	25.2	Yellow gum
ZC22	84.9	Brown gum
ZC23	15.2	Colorless gum
ZC24	3.0	Brown gum

Subfraction ZC21 displayed a long tail under UV-S on reverse phase TLC using 50% methanol in water as a mobile phase. This subfraction was subjected to acetylation reaction. Unfortunately, the reaction mixture was decomposed.

Subfraction ZC22 showed two UV-active spots on normal phase TLC using 3% methanol in dichloromethane as a mobile phase with the R_f values of 0.25 and 0.33. It was further separated by column chromatography over Sephadex LH-20. Elution was performed with 50% methanol in dichloromethane. Fractions with the similar chromatogram were combined and evaporated to dryness under reduced pressure to afford three subfractions as shown in **Table 88**.

Table 88 Subfractions obtained from **subfraction ZC22** by column chromatography over Sephadex LH-20

Subfraction	Weight (mg)	Physical appearance
ZC221	2.4	Brown gum
ZC222	79.3	Brown gum
ZC223	3.5	Brown gum

Subfraction ZC221 displayed a long tail under UV-S on normal phase TLC using 3% methanol in dichloromethane as a mobile phase. The ^{1}H NMR spectrum displayed signals of plasticizer. Thus, it was not further investigated.

Subfraction ZC222 showed two UV-active spots on normal phase TLC using 40% ethyl acetate in petroleum ether (5 runs) as a mobile phase with the R_f values of 0.40 and 0.53. It was further separated by flash column chromatography over silica gel. Elution was initially performed with 40% ethyl acetate in petroleum ether and gradually enriched with ethyl acetate and then methanol until pure methanol. Fractions with the similar chromatogram were combined and evaporated to dryness under reduced pressure to afford five subfractions as shown in **Table 89**.

Table 89 Subfractions obtained from **subfraction ZC222** by flash column chromatography over silica gel

Subfraction	Elution	Weight (mg)	Physical appearance
ZC2221	40-60% EtOAc/Petrol	3.3	Brown gum
ZC2222	60-70% EtOAc/Petrol	2.1	Yellow gum
ZC2223	70-80% EtOAc/Petrol	19.4	Yellow gum
ZC2224	80-90% EtOAc/Petrol	33.6	Colorless gum
ZC2225	100% EtOAc-100%MeOH	20.1	Brown gum

Subfraction ZC2221 displayed a long tail under UV-S on normal phase TLC using 40% ethyl acetate in petroleum ether (5 runs) as a mobile phase. The ^{1}H NMR spectrum displayed signals of plasticizer. Thus, it was not further investigated.

Subfraction ZC2222 showed one UV-active spot on normal phase TLC using 40% ethyl acetate in petroleum ether (5 runs) as a mobile phase with the R_f value of 0.46. Because of the minute quantity, it was not further investigated.

Subfraction ZC2223 showed two UV-active spots on normal phase TLC using 30% ethyl acetate in petroleum ether (5 runs) as a mobile phase with the R_f values of 0.35 and 0.60. It was further separated by flash column chromatography over silica gel. Elution was initially performed with 30% ethyl acetate in petroleum ether and gradually enriched with ethyl acetate and then methanol until pure methanol. Fractions with the similar chromatogram were combined and evaporated to dryness under reduced pressure to afford three subfractions as shown in **Table 90**.

Table 90 Subfractions obtained from **subfraction ZC2223** by flash column chromatography over silica gel

Subfraction	Elution	Weight (mg)	Physical appearance
ZC22231	30-50% EtOAc/Petrol	2.9	Yellow gum
ZC22232	50-70% EtOAc/Petrol	14.0	Yellow gum
ZC22233	70% EtOAc/Petrol – 100% MeOH	2.4	Yellow gum

Subfraction ZC22231 showed one UV-active spot on normal phase TLC using 30% ethyl acetate in petroleum ether (7 runs) as a mobile phase with the R_f value of 0.81. Because of the minute quantity, it was not further investigated.

Subfraction ZC22232 displayed a long tail under UV-S on normal phase TLC using 30% ethyl acetate in petroleum ether (7 runs) as a mobile phase. This subfraction was subjected to acetylation reaction. After working up, the reaction mixture was obtained

as a yellow gum (24.9 mg) and showed three UV-active spots on normal phase TLC using 10% acetone in petroleum ether as a mobile phase with the R_f values of 0.29, 0.43 and 0.55. It was then purified by flash column chromatography over silica gel. Elution was initially performed with 10% acetone in petroleum ether and gradually enriched with acetone until pure acetone. Fractions with the similar chromatogram were combined and evaporated to dryness under reduced pressure to afford six subfractions as shown in **Table 91**.

Table 91 Subfractions obtained from **subfraction ZC22232** by flash column chromatography over silica gel

Subfraction	Elution	Weight (mg)	Physical appearance
ZC222321	10% Acetone/Petrol	0.5	Colorless gum
ZC222322	10% Acetone/Petrol	10.4	Colorless gum
ZC222323	10% Acetone/Petrol	2.0	Colorless gum
ZC222324	10% Acetone/Petrol	4.7	Colorless gum
ZC222325	10-30% Acetone/Petrol	2.2	Yellow gum
ZC222326	50% Acetone/Petrol – 100% Acetone	5.1	Yellow gum

Subfraction ZC222321 showed one UV-active spot on normal phase TLC using 10% acetone in petroleum ether (7 runs) as a mobile phase with the R_f value of 0.56. The ^{1}H NMR spectrum indicated that it was a triacetate derivative of **AR29**.

Subfraction ZC222322 showed two UV-active spots on normal phase TLC using 10% acetone in petroleum ether (7 runs) as a mobile phase with the R_f values of 0.46 and 0.56. It was then purified by precoated TLC with 10% acetone in petroleum ether as a mobile phase (7 runs) to afford two bands.

Band 1 (the triacetate derivative of AR29) was a colorless gum (3.9 mg). Its chromatogram showed one UV-active spot on normal phase TLC using 10% acetone in petroleum ether (7 run) as a mobile phase with the R_f value of 0.54.

$[\alpha]_D^{26}$	-11.9 (c = 1.0, $CHCl_3$)
UV λ_{max}(nm)(MeOH)(log ε)	208 (3.69)
FTIR(neat) : $\upsilon(cm^{-1})$	3372 (O-H stretching), 1738 (C=O stretching)
^{1}H NMR($CDCl_3$)(δ_{ppm})(300 MHz) :	6.93 (*dd, J* = 15.9, 9.0 Hz, 1H), 6.46 (*d, J* = 15.9, Hz, 1H), 5.96 (*dd, J* = 9.9, 2.4 Hz, 1H), 5.54 (*td, J* = 9.9, 5.1 Hz, 1H), 5.45 (*dd, J* = 9.0, 3.6 Hz, 1H), 5.16 (*t, J* = 9.9 Hz, 1H), 5.01 (*m*, 1H), 4.97 (*dd, J* = 8.7, 2.4 Hz, 1H), 4.46 (*dd, J* = 8.7, 3.6 Hz, 1H), 2.55 (*m*, 1H), 2.17 (*s*, 3H), 2.14 (*s*, 3H), 2.12 (*s*, 3H), 1.87 (*m*, 1H), 1.85 (*m*, 1H), 1.69 (*m*, 1H), 1.51 (*m*, 1H), 1.32 (*d*, *J* = 6.3 Hz, 3H), 1.13 (*m*, 1H)
^{13}C NMR($CDCl_3$)(δ_{ppm})(75 MHz) :	170.47, 169.65, 169.38, 165.09, 136.22, 136.06, 130.11, 122.94, 74.21, 73.98, 71.49, 67.23, 60.75, 34.84, 30.42, 25.82, 20.85, 20.76, 20.73, 20.51
CH :	136.22, 136.06, 130.11, 122.94, 74.21, 73.98, 71.49, 67.23, 60.75
CH_2 :	34.84, 30.42, 25.82
CH_3 :	20.85, 20.76, 20.73, 20.51

<u>Band 2</u> (the diacetate derivative of AR28) was a colorless gum (3.3 mg). Its chromatogram showed one UV-active spot on normal phase TLC using 10% acetone in petroleum ether (7 run) as a mobile phase with the R_f value of 0.45.

$[\alpha]_D^{25}$	+65.8 (c = 1.45, $CHCl_3$)
UV λ_{max}(nm)(MeOH)(log ε)	208 (3.60)
FTIR(neat) : $\upsilon(cm^{-1})$	1743 (C=O stretching)
^{1}H NMR($CDCl_3$)(δ_{ppm})(300 MHz) :	6.77 (*dd, J* = 15.6, 7.5 Hz, 1H), 6.13 (*dd, J* = 15.6, 1.2 Hz, 1H), 5.51 (*td, J* = 10.1, 3.0

	Hz, 1H), 5.38 (*t, J* = 9.6 Hz, 1H), 5.33 (*m*, 1H), 5.28 (*m*, 1H), 4.98 (*m*, 1H), 3.26 (*dd, J* = 6.3, 4.2 Hz, 1H), 3.02 (*dd, J* = 8.4, 4.2 Hz, 1H), 2.44 (*m*, 1H), 2.07 (*s*, 3H), 2.05 (*m*, 1H), 2.02 (*s*, 3H), 1.81 (*m*, 1H), 1.75 (*m*, 1H), 1.43 (*m*, 1H), 1.21 (*d*, *J* = 6.3 Hz, 3H), 1.17 (*m*, 1H)
^{13}C NMR($CDCl_3$)(δ_{ppm})(75 MHz) :	169.82, 169.34, 165.30, 138.51, 137.96, 126.09, 123.73, 73.09, 72.89, 66.01, 58.88, 55.79, 33.34, 28.77, 24.94, 21.00, 20.80, 19.78
CH :	138.51, 137.96, 126.09, 123.73, 73.09, 72.89, 66.01, 58.88, 55.79
CH_2 :	33.34, 28.77, 24.94
CH_3 :	21.00, 20.80, 19.78

Subfraction ZC222323 showed one UV-active spot on normal phase TLC using 10% acetone in petroleum ether (7 runs) as a mobile phase with the R_f value of 0.46. The ^{1}H NMR spectrum indicated that it was **the diacetate derivative of AR28**.

Subfraction ZC222324 showed two UV-active spots on normal phase TLC using 10% acetone in petroleum ether (7 runs) as a mobile phase with the R_f values of 0.39 and 0.46. It was then purified by precoated TLC with 10% acetone in petroleum ether as a mobile phase (7 runs) to afford two bands.

Band 1 (ZC2223241) was a colorless gum (1.4 mg). Its chromatogram showed one UV-active spot on normal phase TLC using 10% acetone in petroleum ether (7 run) as a mobile phase with the R_f value of 0.45. The ^{1}H NMR spectrum indicated that it was **the diacetate derivative of AR28**.

Band 2 (AR27) was a colorless gum (2.0 mg). Its chromatogram showed one UV-active spot on normal phase TLC using 10% acetone in petroleum ether (7 run) as a mobile phase with the R_f value of 0.38.

$[\alpha]_D^{25}$	+69.9 (c = 1.45, $CHCl_3$)
UV λ_{max}(nm)(MeOH)(log ε)	208 (3.61)
FTIR(neat) : $\upsilon(cm^{-1})$	1715 (C=O stretching)
^{1}H NMR($CDCl_3$)(δ_{ppm})(500 MHz) :	7.01 (*dd, J* = 15.5, 4.5 Hz, 1H), 6.16 (*ddd, J* = 15.5, 10.0, 5.5 Hz, 1H), 5.95 (*dd, J* = 15.5, 2.0 Hz, 1H), 5.47 (*dd, J* = 15.5, 8.5 Hz, 1H), 5.34 (*ddd, J* = 6.0, 4.5, 2.0 Hz, 1H), 5.14 (*t, J* = 8.5 Hz, 1H), 4.78 (*dqd, J* = 10.0, 6.0, 2.0 Hz, 1H), 3.25 (*dd, J* = 6.5, 4.5 Hz, 1H), 3.22 (*dd, J* = 8.5, 4.5 Hz, 1H), 2.20 (*s*, 3H), 2.16 (*m*, 1H), 2.12 (*s*, 3H), 2.06 (*m*, 1H), 1.90 (*m*, 1H), 1.80 (*m*, 1H), 1.56 (*m*, 1H), 1.27 (*d*, *J* = 6.0 Hz, 3H), 1.13 (*m*, 1H)
^{13}C NMR($CDCl_3$)(δ_{ppm})(125 MHz) :	169.88, 169.79, 164.91, 140.89, 139.48, 124.46, 122.40, 73.02, 72.37, 72.34, 58.02, 55.29, 34.37, 33.13, 24.46, 21.22, 20.71, 20.17
CH :	140.89, 139.48, 124.46, 122.40, 73.02, 72.37, 72.34, 58.02, 55.29
CH_2 :	34.37, 33.13, 24.46
CH_3 :	21.22, 20.71, 20.17
EIMS *m/z* (% relative intensity) :	352 (1), 310 (7), 268 (6), 250 (28), 167 (54), 126 (53), 97 (83), 81 (100)

Subfraction ZC222325 displayed a long tail under UV-S on normal phase TLC using 10% acetone in petroleum ether (7 runs) as a mobile phase. Because of the minute quantity and the absence of olefinic and aromatic protons in the ^{1}H NMR spectrum, it was not further investigated.

Subfraction ZC222326 displayed a long tail under UV-S on normal phase TLC using 10% acetone in petroleum ether (7 runs) as a mobile phase. The ^{1}H NMR spectrum displayed signals in the high field region. Thus, it was not investigated.

Subfraction ZC22233 did not show any UV-active spots on normal phase TLC using 30% ethyl acetate in petroleum ether (7 runs) but showed one spot after dipping the TLC plate in anisaldehyde reagent and subsequently heating with the R_f value of 0.17. Because of the minute quantity, it was not further investigated.

Subfraction ZC2224 showed two UV-active spots on normal phase TLC using 3% methanol in dichloromethane (7 runs) as a mobile phase with the R_f values of 0.36 and 0.46. It was further separated by column chromatography over silica gel. Elution was initially performed with 3% methanol in dichloromethane and gradually enriched with methanol until pure methanol. Fractions with the similar chromatogram were combined and evaporated to dryness under reduced pressure to afford four subfractions as shown in **Table 92**.

Table 92 Subfractions obtained from **subfraction ZC2224** by column chromatography over silica gel

Subfraction	Elution	Weight (mg)	Physical appearance
ZC22241	3% MeOH/CH_2Cl_2	2.7	Colorless gum
ZC22242	3% MeOH/CH_2Cl_2	16.6	Colorless gum
ZC22243	3-10% MeOH/CH_2Cl_2	6.2	Colorless gum
ZC22244	30% MeOH/CH_2Cl_2-100% MeOH	6.7	Yellow gum

Subfraction ZC22241 (AR28) showed one UV-active spot on normal phase TLC using 3% methanol in dichloromethane (2 runs) as a mobile phase with the R_f value of 0.32.

$[\alpha]_D^{25}$	+64.1 (c = 1.45, $CHCl_3$)
UV λ_{max}(nm)(MeOH)(log ε)	209 (3.58)
FTIR(neat) : $\upsilon(cm^{-1})$	3395 (O-H stretching), 1715 (C=O stretching)
^{1}H NMR($CDCl_3$)(δ_{ppm})(300 MHz) :	6.85 (*dd, J* = 15.9, 6.6 Hz, 1H), 6.15 (*dd, J* = 15.6, 1.5 Hz, 1H), 5.57 (*td, J* = 10.5, 3.6 Hz, 1H), 5.39 (*tdd, J* = 10.5, 2.4, 1.5 Hz, 1H), 4.95 (*m*, 1H), 4.32 (*t, J* = 6.3 Hz, 1H), 4.23 (*t, J* = 8.7 Hz, 1H), 3.26 (*dd, J* = 6.3, 4.5 Hz, 1H), 3.03 (*dd, J* = 8.7, 4.5 Hz, 1H), 2.45 (*m*, 1H), 2.09 (*m*, 1H), 1.90 (*m*, 1H), 1.77 (*m*, 1H), 1.47 (*m*, 1H), 1.30 (*d*, *J* = 6.0 Hz, 3H), 1.22 (*m*, 1H)
^{13}C NMR($CDCl_3$)(δ_{ppm})(75 MHz) :	165.70, 142.44, 135.69, 127.20, 123.86, 73.08, 72.13, 64.40, 62.58, 58.80, 33.56, 28.95, 25.13, 19.95
CH :	142.44, 135.69, 127.20, 123.86, 73.08, 72.13, 64.40, 62.58, 58.80
CH_2 :	33.56, 28.95, 25.13
CH_3 :	19.95

Subfraction ZC22242 displayed a long tail under UV-S on normal phase TLC using 3% methanol in dichloromethane (2 runs) as a mobile phase. This subfraction was subjected to acetylation reaction. After working up, the reaction mixture was obtained as a yellow gum (21.4 mg) and showed three UV-active spots on normal phase TLC using 1% methanol in dichloromethane as a mobile phase with the R_f values of 0.10, 0.20 and 0.68. It was then purified by column chromatography over silica gel. Elution was initially performed with 1% methanol in dichloromethane and gradually enriched methanol until pure methanol. Fractions with the similar chromatogram were combined and evaporated to dryness under reduced pressure to afford three subfractions as shown in **Table 93**.

Table 93 Subfractions obtained from **subfraction ZC22242** by column chromatography over silica gel

Subfraction	Elution	Weight (mg)	Physical appearance
ZC222421	1% MeOH/CH_2Cl_2	16.1	Colorless gum
ZC222422	2-30% MeOH/CH_2Cl_2	2.0	Colorless gum
ZC222423	30% MeOH/CH_2Cl_2-100% MeOH	3.3	Yellow gum

Subfraction ZC222421 showed three UV-active spots on normal phase TLC using 10% ethyl acetate in petroleum ether (5 runs) as a mobile phase with the R_f values of 0.36, 0.49 and 0.59. It was further separated by column chromatography over silica gel. Elution was initially performed with 10% ethyl acetate in petroleum ether and gradually enriched with ethyl acetate and then methanol until pure methanol. Fractions with the similar chromatogram were combined and evaporated to dryness under reduced pressure to afford six subfractions as shown in **Table 94**.

Table 94 Subfractions obtained from **subfraction ZC222421** by column chromatography over silica gel

Subfraction	Elution	Weight (mg)	Physical appearance
ZC2224211	10% EtOAc/Petrol	1.2	Colorless gum
ZC2224212	10% EtOAc/Petrol	1.4	Colorless gum
ZC2224213	10-30% EtOAc/Petrol	1.2	Colorless gum
ZC2224214	30-50% EtOAc/Petrol	2.4	Colorless gum
ZC2224215	50-70% EtOAc/Petrol	1.2	Colorless gum
ZC2224216	70% EtOAc/Petrol – 100% MeOH	8.5	Yellow gum

Subfraction ZC2224211 showed one UV-active spot on normal phase TLC using 20% ethyl acetate in petroleum ether (2 runs) as a mobile phase with the R_f value of 0.62. The ^{1}H NMR spectrum indicated that it was **the triacetate derivative of AR29**.

Subfraction ZC2224212 showed two UV-active spots on normal phase TLC using 20% ethyl acetate in petroleum ether (2 runs) as a mobile phase with the R_f values of 0.51 and 0.62. Because of the minute quantity, it was not further investigated.

Subfraction ZC2224213 showed one UV-active spot on normal phase TLC using 20% ethyl acetate in petroleum ether (2 runs) as a mobile phase with the R_f value of 0.51. The ^{1}H NMR spectrum indicated that it was **the diacetate derivative of AR28**.

Subfraction ZC2224214 showed two UV-active spots on normal phase TLC using 20% ethyl acetate in petroleum ether (2 runs) as a mobile phase with the R_f values of 0.44 and 0.51. Because of the low quantity, it was not further investigated.

Subfraction ZC2224215 showed one UV-active spot on normal phase TLC using 20% ethyl acetate in petroleum ether (2 runs) as a mobile phase with the R_f value of 0.44. Because of the minute quantity, it was not further investigated.

Subfraction ZC2224216 did not show any UV-active spots on normal phase TLC using 20% ethyl acetate in petroleum ether (2 runs) but showed long tail after dipping the TLC plate in anisaldehyde reagent and subsequently heating. The ^{1}H NMR spectrum displayed signals in the high field region. Thus, it was not investigated.

Subfraction ZC222422 displayed a long tail under UV-S on normal phase TLC using 2% methanol in dichloromethane as a mobile phase. Because of the minute quantity, it was not further investigated.

Subfraction ZC222423 contained many spots on TLC without major components. No further separation was conducted.

Subfraction ZC22243 displayed a long tail under UV-S on normal phase TLC using 3% methanol in dichloromethane (2 runs) as a mobile phase. Its ^{1}H NHR spectrum was similar to that of **ZC22242**. No further purification was carried out.

Subfraction ZC22244 displayed a long tail under UV-S on normal phase TLC using 3% methanol in dichloromethane (2 runs) as a mobile phase. The ^{1}H NMR spectrum indicated the absence of olefinic and aromatic protons. Thus, it was not further investigated.

Subfraction ZC2225 displayed a long tail under UV-S on normal phase TLC using 40% ethyl acetate in petroleum ether (5 runs) as a mobile phase. The ^{1}H NMR spectrum displayed signals of plasticizer. Thus, it was not further investigated.

Subfraction ZC223 displayed a long tail under UV-S on normal phase TLC using 3% methanol in dichloromethane as a mobile phase. The ^{1}H NMR spectrum displayed signals of plasticizer. Thus, it was not further investigated.

Subfraction ZC23 showed four UV-active spots on normal phase TLC using 40% acetone in petroleum ether as a mobile phase with the R_f values of 0.12, 0.39, 0.49 and 0.66. It was further separated by column chromatography over silica gel. Elution was initially performed with 40% acetone in petroleum ether and gradually enriched with acetone until pure acetone. Fractions with the similar chromatogram were combined and evaporated to dryness under reduced pressure to afford three subfractions as shown in **Table 95**.

Table 95 Subfractions obtained from **subfraction ZC23** by column chromatography over silica gel

Subfraction	Elution	Weight (mg)	Physical appearance
ZC231	40% Acetone/Petrol	4.9	Colorless gum
ZC232	40-50% Acetone/Petrol	5.8	Colorless gum
ZC233	70% Acetone/Petrol-100% Acetone	2.7	Yellow gum

Subfraction ZC231 showed two UV-active spots on normal phase TLC using 40% acetone in petroleum ether as a mobile phase with the R_f values of 0.48 and 0.68. The

^{1}H NMR spectrum indicated that it contained **AR29** as a major componant. Thus, it was not further investigated.

Subfraction ZC232 showed two UV-active spots on normal phase TLC using 40% acetone in petroleum ether as a mobile phase with the R_f values of 0.40 and 0.49. It was then purified by precoated TLC with 3% methanol in dichloromethane as a mobile phase (6 runs) to afford **AR29** as a colorless gum (2.5 mg). Its chromatogram showed one UV-active spot on normal phase TLC using 3% methanol in dichloromethane (2 runs) as a mobile phase with the R_f value of 0.43.

$[\alpha]_D^{27}$	-13.1 (c = 1.0, $CHCl_3$)
UV λ_{max}(nm)(MeOH)(log ε)	208 (3.66)
FTIR(neat) : υ(cm^{-1})	3404 (OH stretching), 1722 (C=O stretching)
^{1}H NMR($CDCl_3$)(δ_{ppm})(300 MHz) :	6.86 (*dd, J* = 15.6, 5.7 Hz, 1H), 6.26 (*d, J* = 15.6, Hz, 1H), 5.57 (*m*, 1H), 5.47 (*m*, 1H), 5.02 (*m*, 1H), 4.73 (*brs*, 1H), 4.45 (*brs*, 1H), 4.42 (*brs*, 1H), 3.59 (*dd, J* = 6.0, 1.5 Hz, 1H), 2.20 (*m*, 1H), 1.95 (*m*, 1H), 1.84 (*m*, 1H), 1.57 (*m*, 1H), 1.49 (*m*, 1H), 1.30 (*d*, *J* = 6.3 Hz, 3H), 1.11 (*m*, 1H)
^{13}C NMR($CDCl_3$)(δ_{ppm})(75 MHz) :	165.64, 143.03, 132.98, 129.00, 125.59, 73.84, 73.17, 71.91, 68.57, 68.16, 35.03, 29.83, 26.03, 20.55
CH :	143.03, 132.98, 129.00, 125.59, 73.84, 73.17, 71.91, 68.57, 68.16
CH_2 :	35.03, 29.83, 26.03
CH_3 :	20.55
EIMS *m/z* (% relative intensity) :	286 (1), 251 (7), 144 (23), 125 (61), 109 (67), 95 (66), 81 (100)

Subfraction ZC233 showed two UV-active spots on normal phase TLC using 40% acetone in petroleum ether as a mobile phase with the R_f values of 0.17 and 0.27. Because the ^{1}H NMR spectrum showed broad signals, it was not further investigated.

Subfraction ZC24 did not show UV-active spots on reverse phase TLC using 50% methanol in water as a mobile phase. The ^{1}H NMR spectrum displayed signals of plasticizer. Thus, it was not further investigated.

Subfraction ZC3 showed four UV-active spots on normal phase TLC using 30% acetone in petroleum ether (5 runs) as a mobile phase with the R_f values of 0.20, 0.44, 0.56 and 0.71. It was then purified by flash column chromatography over silica gel. Elution was initially performed with 30% acetone in petroleum ether and gradually enriched with acetone until pure acetone. Fractions with the similar chromatogram were combined and evaporated to dryness under reduced pressure to afford seven subfractions as shown in **Table 96**.

Table 96 Subfractions obtained from **subfraction ZC3** by flash column chromatography over silica gel

Subfraction	Elution	Weight (mg)	Physical appearance
ZC31	30% Acetone/Petrol	4.1	Yellow gum
ZC32	30% Acetone/Petrol	2.6	Yellow gum
ZC33	30% Acetone/Petrol	15.8	Yellow gum
ZC34	30% Acetone/Petrol	3.2	Yellow gum
ZC35	30-50% Acetone/Petrol	3.3	Yellow gum
ZC36	50-70% Acetone/Petrol	1.8	Brown gum
ZC37	100% Acetone	22.7	Brown gum

Subfraction ZC31 displayed a long tail under UV-S on normal phase TLC using 30% acetone in petroleum ether (3 runs) as a mobile phase. The ^{1}H NMR spectrum displayed signals in high field region. Thus, it was not investigated.

Subfraction ZC32 showed two UV-active spots on normal phase TLC using 30% acetone in petroleum ether (3 runs) as a mobile phase with the R_f values of 0.44 and 0.66. Because the ^{1}H NMR spectrum showed broad signals, it was not further investigated.

Subfraction ZC33 showed two UV-active spots on normal phase TLC using 30% acetone in petroleum ether (3 runs) as a mobile phase with the R_f values of 0.27 and 0.49. Its ^{1}H NMR spectrum indicated the presence of many components. Thus, it was not further investigated.

Subfraction ZC34 displayed a long tail under UV-S on normal phase TLC using 30% acetone in petroleum ether (3 runs) as a mobile phase. Because of low quantity, it was not further investigated.

Subfraction ZC35 displayed a long tail under UV-S on normal phase TLC using 30% acetone in petroleum ether (3 runs) as a mobile phase. Its ^{1}H NMR spectrum indicated the presence of many components. Thus, it was not further investigated.

Subfraction ZC36 showed one UV-active spot on normal phase TLC using 30% acetone in petroleum ether (3 runs) as a mobile phase with the R_f value of 0.22. The ^{1}H NMR spectrum indicated that it was **AR26**.

Subfraction ZC37 displayed a long tail under UV-S on normal phase TLC using 30% acetone in petroleum ether (3 runs) as a mobile phase. Because of the presence of broad signals in the ^{1}H NMR spectrum, it was not further investigated.

Subfraction ZC4 displayed a long tail under UV-S on normal phase TLC using 3% methanol in dichloromethane. Its ^{1}H NMR spectrum indicated that the major compound was **AR29**. No further purification was carried out.

Subfraction ZC5 displayed a long tail under UV-S on normal phase TLC using 3% methanol in dichloromethane. Because the ^{1}H NMR spectrum indicated the presence of many components, it was not further investigated.

Subfraction ZC6 displayed a long tail under UV-S on normal phase TLC using 3% methanol in dichloromethane. Its ^{1}H NMR spectrum indicated that the major compound was **AR28**. Thus, it was not further investigated.

Subfraction ZC7 displayed a long tail under UV-S on normal phase TLC using 3% methanol in dichloromethane. Its ^{1}H NMR spectrum indicated the presence of many components. Thus, it was not further investigated.

Subfraction ZC8 displayed a long tail under UV-S on normal phase TLC using 3% methanol in dichloromethane. Because the ^{1}H NMR spectrum showed broad signals, it was not further investigated.

Subfraction ZC9 displayed a long tail under UV-S on normal phase TLC using 3% methanol in dichloromethane. The ^{1}H NMR spectrum indicated the absence of olefinic and aromatic protons. Thus, it was not further investigated.

Fraction ZD showed three UV-active spots on reverse phase TLC using 50% methanol in water as a mobile phase with the R_f values of 0.19, 0.29 and 0.44. It was further separated by column chromatography over reverse phase silica gel. Elution was initially performed with 50% methanol in water, followed by reducing the polarity with methanol until pure methanol. Fractions with the similar chromatogram were combined and evaporated to dryness under reduced pressure to afford five subfractions as shown in **Table 97**.

Table 97 Subfractions obtained from **fraction ZD** by column chromatography over reverse phase silica gel

Subfraction	Elution	Weight (mg)	Physical appearance
ZD1	50% MeOH/H_2O	37.8	Brown gum
ZD2	50% MeOH/H_2O	12.3	Brown gum
ZD3	50% MeOH/H_2O	17.2	Brown gum
ZD4	50-80% MeOH/H_2O	8.7	Brown gum
ZD5	80% MeOH/H_2O-100% MeOH	25.2	Brown gum

Subfraction ZD1 showed three UV-active spots on normal phase TLC using 2% methanol in dichloromethane (2 runs) as a mobile phase with the R_f values of 0.07, 0.56 and 0.73. It was further separated by column chromatography over Sephadex LH-20. Elution was performed with 50% methanol in dichloromethane. Fractions with the similar chromatogram were combined and evaporated to dryness under reduced pressure to afford five subfractions as shown in **Table 98**.

Table 98 Subfractions obtained from **subfraction ZD1** by column chromatography over Sephadex LH-20

Subfraction	Elution	Weight (mg)	Physical appearance
ZD11	50% MeOH/CH_2Cl_2	8.0	Brown gum
ZD12	50% MeOH/CH_2Cl_2	2.3	Brown gum
ZD13	50% MeOH/CH_2Cl_2	11.4	Brown gum
ZD14	50% MeOH/CH_2Cl_2	2.6	Colorless gum
ZD15	50% MeOH/CH_2Cl_2	12.4	Brown gum

Subfraction ZD11 did not show UV-active spots on normal phase TLC using 5% methanol in dichloromethane as a mobile phase. The ^1H NMR spectrum indicated the absence of olefinic and aromatic protons. Thus, it was not further investigated.

Subfraction ZD12 showed three UV-active spots on normal phase TLC using 5% methanol in dichloromethane as a mobile phase with the R_f values of 0.56, 0.64 and 0.69. Because of low quantity, it was not further investigated.

Subfraction ZD13 showed three UV-active spots on normal phase TLC using 5% methanol in dichloromethane as a mobile phase with the R_f values of 0.10, 0.56 and 0.62. It was then purified by flash column chromatography over silica gel. Elution was performed initially with 5% methanol in dichloromethane, followed by increasing the polarity with methanol until pure methanol. Fractions with the similar chromatogram were combined and evaporated to dryness under reduced pressure to afford three subfractions as shown in **Table 99**.

Table 99 Subfractions obtained from **subfraction ZD13** by flash column chromatography over silica gel

Subfraction	Elution	Weight (mg)	Physical appearance
ZD131	5% MeOH/CH_2Cl_2	1.0	Yellow gum
ZD132	5-50% MeOH/CH_2Cl_2	1.6	Colorless gum
ZD133	70% MeOH/CH_2Cl_2-100% MeOH	8.6	Yellow gum

Subfraction ZD131 showed two UV-active spots on normal phase TLC using 5% methanol in dichloromethane as a mobile phase with the R_f values of 0.63 and 0.55. Because of the minute quantity, it was not further investigated.

Subfraction ZD132 (AR30) showed one UV-active spot on normal phase TLC using 5% methanol in dichloromethane as a mobile phase with the R_f value of 0.38.

UV λ_{max}(nm)(MeOH)(log ε)	207 (2.97), 221 (3.00), 277 (2.40)
FTIR(neat) : υ(cm^{-1})	3422 (O-H stretching)
^{1}H NMR($CDCl_3$)(δ_{ppm})(300 MHz) :	7.11 (*d, J* = 9.0 Hz, 2H), 6.79 (*d, J* = 9.0

	Hz, 2H), 3.83 (*d, J* = 6.0 Hz, 2H), 2.81 (*d, J* = 6.0 Hz, 2H)
^{13}C NMR($CDCl_3$)(δ_{ppm})(75 MHz) :	154.22, 130.55, 130.15, 115.45, 63.80, 38.27
CH :	130.15, 115.45
CH_2 :	63.80, 38.27

Subfraction ZD133 showed two UV-active spots on normal phase TLC using 5% methanol in dichloromethane as a mobile phase with the R_f values of 0.25 and 0.18. The ^{1}H NMR spectrum indicated the absence of olefinic and aromatic protons. Thus, it was not further investigated.

Subfraction ZD14 (AR31) showed one UV-active spot on normal phase TLC using 5% methanol in dichloromethane as a mobile phase with the R_f value of 0.33.

UVλ_{max}(nm)(MeOH)(log ε)	207 (3.60), 252 (3.52)
FTIR(neat) : υ(cm^{-1})	3366 (O-H stretching), 1686 (C=O stretching)
^{1}H NMR($CDCl_3$)(δ_{ppm})(300 MHz) :	7.90 (*d, J* = 9.0 Hz, 2H), 6.85 (*d, J* = 9.0 Hz, 2H), 2.20 (*s,* 3H)
^{13}C NMR($CDCl_3$)(δ_{ppm})(75 MHz) :	196.92, 160.10, 130.94, 130.48, 115.29, 26.30
CH :	130.94, 115.29
CH_3 :	26.30

Subfraction ZD15 did not show UV-active spots on normal phase TLC using 5% methanol in dichloromethane as a mobile phase. Its ^{1}H NMR spectrum indicated the absence of olefinic and aromatic protons. Thus, it was not further investigated.

Subfraction ZD2 showed two UV-active spots on normal phase TLC using 2% methanol in dichloromethane as a mobile phase with the R_f values of 0.20 and 0.39.

Its ^{1}H NMR spectrum indicated that the major compound was **AR29**. Thus, it was not further investigated.

Subfraction ZD3 showed three UV-active spots on normal phase TLC using 30% acetone in petroleum ether (3 runs) as a mobile phase with the R_f values of 0.20, 0.37 and 0.68. It was then purified by flash column chromatography over silica gel. Elution was initially performed with 30% acetone in petroleum ether and gradually enriched with acetone until pure Acetone. Fractions with the similar chromatogram were combined and evaporated to dryness under reduced pressure to afford four subfractions as shown in **Table 100**.

Table 100 Subfractions obtained from **subfraction ZD3** by flash column chromatography over silica gel

Subfraction	Elution	Weight (mg)	Physical appearance
ZD31	30% Acetone/Petrol	1.9	Yellow gum
ZD32	30-40% Acetone/Petrol	2.5	Colorless gum
ZD33	40-60% Acetone/Petrol	4.8	Colorless gum
ZD34	60% Acetone/Petrol-100% Acetone	7.8	Brown gum

Subfraction ZD31 showed one UV-active spot on normal phase TLC using 30% acetone in petroleum ether (2 runs) as a mobile phase with the R_f value of 0.71. Because of the minute quantity, it was not further investigated.

Subfraction ZD32 showed one UV-active spot on normal phase TLC using 30% acetone in petroleum ether (2 runs) as a mobile phase with the R_f value of 0.46. Because the ^{1}H NMR spectrum showed broad signals, it was not further investigated.

Subfraction ZD33 showed one UV-active spot on normal phase TLC using 30% acetone in petroleum ether (2 runs) as a mobile phase with the R_f value of 0.37. Its ^{1}H

NMR spectrum indicated the presence of many components. Thus, it was not further investigated.

Subfraction ZD34 showed a long tail under UV-S on normal phase TLC using 30% acetone in petroleum ether (2 runs) as a mobile phase. Because the ^{1}H NMR spectrum showed broad signals, it was not investigated.

Subfraction ZD4 showed two UV-active spots on normal phase TLC using 2% methanol in dichloromethane (2 runs) as a mobile phase with the R_f values of 0.24 and 0.39. Its ^{1}H NMR spectrum indicated the presence of many components. Thus, it was not further investigated.

Subfraction ZD5 displayed a long tail under UV-S on normal phase TLC using 2% methanol in dichloromethane. The ^{1}H NMR spectrum indicated the absence of olefinic and aromatic protons. Thus, it was not further investigated.

Fraction ZE displayed a long tail under UV-S on normal phase TLC using 3% methanol in dichloromethane as a mobile phase. The ^{1}H NMR spectrum indicated the absence of olefinic and aromatic protons. Thus, it was not further investigated.

CHAPTER 3.3

RESULTS AND DISCUSSION

Two new compounds **(AR27** and **29)** and three known compounds **(AR28** and **AR 30-31)** were isolated from the broth extract. Furthermore, compound **AR27** was isolated as its acetate derivative.

3.3.1 Compound AR28 and its diacetate derivative

Compound **AR28** was obtained as a colorless gum. The UV spectrum showed an absorption band at λ_{max} 209 nm. The IR spectrum displayed absorption bands at 3395 and 1715 cm^{-1} for hydroxyl and ester carbonyl groups, respectively. The ^{1}H NMR spectrum (**Figure 68**) (**Table 101**) contained signals for two *trans*-olefinic protons of an α,β-unsaturated carbonyl unit [δ_H 6.85 (*dd*, *J* = 15.6, 6.6 Hz, 1H) and 6.15 (*dd*, *J* = 15.6, 1.5 Hz, 1H)], two *cis*-olefinic protons [δ_H 5.57 (*td*, *J* = 10.5, 3.6 Hz, 1H) and 5.39 (*tdd*, *J* = 10.5, 2.4, 1.5 Hz, 1H)], three oxymethine protons [δ_H 4.95 (*m*, 1H), 4.32 (*t*, *J* = 6.3 Hz, 1H) and 4.23 (*t*, *J* = 8.7 Hz, 1H)], two *cis*-epoxymethine protons [δ_H 3.26 (*dd*, *J* = 6.3, 4.5 Hz, 1H) and 3.03 (*dd*, *J* = 8.7, 4.5 Hz, 1H)], three sets of nonequivalent methylene protons [δ_H 2.45 (*m,* 1H)/2.09 (*m,* 1H), 1.90 (*m*, 1H)/1.47 (*m*, 1H) and 1.77 (*m*, 1H)/1.22 (*m*, 1H)] and one methyl group (δ_H 1.30, *d*, *J* = 6.0 Hz, 3H). The ^{13}C NMR spectrum (**Figure 69**) (**Table 101**) displayed one carbonyl carbon of the α,β-unsaturated ester (δ_C 165.70), four methine carbons (δ_C 142.44, 135.69, 127.20 and 123.86), five oxymethine carbons (δ_C 73.08, 72.13, 64.40, 62.58 and 58.80), three methylene carbons (δ_C 33.56, 28.95 and 25.13) and one methyl carbon (δ_C 19.95). The *trans*-olefinic protons resonating at δ_H 6.13 and 6.77 were assigned to H-2 and H-3, respectively, on the basis of their HMBC correlations with C-1 (δ_C 165.70) as well as their chemical shifts. The oxymethine proton, H-4 (δ_H 4.32), showed the ^{1}H-^{1}H COSY correlations with H-3 and one of *cis*-epoxymethine protons, H-5 (δ_H 3.26). The other *cis*-epoxymethine proton, H-6 (δ_H 3.03), displayed

the same correlations with H-5 and H-7 (δ_H 4.23). The *cis*-olefinic proton, H-8 (δ_H 5.39), was coupled with H-7 and H-9 (δ_H 5.57). The nonequivalent methylene protons, H_{ab}-10 (δ_H 2.45 and 2.09), showed the ^1H-^1H COSY cross peaks with H-9 and H_{ab}-11 (δ_H 1.77 and 1.22). The methylene protons, H_{ab}-12 (δ_H 1.90 and 1.47), displayed the same correlations with H_{ab}-11 and H-13 (δ_H 4.95) which was further coupled with H_3-14 (δ_H 1.30). In addition, H-13 showed the HMBC correlation with the ester carbonyl carbon, C-1, constructing a 14-membered lactone ring. Compound **AR28** was identified as seiricuprolide (Ballio *et al*., 1988). The observed optical rotation of **AR28**, $[\alpha]_D^{25}$ +64.1 (c = 1.45, $CHCl_3$), was almost identical to that of seiricuprolide, $[\alpha]_D^{25}$ +67.2 (c = 1.45, $CHCl_3$), indicating that all chiral carbons of **AR28** possessed the same absolute configuration (4*R*,5*S*,6*R*,7*S*,13*S*) as those of seiricuprolide (Ballio *et al*., 1988).

The diacetate derivative of **AR28** was obtained as a colorless gum and exhibited UV and IR absorption bands similar to those of **AR28**. The ^1H NMR data (**Figure 70**) (**Table 103**) were almost identical to those of compound **AR28** except for the appearance of the oxymethine protons, H-4 (δ_H 5.33) and H-7 (δ_H 5.38) at much lower field. Two singlets of the acetoxyl groups were also observed. The HMBC correlations of H_3-16 (δ_H 2.07) to C-4 (δ_C 73.09) and H_3-18 (δ_H 2.02) to C-7 (δ_C 66.01) indicated that the acetoxyl groups (δ_H 2.07 and 2.02) were attached at C-4 and C-7 of the 14-membered lactone ring. Irradiation of H-6 in the NOEDIFF experiment (**Table 103**), enhanced signal intensity of H-5 and H-7, indicating their *cis*-relationship. In addition, irradiation of H-5 affected signal intensity of H-6, but not H-4, indicating that H-5 was *cis* to H-6 but *trans* to H-4. These NOEDIFF data confirmed that compound **AR28** and its diacetate derivative had the absolute configuration identical to that of seiricuprolide.

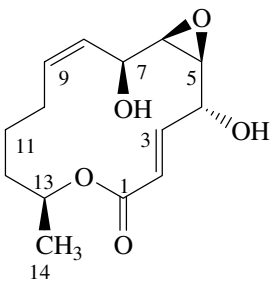

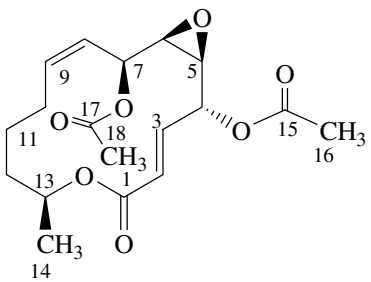

Table 101 The ^{1}H and ^{13}C NMR data of compound **AR28** and seiricuprolide in $CDCl_3$

position	**AR28**		**Seiricuprolide**	
	δ_H (*mult*., J_{Hz})	δ_C (C-Type)	δ_H (*mult*., J_{Hz})	δ_C (C-Type)
1	-	165.70 (C=O)	-	166.0 (C=O)
2	6.15 (*dd*, 15.6, 1.5)	123.86 (CH)	6.14 (*dd*, 15.4, 1.5)	123.8 (CH)
3	6.85 (*dd*, 15.6, 6.6)	142.44 (CH)	6.84 (*dd*, 15.4, 6.1)	142.9 (CH)
4	4.32 (*t*, 6.3)	72.13 (CH)	4.32 (*ddd*, 6.3, 6.1, 1.5)	71.9 (CH)
5	3.26 (*dd*, 6.3, 4.5)	62.58 (CH)	3.23 (*dd*, 6.3, 4.4)	62.6 (CH)
6	3.03 (*dd*, 8.7, 4.5)	58.80 (CH)	3.01 (*dd*, 7.8, 4.4)	58.9 (CH)
7	4.23 (*t*, 8.7)	64.40 (CH)	4.23 (*dd*, 8.5, 8.5)	64.4 (CH)
8	5.39 (*tdd,* 10.5, 2.4, 1.5)	127.20 (CH)	5.37 (*ddd*, 11.0, 8.5, 2.6)	127.4 (CH)
9	5.57 (*td*, 10.5, 3.6)	135.69 (CH)	5.54 (*ddd*, 11.0, 9.6, 3.3)	135.5 (CH)
10	a: 2.45 (*m*) b: 2.09 (*m*)	28.95 (CH_2)	a: 2.43 (*m*) b: 2.07 (*m*)	28.8 (CH_2)
11	a: 1.77 (*m*) b: 1.22 (*m*)	25.13 (CH_2)	a: 1.78 (*m*) b: 1.23 (*m*)	25.1 (CH_2)
12	a: 1.90 (*m*) b: 1.47 (*m*)	33.56 (CH_2)	a: 1.86 (*ddd*, 13.6, 10.6, 2.5) b: 1.44 (*ddd*, 13.6, 7.4, 7.4)	35.0 (CH_2)
13	4.95 (*m*)	73.08 (CH)	4.91 (*ddq*, 7.4, 6.6, 2.5)	73.1 (CH)
14	1.30 (*d*, 6.0)	19.95 (CH_3)	1.26 (*d*, 6.6)	19.8 (CH_3)

Ballio *et al*., 1988.

Table 102 The HMBC and COSY data of compound **AR28** in $CDCl_3$

position	HMBC Correlation	COSY
H-2	C-1, C-3, C-4	H-3, H-4
H-3	C-1, C-2, C-4, C-5	H-2, H-4
H-4	C-2, C-3, C-5	H-2, H-3, H-5
H-5	C-4, C-6, C-7	H-4,H-6
H-6	C-4, C-5, C-7, C-8	H-5, H-7
H-7	C-5, C-6, C-8, C-9	H-6, H-8, H-9
H-8	C-6, C-9, C-10	H-7, H-9, H_b-10
H-9	C-7, C-8, C-10, C-11	H-7, H-8, H_{ab}-10
H_a-10	C-8, C-9, C-11	H-9, H_b-10, H_{ab}-11
H_b-10	C-8, C-9, C-11	H-8, H-9, H_a-10, H_{ab}-11
H_a-11	C-9, C-10, C-12	H_{ab}-10, H_b-11, H_{ab}-12
H_b-11	C-9, C-10, C-12	H_{ab}-10, H_a-11, H_{ab}-12
H_a-12	C-10, C-11, C-13, C-14	H_{ab}-11, H_b-12, H-13
H_b-12	C-10, C-11, C-13, C-14	H_{ab}-11, H_a-12, H-13
H-13	C-1, C-11, C-12, C-14	H_3-14, H_{ab}-12
H_3-14	C-12, C-13	H-13

Table 103 The NMR data of the diacetate derivative of **AR28** in $CDCl_3$

position	**Diacetate derivative of AR28**		HMBC Correlation	NOE
	δ_H (*mult.*, J_{Hz})	δ_C (C-Type)		
1	-	165.30 (C=O)	-	*
2	6.13 (*dd*, 15.6, 1.2)	126.09 (CH)	C-1, C-4	H-4, H_3-16
3	6.77 (*dd*, 15.6, 7.5)	138.51 (CH)	C-1, C-2, C-4	H-4, H-5, H-7
4	5.33 (*m*)	73.09 (CH)	C-2, C-3, C-5, C-15	H-2, H-3, H_3-16

Table 103 Continued

position	**Diacetate derivative of AR28**		HMBC Correlation	NOE
	δ_H (*mult*., J_{Hz})	δ_C (C-Type)		
5	3.26 (*dd*, 6.3, 4.2)	58.88 (CH)	C-6, C-7	H-3, H-6
6	3.02 (*dd*, 8.4, 4.2)	55.79 (CH)	C-5, C-7, C-8	H-5, H-7
7	5.38 (*t*, 9.6)	66.01 (CH)	C-5, C-6, C-8, C-9, C-17	H-3, H-6
8	5.28 (*m*)	123.73 (CH)	C-9, C-10	*
9	5.51 (*td*, 10.1, 3.0)	137.96 (CH)	C-7, C-10, C-11	H-8
10	a: 2.44 (*m*)	28.77 (CH_2)	C-8, C-9, C-11	*
	b: 2.05 (*m*)		C-8, C-9, C-11	*
11	a: 1.75 (*m*)	24.94 (CH_2)	C-9	*
	b: 1.17 (*m*)		C-9	*
12	a: 1.81 (*m*)	33.34 (CH_2)	C-10, C-11, C-13, C-14	*
	b: 1.43 (*m*)		C-10, C-11, C-13, C-14	*
13	4.98 (*m*)	72.89 (CH)	C-1, C-14	*
14	1.21 (*d*, 6.3)	19.78 (CH_3)	C-12, C-13	H-13
15	-	169.34 (C=O)	-	*
16	2.07 (*s*)	20.80 (CH_3)	C-4, C-15	*
17	-	169.82 (C=O)	-	*
18	2.02 (*s*)	21.00 (CH_3)	C-7, C-17	*

* not determined

3.3.2 Compound AR27

Compound **AR27** with the molecular formula $C_{18}H_{24}O_7$ by EIMS [*m/z* 310 $(M-C_2H_2O)^+$] (**Figure 74**) was obtained as a colorless gum and exhibited UV and IR absorption bands similar to those of the diacetate derivative of **AR28**. The ^1H NMR data (**Figure 72**) (**Table 104**) were almost identical to those of the diacetate

derivative of **AR28** except for the replacement of signals for two *cis*-olefinic protons (δ_H 5.51, H-9 and 5.28, H-8) in the diacetate derivative of **AR28** with those for two *trans*-olefinic protons (δ_H 6.16 and 5.47). The ^3J HMBC correlations of H-8/C-6 (δ_C 55.29) and C-10 (δ_C 33.13) and those of H-9/C-7 (δ_C 73.02) and C-11 (δ_C 24.46) confirmed above conclusion. The remaining substitutents were located at the same position as those in the diacetate derivative of **AR28** according to the HMBC correlation data. The observed optical rotation of **AR27**, $[\alpha]_D^{25}$ +69.9 (c = 1.45, $CHCl_3$), was almost identical to that of the diacetate derivative of **AR28**, $[\alpha]_D^{25}$ +65.8 (c = 1.45, $CHCl_3$), indicating that all chiral carbons of **AR27** possessed the same configuration as those of the diacetate derivative of **AR28**. Therefore, **AR27** was identified as the diacetate derivative of a new seiricuprolide.

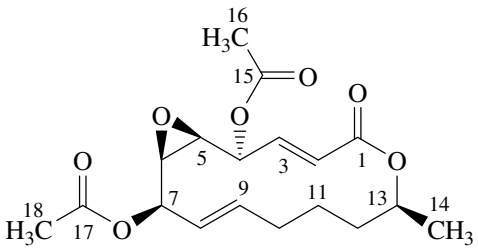

Table 104 The ^{1}H and ^{13}C NMR data of compound **AR27** and the diacetate derivative of **AR28** in $CDCl_3$

position	**AR27**		**Diacetate derivative of AR28**	
	δ_H (*mult.*, J_{Hz})	δ_C (C-Type)	δ_H (*mult.*, J_{Hz})	δ_C (C-Type)
1	-	164.91 (C=O)	-	165.30 (C=O)
2	5.95 (*dd*, 15.5, 2.0)	122.40 (CH)	6.13 (*dd*, 15.6, 1.2)	126.09 (CH)
3	7.01 (*dd*, 15.5, 4.5)	140.89 (CH)	6.77 (*dd*, 15.6, 7.5)	138.51 (CH)
4	5.34 (*ddd*, 6.0, 4.5, 2.0)	72.37 (CH)	5.33 (*m*)	73.09 (CH)
5	3.25 (*dd*, 6.5, 4.5)	58.02 (CH)	3.26 (*dd*, 6.3, 4.2)	58.88 (CH)
6	3.22 (*dd*, 8.5, 4.5)	55.29 (CH)	3.02 (*dd*, 8.4, 4.2)	55.79 (CH)

Table 104 Continued

position	**AR27**		**Diacetate derivative of AR28**	
	δ_H (*mult*., J_{Hz})	δ_C (C-Type)	δ_H (*mult*., J_{Hz})	δ_C (C-Type)
7	5.14 (*t*, 8.5)	73.02 (CH)	5.38 (*t*, 9.6)	66.01 (CH)
8	5.47 (*dd,* 15.5, 8.5)	124.46 (CH)	5.28 (*m*)	123.73 (CH)
9	6.16 (*ddd*, 15.5, 10.0, 5.5)	139.48 (CH)	5.51 (*td*, 10.1, 3.0)	137.96 (CH)
10	a: 2.16 (*m*) b: 2.06 (*m*)	33.13 (CH_2)	a: 2.44 (*m*) b: 2.05 (*m*)	28.77 (CH_2)
11	a: 1.90 (*m*) b: 1.13 (*m*)	24.46 (CH_2)	a: 1.75 (*m*) b: 1.17 (*m*)	24.94 (CH_2)
12	a: 1.80 (*m*) b: 1.56 (*m*)	34.37 (CH_2)	a: 1.81 (*m*) b: 1.43 (*m*)	33.34 (CH_2)
13	4.78 *(dqd*, 10.0, 6.0, 2.0)	72.34 (CH)	4.98 (*m*)	72.89 (CH)
14	1.27 (*d*, 6.0)	20.17 (CH_3)	1.21 (*d*, 6.3)	19.78 (CH_3)
15	-	169.79 (C=O)	-	169.34 (C=O)
16	2.20 (*s*)	20.71 (CH_3)	2.07 (*s*)	20.80 (CH_3)
17	-	169.88 (C=O)	-	169.82 (C=O)
18	2.20 (*s*)	21.22 (CH_3)	2.02 (*s*)	21.00 (CH_3)

Table 105 The HMBC and COSY data of compound **AR27** in $CDCl_3$

position	HMBC Correlation	COSY
H-2	C-1, C-3, C-4	H-3, H-4
H-3	C-1, C-2, C-4, C-5	H-2, H-4
H-4	C-2, C-5, C-15	H-3, H-5
H-5	C-7, C-8	H-4,H-6
H-6	C-7, C-8	H-5, H-7

Table 105 Continued

position	HMBC Correlation	COSY
H-7	C-5, C-8, C-9, C-17	H-6, H-8
H-8	C-6, C-7, C-10	H-7, H-9
H-9	C-7, C-10, C-11	H-8, H_{ab}-10
H_a-10	C-8, C-9	H-9, H_b-10, H_{ab}-11
H_b-10	C-8, C-9	H-9, H_a-10, H_{ab}-11
H_a-11	C-9, C-10, C-12, C13	H_{ab}-10, H_b-11, H_{ab}-12
H_b-11	C-9, C-10, C-12, C-13	H_{ab}-10, H_a-11, H_{ab}-12
H_a-12	C-10, C-11, C-13	H_{ab}-11, H_b-12, H-13
H_b-12	C-10, C-11, C-13	H_{ab}-11, H_a-12, H-13
H-13	C-1, C-11	H_3-14, H_{ab}-12
H_3-14	C-12, C-13	H-13
H_3-16	C-4, C-15	-
H_3-18	C-7, C-17	-

3.3.3 Compound AR29 and its triacetate derivative

Compound **AR29** with the molecular formula $C_{14}H_{22}O_6$ by EIMS [*m/z* 268 $(M-H_2O)^+$] (**Figure 77**) was obtained as a colorless gum. It exhibited UV and IR absorption bands similar to those of **AR28**. The ^{1}H NMR data (**Figure 75**) (**Table 106**) were almost identical to those of **AR28** except for the replacement of signals for two *cis*-epoxymethine protons in compound **AR28** with those of two hydroxymethine protons (H-5, δ_H 4.42 and H-6, δ_H 3.59). The ^3J HMBC correlations of H-5/C-3 (δ_C 143.03) and C-7 (δ_C 68.57) and those of H-6/C-4 (δ_C 71.91) supported the conclusion. Therefore, **AR29** was a new 4,5-dihydroxy derivative of seiricuprolide.

A triacetate derivative of **AR29** was obtained as a colorless gum and exhibited UV and IR absorption bands similar to those of **AR29**. The ^{1}H NMR data (**Figure 78**) (**Table 106**) were almost identical to those of compound **AR29** except for

the appearance of signals for three oxymethine protons H-4 (δ_H 5.45), H-6 (δ_H 4.97) and H-7 (δ_H 5.96) at much lower field and three additional singlets for three acetoxyl groups, H_3-16 (δ_H 2.12), H_3-18 (δ_H 2.14) and H_3-20 (δ_H 2.17). The HMBC correlations of H_3-16 to C-4 (δ_C 71.49), H_3-18 to C-6 (δ_C 73.98) and H_3-20 to C-7 (δ_C 67.23) indicated that the acetoxyl groups were attached at C-4, C-6 and C-7. The remaining substitutents were located at the same position as those in **AR29** according to the HMBC correlations. Irradiation of H-5 in the NOEDIFF experiment (**Table 108**) enhanced signal intensity of H-4, while irradiation of H-7 affected signal intensity of H-6. These results indicated *cis*-relationship of H-4/H-5 and H-6/H-7 as well as *trans*-relationship of H-5/H-6. Consequently, compound **AR29** possessed the same relative configuration as its triacetate derivative. As compounds **AR28** and **AR29** were co-metabolites, we proposed that the absolute configuration of C-4 and C-7 in compound **AR29** would have *R* and *S* configuration, respectively, identical to those of compound **AR28**. Thus, both C-5 and C-6 would possess *R*-configuration.

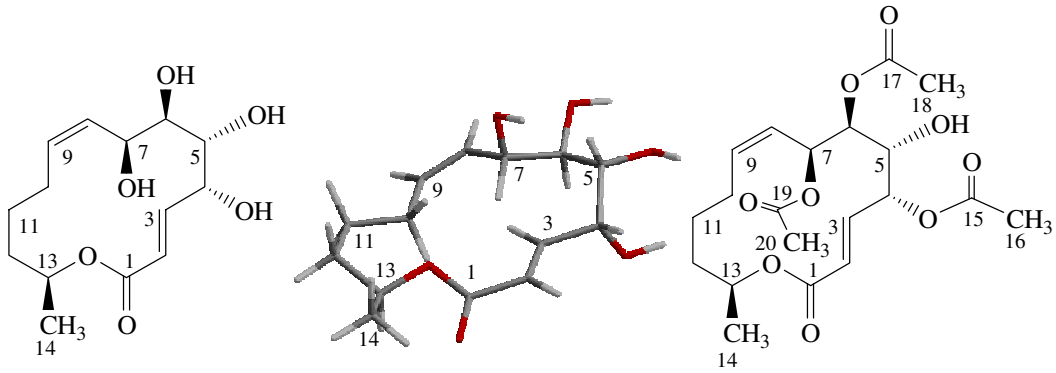

Table 106 The ^1H and ^{13}C NMR data of compound **AR29** and its triacetate derivative in $CDCl_3$

position	**AR29**		**Triacetate derivative of AR29**	
	δ_H (*mult.*, J_{Hz})	δ_C (C-Type)	δ_H (*mult.*, J_{Hz})	δ_C (C-Type)
1	-	165.64 (C=O)	-	165.09 (C=O)
2	6.26 (*d*, 15.6)	125.59 (CH)	6.46 (*d*, 15.9)	130.11 (CH)
3	6.86 (*dd*, 15.6, 5.7)	143.03 (CH)	6.93 (*dd*, 15.9, 9.0)	136.22 (CH)

Table 106 Continued

position	**AR29**		**Triacetate derivative of AR29**	
	δ_H (*mult*., J_{Hz})	δ_C (C-Type)	δ_H (*mult*., J_{Hz})	δ_C (C-Type)
4	4.73 (*brs*)	71.91 (CH)	5.45 (*dd*, 9.0, 3.6)	71.49 (CH)
5	4.42 (*brs*)	68.16 (CH)	4.46 (*dd*, 8.7, 3.6)	60.75 (CH)
6	3.59 (*dd*, 6.0, 1.5)	73.84 (CH)	4.97 (*dd*, 8.7, 2.4)	73.98 (CH)
7	4.45 (*brs*)	68.57 (CH)	5.96 (*dd*, 9.9, 2.4)	67.23 (CH)
8	5.57 (*m*)	129.00 (CH)	5.16 (*t*, 9.9)	122.94 (CH)
9	5.47 (*m*)	132.98 (CH)	5.54 (*td*, 9.9, 5.1)	136.06 (CH)
10	a: 2.20 (*m*)	29.83 (CH_2)	a: 2.55 (*m*)	30.42 (CH_2)
	b: 1.95 (*m*)		b: 1.87 (*m*)	
11	a: 1.57 (*m*)	26.03 (CH_2)	a: 1.69 (*m*)	25.82 (CH_2)
	b: 1.11 (*m*)		b: 1.13 (*m*)	
12	a: 1.84 (*m*)	35.03 (CH_2)	a: 1.85 (*m*)	34.84 (CH_2)
	b: 1.49 (*m*)		b: 1.51 (*m*)	
13	5.02 (*m*)	73.17 (CH)	5.01 (*m*)	74.21 (CH)
14	1.30 (*d*, 6.3)	20.55 (CH_3)	1.32 (*d*, 6.3)	20.73 (CH_3)
15			-	169.65 (C=O)
16			2.12 (*s*)	20.51 (CH_3)
17			-	169.38 (C=O)
18			2.14 (*s*)	20.76 (CH_3)
19			-	170.47 (C=O)
20			2.17 (*s*)	20.85 (CH_3)

Table 107 The HMBC and COSY data of compound **AR29** in $CDCl_3$

position	HMBC Correlation	COSY
H-2	C-1, C-4, C-5	H-3, H-4
H-3	C-1, C-2, C-4, C-5	H-2, H-4
H-4	C-2, C-3, C-5	H-2, H-3, H-5
H-5	C-3, C-4, C-7	H-4, H-6

Table 107 Continued

position	HMBC Correlation	COSY
H-6	C-4, C-5, C-7	H-5, H-7
H-7	C-8, C-9	H-6, H-8
H-8	C-10	H-7, H-9
H-9	C-7, C-10, C-11	H-8, H_{ab}-10
H_a-10	C-8, C-9	H-9, H_b-10, H_{ab}-11
H_b-10	C-8, C-9	H-9, H_a-10, H_{ab}-11
H_a-11	C-10, C-12, C-13	H_{ab}-10, H_b-11, H_{ab}-12
H_b-11	C-10, C-12, C-13	H_{ab}-10, H_a-11, H_{ab}-12
H_a-12	C-10, C-11	H_{ab}-11, H_b-12, H-13
H_b-12	C-10, C-11	H_{ab}-11, H_a-12, H-13
H-13	C-1, C-12, C-14	H_3-14, H_{ab}-12
H_3-14	C-12, C-13	H-13

Table 108 The HMBC, COSY and NOE data of the triacetate derivative of compound **AR29** in $CDCl_3$

position	HMBC Correlation	COSY	NOE
H-2	C-1, C-4, C-5	H-3, H-4	*
H-3	C-1, C-2, C-4, C-5	H-2, H-4	*
H-4	C-2, C-3, C-5, C-15	H-2, H-3, H-5	H-3, H-5
H-5	C-3, C-4, C-7	H-4, H-6	H-4
H-6	C-4, C-5, C-7, C-17	H-5, H-7	H-7
H-7	C-8, C-9, C-19	H-6, H-8	H-6, H-8
H-8	C-10	H-7, H-9	*
H-9	C-7, C-10, C-11	H-8, H_{ab}-10	*
H_a-10	C-8, C-9	H-9, H_b-10, H_{ab}-11	*
H_b-10	C-8, C-9	H-9, H_a-10, H_{ab}-11	*

Table 108 Continued

position	HMBC Correlation	COSY	NOE
H_a-11	C-10, C-12, C-13	H_{ab}-10, H_b-11, H_{ab}-12	*
H_b-11	C-10, C-12, C-13	H_{ab}-10, H_a-11, H_{ab}-12	*
H_a-12	C-10, C-11	H_{ab}-11, H_b-12, H-13	*
H_b-12	C-10, C-11	H_{ab}-11, H_a-12, H-13	*
H-13	C-1, C-12, C-14	H_3-14, H_{ab}-12	*
H_3-14	C-12, C-13	H-13	H-13
H_3-16	C-4, C-15	-	*
H_3-18	C-6, C-17	-	*
H_3-20	C-7, C-19	-	*

* not determined

3.3.4 Compound AR30

Compound **AR30** was obtained as a colorless gum. The UV spectrum showed absorption bands at λ_{max} 207, 221 and 277 nm, indicating the presence of an aromatic chromophore. The IR spectrum displayed an absorption band at 3422 cm^{-1} for a hydroxyl group. The ^1H NMR spectrum showed characteristic signals for a 1,4-disubstituted benzene [δ 7.11 (*d*, *J* = 9.0 Hz, 2H) and 6.79 (*d*, *J* = 9.0 Hz, 2H)] and a hydroxyethyl group [δ 3.83 (*t*, *J* = 6.0 Hz, 2H) and 2.81 (*t*, *J* = 6.0 Hz, 2H)]. These data together with the chemical shift of C-1 (δ 154.22) indicated that the other substituent of the 1,4-disubstituted benzene was a hydroxyl group. The HMBC data supported the assigned structure. Therefore, **AR30** was identified as tyrosol (Guzmán-López *et al*., 2007).

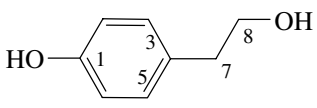

Table 109 The ^{1}H and ^{13}C NMR data of compound **AR30** and tyrosol in $CDCl_3$

position	**AR30**		**Tyrosol**	
	δ_H (*mult*., J_{Hz})	δ_C (C-Type)	δ_H (*mult*., J_{Hz})	δ_C (C-Type)
1	-	154.22 (C)	-	154.1 (C)
2, 6	6.79 (*d*, 9.0)	115.45 (CH)	6.77 (*d*, 8.0)	115.4 (CH)
3, 5	7.11 (*d*, 9.0)	130.15 (CH)	7.09 (*d*, 8.0)	130.0 (CH)
4	-	130.55 (C)	-	130.2 (C)
7	2.81 (*t*, 6.0)	38.27 (CH_2)	2.82 (*t*, 6.4)	38.3 (CH_2)
8	3.83 (*t*, 6.0)	63.80 (CH_2)	3.83 (*t*, 6.4)	63.8 (CH_2)

Guzmán-López *et al*., 2007.

3.3.5 Compound AR31

Compound **AR31** was obtained as a colorless gum. The UV spectrum showed absorption bands at λ_{max} 207 and 252 nm, indicating the presence of an aromatic chromophore. The IR spectrum showed absorption bands at 3366 and 1686 cm^{-1} for hydroxyl and conjugated carbonyl groups, respectively. The ^{1}H NMR spectral data exhibited signals for a *para*-disubstituted benzene [δ_H 7.90 (*d*, *J* = 9.0 Hz, 2H) and 6.85 (*d*, *J* = 9.0 Hz, 2H)] and one acetyl group (δ_H 2.20, *s*, 3H). The aromatic protons at δ_H 7.90 and 6.85 were attributed to H-2, H-6 and H-3, H-5, respectively, on the basis of their chemical shifts. A signal of carbonyl carbon at δ_C 196.92 in the ^{13}C NMR spectrum supported the IR data. The chemical shifts of C-1 (δ_C 130.48) and C-4 (δ_C 160.10) attached the acetyl unit and a hydroxyl group at C-1 and C-4, respectively. Therefore, compound **AR31** was assigned as 4-hydroxyacetophenone which was isolated from the bark of *Salix hulteni* (Jeon *et al*., 2008).

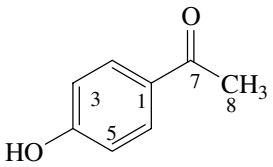

Table 110 The ^{1}H and ^{13}C NMR data of compound **AR31** in $CDCl_3$ and 4-hydroxyacetophenone in DMSO-d_6

position	**AR31**		**4-Hydroxyacetophenone**	
	δ_H (*mult*., J_{Hz})	δ_C (C-Type)	δ_H (*mult*., J_{Hz})	δ_C (C-Type)
1	-	130.48 (C)	**-**	128.84 (C)
2, 6	7.90 (*d*, 9.0)	130.94 (CH)	7.93 (*d*, 7.8)	133.05 (CH)
3, 5	6.85 (*d*, 9.0)	115.29 (CH)	6.97 (*d*, 7.8)	114.44 (CH)
4	-	160.10 (C)	**-**	161.23 (C)
7	**-**	196.92 (C=O)	**-**	195.23 (C=O)
8	2.20 (*s*)	26.30 (CH_3)	2.53 (*s*)	24.65 (CH_3)

Jeon *et al*., 2008.

REFERENCES

Abdel-Lateff, A., König, G.M., Fisch, K.M., Höller, U., Jones, P.G. and Wright, A.D. 2002. New antioxidant hydroquinone derivatives from the algicolous marine fungus *Acremonium* sp. J. Nat. Prod. 65, 1605-1611.

Amagata, T., Morinaka, B.I., Amagata, A., Tenney, K., Valeriote, F.A., Lobkovsky, E., Clardy, J. and Crews, P. 2006. A chemical study of cyclic depsipeptides produced by a sponge-derived fungus. J. Nat. Prod. 69, 1560-1565.

Ayer, W.A. and Miao, S. 1993. Secondary metabolites of the aspen fungus *Stachybotrys cylindrospora*. Can. J. Chem. 71, 487-493.

Ballio, A., Evidente, A., Graniti, A., Randazzo, G. and Sparapano, L. 1988. Seiricuprolide, a new phytotoxic macrolide from a strain of *Seiridium Cupressi* infecting cypress. Phytochemistry 27, 3117-3121.

Bunyapaiboonsri, T., Yoiprommarat, S., Khonsanit, A. and Komwijit, S. 2008. Phenolic glycosides from the filamentous fungus *Acremonium* sp. BCC 14080. J. Nat. Prod. 71, 891-894.

Camarda, L., Merlini, L. and Nasini, G. 1976. Metabolites of *Cercospora*. Taiwapyrone, an α-pyrone of unusual structure from *Cercospora taiwanensis*. Phytochemistry 15, 537-539.

Chinworrungsee, M., Wiyakrutta, S., Sriubolmas, N., Chuailua, P. and Suksamrarn, A. 2008. Cytotoxic activities of trichothecenes isolated from an endophytic fungus belonging to order Hypocreales. Arch. Pharm. Res. 31, 611-616.

Cho, J.-Y., Moon, J.-H., Seong, K.-Y. and Park, K-H. 1998. Antimicrobial activity of 4-hydroxybenzoic acid and *trans* 4-hydroxycinnamic acid isolated and identified from rice hull. Biosci. Biotechnol. Biochem. 62, 2273-2276.

Chu, M., Mierzwa, R., Truumees, I., Gentile, F., Patel, M., Gullo, V., Chan, T.-M. and Puar, M.S. 1993. Two novel diketopiperazines isolated from the fungus *Tolypocladium* sp. Tetrahedron Lett. 34, 7537-7540.

Deyrup, S.T., Swenson, D.C., Gloer, J.B. and Wicklow, D.T. 2006. Caryophyllene sesquiterpenoids from a fungicolous isolate of *Pestalotiopsis disseminate*. J. Nat. Prod. 69, 608-611.

Ding, G., Jiang, L., Guo, L., Chen, X., Zhang, H. and Che, Y. 2008. Pestalazines and pestalamides, bioactive metabolites from the plant pathogenic fungus *Pestalotiopsis theae*. J. Nat. Prod. 71, 1861–1865.

Ding, G., Li, Y., Fu, S., Liu, S., Wei, J. and Che, Y. 2009. Ambuic acid and torreyanic acid derivatives from the endolichenic fungus *Pestalotiopsis* sp. J. Nat. Prod. 72, 182–186.

Ding, G., Liu, S., Guo, L., Zhou, Y. and Che, Y. 2008. Antifungal metabolites from the plant endophytic fungus *Pestalotiopsis foedan*. J. Nat. Prod. 71, 615–618.

Ding, G., Zheng, Z., Liu, S., Zhang, H., Guo, L. and Che, Y. 2009. Photinides A-F, cytotoxic benzofuranone-derived γ-lactones from the plant endophytic fungus *Pestalotiopsis photiniae*. J. Nat. Prod. 72, 942–945.

Gallardo, G.L., Butler, M., Gallo, M.L., Rodríguez, M.A., Eberlin, M.N. and Cabrera, G. M. 2006. Antimicrobial metabolites produced by an intertidal *Acremonium furcatum*. Phytochemistry 67, 2403-2410.

Guzmán-Lopéz, O., Trigos, A., Fernández, F.J., Yañez-Morales, M.deJ. and Saucedo-Castañeda, G. 2007. Tyrosol and tryptophol produced by *Ceratocystis adiposa*. World J. Microbiol. Biotechnol. 23, 1473-1477.

Harper, J.K., Arif, A.M., Ford, E.J., Strobel, G.A., Porco, Jr., J.A., Tomer, D.P., Oneill, K.L., Heider, E.M. and Grant, D.M. 2003. Pestacin: a 1,3-dihydro isobenzofuran from *Pestalotiopsis microspora* possessing antioxidant and antimycotic activities. Tetrahedron 59, 2471–2476.

Isaka, M., Palasarn, S., Auncharoen, P., Komwijit, S. and Jones, E.B.G. 2009. Acremoxanthones A and B, novel antibiotic polyketides from the fungus *Acremonium sp.* BCC 31806. Tetrahedron Lett. 50, 284-287.

Jang, J-H., Kanoh, K., Adachi, K. and Shizuri, Y. 2006. New dihydrobenzofuran derivative, awajanoran, from marine-derived *Acremonium* sp. AWA16-1. J. Antibiot. 59, 428-431.

Jiao, P., Kawasaki M. and Yamamoto, H. 2009. A sequential *o*-nitrosoaldol and Grignard addition process: An enantio- and diastereoselective entry to chiral 1,2-diols. Angew. Chem. Int. Ed. 48, 3333-3336.

Joen, S.H., Chun, W., Choi, Y.J. and Kwon, Y.S. 2008. Cytotoxic constituents from the bark of *Salix hulteni*. Arch. Pharm. Res. 31, 978-982.

Kashiyama, Y., Yoshikuni, Y., Baker, D. and Siegel, J.B. 2009. (Bio Architecture Lab, Inc., USA). Recombinant microbial systems for converting polysaccharides into commodity products such as biofuels. WO 2009046370 A2, April 09.

Kawamura, H., Kaneko, T., Koshino, H., Esumi, Y., Uzawa, J. and Sugawara F. 2000. Penicillides from *Penicillium* sp. isolated from *Taxus cuspidata*. Nat. Prod. Lett. 14, 477-484.

Li, E., Jiang, L., Guo, L., Zhang, H. and Che, Y. 2008. Pestalachlorides A–C, antifungal metabolites from the plant endophytic fungus *Pestalotiopsis adusta*. Bioorg. Med. Chem. 16, 7894–7899.

Li, E., Tian, R., Liu, S., Chen, X., Guo, L. and Che, Y. 2008. Pestalotheols A-D, bioactive metabolites from the plant endophytic fungus *Pestalotiopsis theae*. J. Nat. Prod. 71, 664–668.

Li, J.Y. and Strobel, G.A. 2001. Jesterone and hydroxy-jesterone antioomycete cyclohexenone epoxides from the endophytic fungus *Pestalotiopsis jesteri.* Phytochemistry 57, 261–265.

Liu, L., Li, Y., Liu, S., Zheng, Z., Chen, X., Zhang, H., Guo, L. and Che, Y. 2009. Chloropestolide A, an antitumor metabolite with an unprecedented spiroketal skeleton from *Pestalotiopsis fici*. Org. Lett. 11, 2836-2839.

Liu, L., Liu, S., Chen, X., Guo, L. and Che, Y. 2009. Pestalofones A–E, bioactive cyclohexanone derivatives from the plant endophytic fungus *Pestalotiopsis fici*. Bioorg. Med. Chem. 17, 606–613.

Liu, L., Liu, S., Niu, S., Guo, L., Chen, X. and Che, Y. 2009. Isoprenylated chromone derivatives from the plant endophytic fungus *Pestalotiopsis fici*. J. Nat. Prod. 72, 1482–1486.

Liu, L., Tian, R., Liu, S., Chen, X., Guo, L. and Che, Y. 2008. Pestaloficiols A–E, bioactive cyclopropane derivatives from the plant endophytic fungus *Pestalotiopsis fici.* Bioorg. Med. Chem. 16, 6021–6026.

Magnani, R.F., Rodrigues-Fo, E., Daolioa, C., Ferreira, A.G. and de Souza, A.Q.L. 2003. Three highly oxygenated caryophyllene sesquiterpenes from *Pestalotiopsis* sp., a fungus isolated from bark of *Pinus taeda*. Z. Naturforsch. 58, 319-324.

Mori, H., Urano, Y., Abe, F., Furukawa, S., Furukawa, S., Tsurumi, Y., Sakamoto, K., Hashimoto, M., Takase, S., Hino, M. and Fujii, T. 2003. FR235222, a fungal metabolite, is a novel immunosuppressant that inhibits mammalian histone deacetylase (HDAC). J. Antibiot. 56, 72-79.

Poling, S.M., Wicklow, D.T., Rogers, K.D. and Gloer J.B. 2008. *Acremonium zeae*, a protective endophyte of maize, produces dihydroresorcylide and 7-hydroxydihydroresorcylides. J. Agric. Food. Chem. 56, 3006-3009.

Pontius, A., Mohamed, I., Krick, A., Kehraus, S. and König, G.M. 2008. Aromatic polyketides from marine algicolous fungi. J. Nat. Prod. 71, 272-274.

Shim, S.H., Sy, A.A., Gloer, J.B. and Wicklow, D.T. 2008. Isolation of an isocoumarin and an isobenzofuran derivatives from a fungicolous isolate of *Acremonium crotocinigenum*. Bull. Korean Chem. Soc. 29, 863-865.

Shimada. A., Takahashi. I., Kawano, T. and Kimura, Y. 2001. Chloroisosulochrin, chloroisosulochrin dehydrate, and pestheic acid, plant growth regulators, produced by *Pestalotiopsis theae*. Z. Naturforsch. 56, 797-803.

Strobel, G., Ford, E., Worapong, J., Harper, J.K., Arif, A.M., Grant, D.M., Fung, P.C. W. and Chaud, R.M.W. 2002. Isopestacin, an isobenzofuranone from *Pestalotiopsis microspora*, possessing antifungal and antioxidant activities. Phytochemistry 60, 179–183.

Trisuwan, K., Rukachaisirikul, V., Sukpondma Y., Phongpaichit, S., Preedanon, S. and Sakayaroj, J. 2009. Lactone derivatives from the marine-derived fungus *Penicillium* sp. PSU-F44. Chem. Pharm. Bull. 57, 1100-1102.

Xu, J., Kjer, J., Sendker, J., Wray, V., Guan, H., Edrada, R., Lin, W., Wu, J. and Proksch, P. 2009. Chromones from the endophytic fungus *Pestalotiopsis* sp.

isolated from the Chinese mangrove plant *Rhizophora mucronata*. J. Nat. Prod. 72, 662–665.

Xu, J., Kjer, J., Sendker, J., Wray, V., Guan, H., Edrada, R., Müller, W.E.G., Bayer, M., Lin, W., Wu, J. and Proksch, P. 2009. Cytosporones, coumarins, and an alkaloid from the endophytic fungus *Pestalotiopsis* sp. isolated from the Chinese mangrove plant *Rhizophora mucronata*. Bioorg. Med. Chem. 17, 7362–7367.

Zhang, P., Bao, B., The Dang, H., Hong, J., Lee, H.J., Yoo, E.S., Bae, K.S. and Jung, J.H. 2009. Anti-inflammatory sesquiterpenoids from a sponge-derived fungus *Acremonium* sp. J. Nat. Prod. 72, 270-275.

APPENDIX

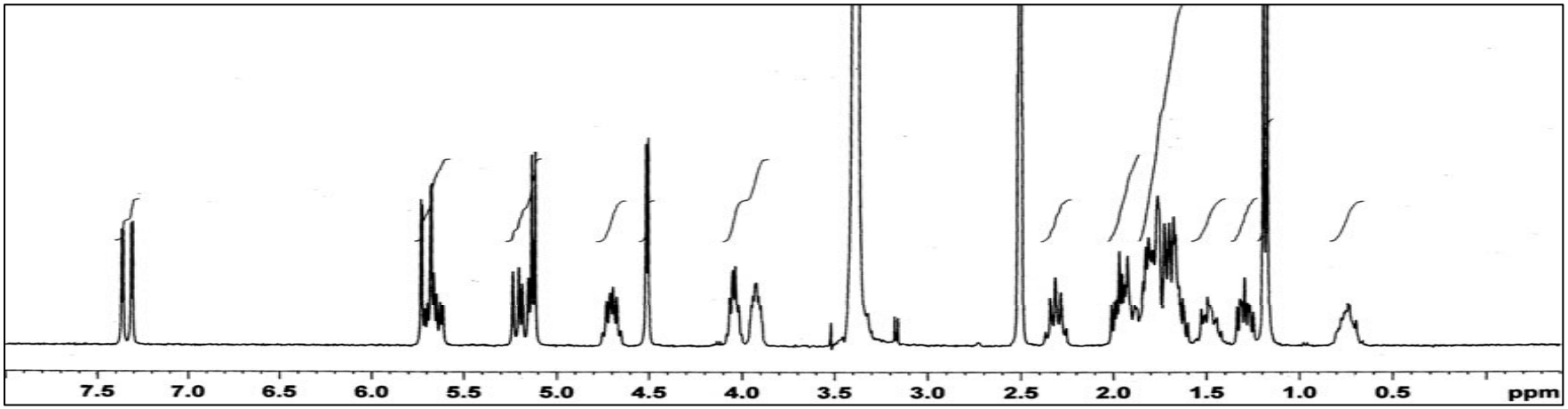

Figure 1 The 300 MHz ^{1}H NMR spectrum of compound **AR1** in DMSO-d_6

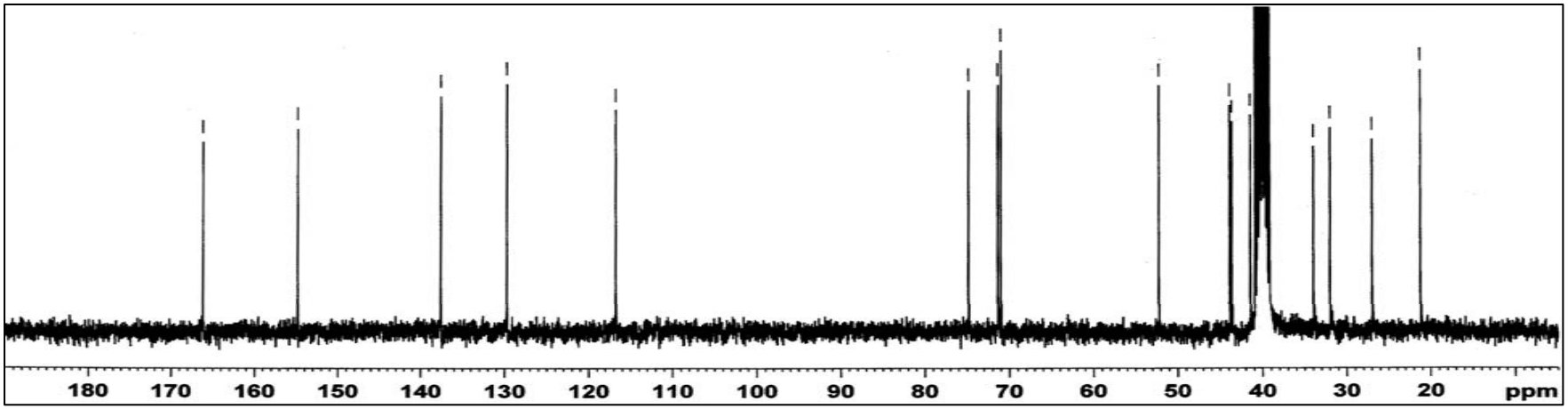

Figure 2 The 75 MHz ^{13}C NMR spectrum of compound **AR1** in DMSO-d_6

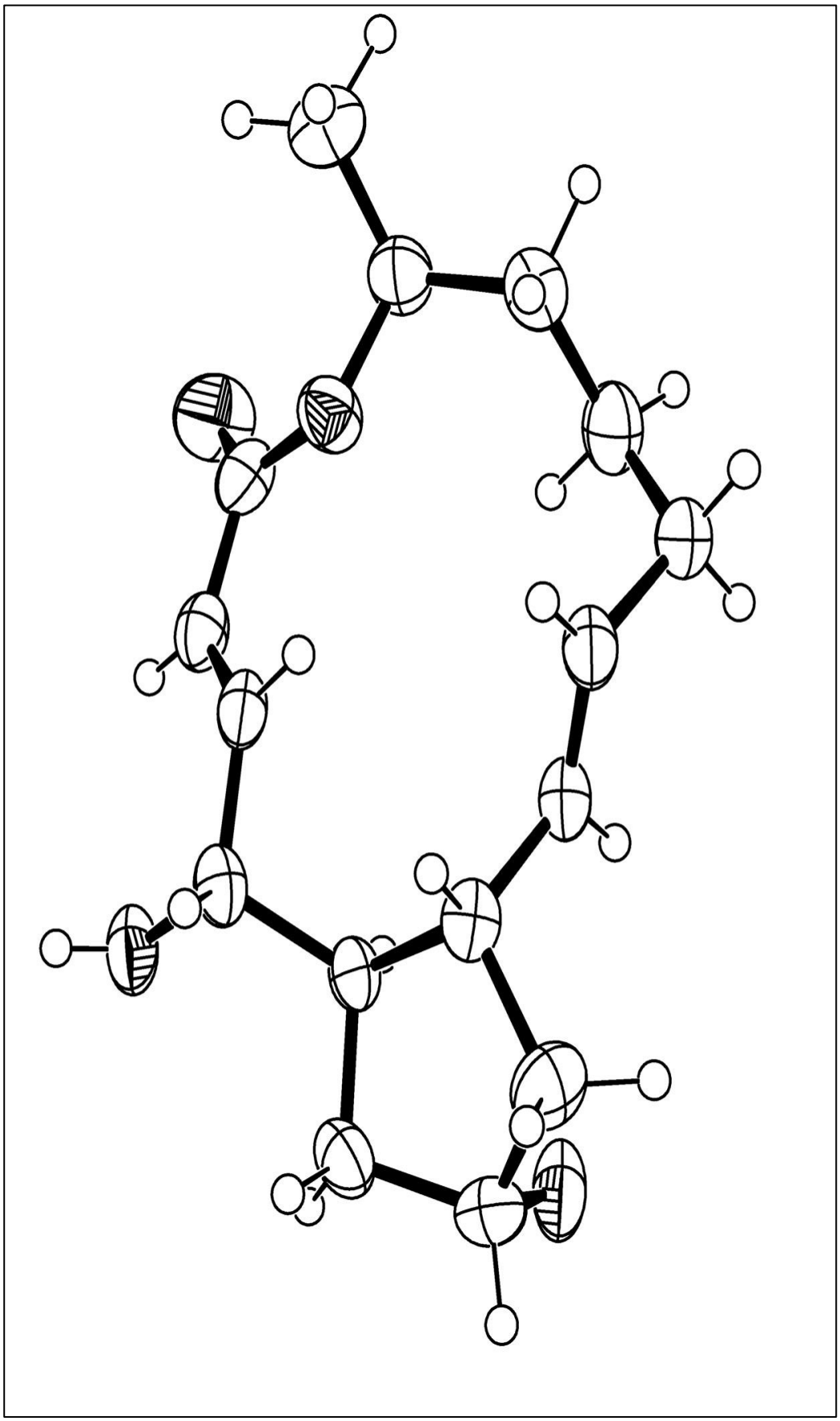

Figure 3 The X-ray structure of compound **AR1**

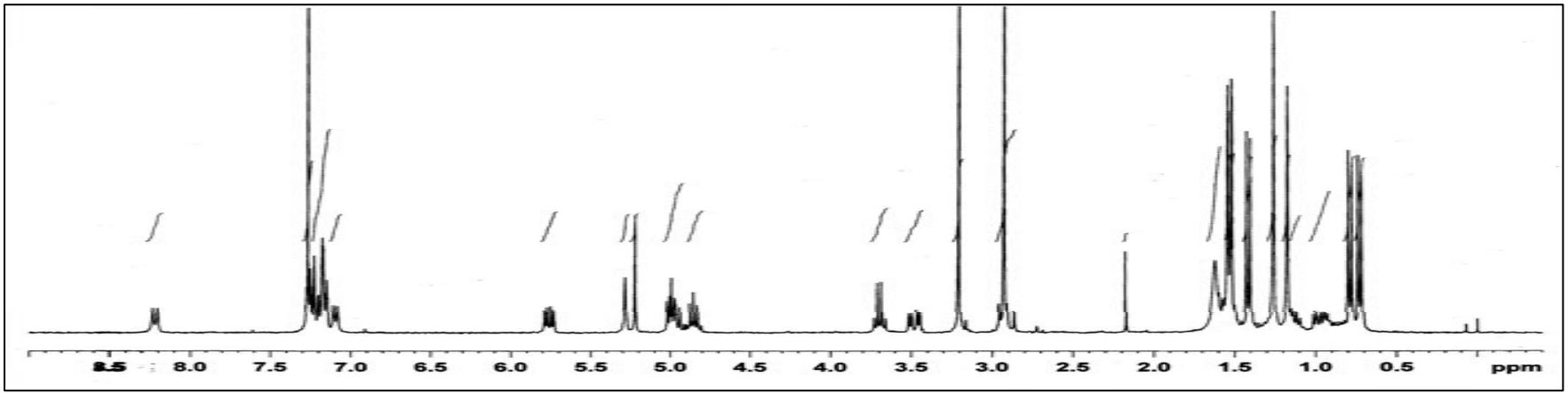

Figure 4 The 300 MHz ^{1}H NMR spectrum of compound **AR2** in $CDCl_3$

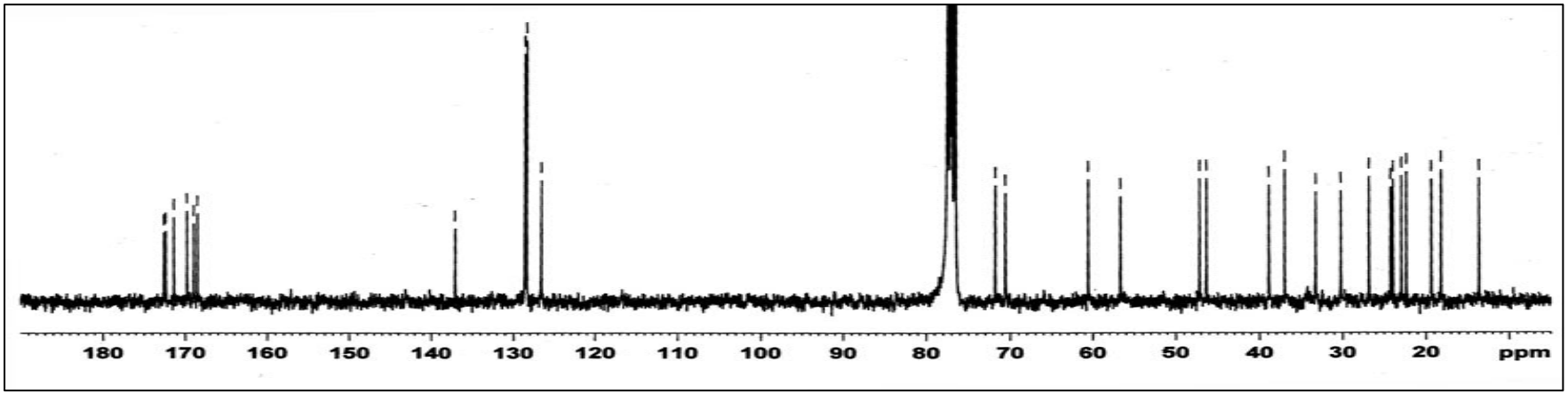

Figure 5 The 75 MHz ^{13}C NMR spectrum of compound **AR2** in $CDCl_3$

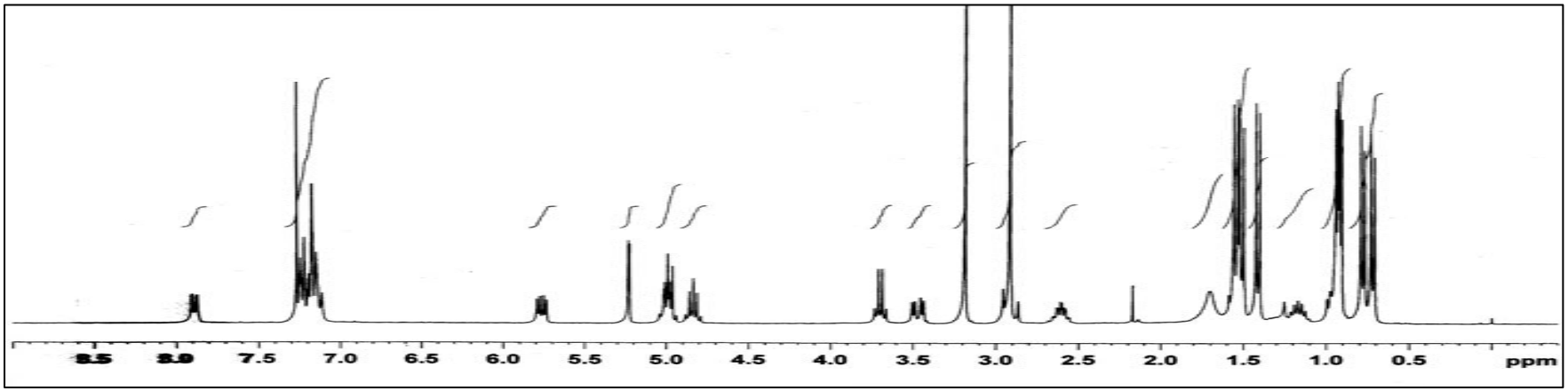

Figure 6 The 300 MHz ^{1}H NMR spectrum of compound **AR3** in $CDCl_3$

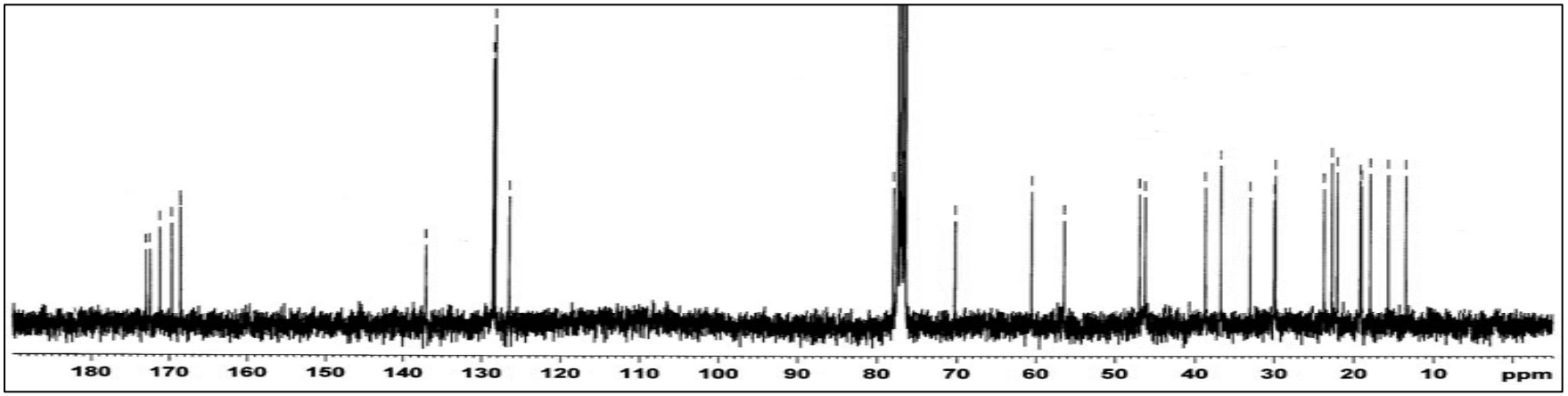

Figure 7 The 75 MHz ^{13}C NMR spectrum of compound **AR3** in $CDCl_3$

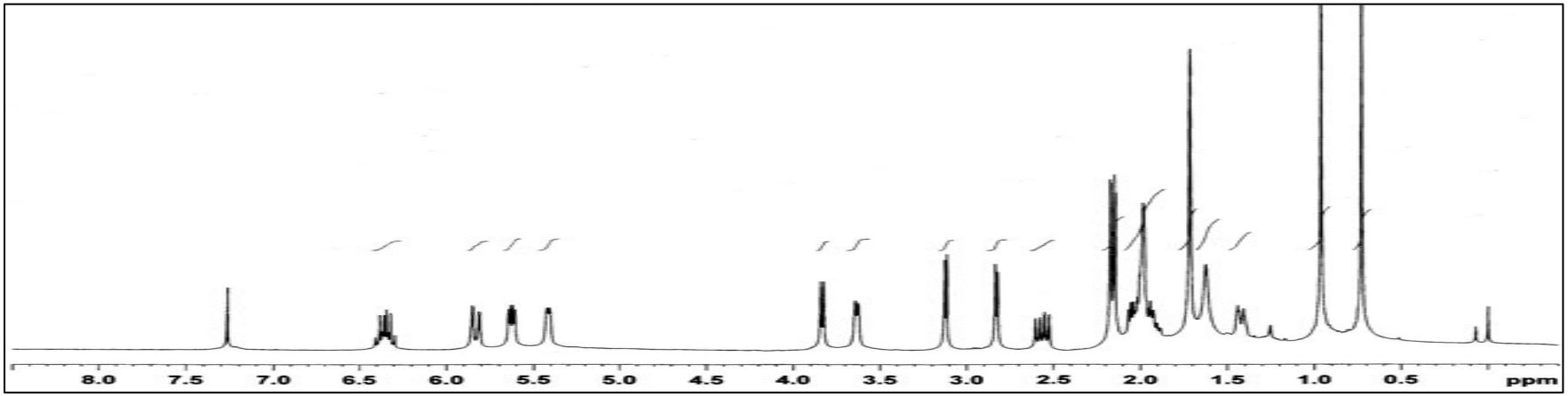

Figure 8 The 300 MHz ^{1}H NMR spectrum of compound **AR4** in $CDCl_3$

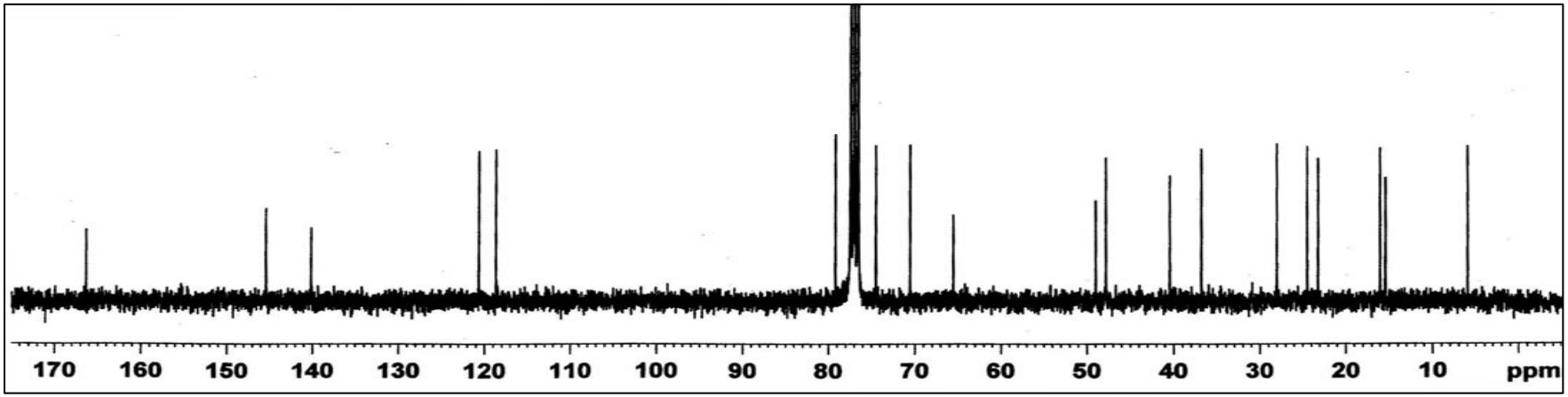

Figure 9 The 75 MHz ^{13}C NMR spectrum of compound **AR4** in $CDCl_3$

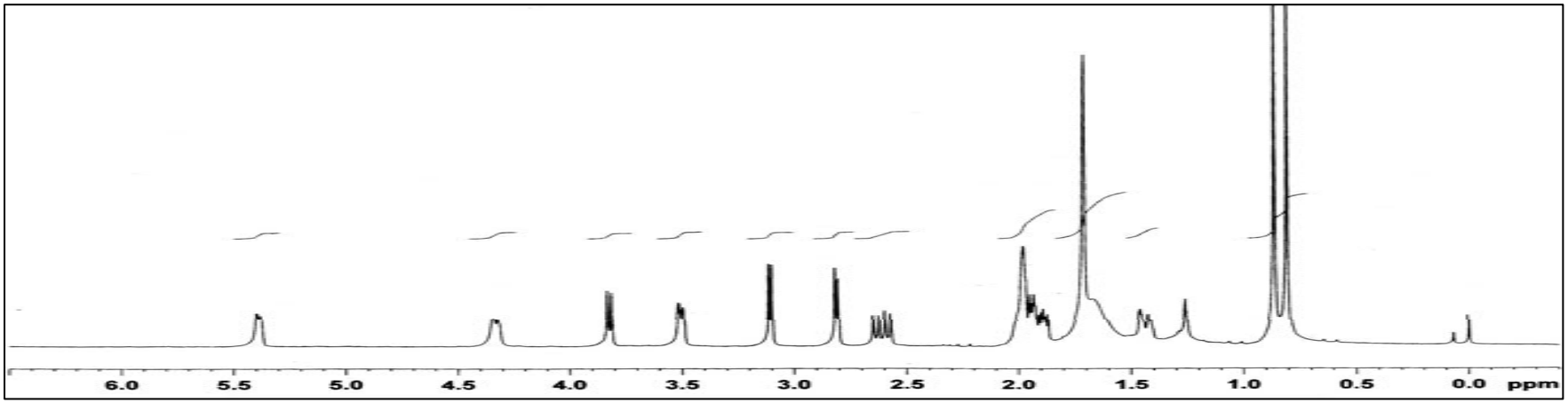

Figure 10 The 300 MHz ^{1}H NMR spectrum of compound **AR7** in $CDCl_3$

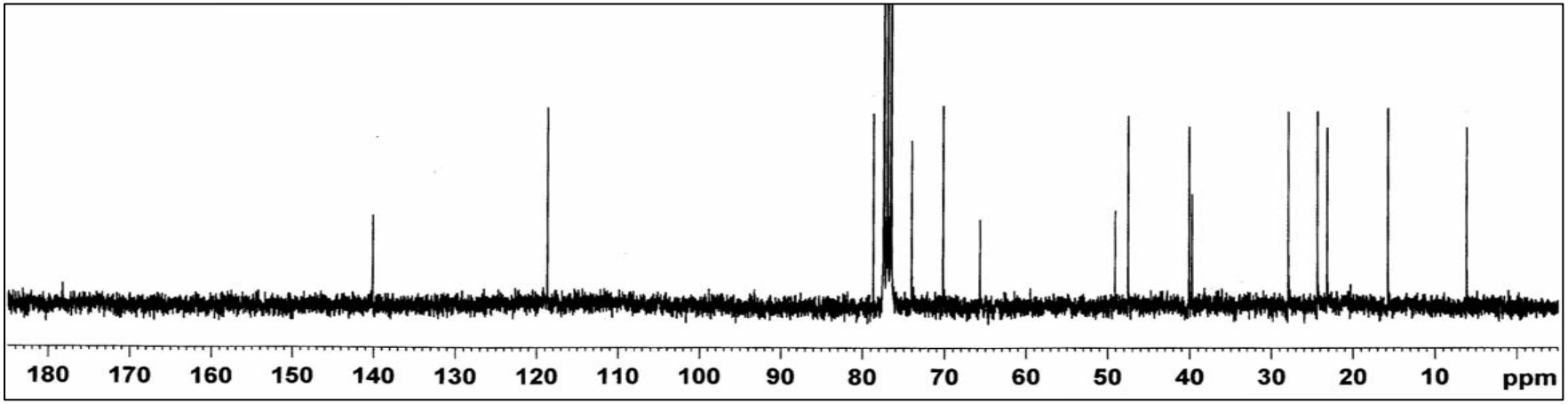

Figure 11 The 75 MHz ^{13}C NMR spectrum of compound **AR7** in $CDCl_3$

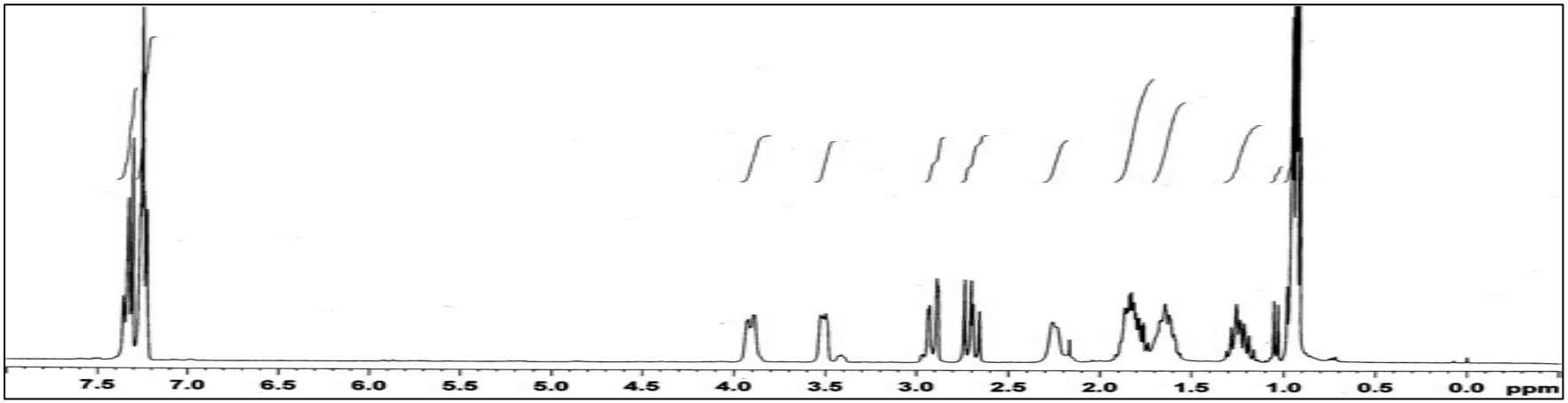

Figure 12 The 300 MHz ^{1}H NMR spectrum of compound **AR5** in $CDCl_3$

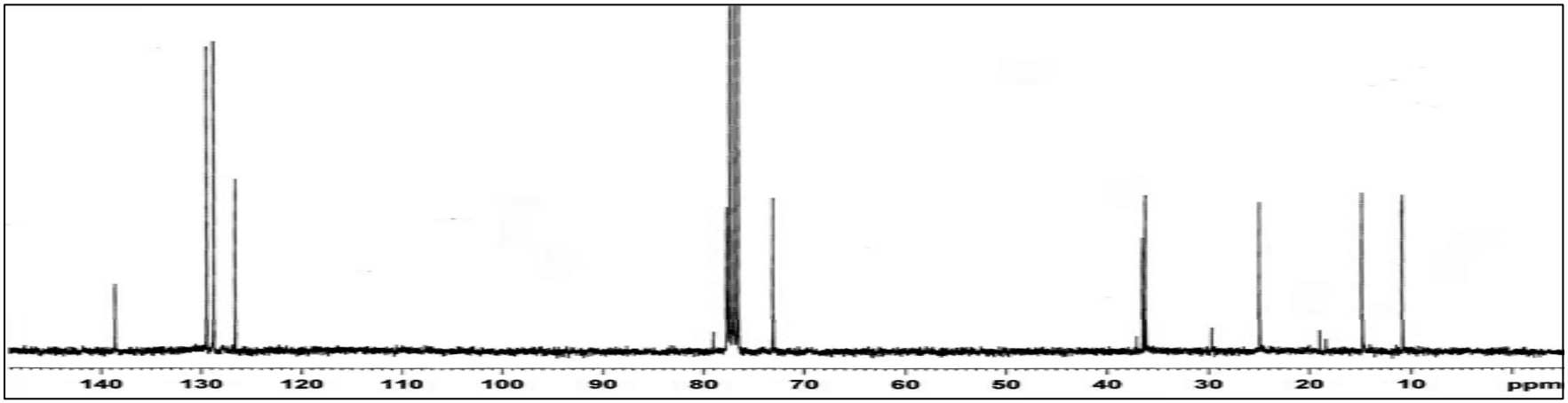

Figure 13 The 75 MHz ^{13}C NMR spectrum of compound **AR5** in $CDCl_3$

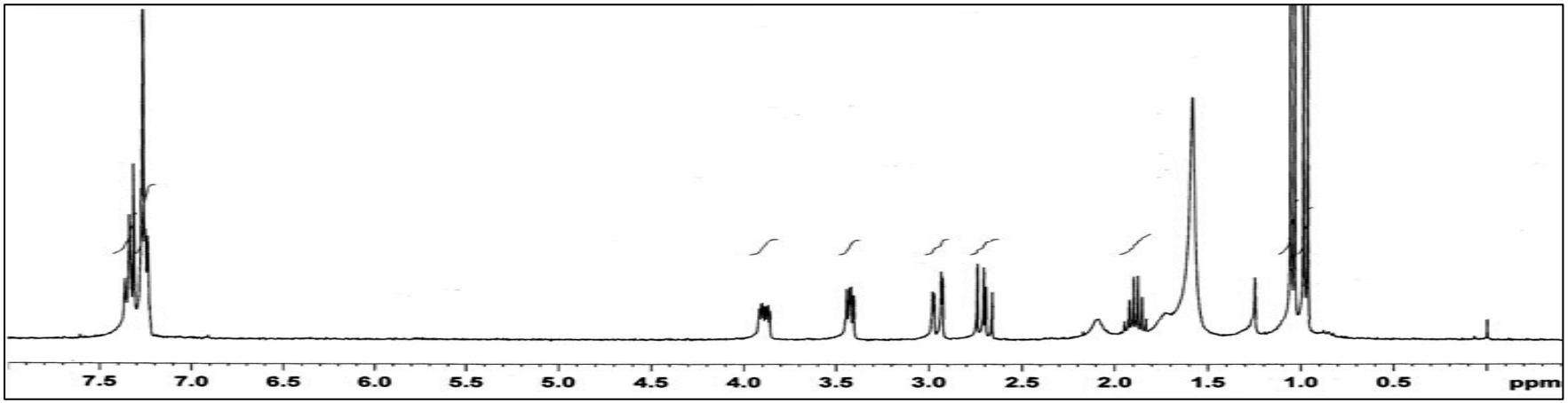

Figure 14 The 300 MHz ^{1}H NMR spectrum of compound **AR6** in $CDCl_3$

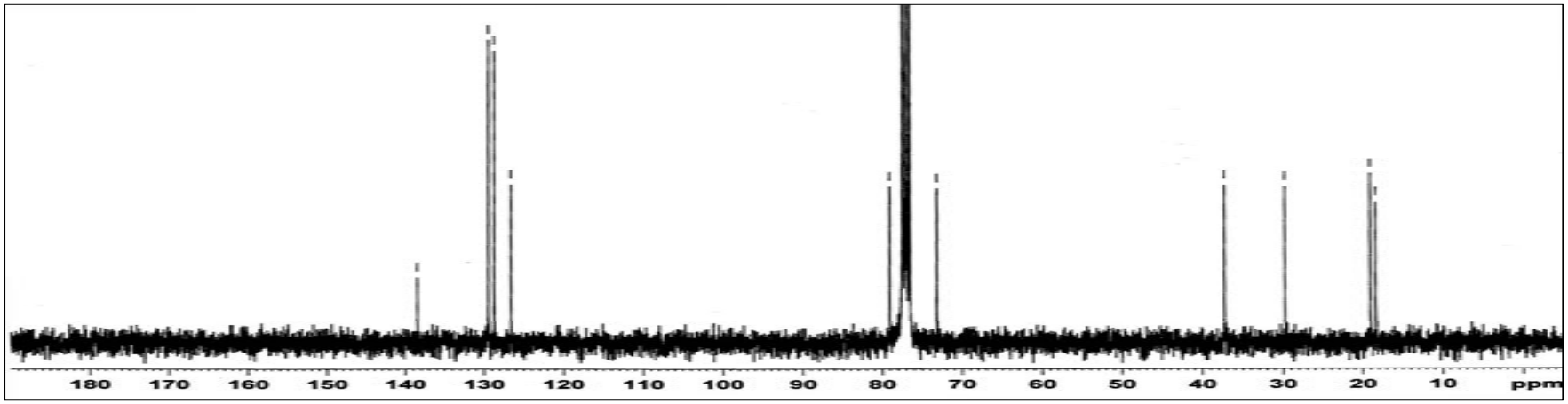

Figure 15 The 75 MHz ^{13}C NMR spectrum of compound **AR6** in $CDCl_3$

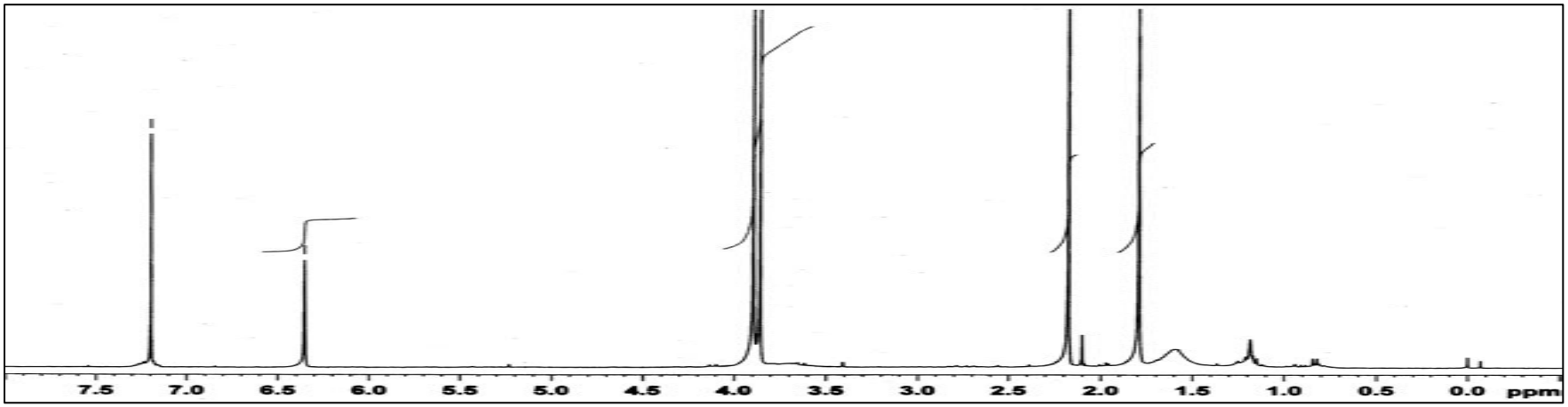

Figure 16 The 300 MHz ^{1}H NMR spectrum of compound **AR8** in $CDCl_3$

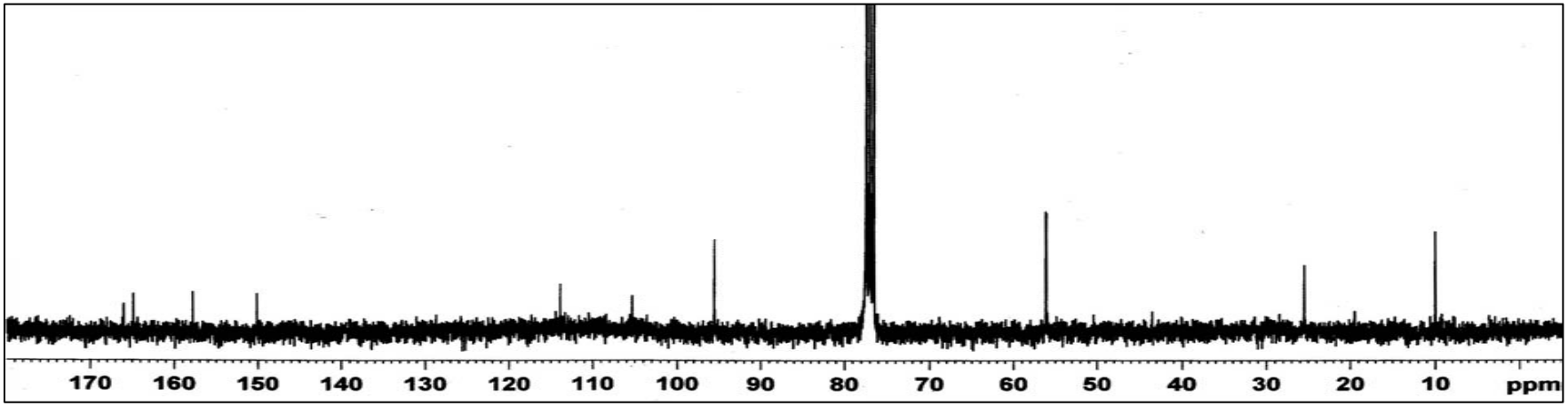

Figure 17 The 75 MHz ^{13}C NMR spectrum of compound **AR8** in $CDCl_3$

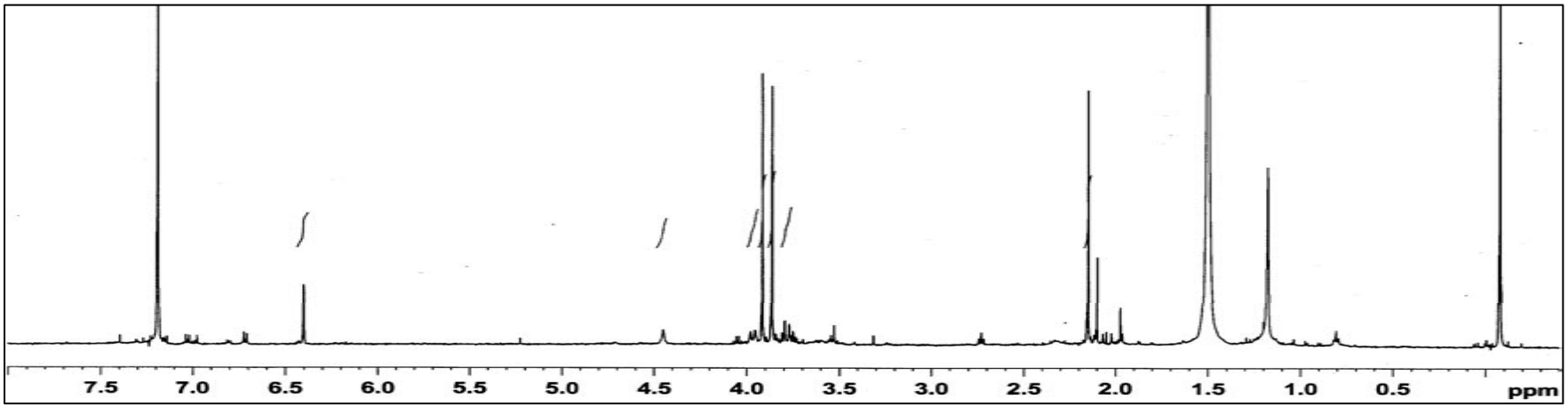

Figure 18 The 500 MHz ^{1}H NMR spectrum of compound **AR11** in $CDCl_3$

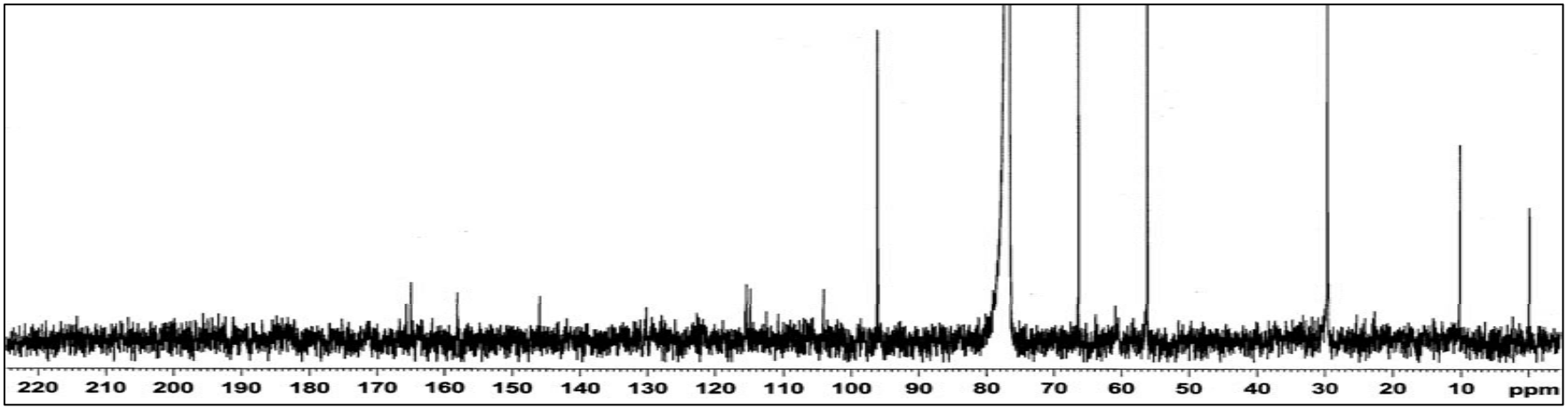

Figure 19 The 125 MHz ^{13}C NMR spectrum of compound **AR11** in $CDCl_3$

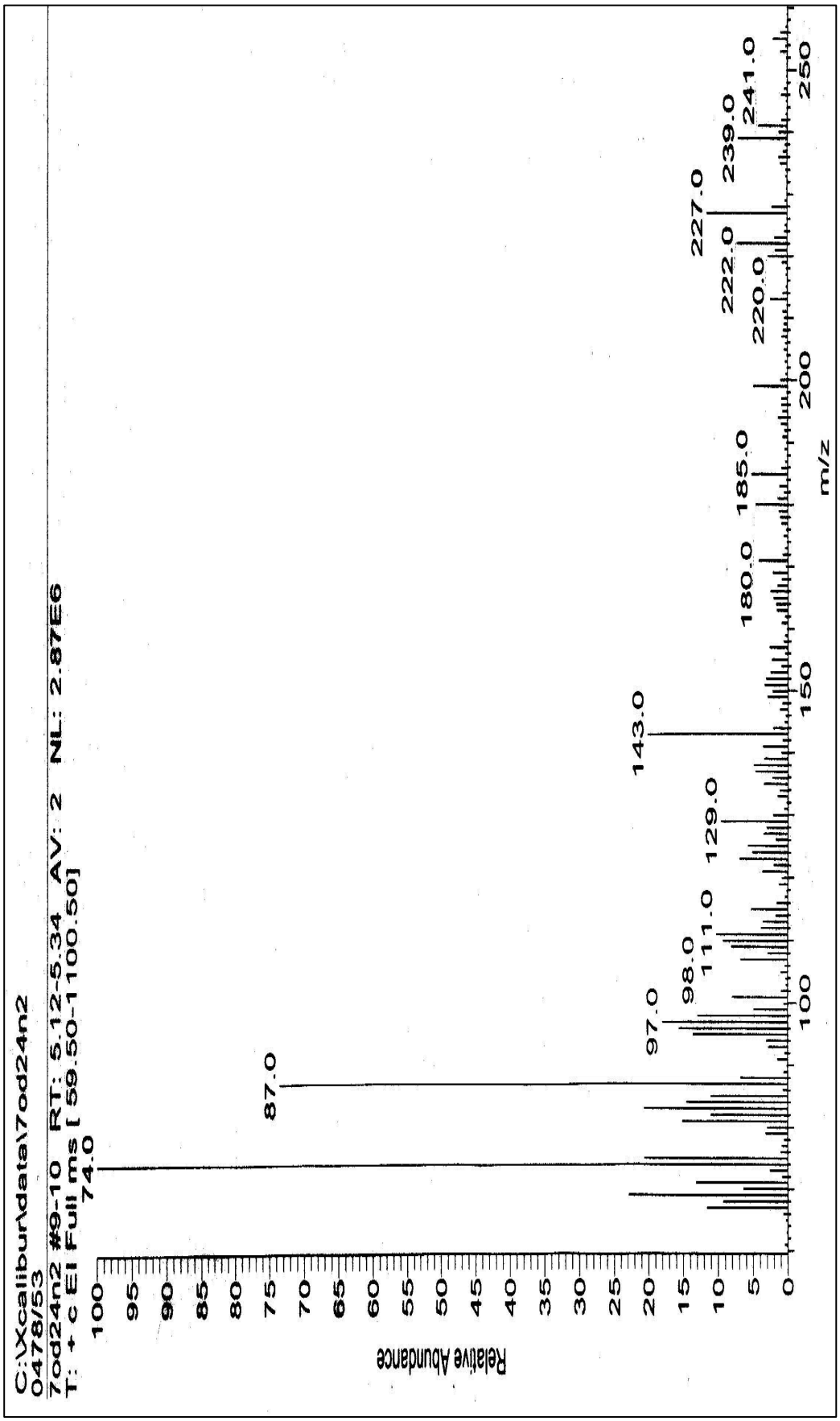

Figure 20 The mass spectrum of compound **AR11**

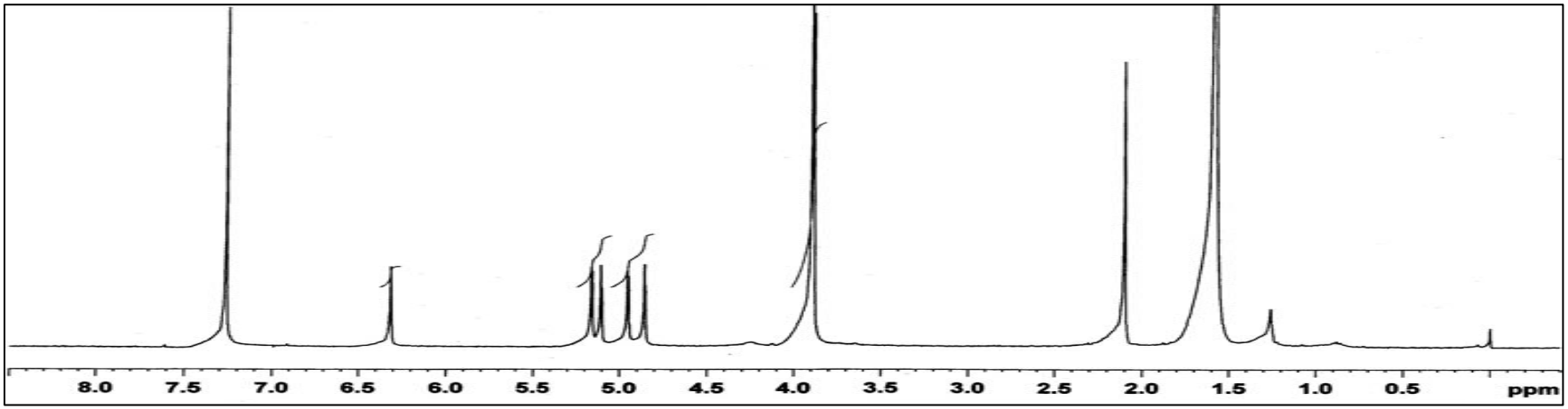

Figure 21 The 300 MHz ^{1}H NMR spectrum of compound **AR15** in $CDCl_3$

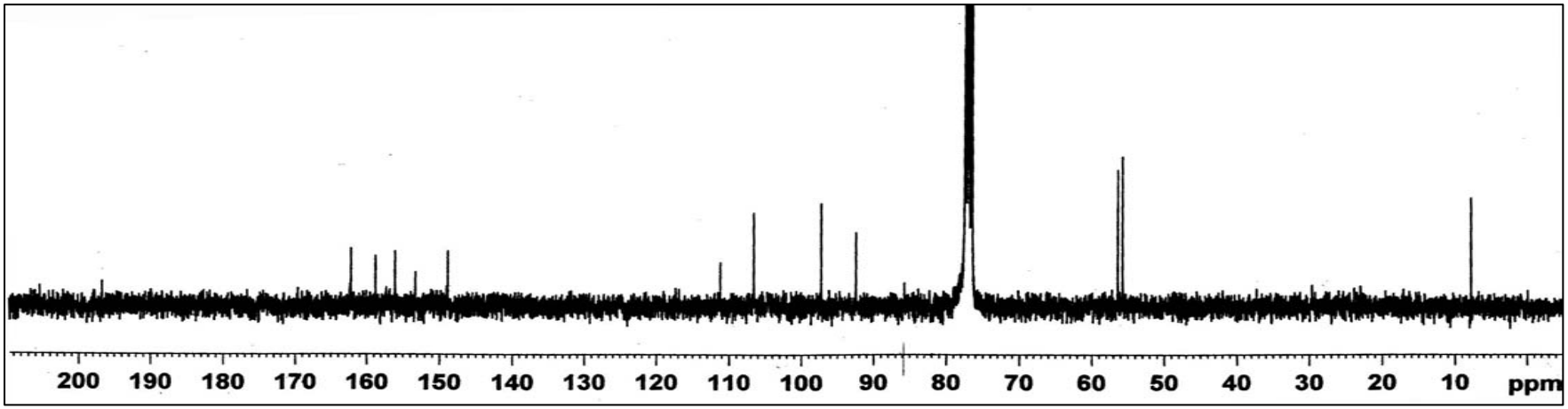

Figure 22 The 75 MHz ^{13}C NMR spectrum of compound **AR15** in $CDCl_3$

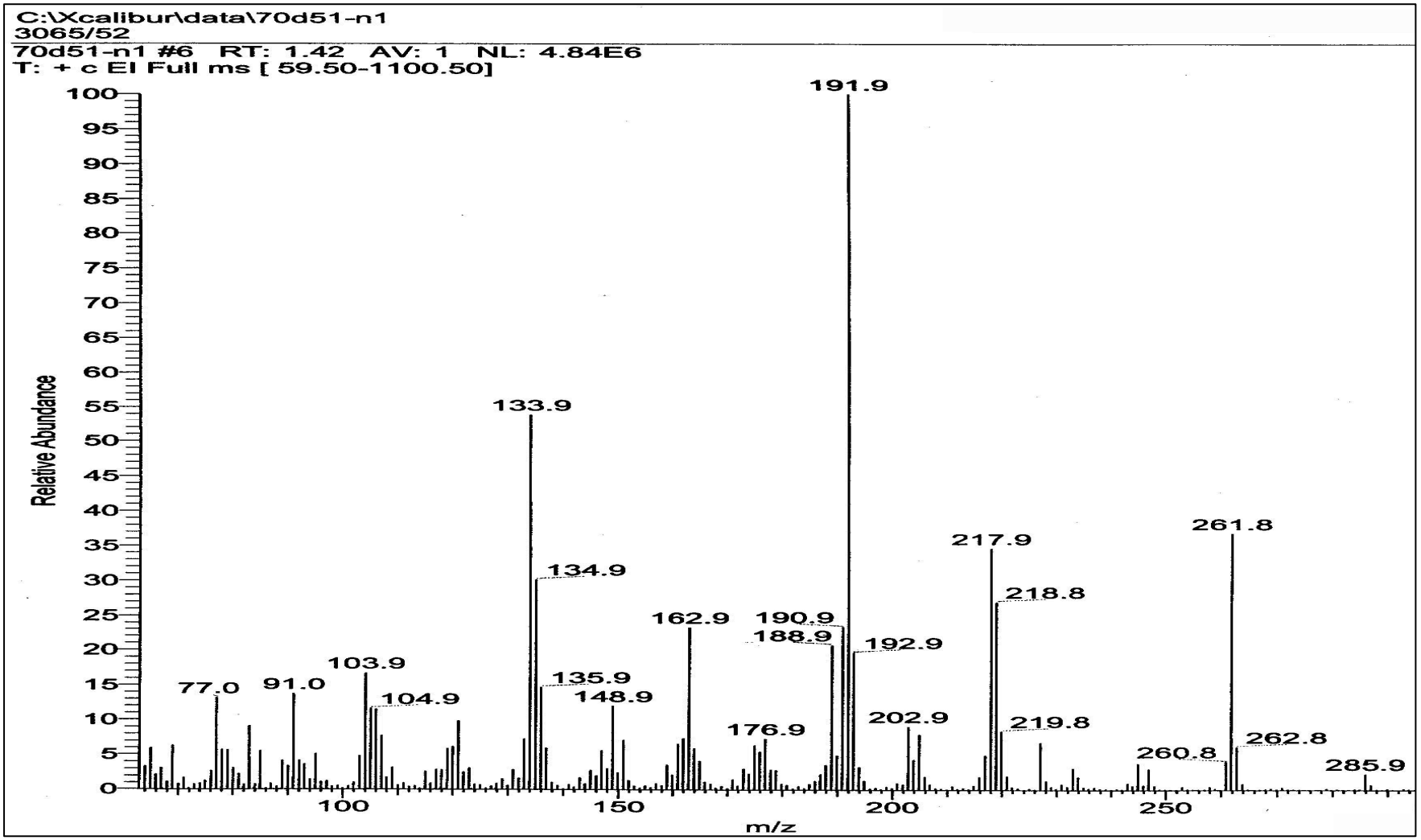

Figure 23 The mass spectrum of compound **AR15**

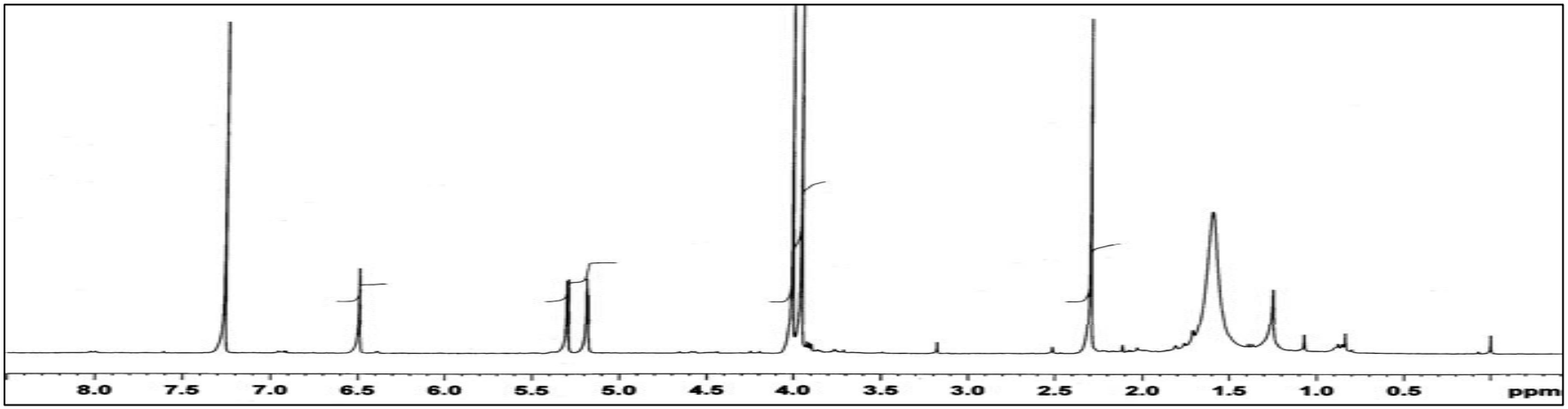

Figure 24 The 300 MHz ^{1}H NMR spectrum of compound **AR16** in $CDCl_3$

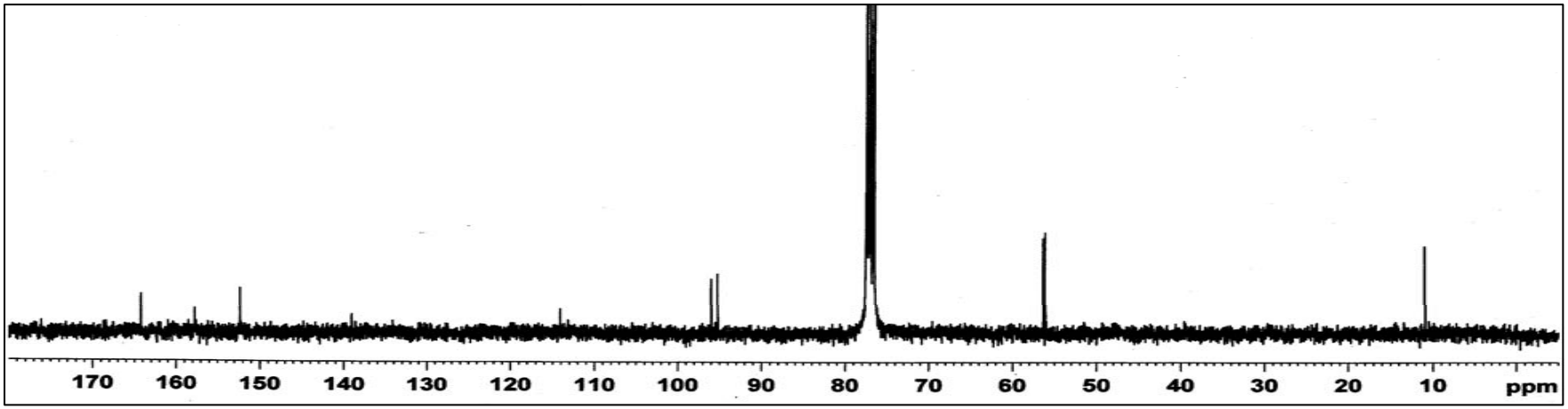

Figure 25 The 75 MHz ^{13}C NMR spectrum of compound **AR16** in $CDCl_3$

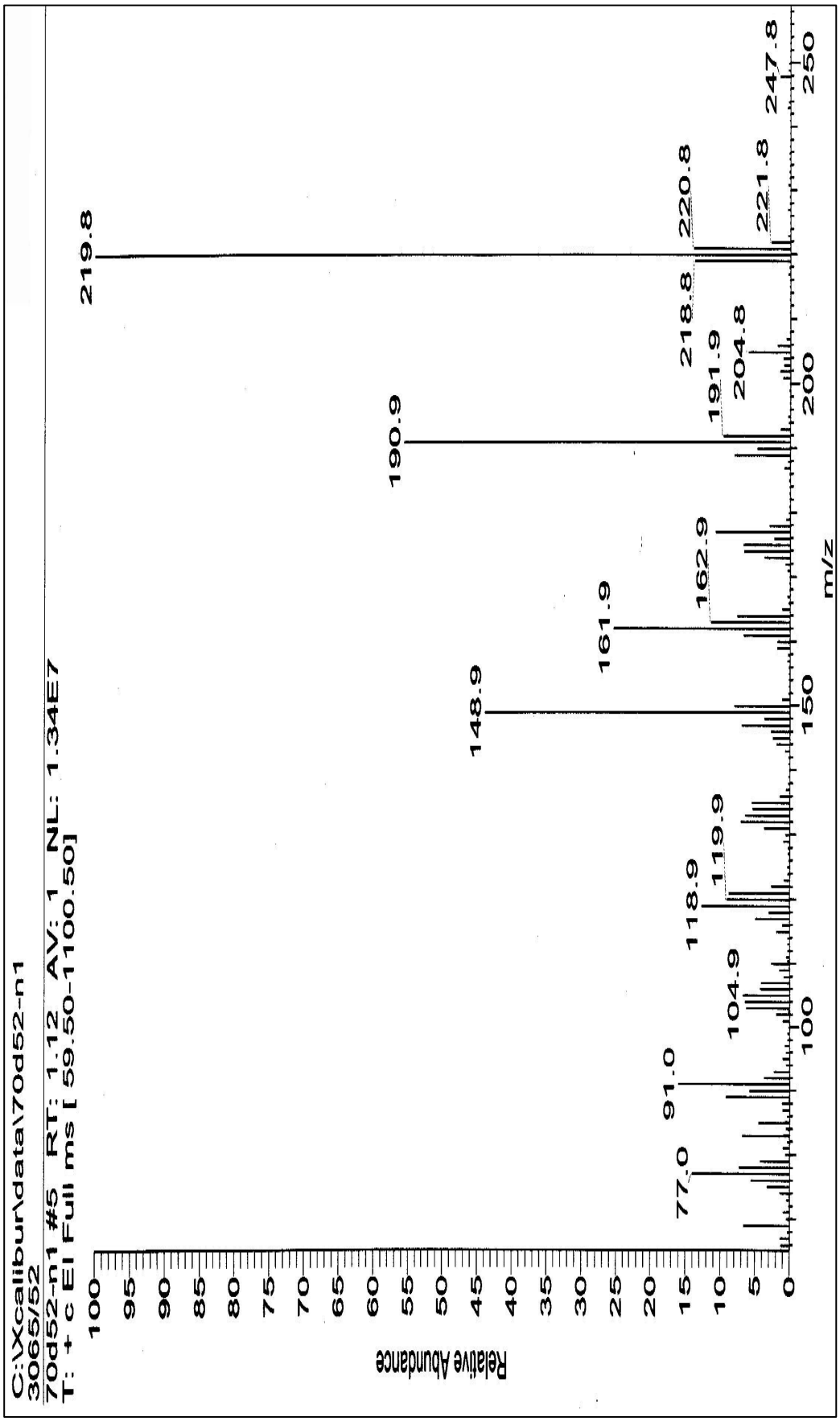

Figure 26 The mass spectrum of compound **AR16**

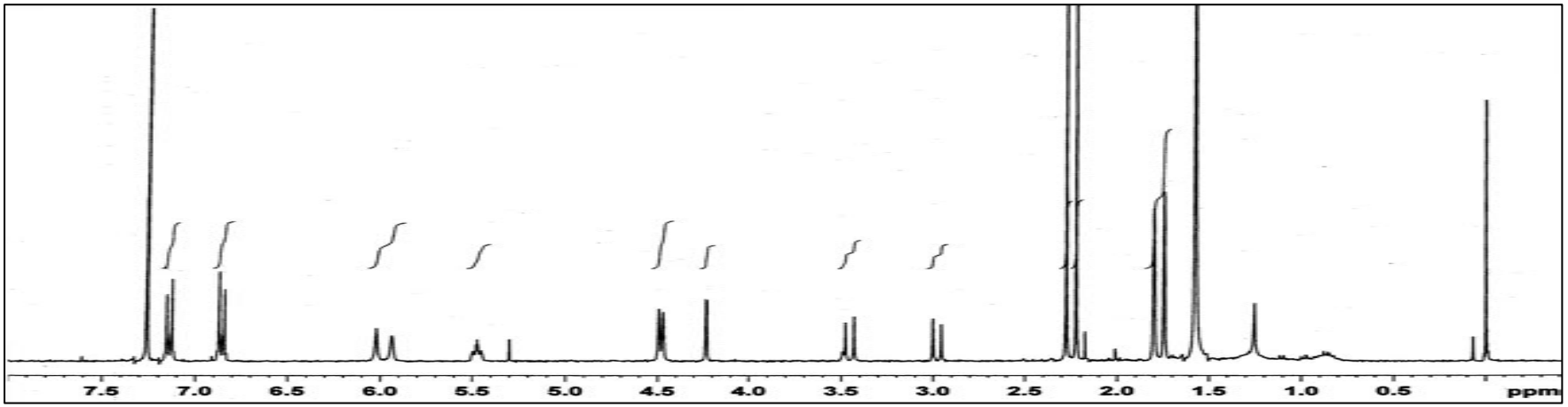

Figure 27 The 300 MHz ^{1}H NMR spectrum of compound **AR9** in $CDCl_3$

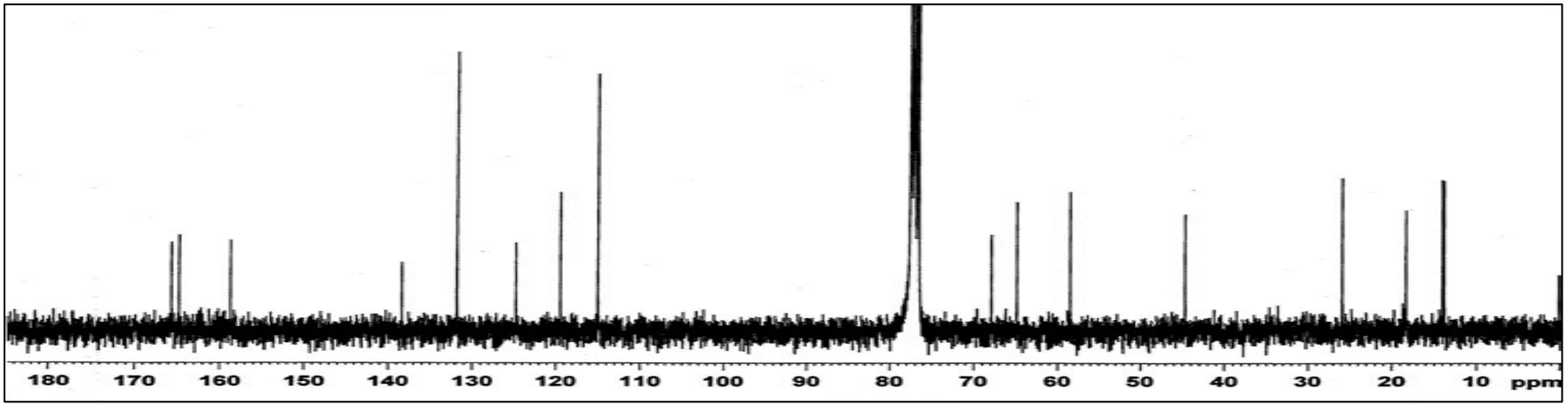

Figure 28 The 75 MHz ^{13}C NMR spectrum of compound **AR9** in $CDCl_3$

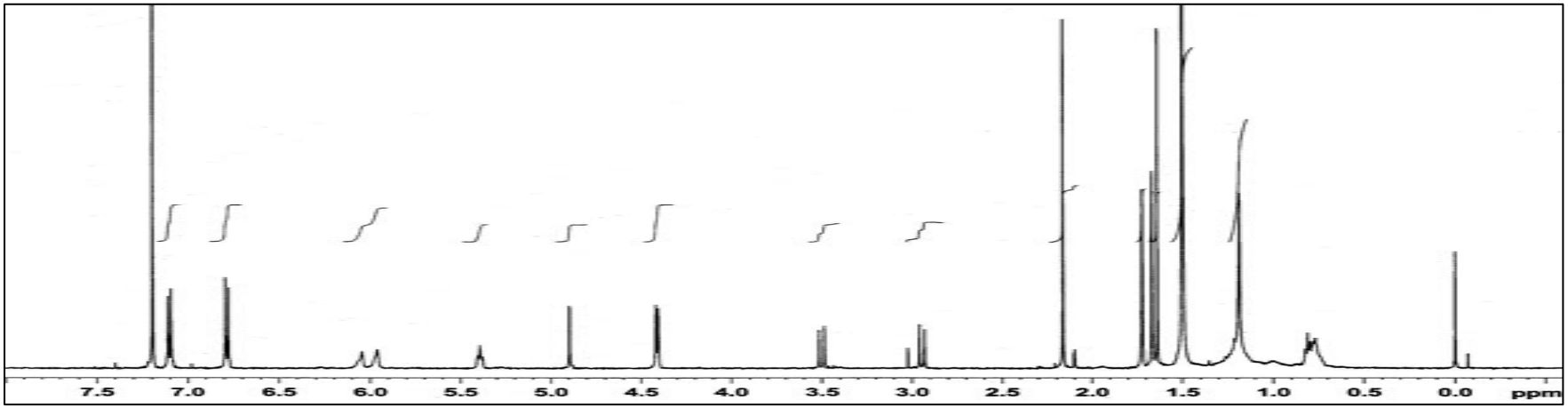

Figure 29 The 500 MHz ^{1}H NMR spectrum of compound **AR10** in $CDCl_3$

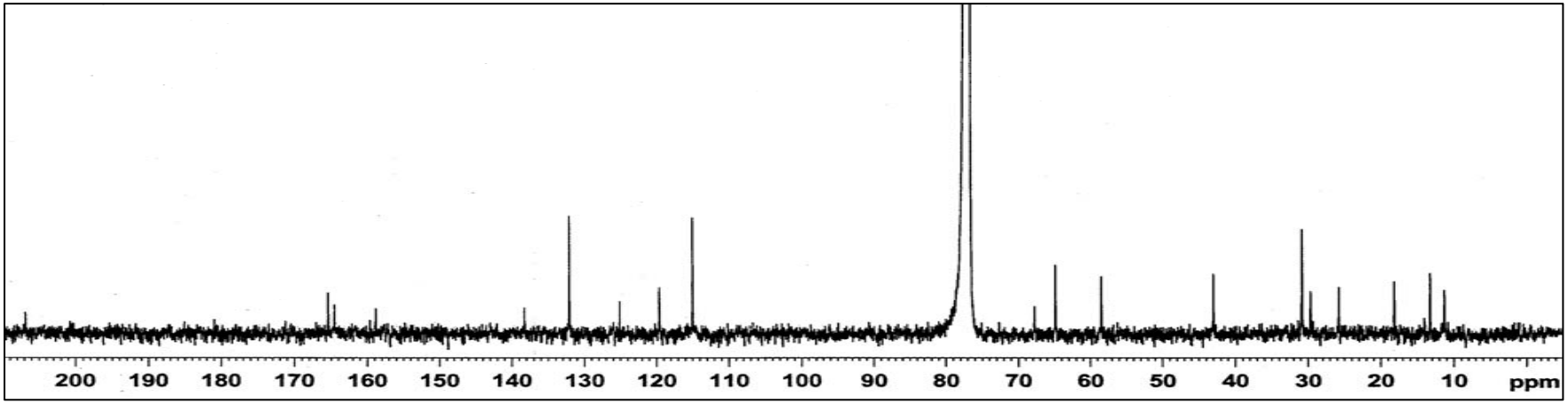

Figure 30 The 125 MHz ^{13}C NMR spectrum of compound **AR10** in $CDCl_3$

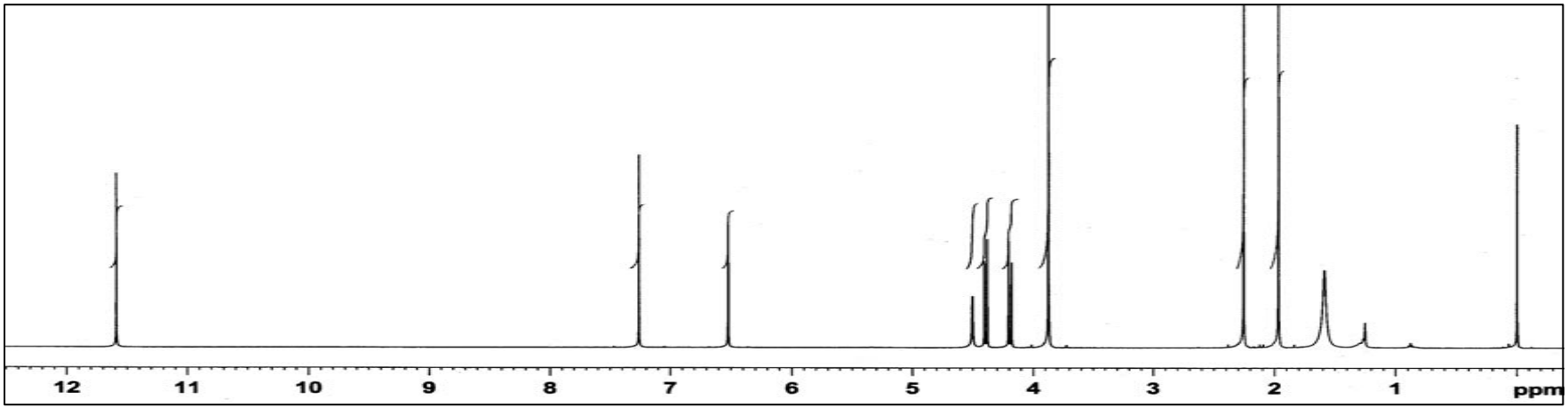

Figure 31 The 500 MHz ^{1}H NMR spectrum of compound **AR12** in $CDCl_3$

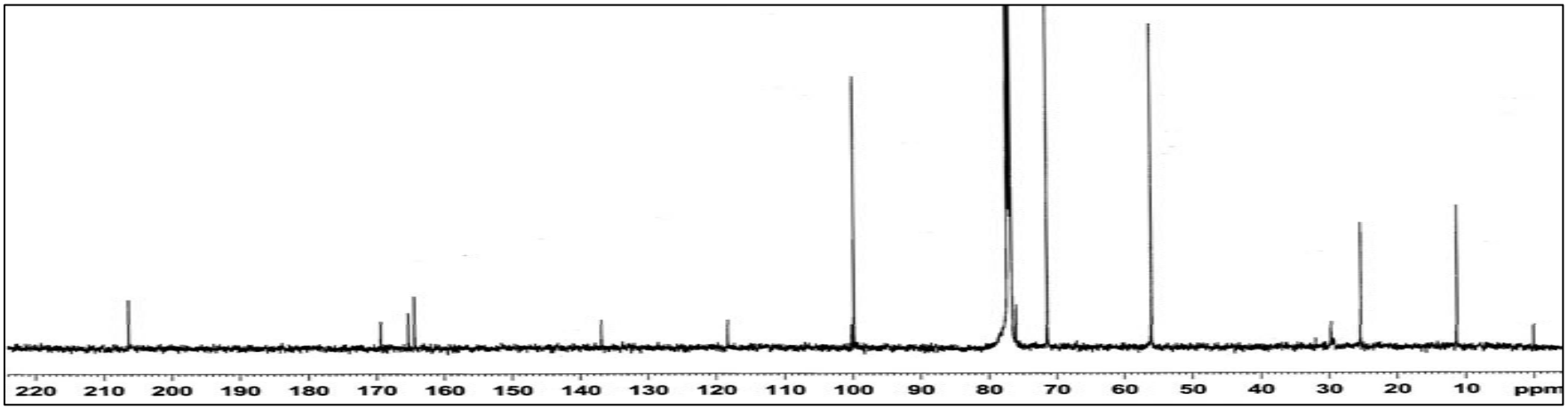

Figure 32 The 125 MHz ^{13}C NMR spectrum of compound **AR12** in $CDCl_3$

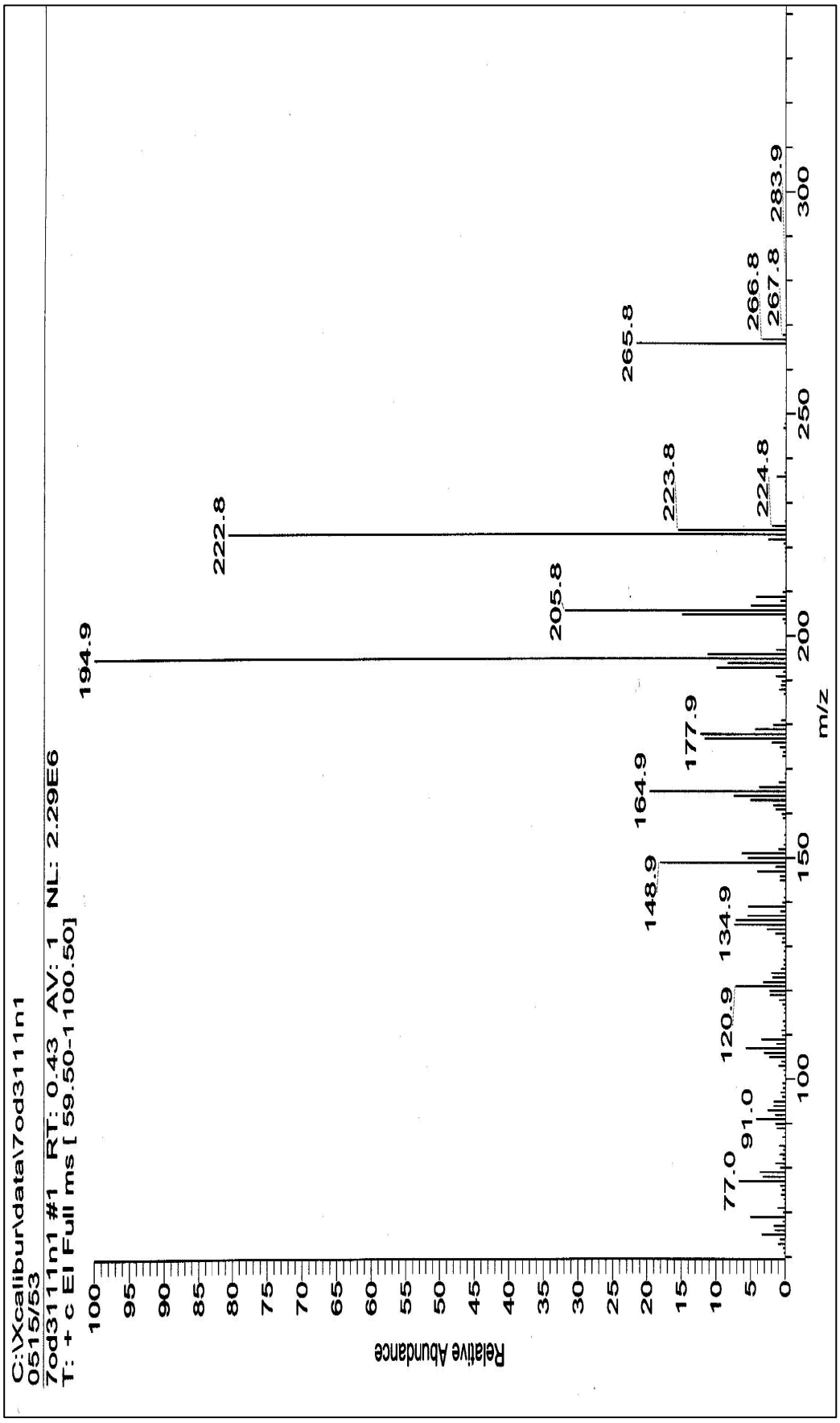

Figure 33 The mass spectrum of compound **AR12**

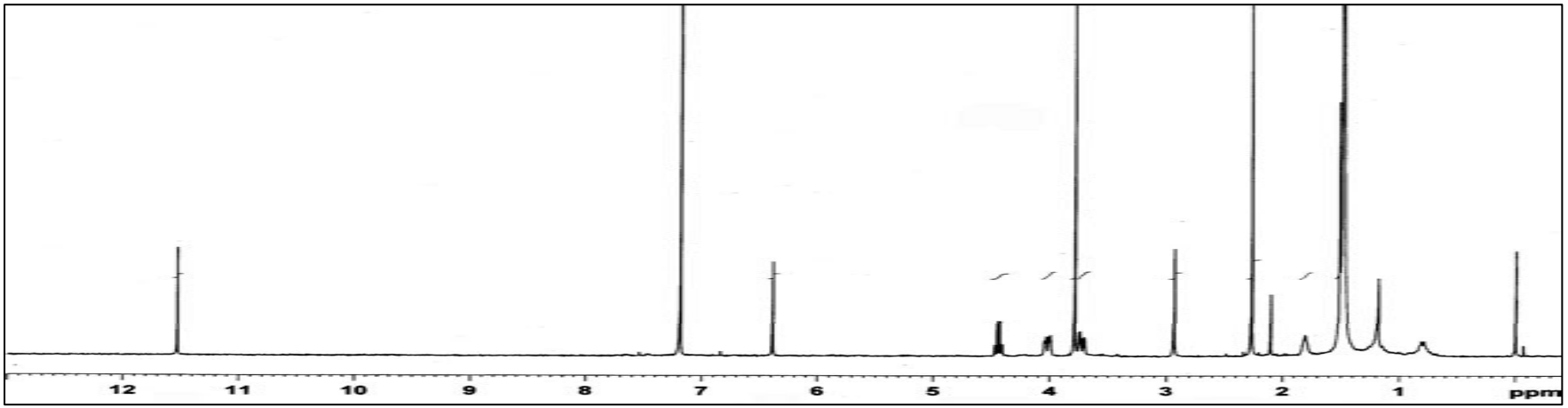

Figure 34 The 500 MHz ^{1}H NMR spectrum of compound **AR13** in $CDCl_3$

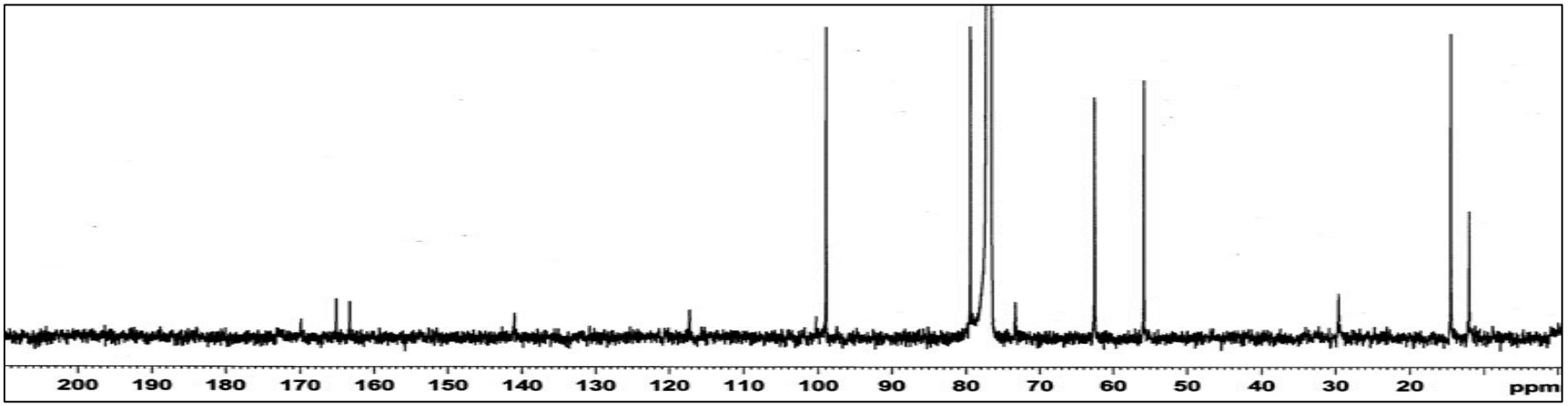

Figure 35 The 125 MHz ^{13}C NMR spectrum of compound **AR13** in $CDCl_3$

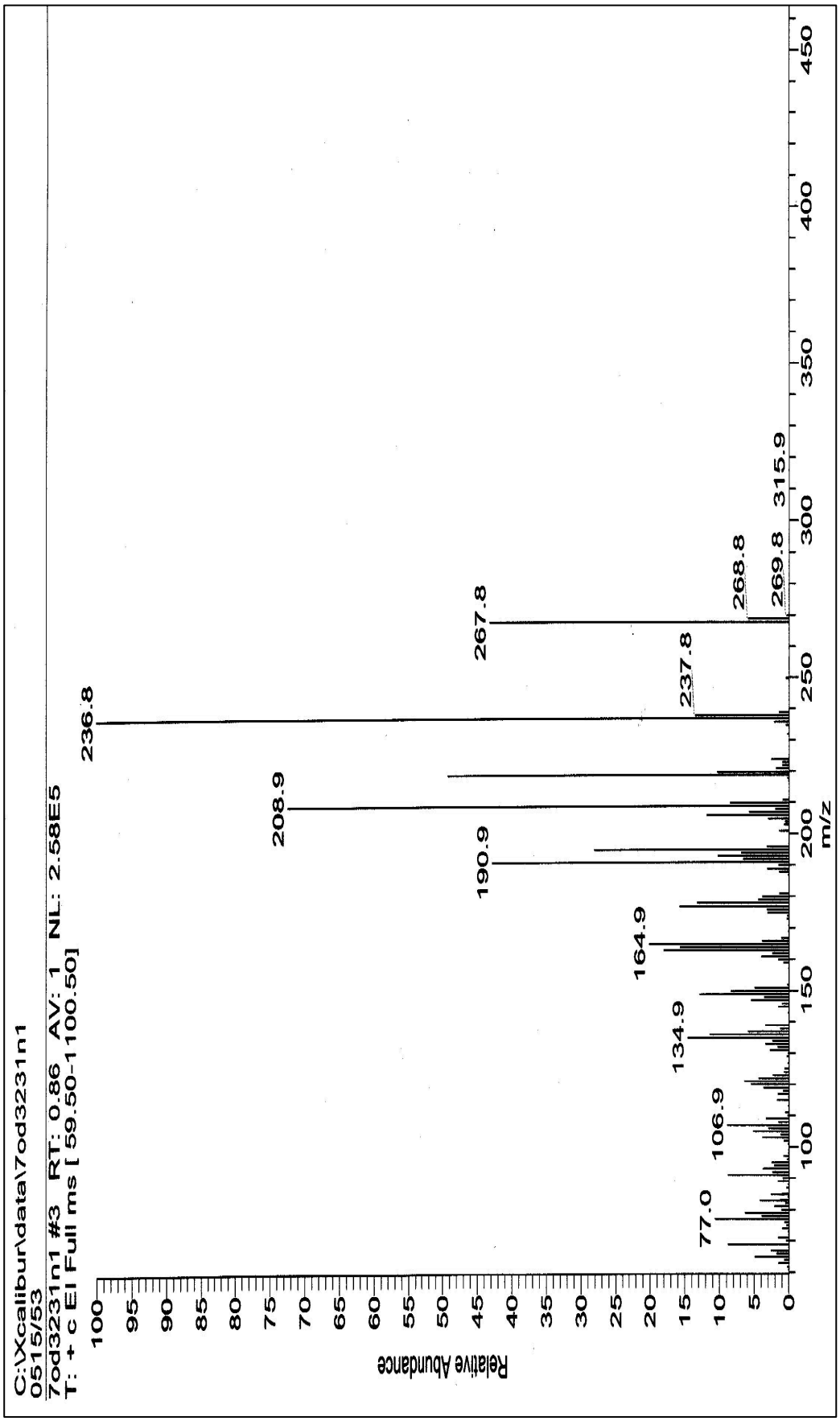

Figure 36 The mass spectrum of compound **AR13**

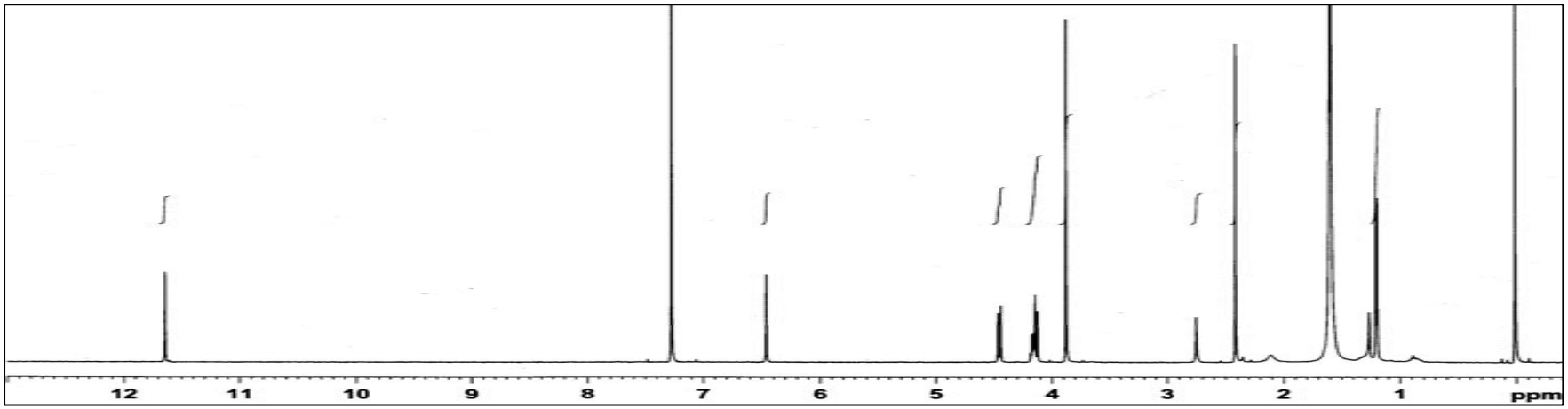

Figure 37 The 500 MHz ^{1}H NMR spectrum of compound **AR17** in $CDCl_3$

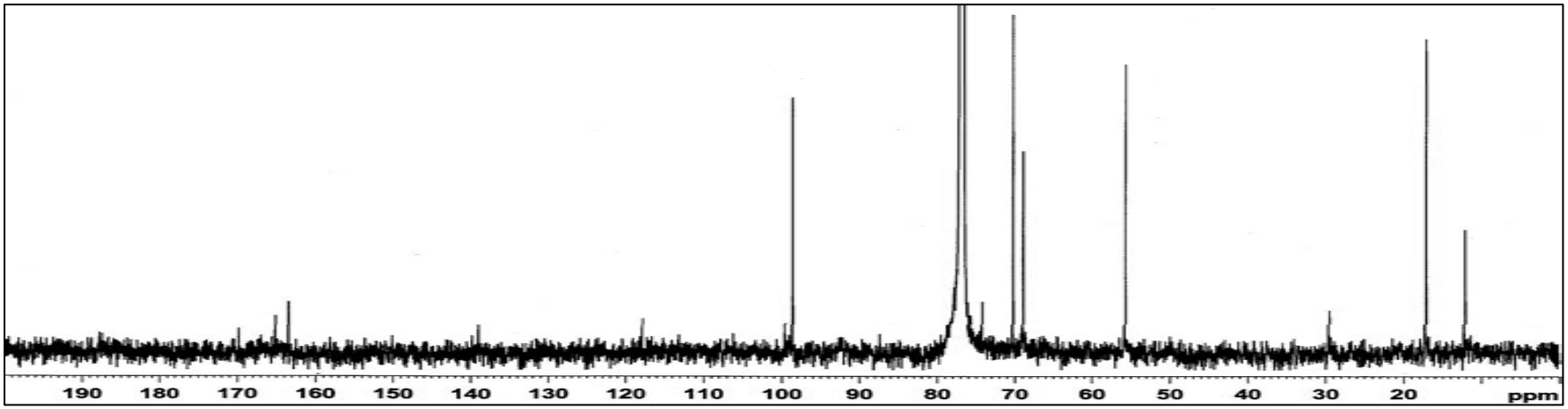

Figure 38 The 125 MHz ^{13}C NMR spectrum of compound **AR17** in $CDCl_3$

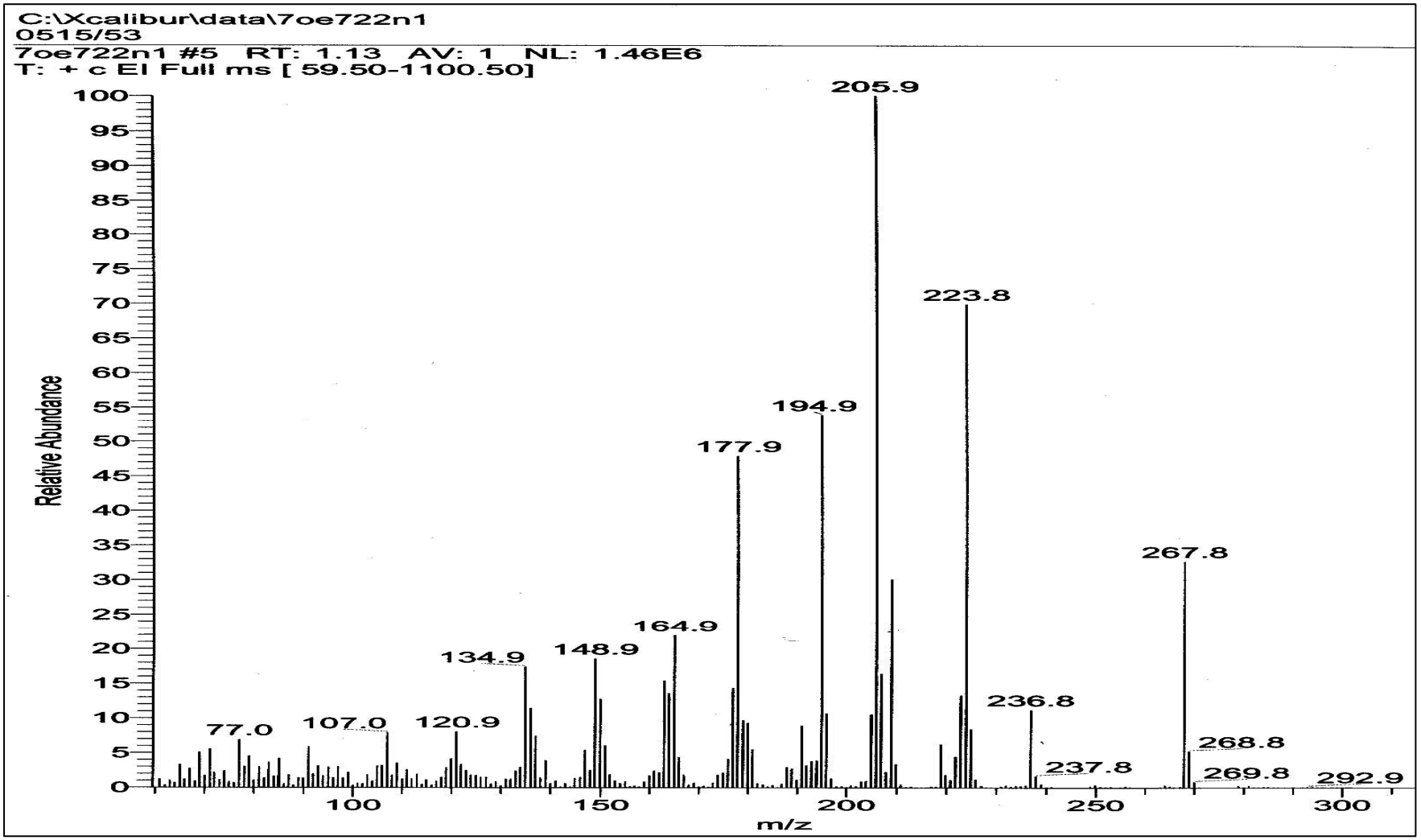

Figure 39 The mass spectrum of compound **AR17**

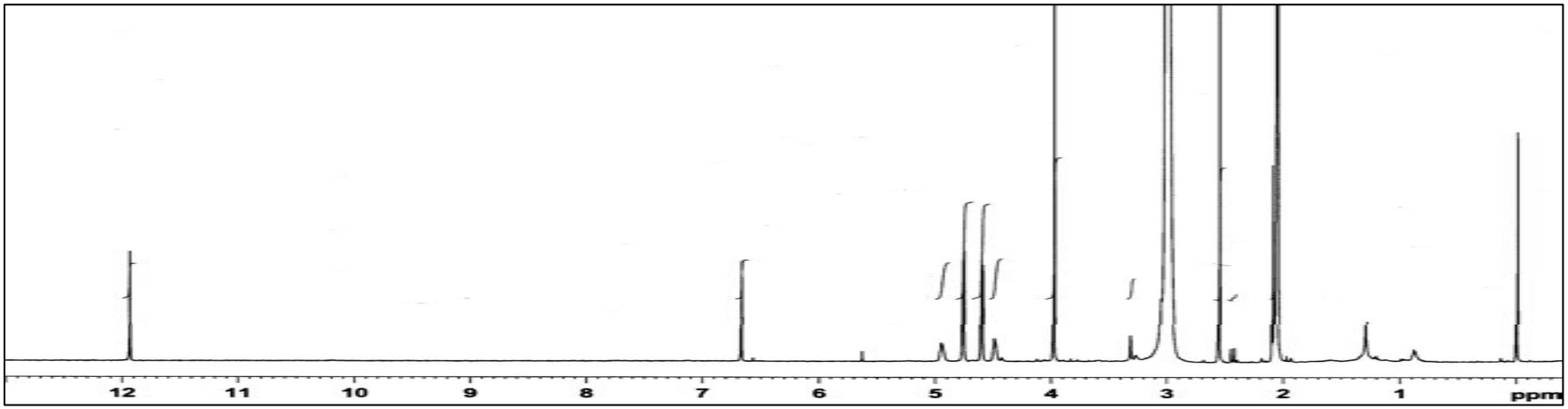

Figure 40 The 500 MHz ^{1}H NMR spectrum of compound **AR18** in Acetone-d_6

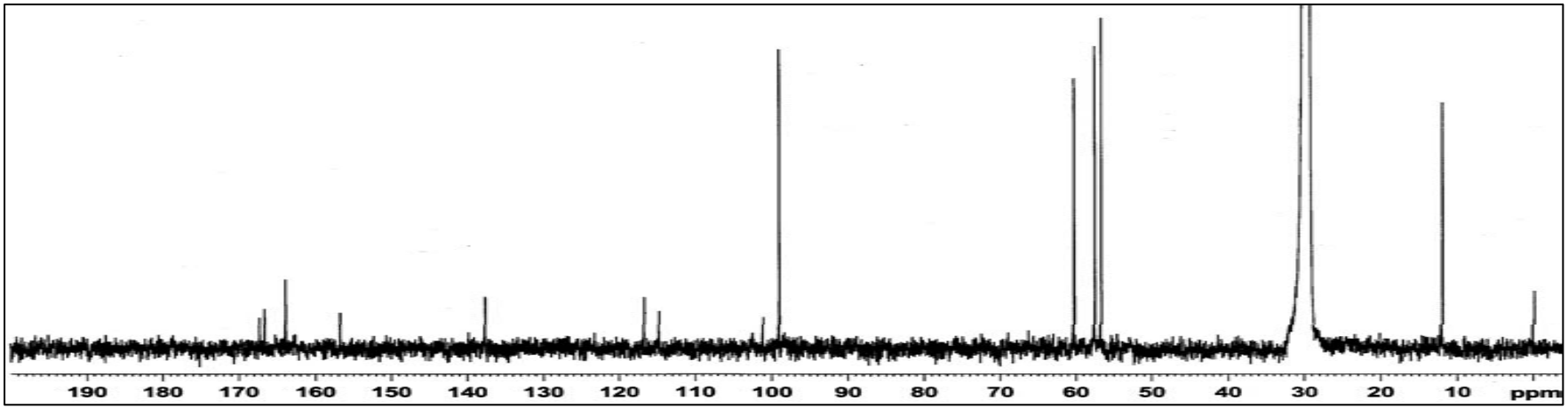

Figure 41 The 125 MHz ^{13}C NMR spectrum of compound **AR18** in Acetone-d_6

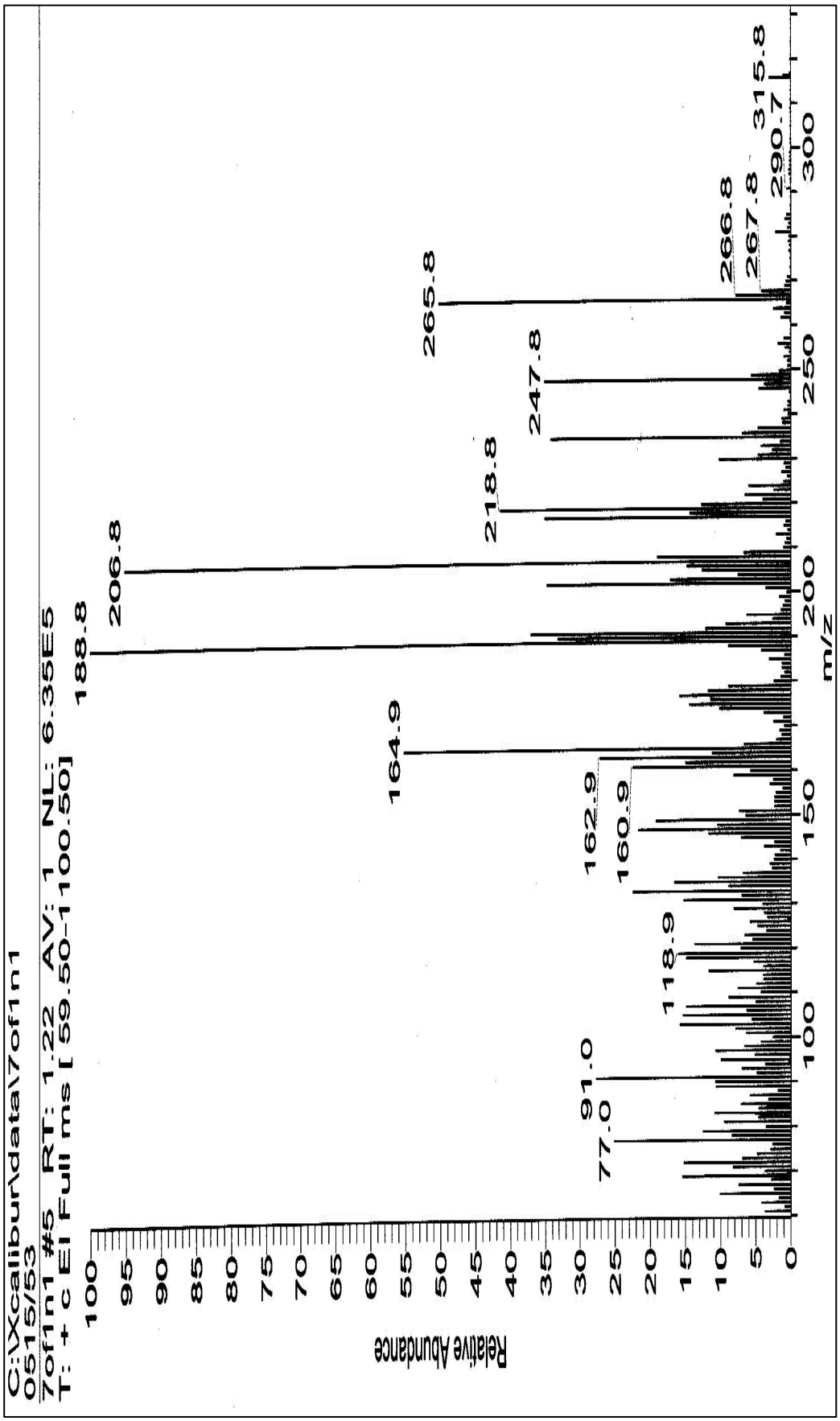

Figure 42 The mass spectrum of compound **AR18**

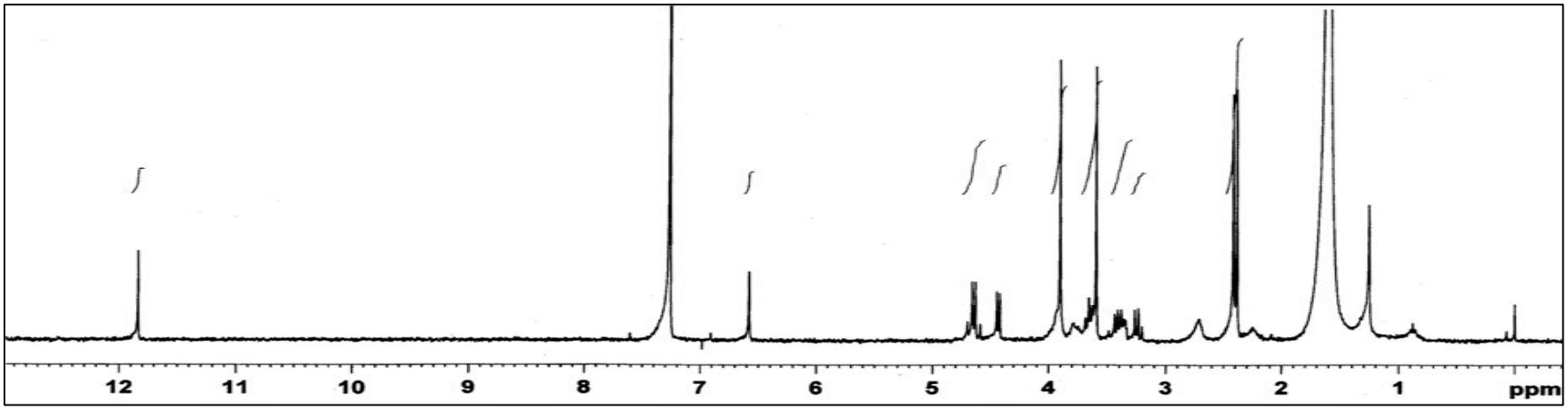

Figure 43 The 500 MHz ^{1}H NMR spectrum of compound **AR14** in $CDCl_3$

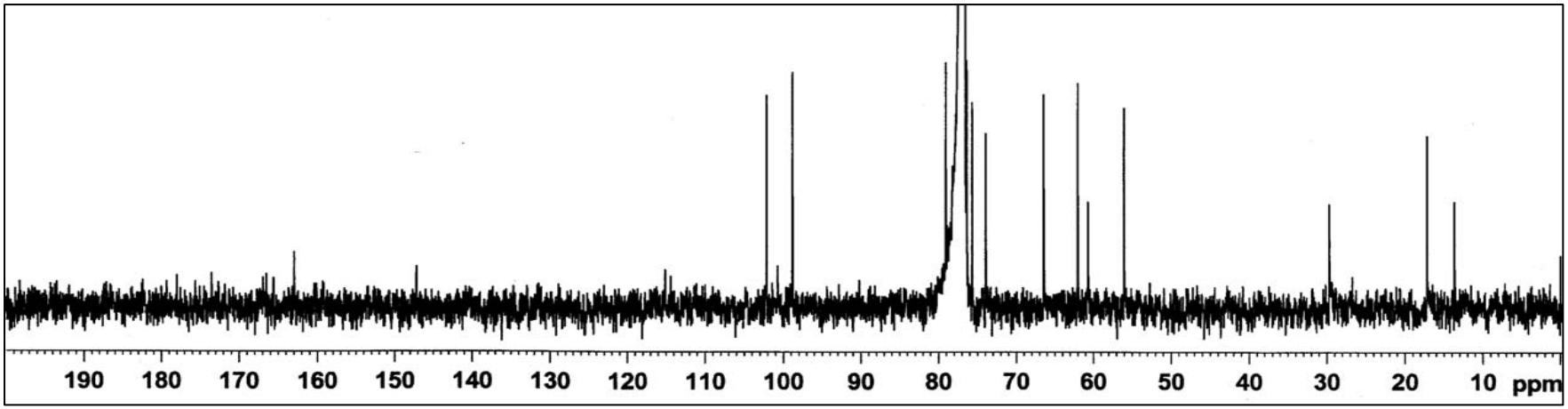

Figure 44 The 125 MHz ^{13}C NMR spectrum of compound **AR14** in $CDCl_3$

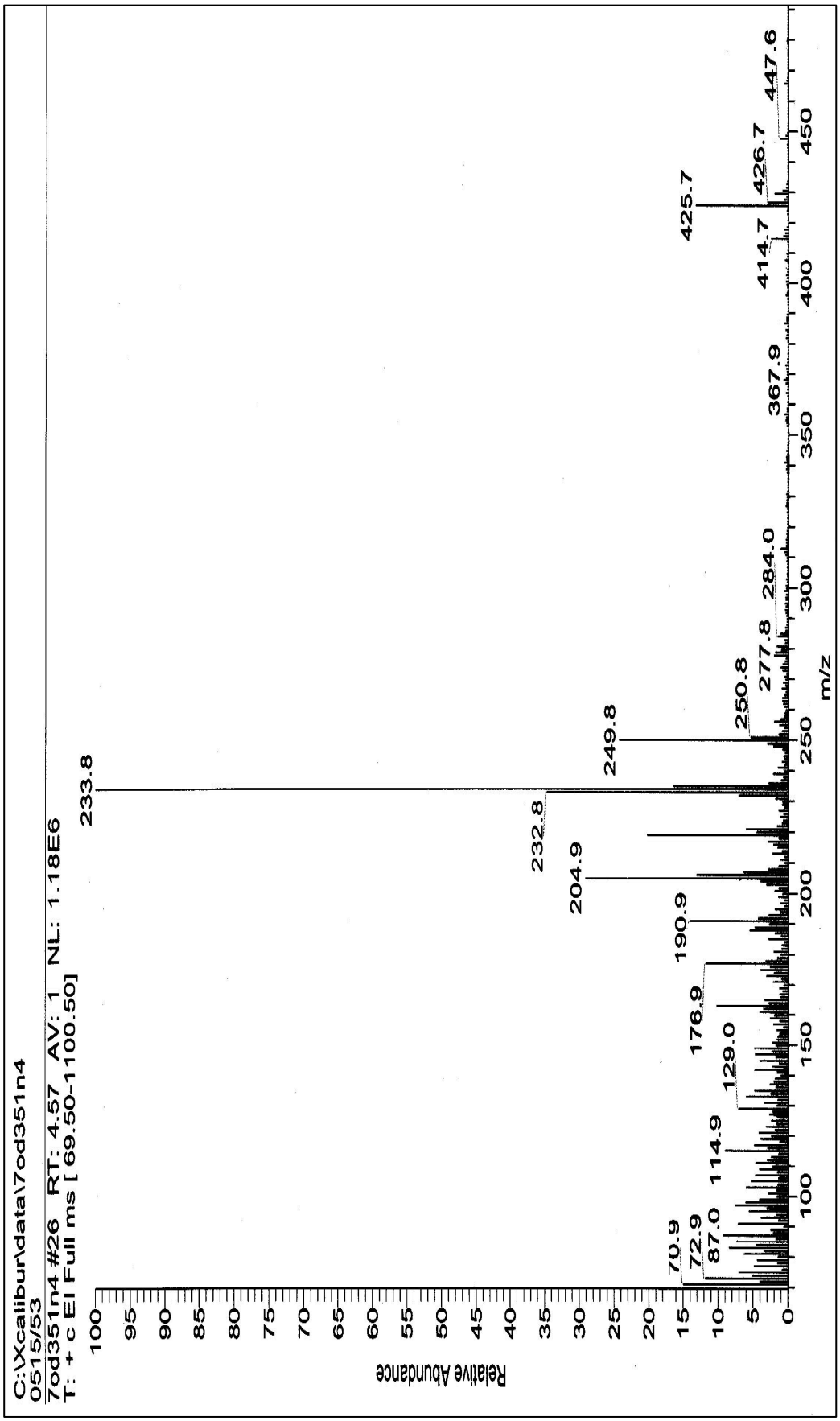

Figure 45 The mass spectrum of compound **AR14**

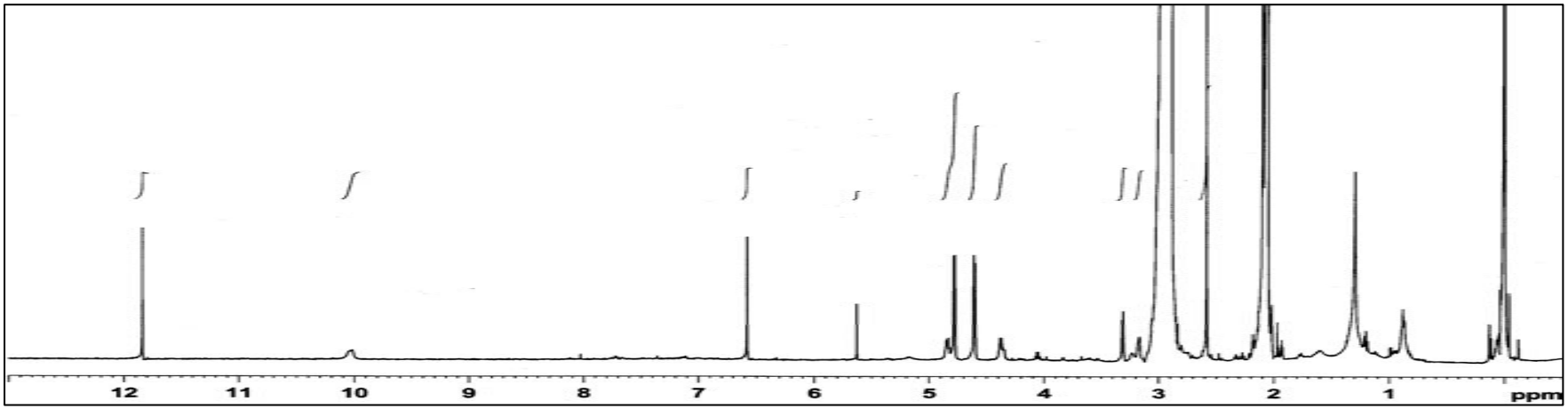

Figure 46 The 500 MHz ^{1}H NMR spectrum of compound **AR20** in Acetone-d_6

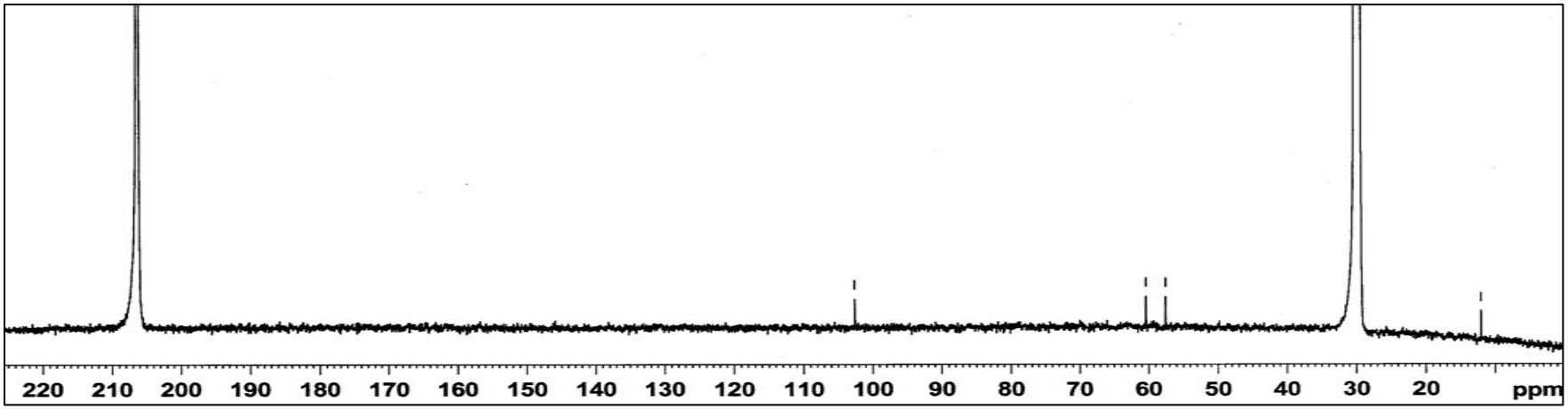

Figure 47 The 125 MHz ^{13}C NMR spectrum of compound **AR20** in Acetone-d_6

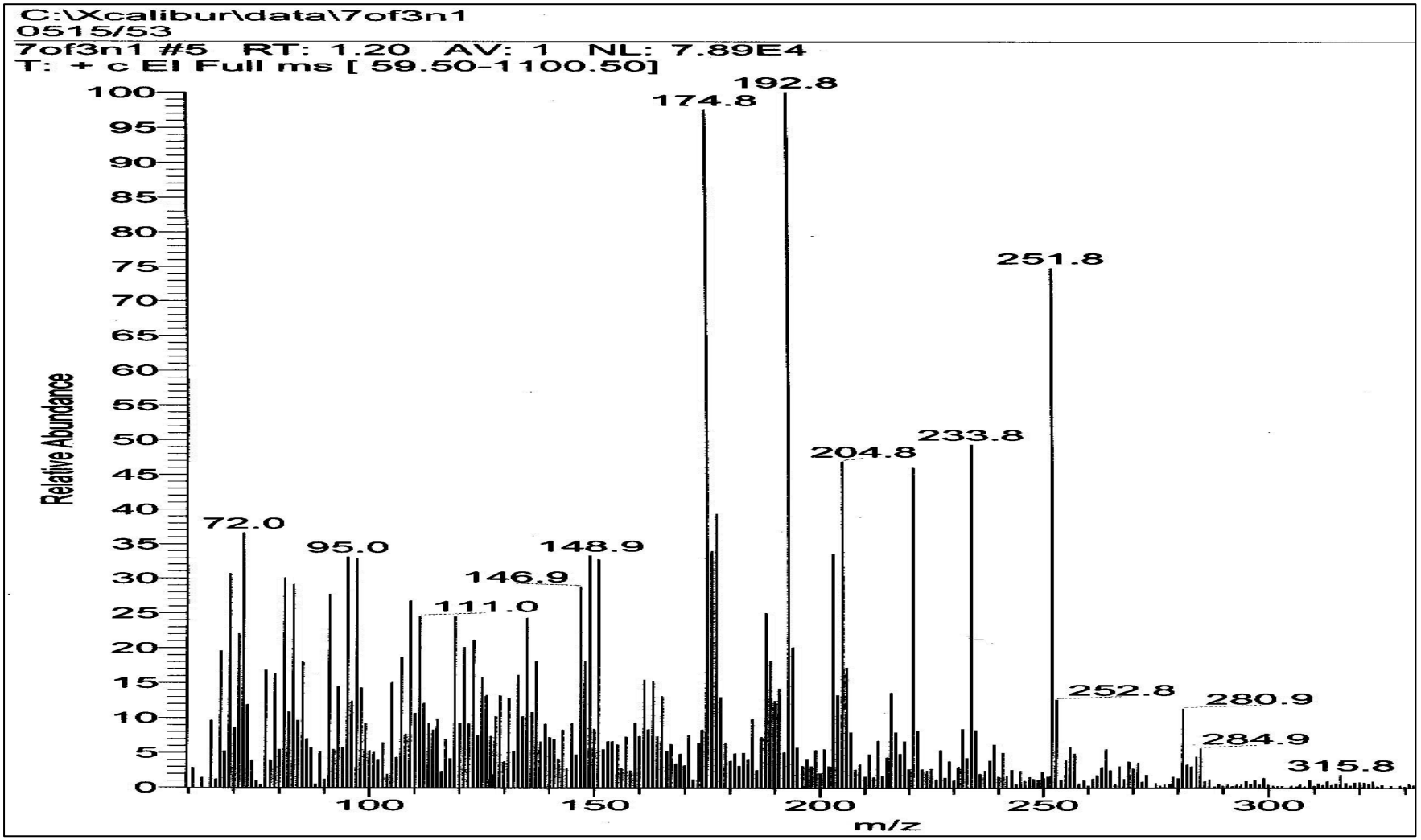

Figure 48 The mass spectrum of compound **AR20**

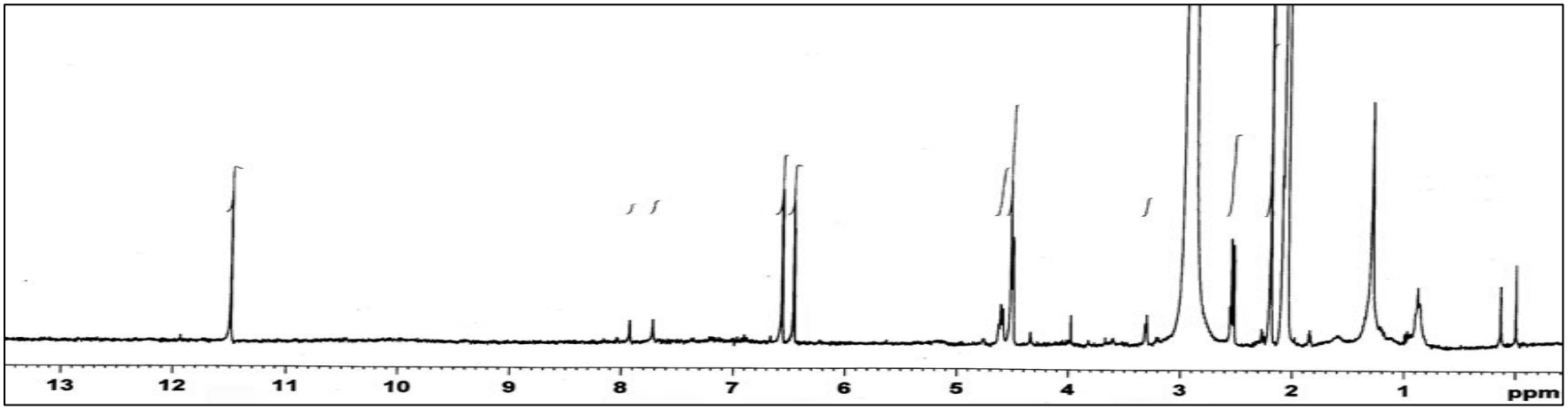

Figure 49 The 500 MHz ^{1}H NMR spectrum of compound **AR19** in Acetone-d_6

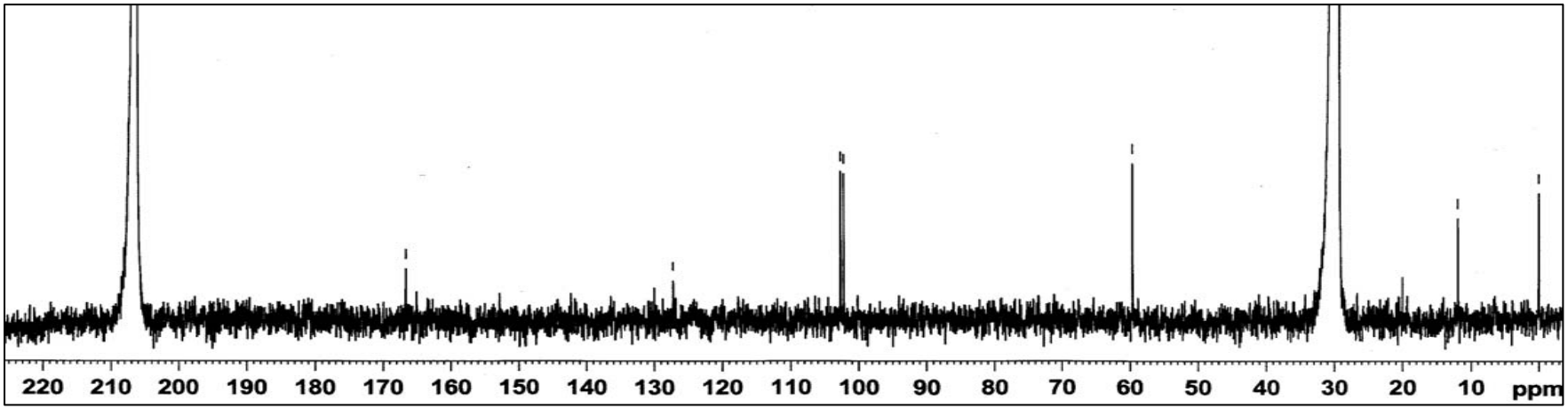

Figure 50 The 125 MHz ^{13}C NMR spectrum of compound **AR19** in Acetone-d_6

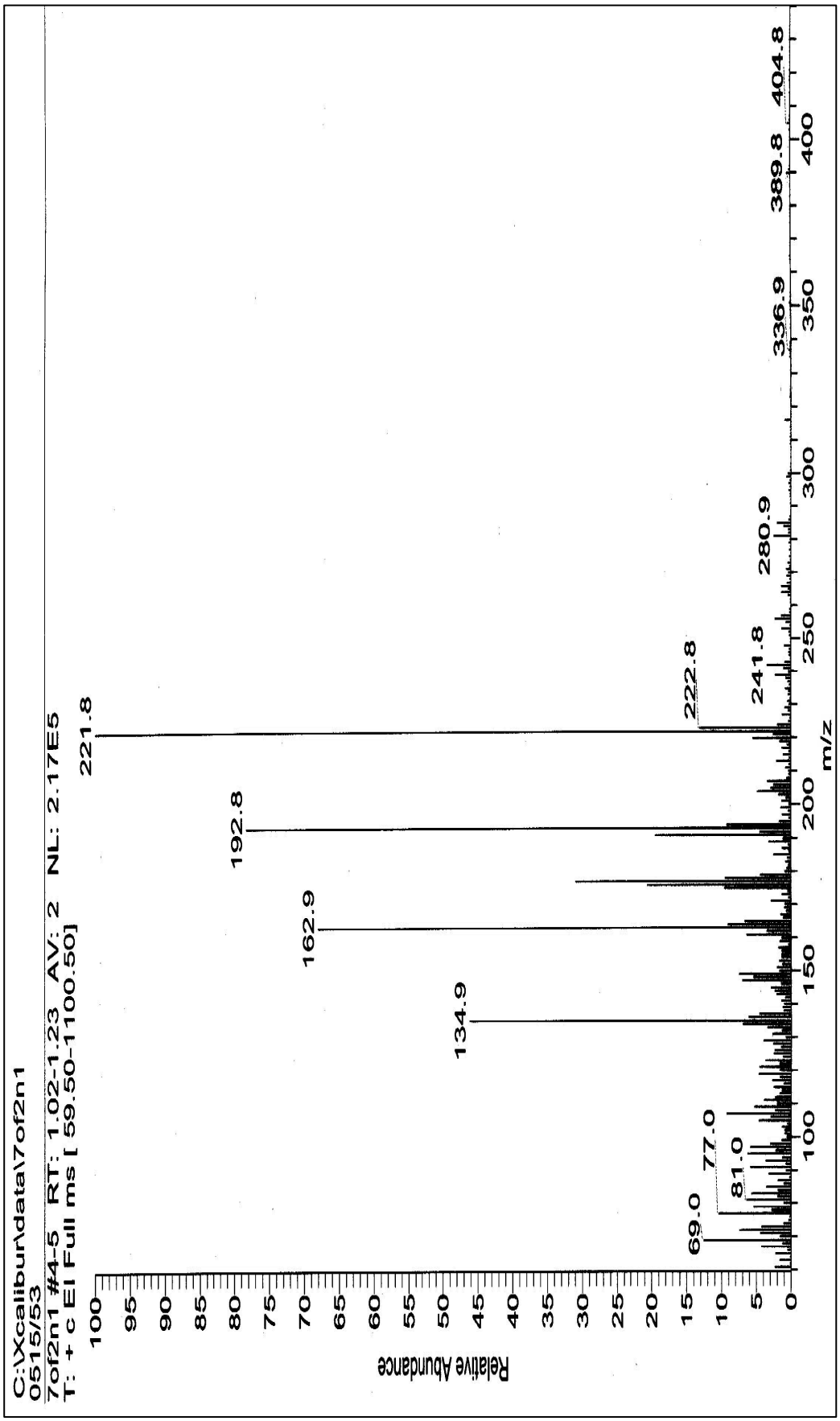

Figure 51 The mass spectrum of compound **AR19**

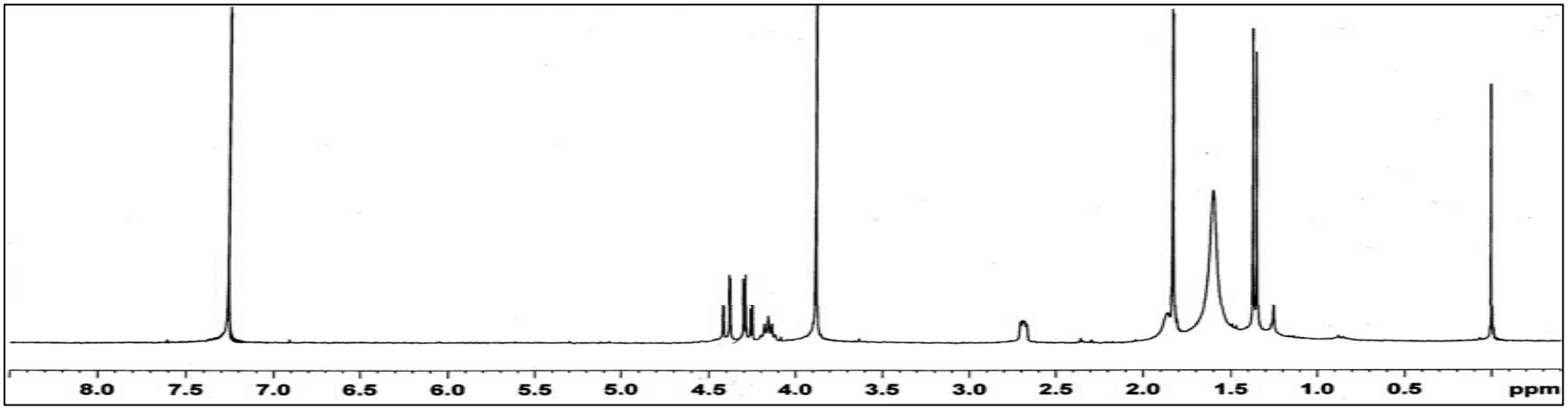

Figure 52 The 300 MHz ^{1}H NMR spectrum of compound **AR21** in $CDCl_3$

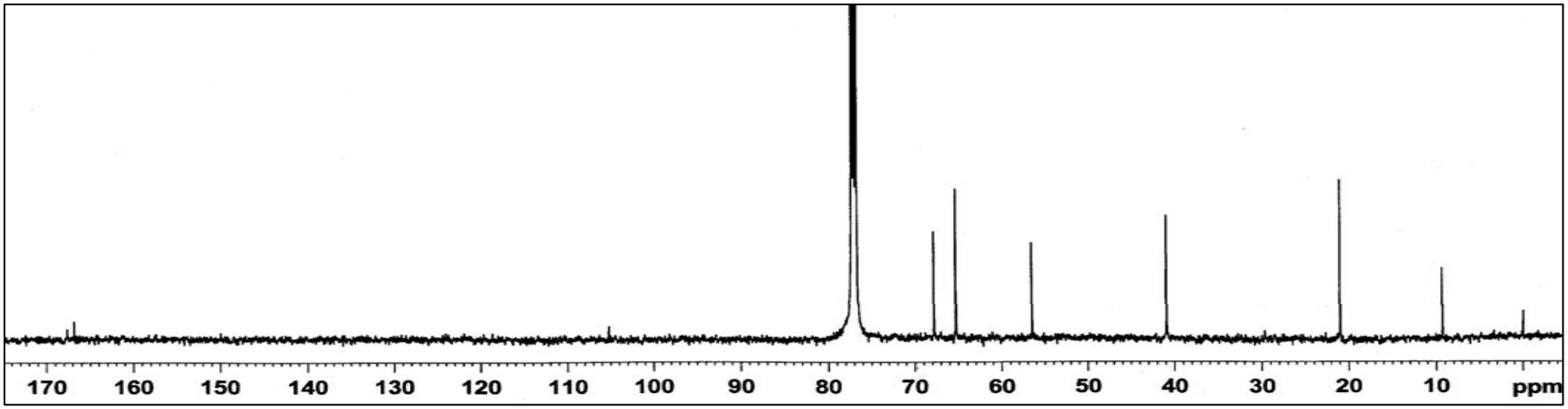

Figure 53 The 125 MHz ^{13}C NMR spectrum of compound **AR21** in $CDCl_3$

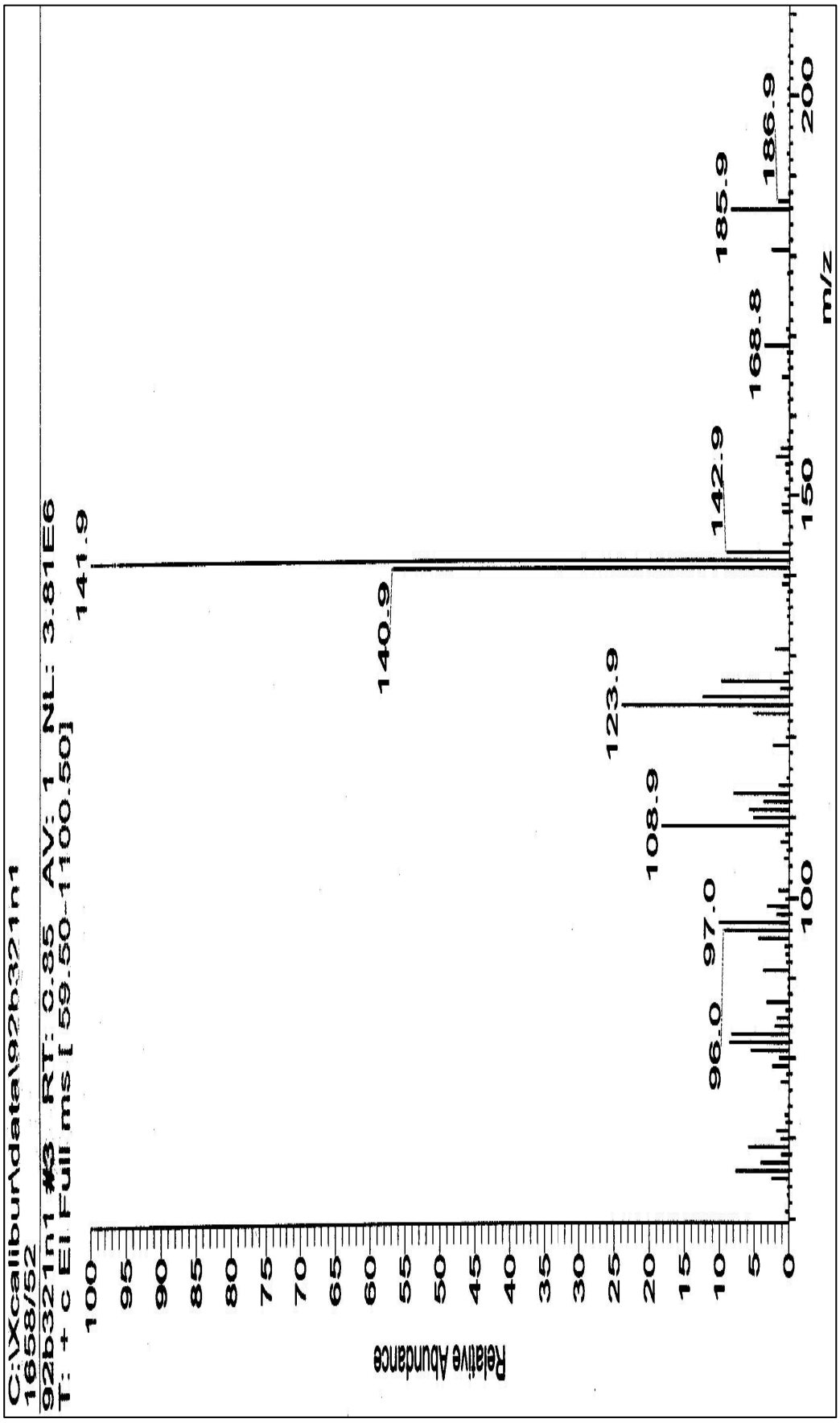

Figure 54 The mass spectrum of compound **AR21**

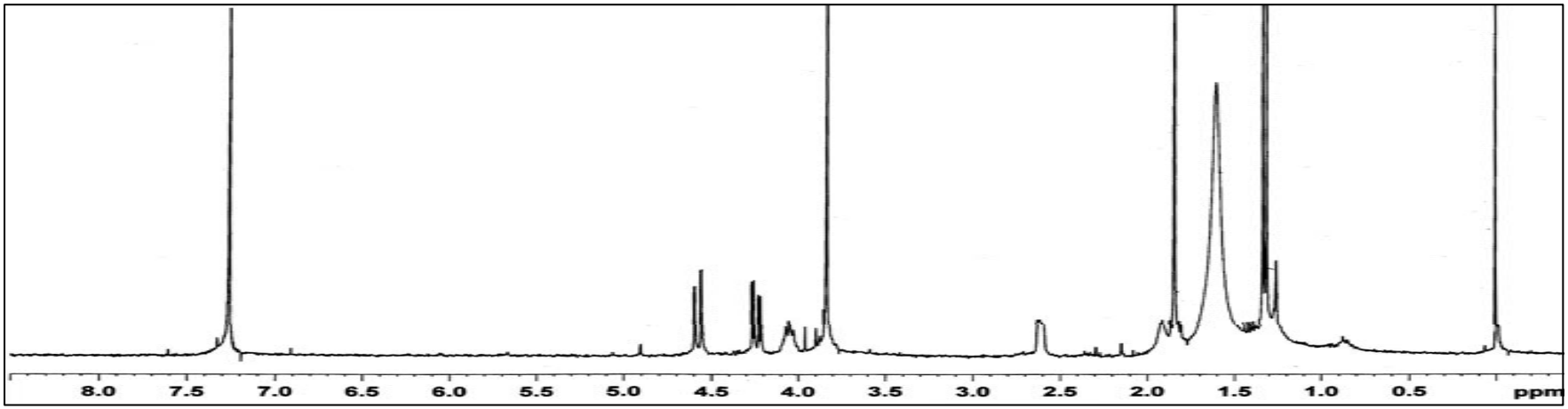

Figure 55 The 300 MHz ^{1}H NMR spectrum of compound **AR22** in $CDCl_3$

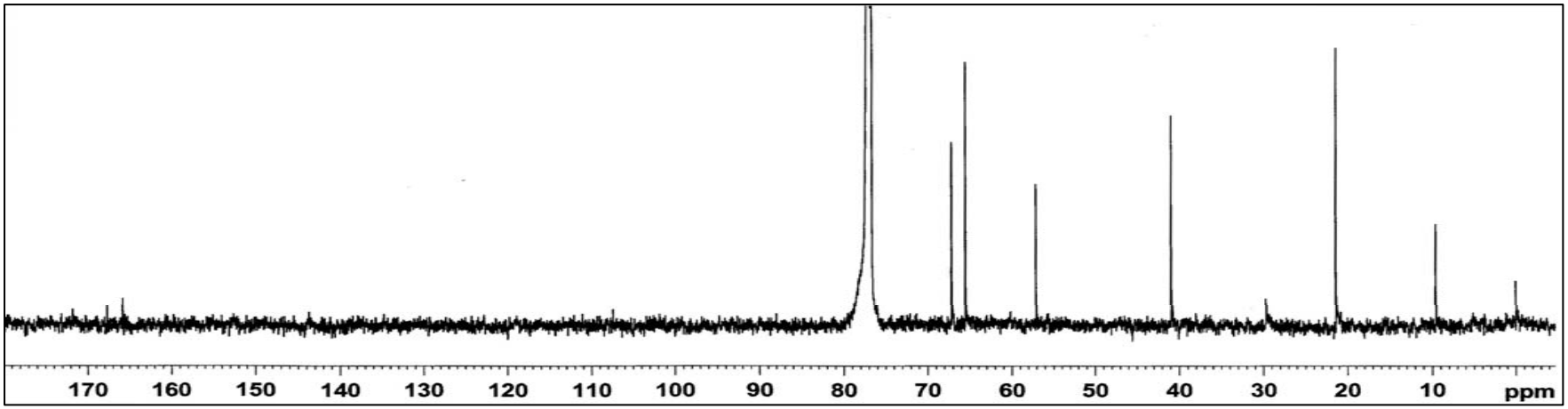

Figure 56 The 125 MHz ^{13}C NMR spectrum of compound **AR22** in $CDCl_3$

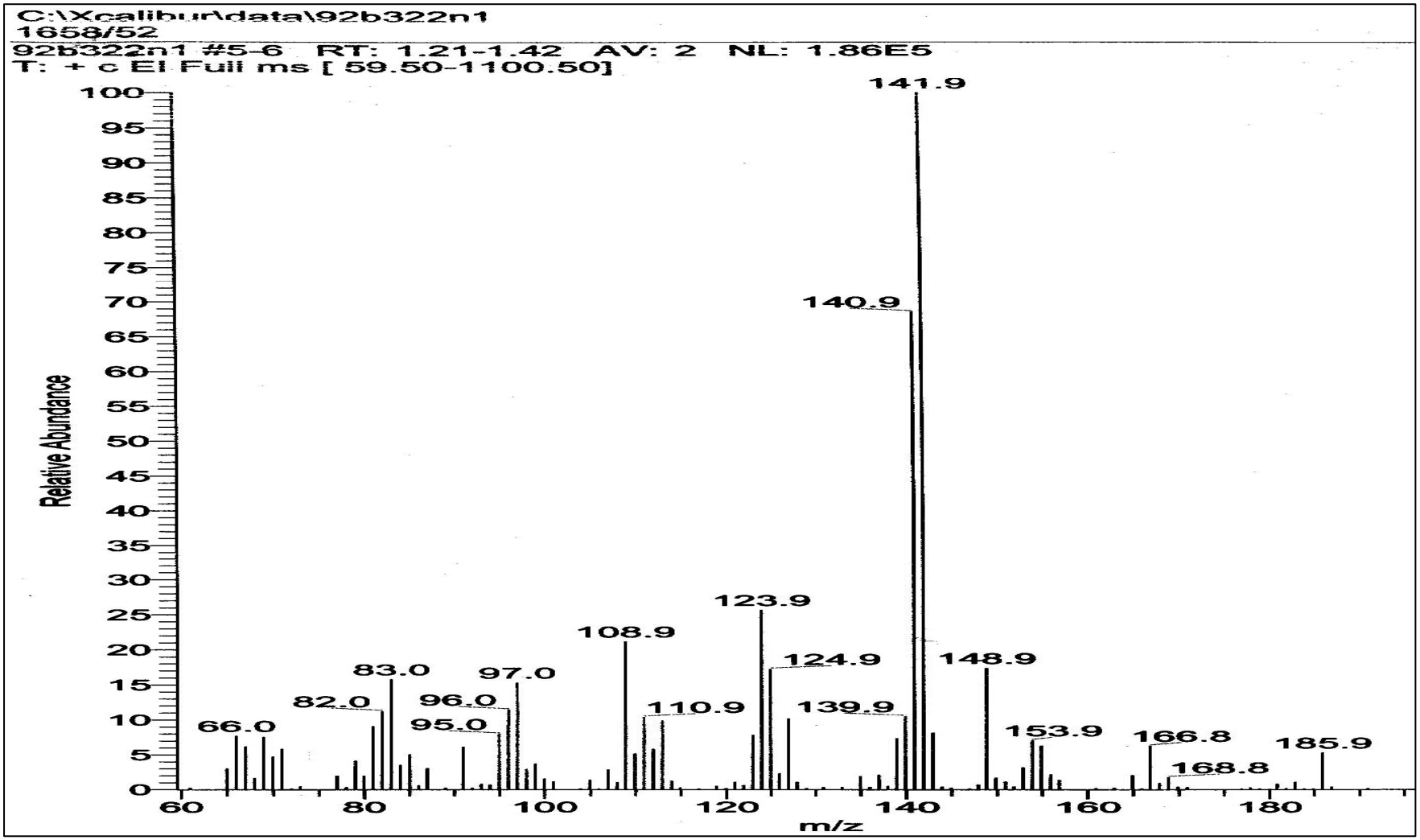

Figure 57 The mass spectrum of compound **AR22**

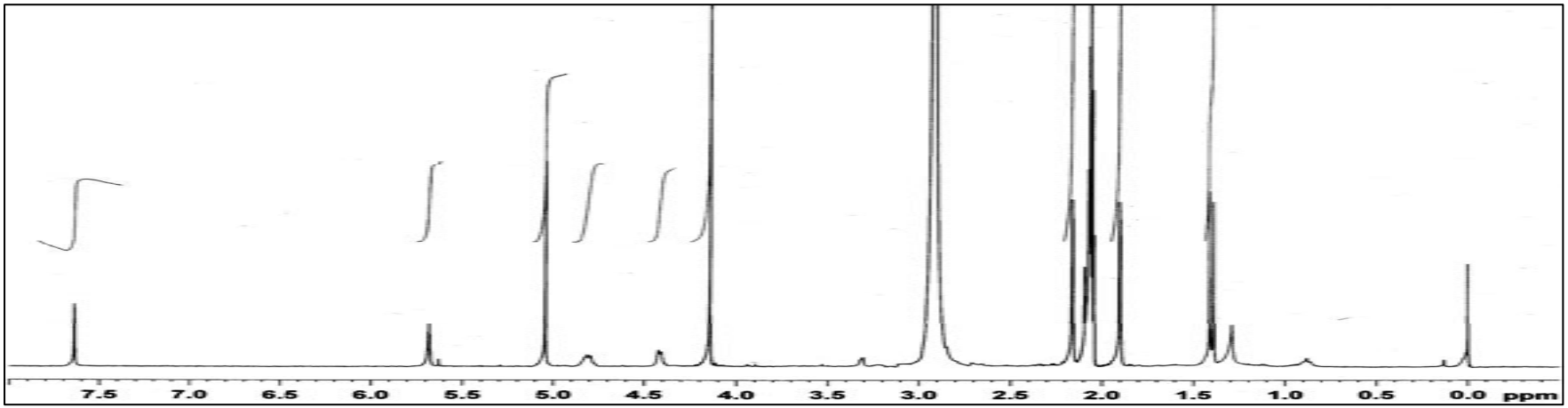

Figure 58 The 300 MHz ^{1}H NMR spectrum of compound **AR23** in Acetone-d_6

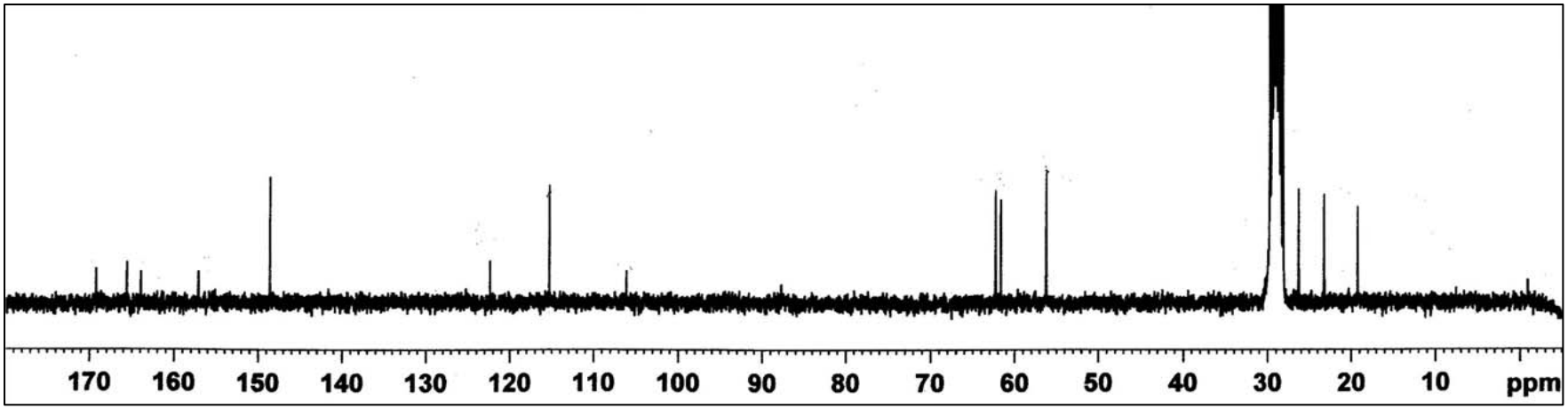

Figure 59 The 75 MHz ^{13}C NMR spectrum of compound **AR23** in Acetone-d_6

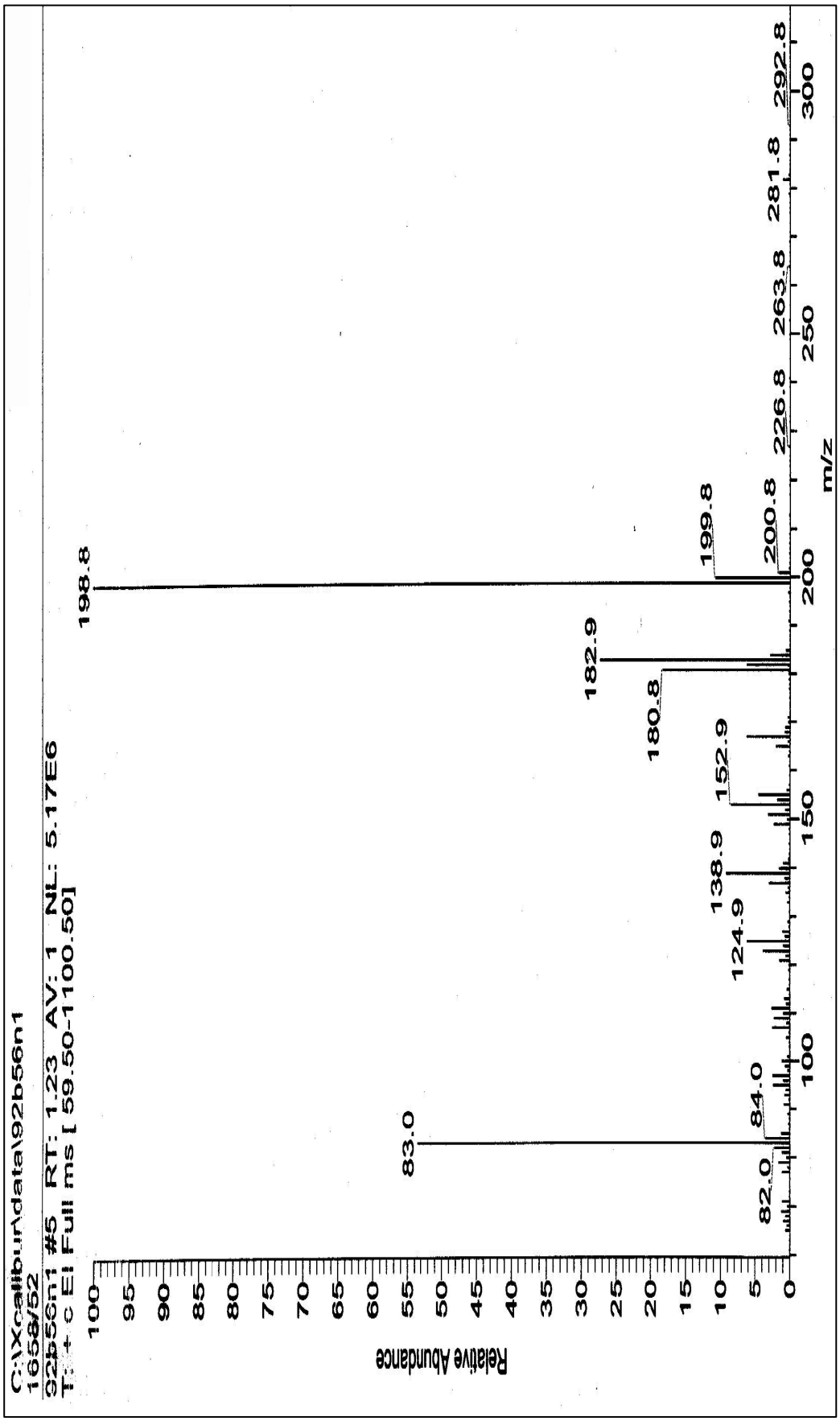

Figure 60 The mass spectrum of compound **AR23**

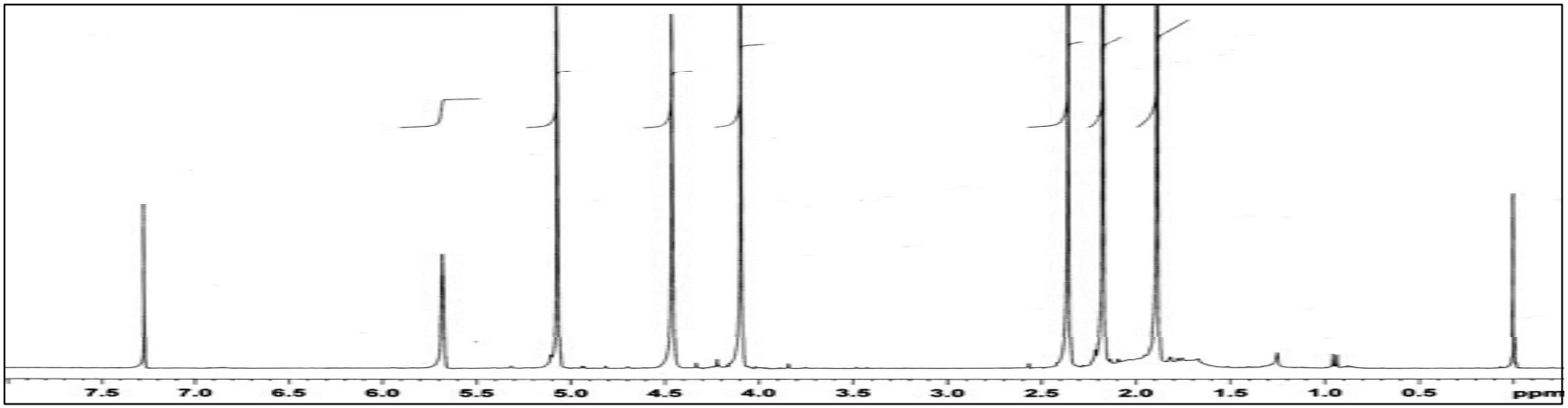

Figure 61 The 300 MHz ^{1}H NMR spectrum of compound **AR24** in $CDCl_3$

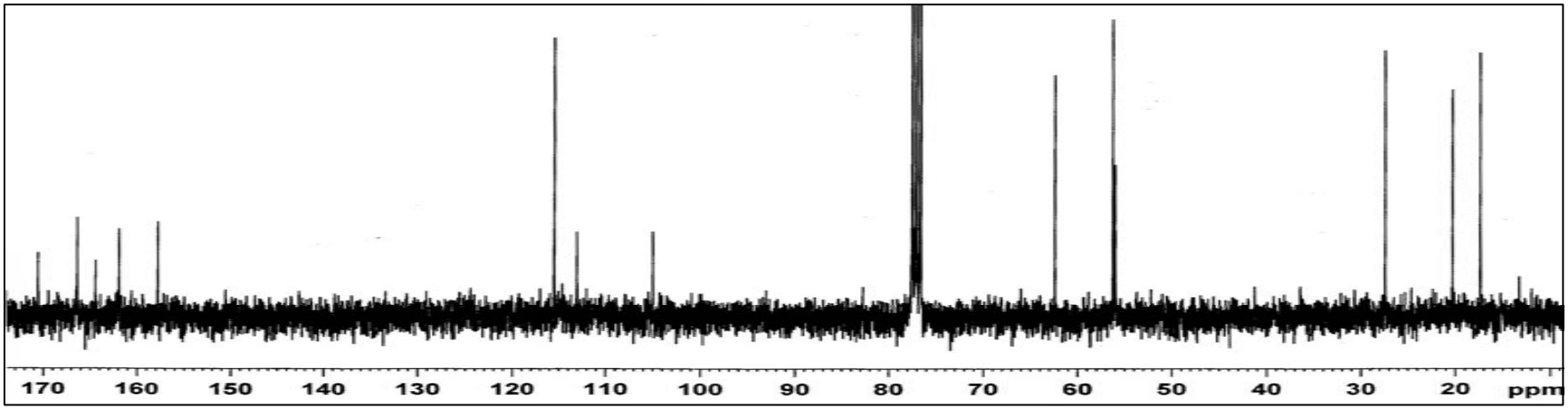

Figure 62 The 75 MHz ^{13}C NMR spectrum of compound **AR24** in $CDCl_3$

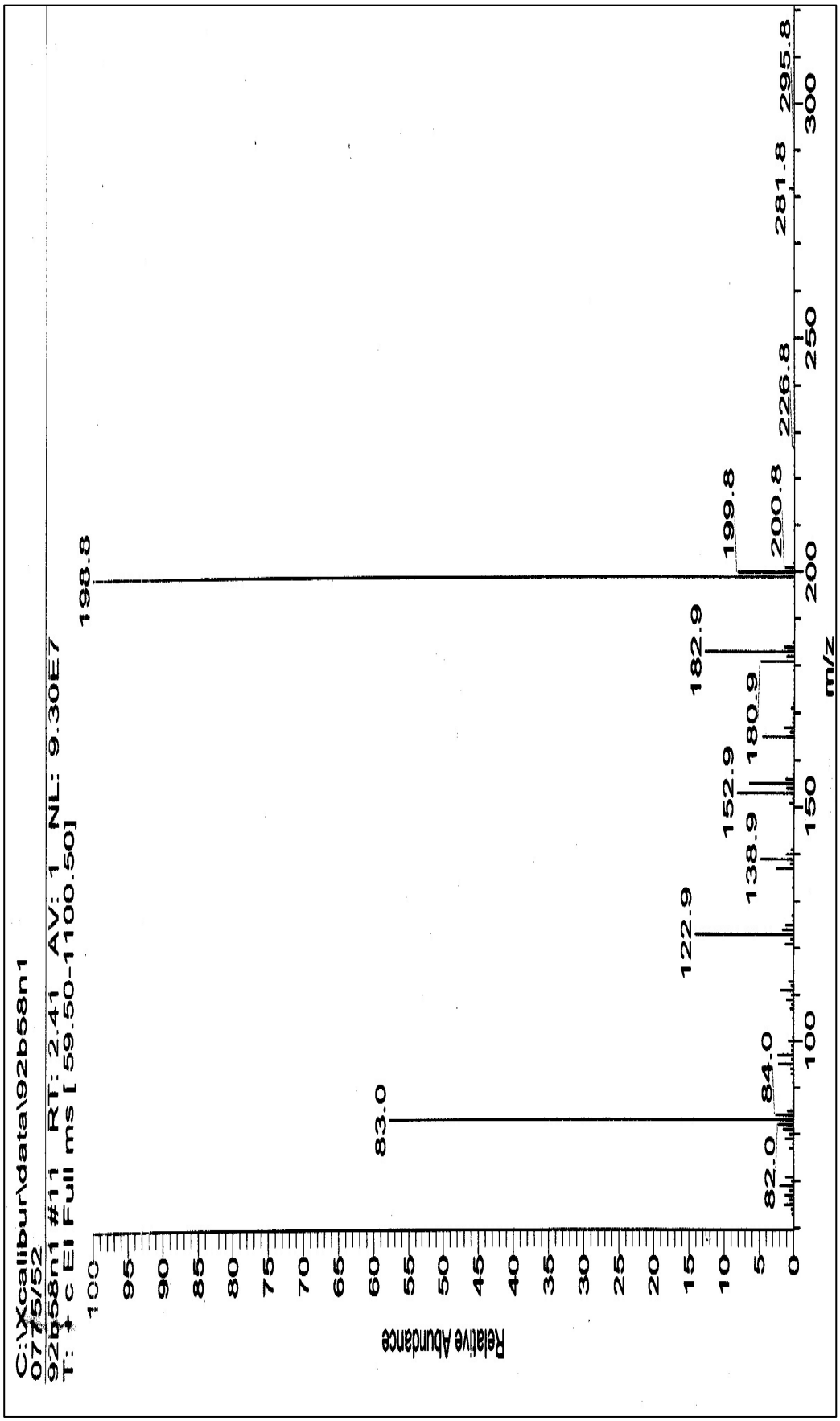

Figure 63 The mass spectrum of compound **AR24**

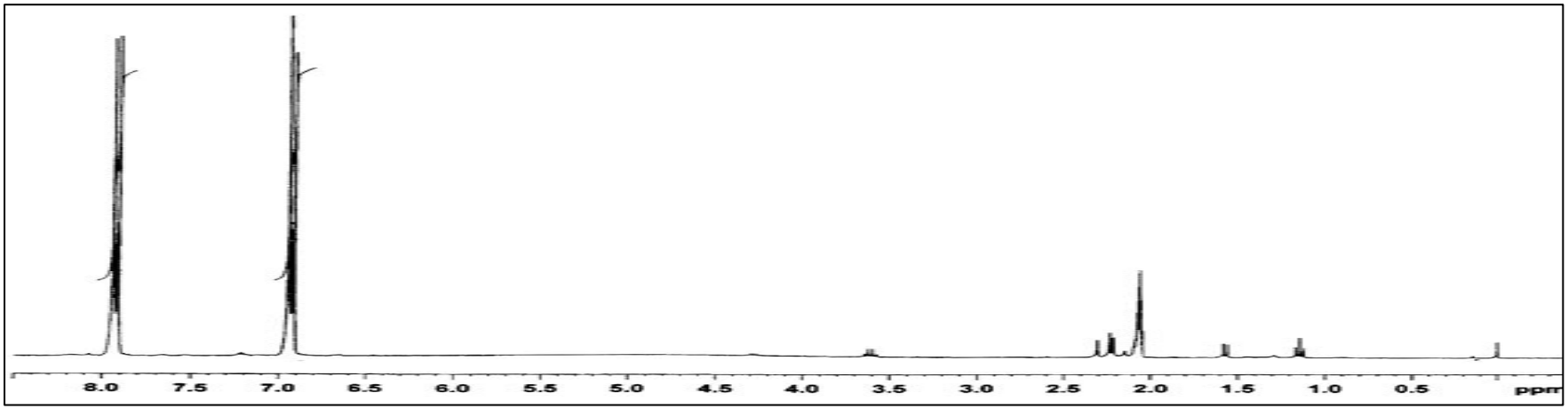

Figure 64 The 300 MHz ^{1}H NMR spectrum of compound **AR25 in** Acetone-d_6

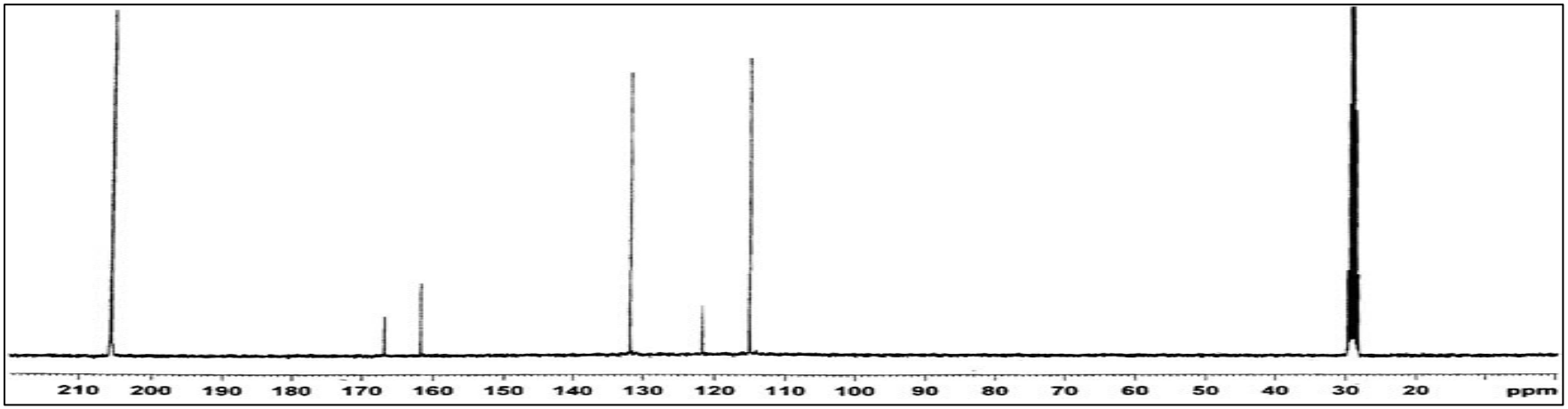

Figure 65 The 75 MHz ^{13}C NMR spectrum of compound **AR25** in Acetone-d_6

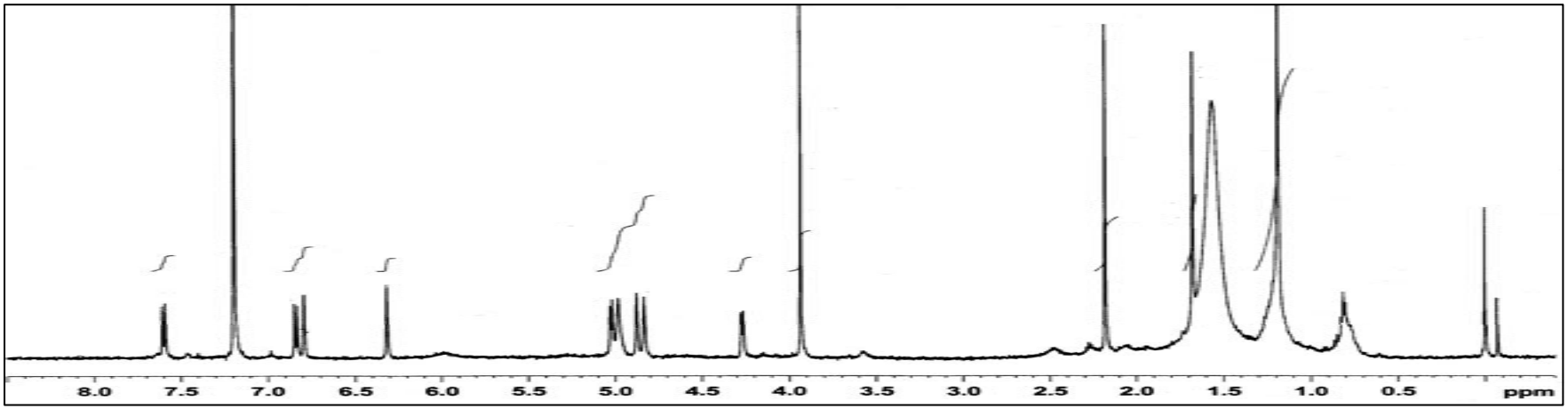

Figure 66 The 500 MHz ^{1}H NMR spectrum of compound **AR26** in $CDCl_3$

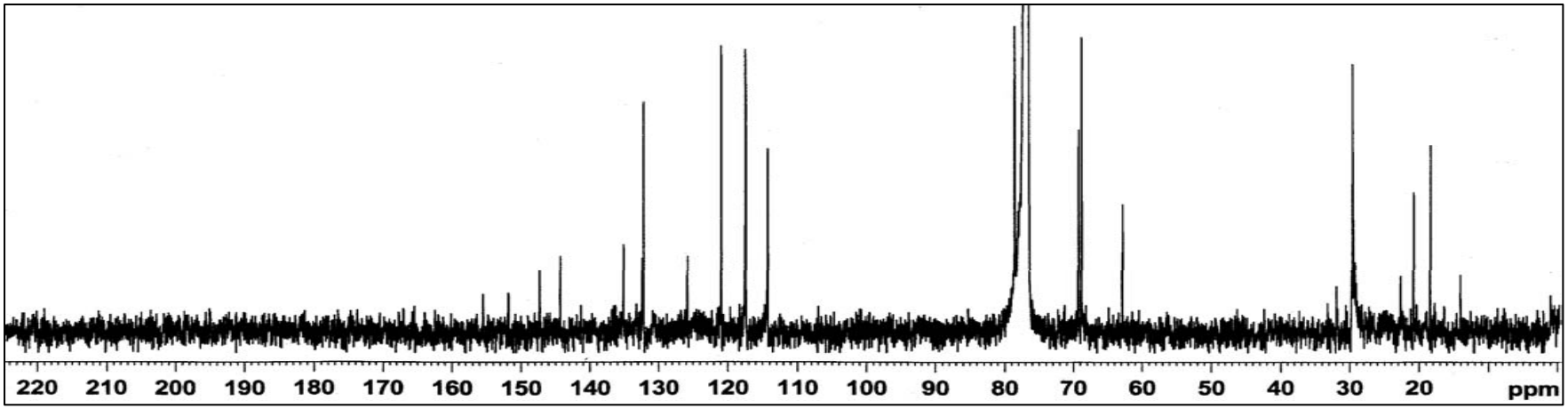

Figure 67 The 125 MHz ^{13}C NMR spectrum of compound **AR26** in $CDCl_3$

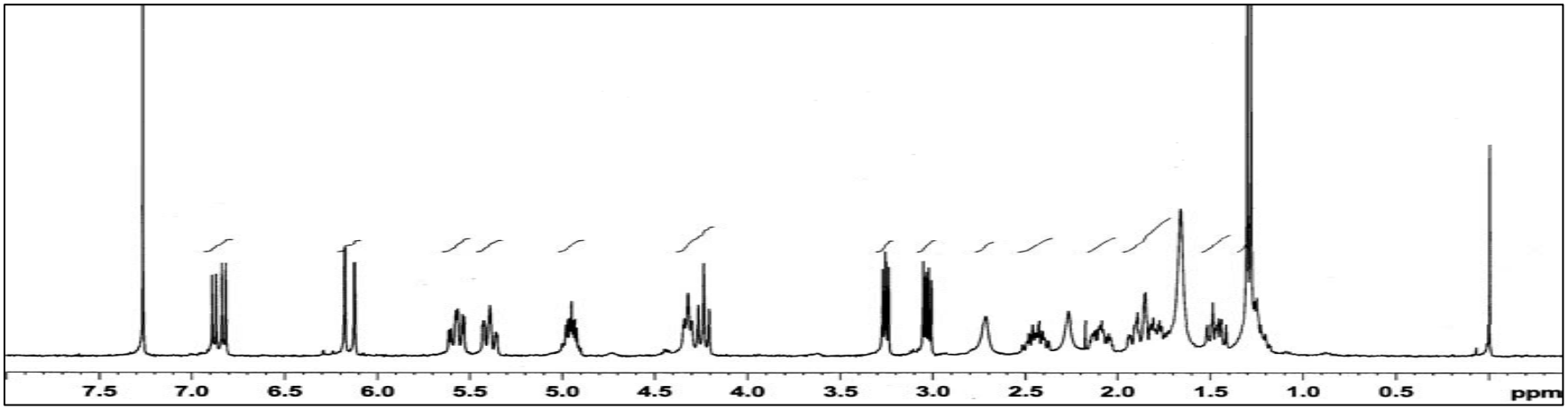

Figure 68 The 300 MHz ^{1}H NMR spectrum of compound **AR28** in $CDCl_3$

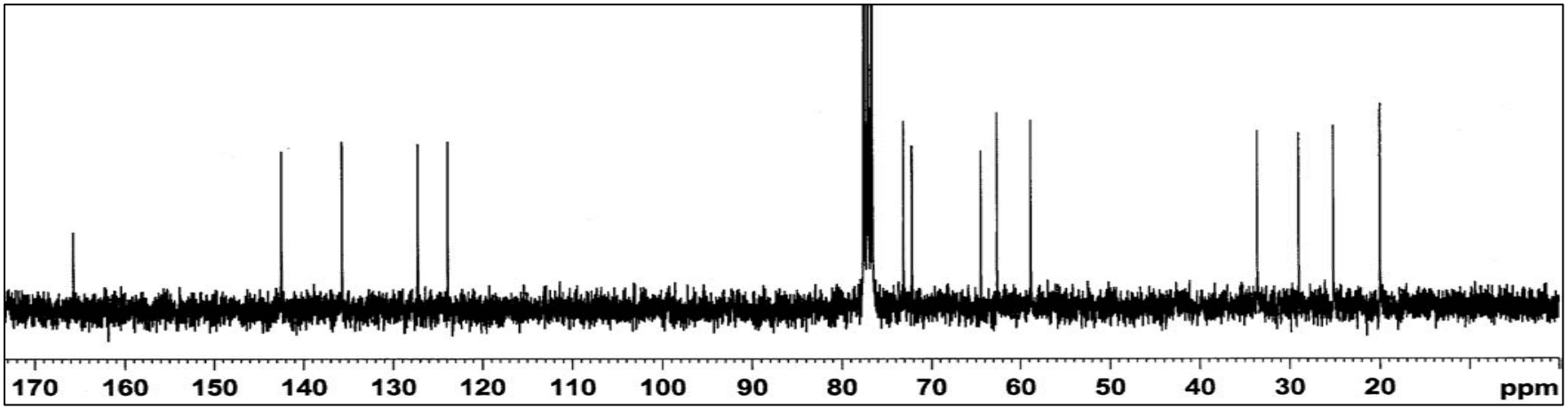

Figure 69 The 75 MHz ^{13}C NMR spectrum of compound **AR28** in $CDCl_3$

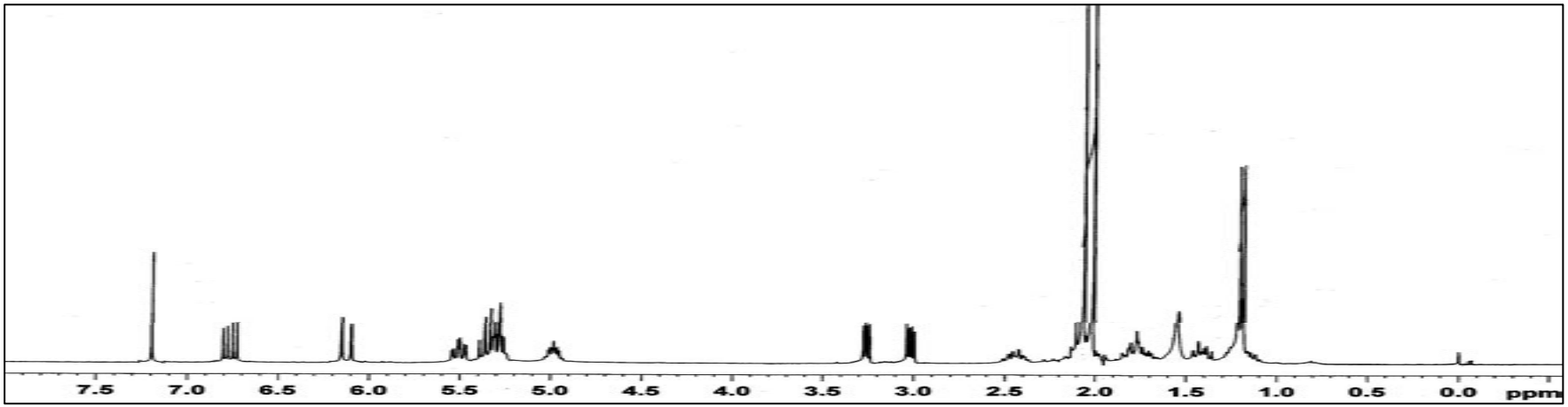

Figure 70 The 300 MHz ^{1}H NMR spectrum of the diacetate derivative of compound **AR28** in $CDCl_3$

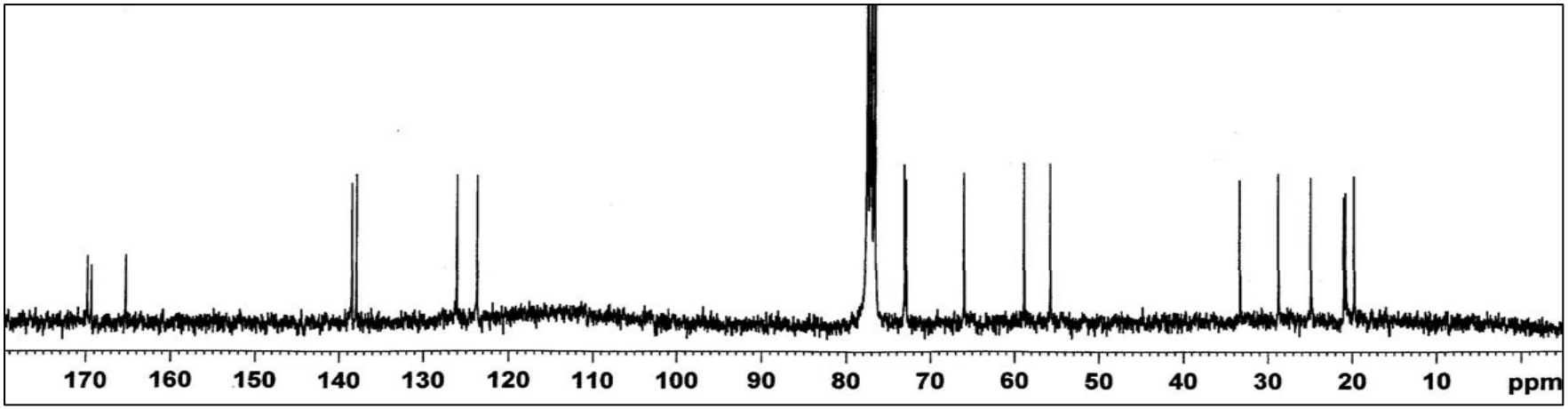

Figure 71 The 75 MHz ^{13}C NMR spectrum of the diacetate derivative of compound **AR28** in $CDCl_3$

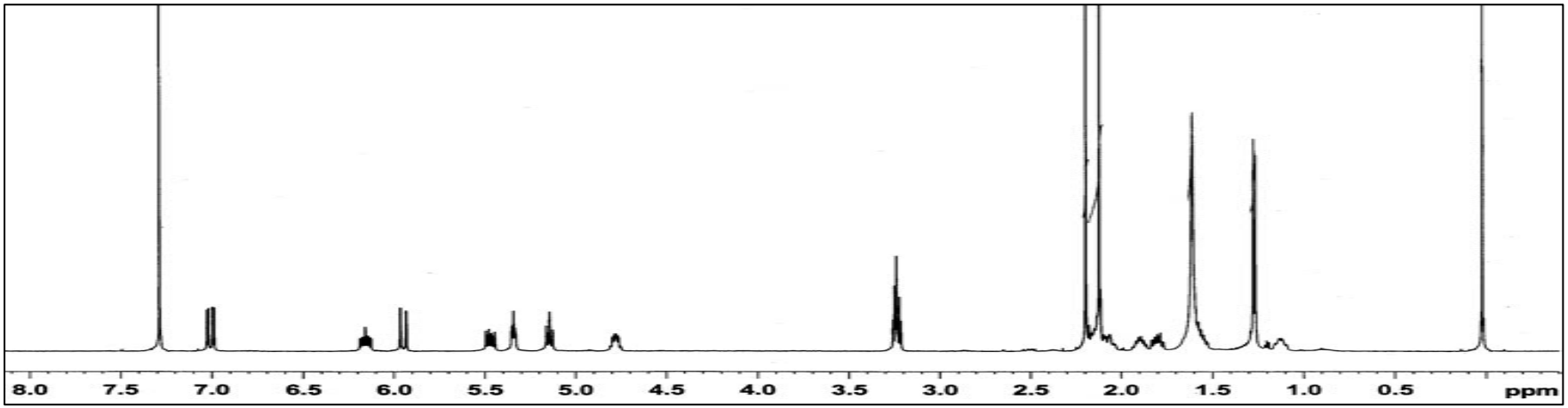

Figure 72 The 500 MHz ^{1}H NMR spectrum of compound **AR27** in $CDCl_3$

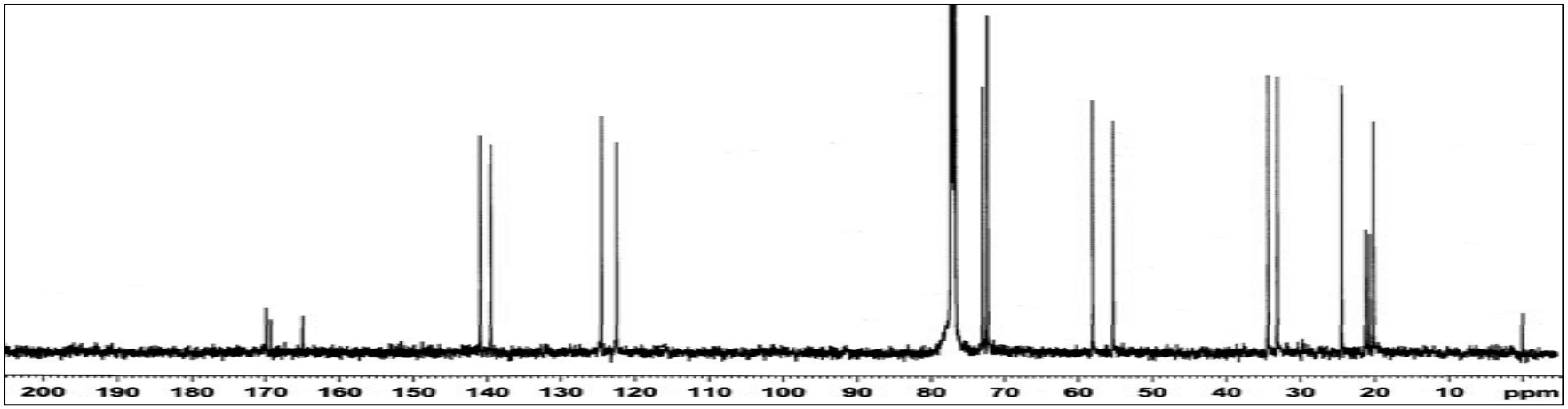

Figure 73 The 125 MHz ^{13}C NMR spectrum of compound **AR27** in $CDCl_3$

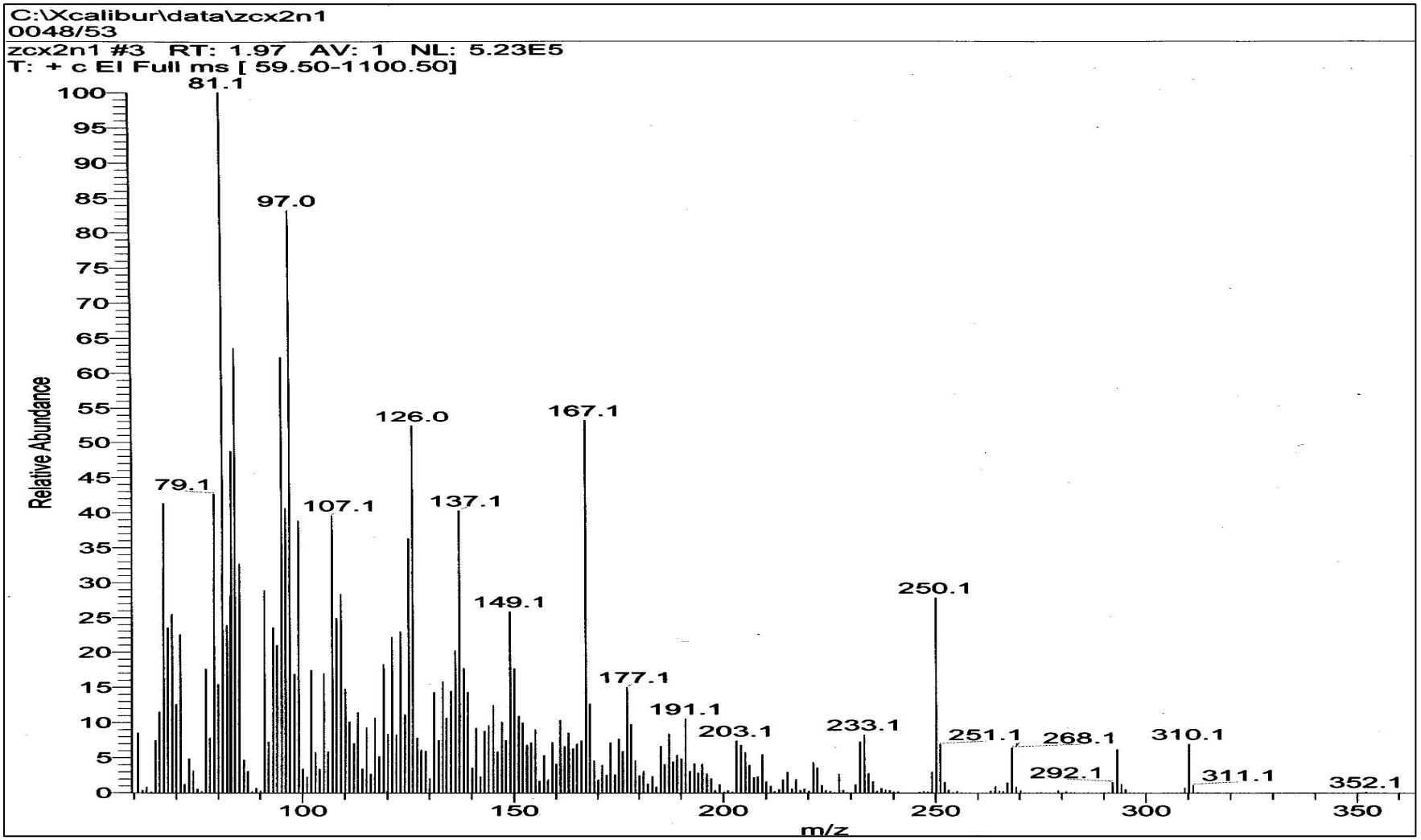

Figure 74 The mass spectrum of compound **AR27**

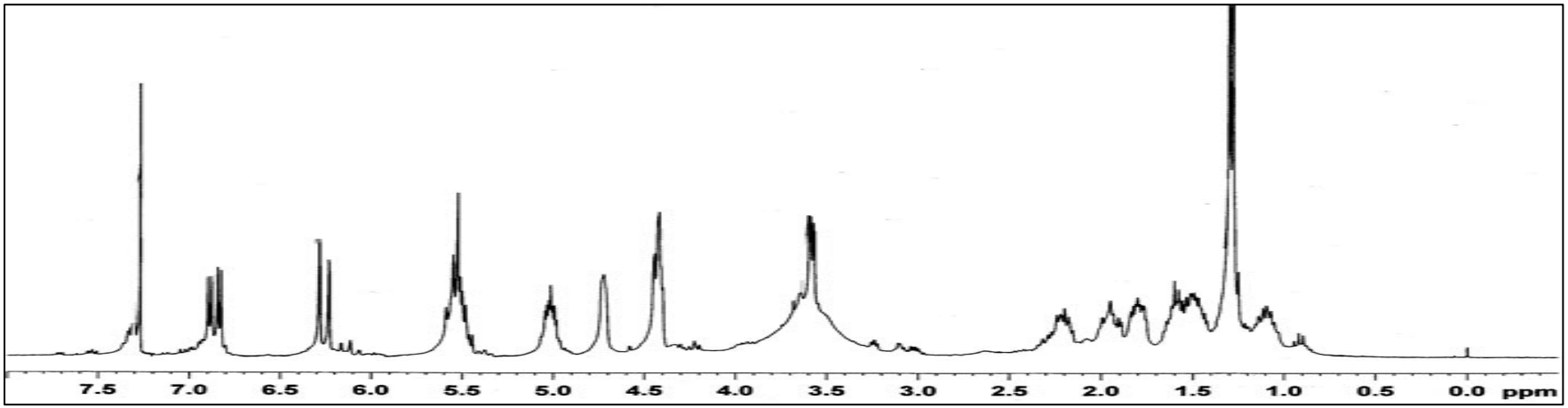

Figure 75 The 300 MHz ^{1}H NMR spectrum of compound **AR29** in $CDCl_3$

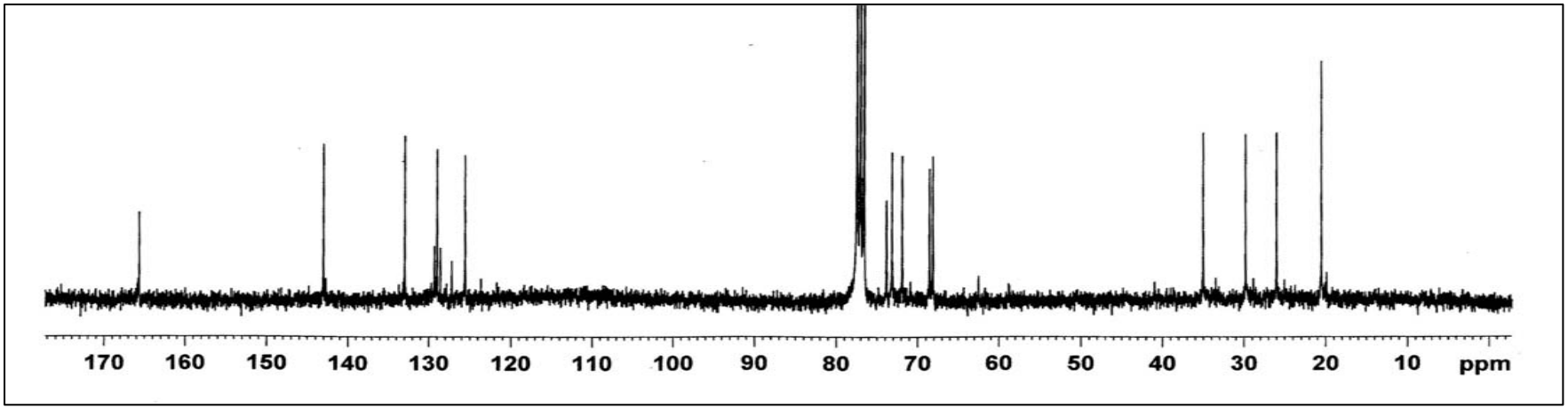

Figure 76 The 75 MHz ^{13}C NMR spectrum of compound **AR29** in $CDCl_3$

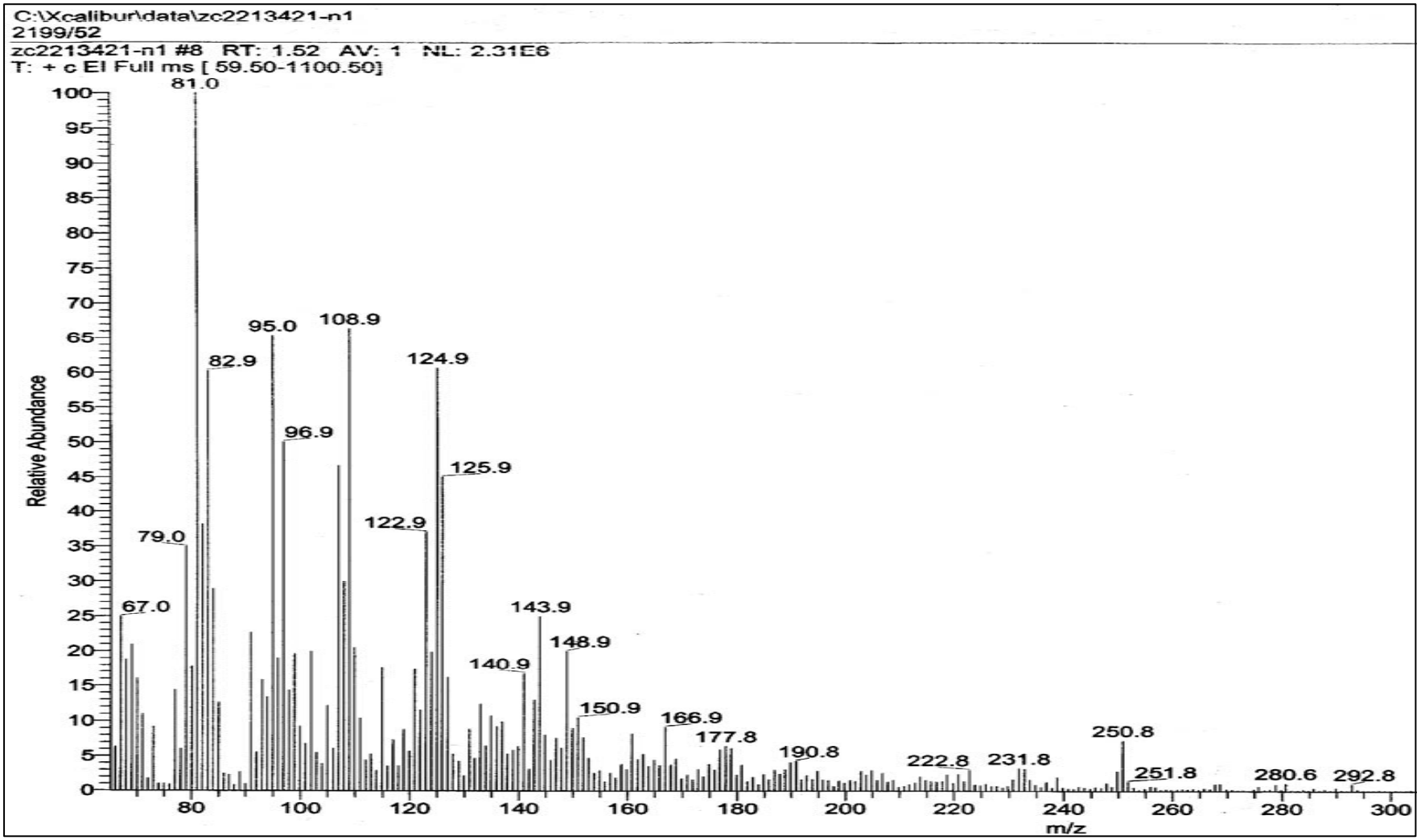

Figure 77 The mass spectrum of compound **AR29**

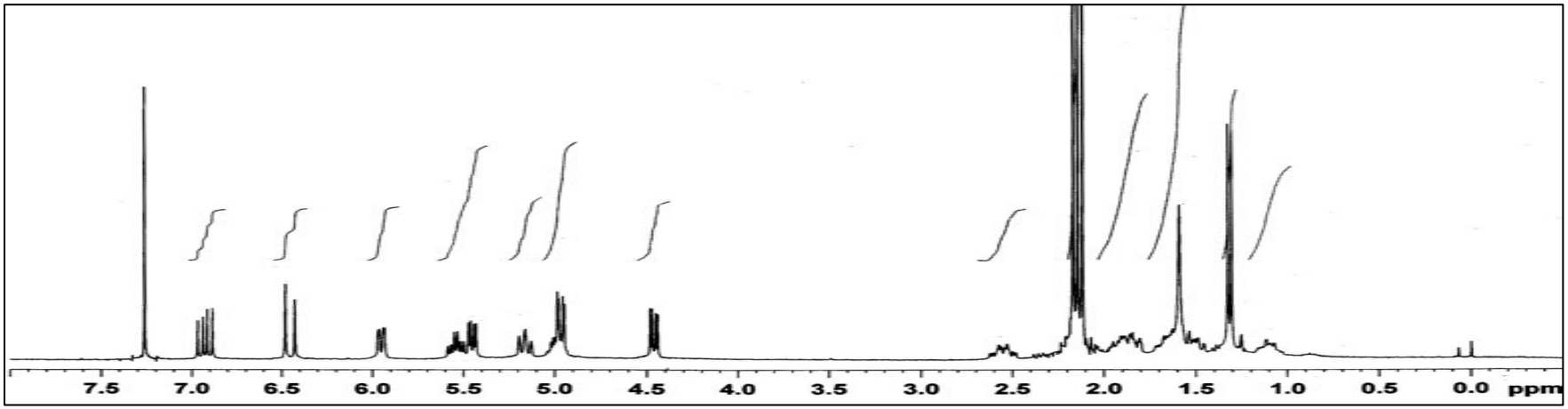

Figure 78 The 300 MHz ^{1}H NMR spectrum of the triacetate derivative of compound **AR29** in $CDCl_3$

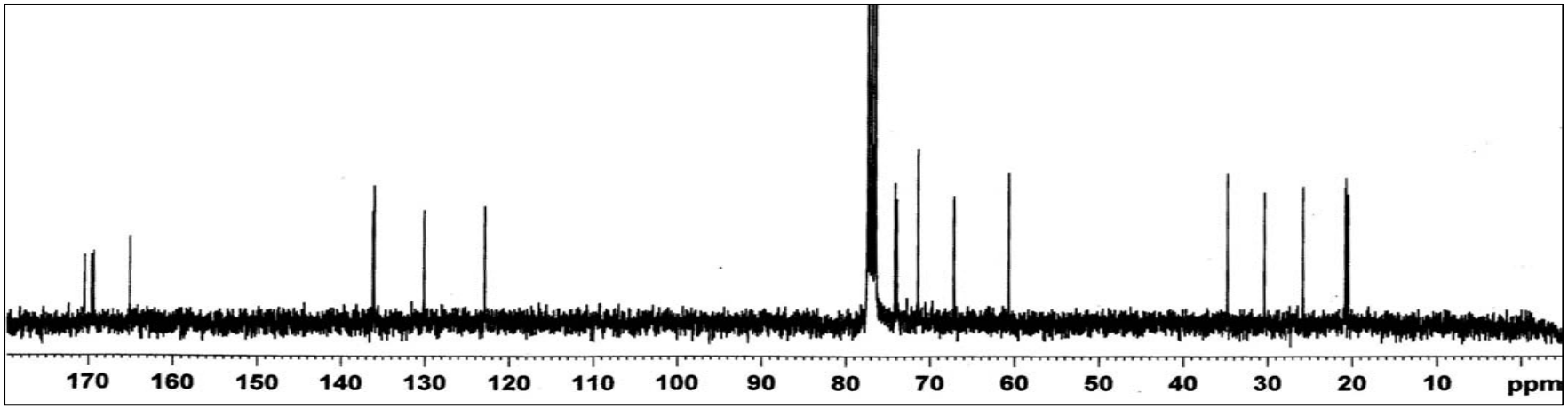

Figure 79 The 75 MHz ^{13}C NMR spectrum of the triacetate derivative of compound **AR29** in $CDCl_3$

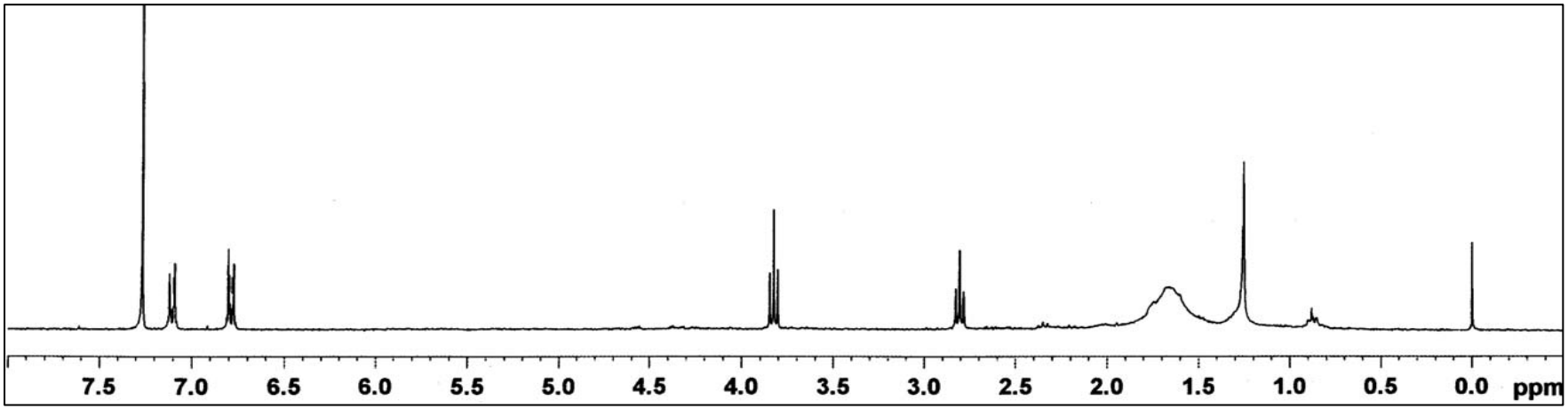

Figure 80 The 300 MHz ^{1}H NMR spectrum of compound **AR30** in $CDCl_3$

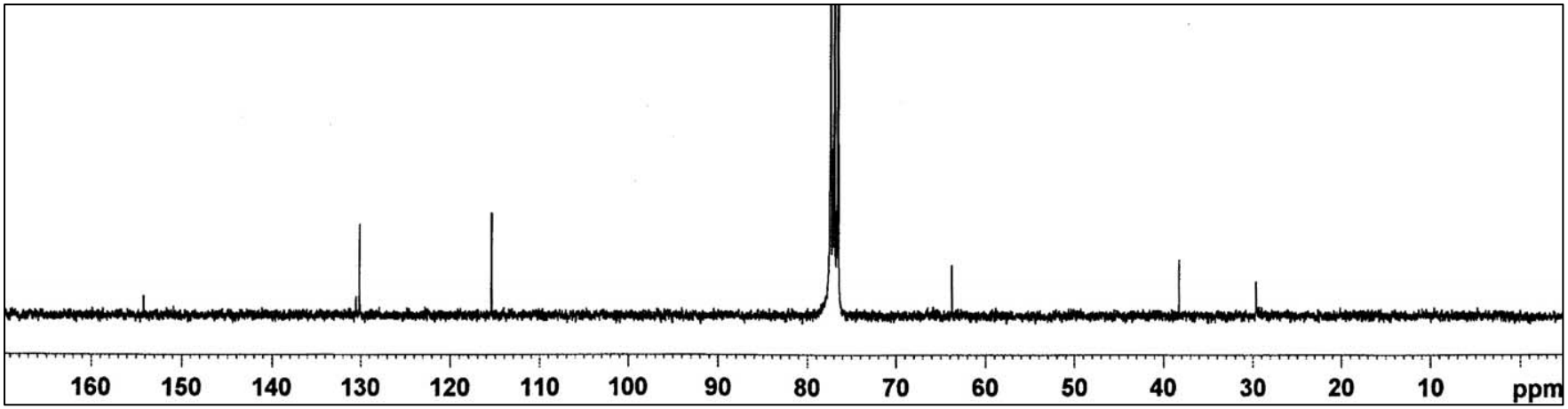

Figure 81 The 75 MHz ^{13}C NMR spectrum of compound **AR30** in $CDCl_3$

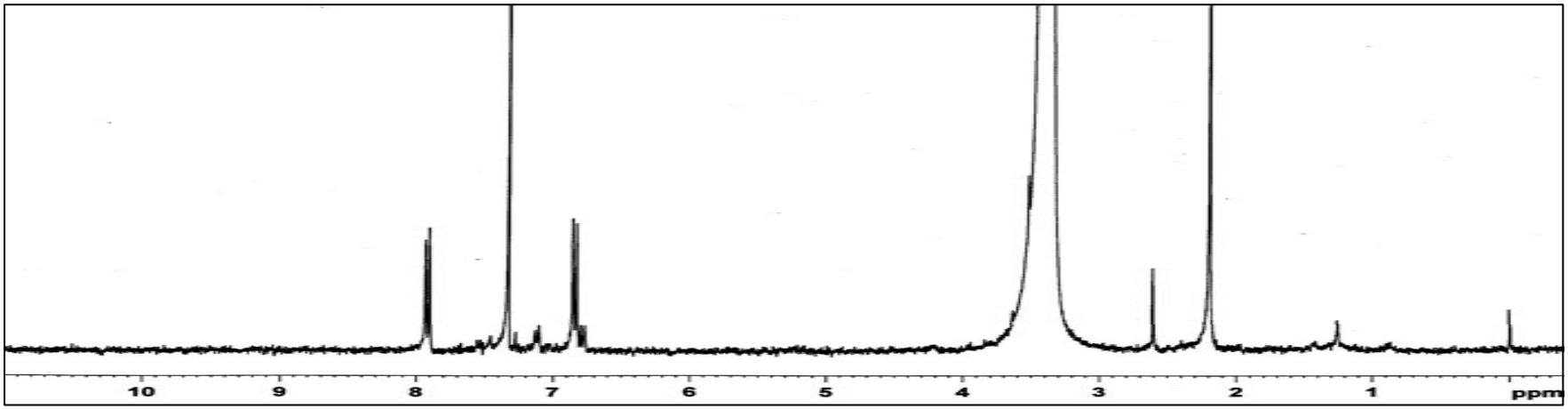

Figure 82 The 300 MHz ^{1}H NMR spectrum of compound **AR31** in $CDCl_3$

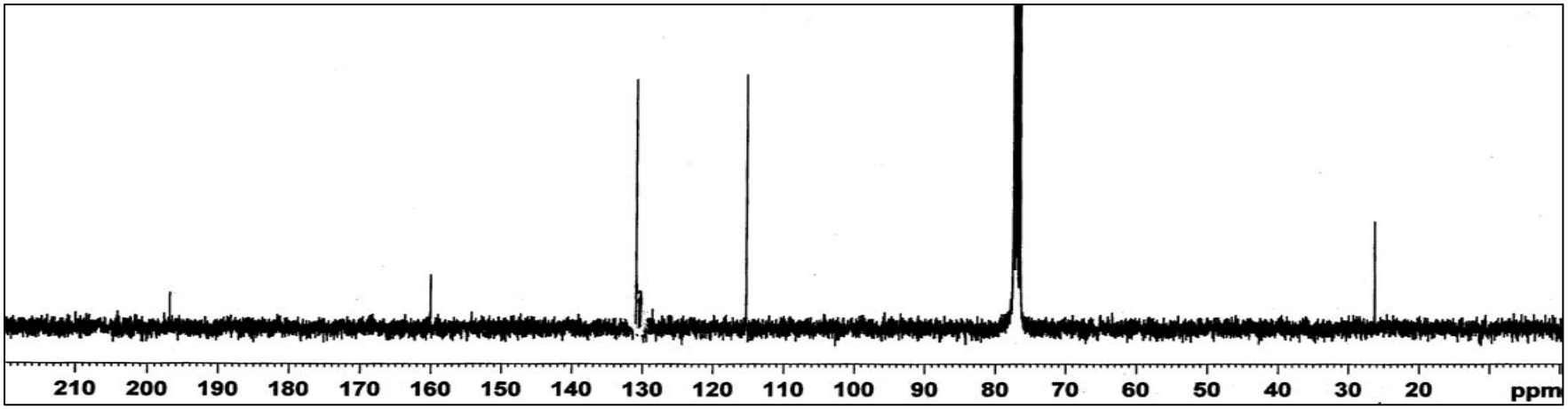

Figure 83 The 75 MHz ^{13}C NMR spectrum of compound **AR31** in $CDCl_3$

VITAE

Name Mr. Aekkachai Rodglin

Student ID 5110220107

Educational Attainment

Degree	Name of Institution	Year of Graduation
B.Sc. (Chemistry)	Thaksin University	2005

Scholarship Awards during Enrolment

The Center for Innovation in Chemistry: Postgraduate Education and Research Program in Chemistry (PERCH-CIC)

List of Publication and Proceedings

Proceedings

1. Rodglin, A., Rukachaisirikul, V., Phongpaichit, S. and Buatong, J. 2009. Seiricuprolide, tyrosol and 4-hydroxyacetophenone from the broth extract of the mangrove-derived fungus *Pestalotiopsis* sp. PSU-MA119. Proceeding of the 14th National Graduate Research Conference. King Mongkut's University of Technology North Bangkok, September 10-11, 2009. pp.71.

2. Rodglin, A., Rukachaisirikul, V., Phongpaichit, S. and Buatong, J. 2009. Metabolites from mangrove-derived fungus *Pestalotiopsis* sp. PSU-MA119. Proceeding of the 35th Congress on Science and Technology of Thailand. The Tide Resort (Bangsaen Beach), Chonburi, Thailand, October 15-17, 2009. pp.150.